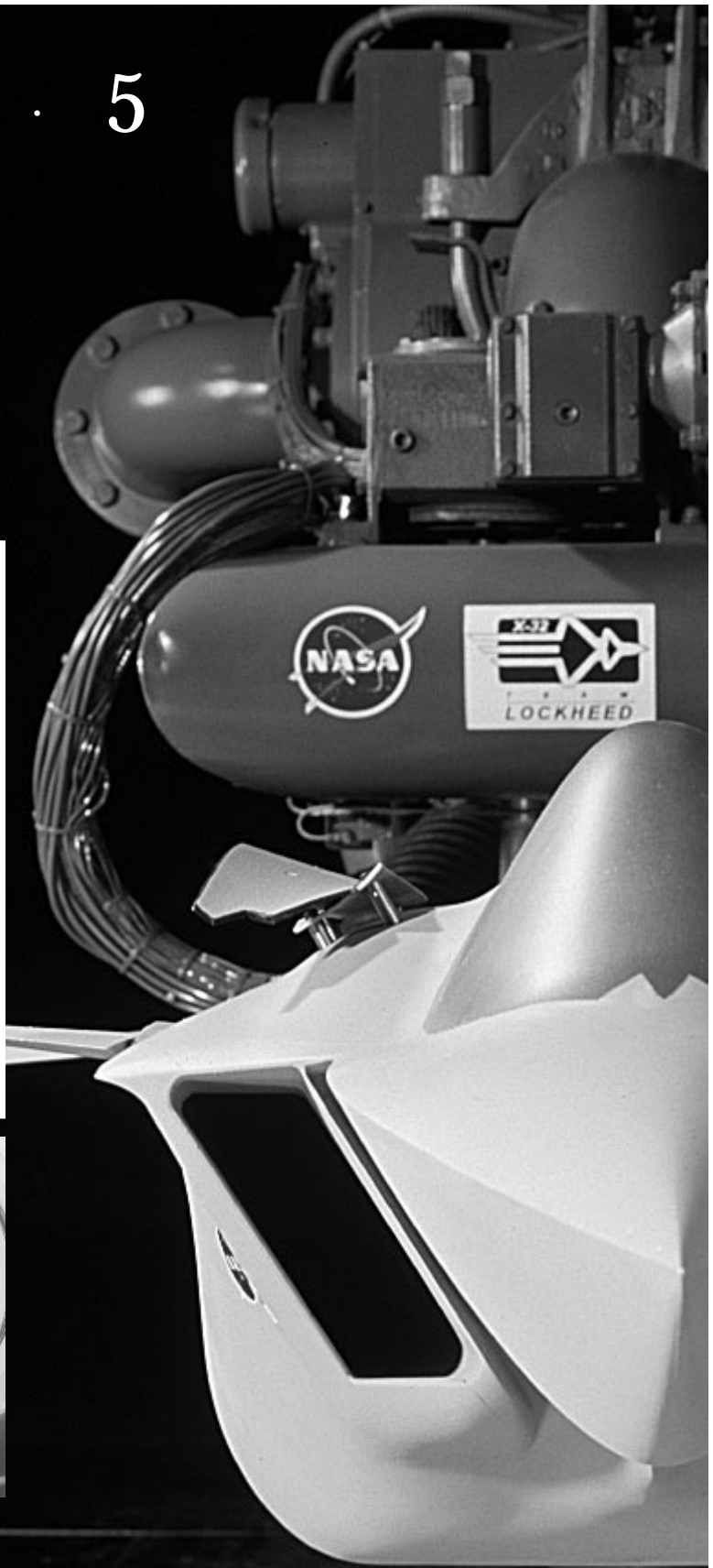
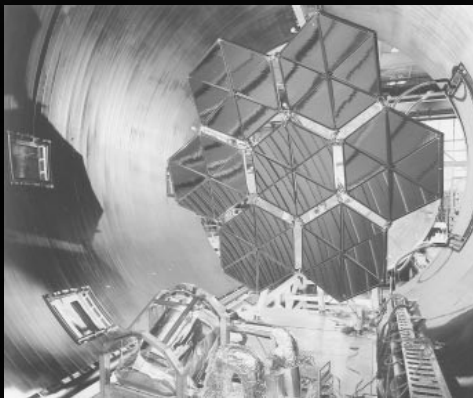
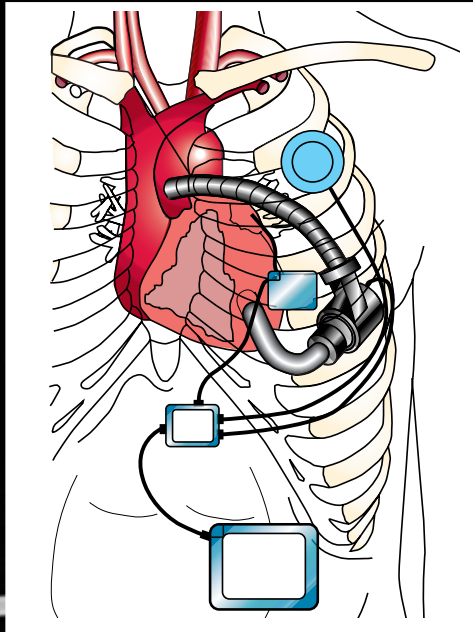


1 · 9 · 9 · 5

R&T

Research & Technology



National Aeronautics and
Space Administration
Lewis Research Center
Cleveland, Ohio 44135

Technical Memorandum 107111

About the cover:

Top left: Lewis/Cleveland Clinic Foundation heart pump (see p. 39).

Bottom left: Solar dynamic system installed in tank 6 (see p. 115).

Right: Front view of ASTOVL model (see p. 27).

Research & Technology 1995



National Aeronautics and
Space Administration

Lewis Research Center
Cleveland, Ohio 44135

TM-107111

Trade names or manufacturers' names are used in this report for identification only. This usage does not constitute an official endorsement, either expressed or implied, by the National Aeronautics and Space Administration.



Introduction

The NASA Lewis Research Center is a unique facility with a long and distinguished history of performing research and developing technology in support of NASA's mission and the Nation's needs. Over the past year, Lewis underwent changes that put special emphasis on realigning our activities in space and aeronautics with the Agency's mission. Part of that realignment focuses on transferring our technology and creating opportunities: transforming our cutting-edge technology into solutions that will benefit the whole Nation and making our resources and knowledge more easily available to the private sector. This report is part of the second focus.

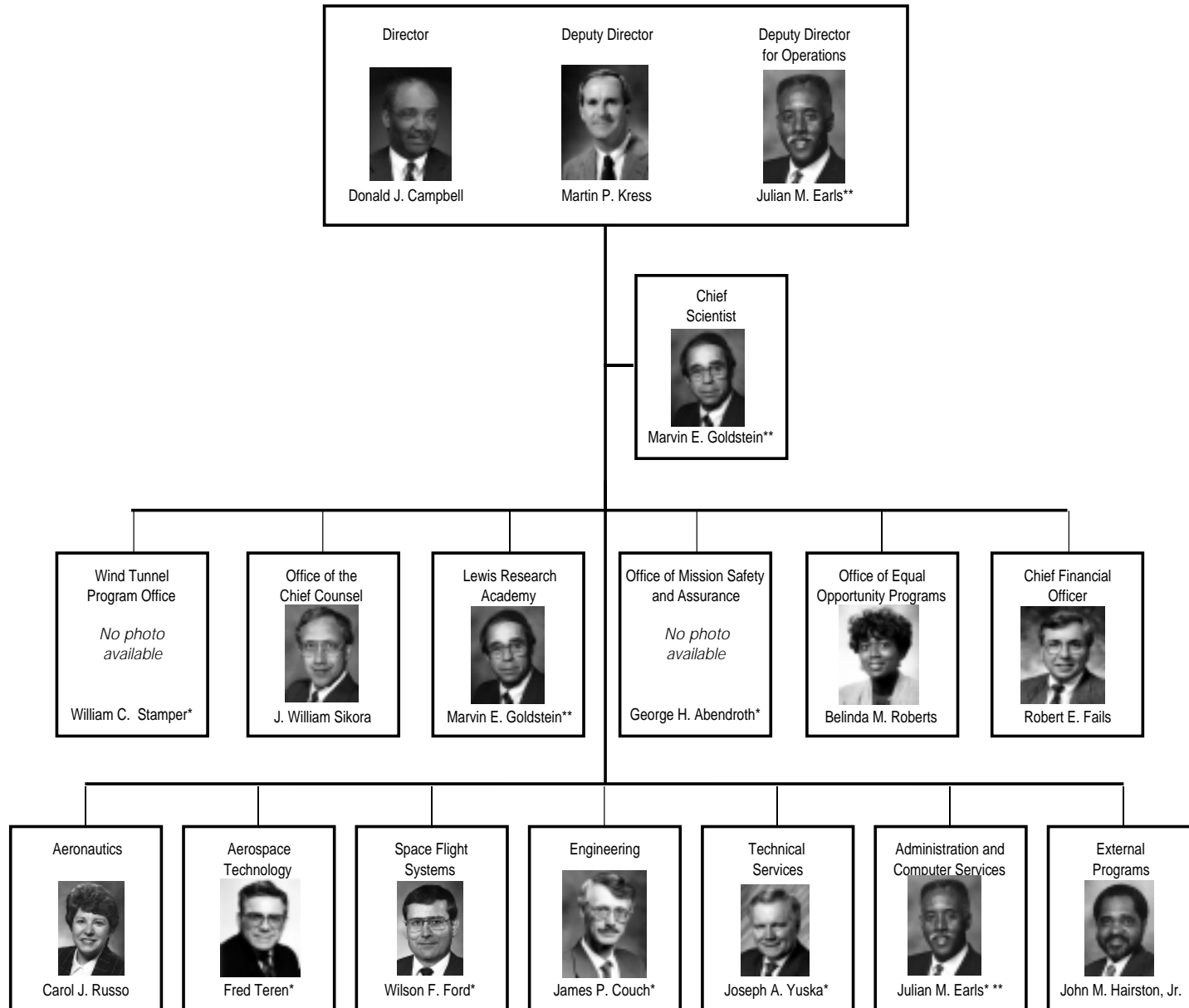
Lewis' Research & Technology 1995 report gives a brief, but comprehensive, review of Lewis' technical accomplishments during the past year. It is a testimony to the dedication and competence of all the employees, civil servants and contractors alike, who make up the staff. This report helps us to make others aware of our technical accomplishments and to inspire them to seize the opportunities to expand on their application.

The report is organized so that a broad cross section of the community can readily use it. A short introductory paragraph begins each article and will prove to be an invaluable tool for the layperson. The articles summarize the progress made during the year in various technical areas and portray the technical and administrative support associated with Lewis' technology programs. We hope this information is useful to all. If additional information is desired, readers are encouraged to contact the researchers identified in the articles and to visit Lewis on the World Wide Web (<http://www.lerc.nasa.gov>). This document is available on the World Wide Web (<http://www.lerc.nasa.gov/WWW/RT1995/>).

A handwritten signature in cursive script that reads "D. J. Campbell". The signature is written in dark ink on a white background.

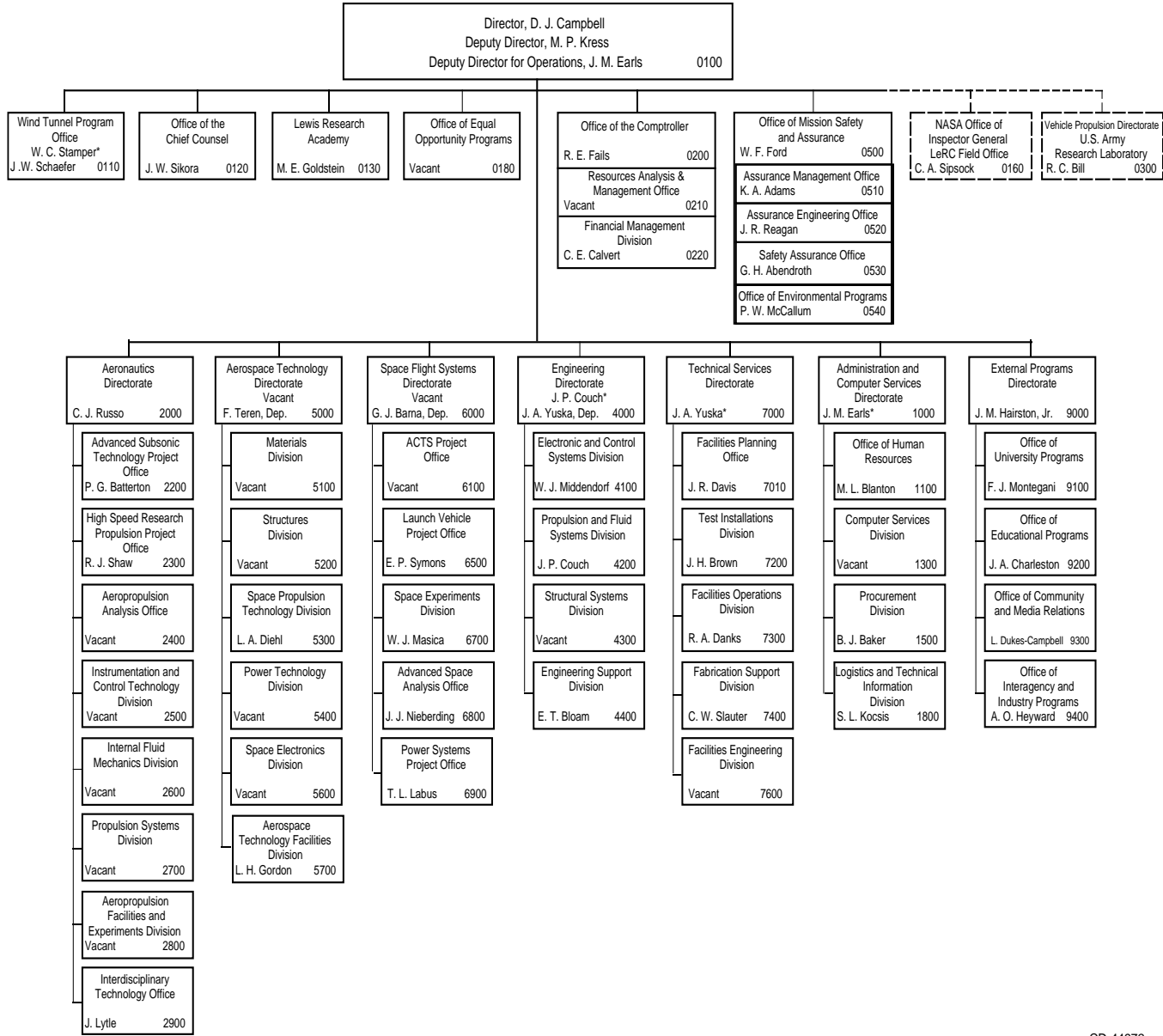
Donald J. Campbell
Director

NASA Lewis Research Center Senior Management



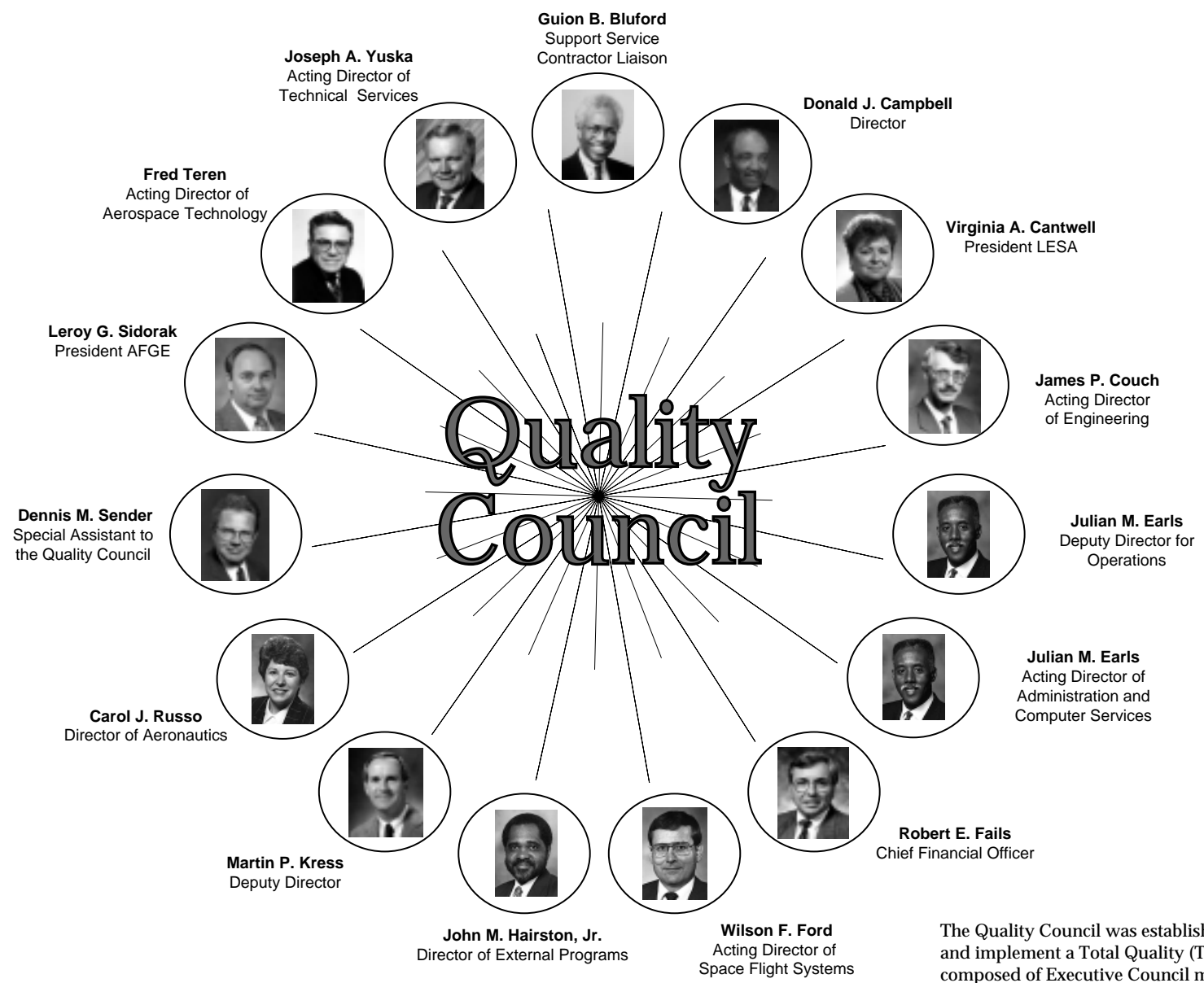
* Acting
** Dual Capacity

NASA Lewis Research Center



* Acting

Quality Council



The Quality Council was established in October 1992 to adopt and implement a Total Quality (TQ) plan for Lewis. It is composed of Executive Council members as well as the president of the American Federation of Government Employees (AFGE), Local 2812, and the president of the Lewis Engineers and Scientists Association (LESA), IFPTE Local 28. A representative of major onsite support service contractors serves a liaison.

Contents

Aeronautics

| | |
|---|----|
| Advanced Subsonic Technology | 1 |
| Advanced Subsonic Combustion Rig Developed | 1 |
| Aeropropulsion Analysis | 2 |
| Performance of Gas Turbine Engines Using Wave Rotors Modeled | 2 |
| Instrumentation and Control Technology | 3 |
| High-Temperature, Thin-Film Strain Gages Improved | 3 |
| Silicon Carbide High-Temperature Power Rectifiers Fabricated and Characterized | 4 |
| Automated Hydrogen Gas Leak Detection System | 5 |
| Fuzzy Logic Particle Tracking | 6 |
| Fiber Optic Repair and Maintainability (FORM) Program Progresses | 7 |
| Transient Wave Rotor Performance Investigated | 8 |
| Concept Designed and Developed for Distortion-Tolerant, High-Stability Engine Control | 9 |
| Internal Fluid Mechanics | 10 |
| Coupled Monte Carlo Probability Density Function/SPRAY/CFD Code Developed for Modeling Gas-Turbine Combustor Flows | 10 |
| CFD-Based Design Optimization Tool Developed for Subsonic Inlet | 11 |
| User Interface Developed for Controls/CFD Interdisciplinary Research | 12 |
| Wavelet Techniques Applied to Modeling Transitional/Turbulent Flows in Turbomachinery | 13 |
| Effect of Shrouded Stator Leakage Flows on Core Compressor Studied | 14 |
| Stable Lobed Mixer With Combustion Demonstrated and Measured | 15 |
| Effect of Tabs on a Rectangular Nozzle Studied | 16 |
| Propulsion Systems | 17 |
| Spherical Joint Piston and Connecting Rod Developed | 17 |
| Mach 6 Integrated Systems Tests of Lewis' Hypersonic Tunnel Facility | 18 |
| Capabilities Enhanced for Researching the Reduction of Emissions in Future Aircraft | 19 |
| Aircraft Ice Accretion Due to Large-Droplet Icing Clouds | 20 |
| Shape-Memory-Alloy-Based Deicing System Developed | 21 |
| Laser Sheet Flow Visualization Developed for Lewis' Icing Research Tunnel | 22 |
| Gear Crack Propagation Investigation | 23 |
| Study of Gear Dynamic Forces Completed | 24 |
| Code to Optimize Load Sharing of Split-Torque Transmissions Applied to the Comanche Helicopter | 25 |
| Face Gear Technology for Aerospace Power Transmission Progresses | 26 |
| Advanced Short Takeoff and Vertical Landing (ASTOVL) Concepts Tested | 27 |
| NPARC Code Upgraded With Two-Equation Turbulence Models | 27 |
| Mixing Process in Ejector Nozzles Studied at Lewis' Aero-Acoustic Propulsion Laboratory | 28 |
| F119 Nozzle Flaps Tested at Lewis' CE-22 Facility | 29 |
| Prediction Capability for Transonic Nozzle Afterbodies Improved | 30 |
| Thin-Film Thermocouple Technology Demonstrated for Reliable Heat Transfer Measurements | 31 |
| Effect of Brush Seals on Wave Rotor Performance Assessed | 32 |
| Scale-Model, Low-Tip-Speed Turbofan Tested at Simulated Takeoff and Approach Conditions | 33 |

| | |
|---|----|
| First Test of Fan Active Noise Control (ANC) Completed | 34 |
| Subsonic Jet Noise Reduced With Improved Internal Exhaust Gas Mixers | 35 |
| Aeropropulsion Facilities and Experiments | 36 |
| Drive Motor Improved for 8- by 6-Foot Supersonic Wind Tunnel/9- by 15-Foot Low-Speed Wind Tunnel Complex | 36 |
| Testing Efficiency Improved by Addition of Remote Access Control Room | 37 |
| Interdisciplinary Technology Office | 38 |
| Lewis/ACTS/Boeing Experiment Demonstrates Gigabit Application Using ACTS | 38 |
| Heart Pump Design for Cleveland Clinic Foundation | 39 |
| Coupled Aerodynamic-Thermal-Structural (CATS) Analysis | 40 |
| NASA Lewis IITA Kindergarten to 12th Grade Program | 41 |

Aerospace Technology

| | |
|---|----|
| Materials | 43 |
| Advanced High Temperature Engine Materials Technology Progresses | 43 |
| Stereo Imaging Velocimetry | 44 |
| Source of Scatter in the Creep Lives of NiAl(Hf) Single Crystals Revealed | 45 |
| Creep Testing of High-Temperature Cu-8 Cr-4 Nb Alloy Completed | 47 |
| Ceramic Composites Used in High-Speed Turbines for Rocket Engines | 48 |
| Affordable Fiber-Reinforced Ceramic Composites Win 1995 R&D 100 Award | 49 |
| Thermomechanical Property Data Base Developed for Ceramic Fibers | 50 |
| Silicon Carbide Epitaxial Films Studied by Atomic Force Microscopy | 51 |
| Self-Lubricating, Wear-Resistant Diamond Films Developed for Use in Vacuum Environment | 52 |
| Lubricous Deposit Formed In Situ Between Wearing Surfaces at High Temperatures | 54 |
| DMBZ Polyimides Provide an Alternative to PMR-15 for High-Temperature Applications | 55 |
| Low-Cost Resin Transfer Molding Process Developed for High-Temperature Polyimide Matrix Composites | 56 |
| Nuclear Magnetic Resonance Used to Quantify the Effect of Pyrolysis Conditions on the Oxidative Stability of Silicon Oxycarbide Ceramics | 57 |
| Thermochemical Degradation Mechanisms for Reinforced Carbon/Carbon Panels on the Space Shuttle | 58 |
| Structures | 59 |
| Cascade Optimization Strategy Maximizes Thrust for High-Speed Civil Transport Propulsion System Concept | 59 |
| Impact Properties of Metal Fan Containment Materials Being Evaluated for the High-Speed Civil Transport (HSCT) | 60 |
| Active Piezoelectric Structures for Tip Clearance Management Assessed | 60 |
| Microalloying Improves the Low-Cycle Fatigue Behavior of Powder-Extruded NiAl | 61 |
| Effects of Control Mode and R-Ratio on the Fatigue Behavior of a Metal Matrix Composite | 62 |
| Thermomechanical Fatigue Behavior of Coated and Uncoated Enhanced SiC/SiC Studied | 64 |
| Micromechanics Analysis Code (MAC) Developed | 65 |
| Fully Associative, Nonisothermal, Potential-Based Unified Viscoplastic Model for Titanium-Based Matrices | 67 |
| Thermal and Structural Analysis Conducted on Hollow-Core Turbine Blade of the Space Shuttle Main Engine | 68 |
| Thermomechanical Multiaxial Fatigue Testing Capability Developed | 69 |

| | |
|---|-----|
| Fatigue Behavior and Deformation Mechanisms in Inconel 718 Superalloy Investigated | 70 |
| High-Temperature Extensometry and PdCr Temperature-Compensated Wire Resistance Strain Gages Compared | 72 |
| Temperature-Dependent Effects on the Mechanical Behavior and Deformation Substructure of Haynes 188 Under Low-Cycle Fatigue | 74 |
| New Method Developed for Aeroelastic Stability Analysis | 75 |
| High-Temperature Magnetic Bearings for Gas Turbine Engines | 76 |
| Lewis-Developed Seals Serve General Electric Technology Needs | 77 |
| Lewis' Ultrasonic Imaging Technology Helps American Manufacturer of Nondestructive Evaluation Equipment Become More Competitive in the Global Market | 78 |
| Integrated Design Software Predicts the Creep Life of Monolithic Ceramic Components | 78 |
| Methodology Developed for Modeling the Fatigue Crack Growth Behavior of Single- Crystal, Nickel-Base Superalloys | 80 |
| Space Propulsion Technology | 81 |
| Three Phases of Low-Cost Rocket Engine Demonstration Program Completed | 81 |
| High-Aspect-Ratio Cooling Channel Concept Tested in Lewis' Rocket Engine Test Facility..... | 83 |
| Fluid Film Bearing Code Development | 84 |
| Cooperative Testing of Rocket Injectors That Use Gaseous Oxygen and Hydrogen | 85 |
| Lessons Learned With Metallized Gelled Propellants | 86 |
| 1025:1 Area Ratio Nozzle Evaluated at High Combustion Chamber Pressures | 87 |
| Diagnostics Adapted for Heat-Treating Furnace Environment | 88 |
| Rhenium Rocket Manufacturing Technology | 89 |
| NSTAR Ion Propulsion System Power Electronics | 90 |
| Pulsed Plasma Thruster Technology | 91 |
| Thermodynamic Vent System Applied as Propellant Delivery System for Air Force | 92 |
| Power Technology | 94 |
| SCARLET Solar Array Delivered for METEOR Mission | 94 |
| Valuable Data Provided by PASP Plus Flight Experiment After 1 Year in Orbit | 95 |
| Separator Materials Used in Secondary Alkaline Batteries Characterized and Evaluated | 96 |
| Regenerative Fuel Cell System Testbed Program for Government and Commercial Applications | 97 |
| Power-by-Wire Development and Demonstration for Subsonic Civil Transport | 98 |
| Advanced Power Regulator Developed for Spacecraft | 99 |
| SAMPIE Measurements of the Space Station Plasma Current Analyzed | 100 |
| Molecular Dynamics Calculations | 101 |
| Mars Pathfinder: The Wheel Abrasion Experiment | 102 |
| EWB: The Environment WorkBench Version 4.0 | 103 |
| Protective, Abrasion-Resistant Coatings With Tailorable Properties | 105 |
| Technique to Predict Ultraviolet Radiation Embrittlement of Polymers in Space | 106 |
| Transparent, Conductive Coatings Developed for Arc-Proof Solar Arrays | 107 |
| Radiation Protection of New Lightweight Electromagnetic Interference Shielding Materials Determined | 107 |
| Silicone Contamination Camera Developed for Shuttle Payloads | 108 |
| Iron-Containing Carbon Materials Fabricated | 109 |
| Passive Optical Sample Assembly (POSA-2) Space Flight Experiment | 110 |
| Aperture Shield Materials Characterized and Selected for Solar Dynamic Space Power System | 111 |
| Atomic-Oxygen-Durable Microsheet Glass Reflector | 112 |
| Environmental Influence of Gravity and Pressure on Arc Tracking of Insulated Wires Investigated | 112 |
| Experimental Results From the Thermal Energy Storage-1 (TES-1) Flight Experiment | 113 |
| 2-kW Solar Dynamic Space Power System Tested in Lewis' Thermal Vacuum Facility | 114 |

| | |
|---|-----|
| Space Electronics | 116 |
| Digital Audio Radio Broadcast Systems Laboratory Testing Nearly Complete | 116 |
| Role of Communications Satellites in the National and Global Information Infrastructure | 117 |
| Lewis Helps Examine Feasibility of Fixed Satellite Service and Local Multipoint Distribution Service Sharing the Same Frequency Band | 119 |
| Potential Market for Satellite Technology in Meeting Telecommunication Needs of Developing Nations | 120 |
| Highly Efficient Amplifier for Ka-Band Communications | 121 |
| Chemical Vapor-Deposited (CVD) Diamond Films for Electronic Applications | 122 |
| Monolithic Microwave Integrated Circuit (MMIC) Phased Array Demonstrated With ACTS | 122 |
| B-ISBN Onboard Processing Fast Packet Switch Developed | 123 |
| Low-Complexity, Digital Encoder/Modulator Developed for High-Data-Rate Satellite B-ISDN Applications | 124 |
| Multichannel Error Correction Code Decoder | 125 |
| INTEX Ka-Band Experiment Ground Terminal | 127 |
| Telemammography Using Satellite Communications | 127 |

Space Flight Systems

| | |
|---|-----|
| ACTS Project | 129 |
| Compilation and Analysis of 20- and 30-GHz Rain Fade Events at the ACTS NASA Ground Station: Statistics and Model Assessment | 129 |
| Using the ACTS Rain Attenuation Prediction Model to Identify and Specify Communications System Performance Parameters | 129 |
| Implications of ACTS Technology on the Requirements of Rain Attenuation Modeling for Communication System Specification and Analysis at the Ka-Band and Beyond | 130 |
| ACTS Aeronautical Terminal Experiment (AERO-X) | 130 |
| Advanced Communication Technology Satellite (ACTS) Multibeam Antenna On-Orbit Performance | 132 |
| Space Experiments | 133 |
| Radiative Ignition and the Transition to Flame Spread Investigated in the Japan Microgravity Center's 10-sec Drop Shaft | 133 |
| Soot Imaging and Measurement | 134 |
| Microgravity Turbulent Gas-Jet Diffusion Flames | 136 |
| Spread Across Liquids: The World's First Microgravity Combustion Experiment on a Sounding Rocket | 137 |
| Two U.S. Experiments to Fly Aboard European Spacelab Facility in 1996 | 139 |
| Interface Configuration Experiments (ICE) Explore the Effects of Microgravity on Fluids | 140 |
| Combustion Module 1: Spacelab Racks Integrated at the Lewis Research Center for the First Time | 141 |
| Pool Boiling Experiment Has Successful Flights | 142 |
| Successful Isothermal Dendritic Growth Experiment (IDGE) Proves Current Theories of Dendritic Solidification are Flawed | 143 |
| Microgravity Smoldering Combustion Takes Flight | 144 |
| Solid Surface Combustion Experiment Completes a Series of Eight Successful Flights | 145 |
| New Low-Gravity Research Aircraft Takes to the Skies | 146 |
| Real-Time Data From the Orbital Acceleration Research Experiment (OARE) | 148 |
| Microgravity Environment Measured During Shuttle-Mir Science Program | 149 |

| | |
|---|-----|
| Advanced Space Analysis | 150 |
| Lewis Mars Pathfinder Microrover Experiments | 150 |
| TEMPEST: Twin Electric Magnetospheric Probes Exploring on Spiral Trajectories— A Proposal to the Medium Class Explorer Program | 151 |

Engineering Support

| | |
|---|-----|
| Structural Systems | 153 |
| Improved Acoustic Blanket Developed and Tested | 153 |
| MSC/NASTRAN DMAP Alter Used for Closed-Form Static Analysis With Inertia Relief and Displacement-Dependent Loads | 154 |

Lewis Research Academy

| | |
|--|-----|
| Turbomachinery Flows Modeled | 155 |
| Mixing and Transition Control Studied | 155 |
| Transient Analysis Used to Study Thermal Radiation Effects in Single and Composite Semitransparent Layers | 156 |
| New Theoretical Technique Developed for Predicting the Stability of Alloys | 157 |

Technology Transfer

| | |
|---|-----|
| CARES/LIFE Software Commercialization | 158 |
| Combustion Technology Outreach | 158 |
| Technology Transferred to the Kirby Company | 159 |
| Flow Visualization Proposed for Vacuum Cleaner Nozzle Designs | 160 |
| CommTech: The Commercial Technology Consultants Program | 160 |

Appendixes

| | |
|---|-----|
| NASA Headquarters Program Offices | 161 |
| Index of Authors and Contacts | 162 |

1995 R&T Aeronautics

Advanced Subsonic Technology

Advanced Subsonic Combustion Rig Developed

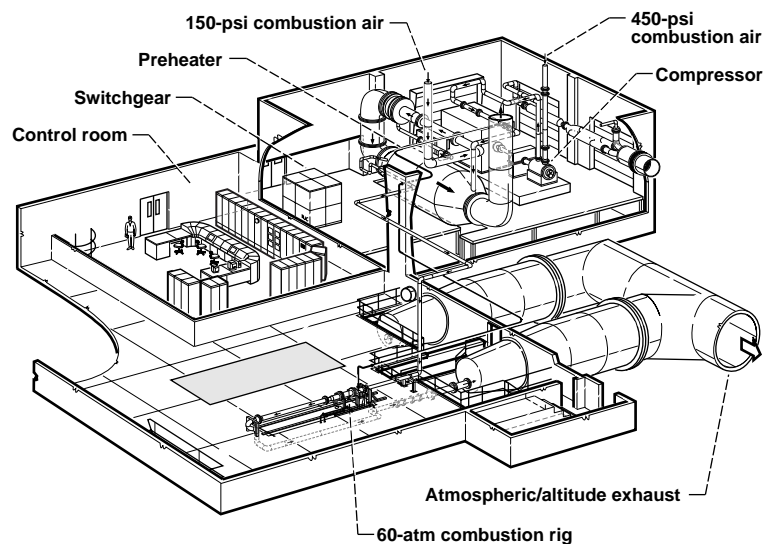
The Advanced Subsonic Combustion Rig (ASCR), a unique, state-of-the-art facility for conducting combustion research, is located at the NASA Lewis Research Center in Cleveland, Ohio. The ASCR, which was nearing completion at the close of 1995, will be capable of simulating the very high pressure and high temperature conditions that are expected to exist in future, advanced subsonic gas turbine (jet) engines. Future environmental regulations will require much cleaner burning (more environmentally friendly) aircraft engines. The ASCR is critical to the development of these cleaner engines. It will allow NASA and U.S. aircraft engine industry researchers to identify and test promising clean-burning gas turbine engine combustion concepts under the pressure and temperature conditions that are expected for those future engines. Combustion processes will be investigated for a variety of next-generation aircraft engine sizes, including engines for large, long-range aircraft (with typical trip lengths of about 3000 mi) and for regional aircraft (with typical trip lengths of about 400 mi).

The ASCR design was conceived and initiated in 1993, and fabrication and construction of the rig, including the buildup of an advanced control room, took place throughout 1994 and 1995. In early 1996, the ASCR will be operational for obtaining research data.

The ASCR is an intricate part of the NASA Advanced Subsonic Technology Propulsion Program, which is aimed at developing technologies critical to the next generation of gas turbine engines. This effort is in collaboration with the U.S. aircraft gas turbine engine industry. A goal of the Advanced Subsonic Technology Propulsion Program is to develop combustion concepts and technologies that will result in gas turbine engines that produce 50 percent less nitrous oxide (NO_x) pollutants than current engines do.

This facility is unique in its capability to simulate advanced subsonic engine pressure, temperature, and air flow rate conditions. Specifically, it will provide operating temperatures up to 3000 °F and pressures up to 60 atm. Under these conditions, researchers will obtain detailed combustion temperatures, pressures, and flow velocities as well as the chemical compositions of the combustion exhaust. Researchers also will be able to obtain data by using nonintrusive laser diagnostic techniques. The ASCR facility will be used to test fundamental combustion configurations (flametubes) for detailed study of combustion processes, to test sectors of gas turbine combustors to study the process in configurations more like those of aircraft engines, and in some cases to test full annular combustors.

Lewis contact: Barbara E. Wiedenmannott, (216) 433-8707
Headquarters program office: OA



Advanced Subsonic Combustion Rig.

Aeropropulsion Analysis

Performance of Gas Turbine Engines Using Wave Rotors Modeled

A wave rotor is a device that can boost the pressure and temperature of an airflow. When used as part of the core of a gas turbine engine, a wave rotor can significantly improve the thrust or shaft horsepower by boosting the flow pressure without raising the turbine inlet temperature.

The NASA Lewis Research Center's Aeropropulsion Analysis Office, which is identifying technologies and research opportunities that will enhance the technical and economic competitiveness of the U.S. aeronautics industry, is evaluating the wave rotor to quantify the potential benefits of this device. Preliminary studies such as these are critical to identifying technologies that have high payoffs.

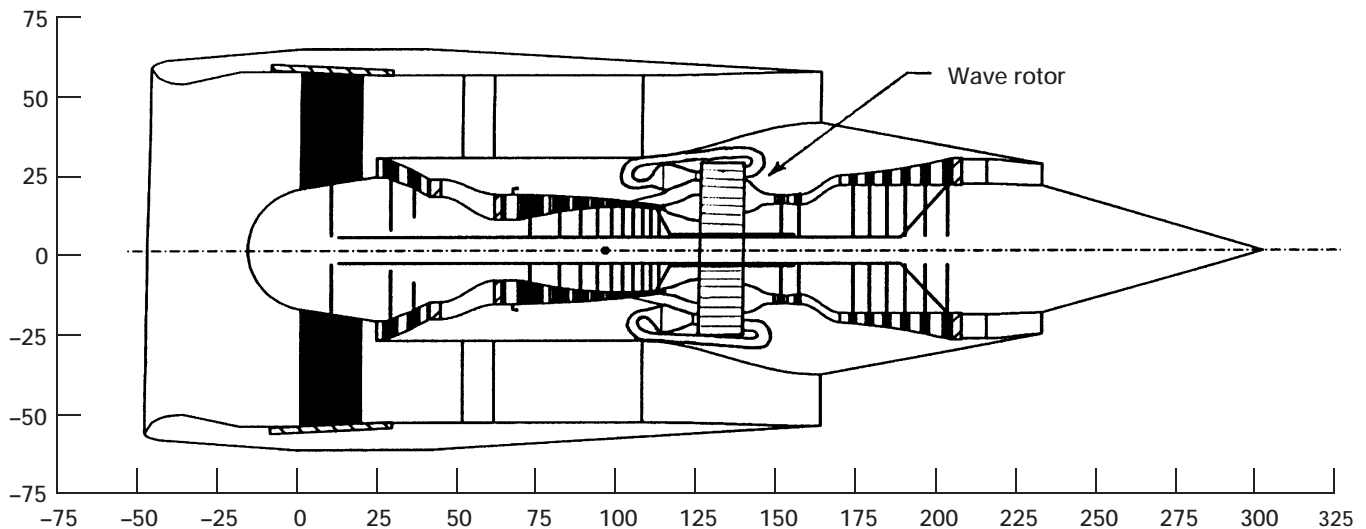
Ongoing cycle, weight, and mission studies will determine the benefits of incorporating a wave rotor into a gas turbine engine core. The engine types being modeled include a high-bypass turbofan and several turboshaft engines. The performance of the wave rotor component is being modeled by Lewis' Turbomachinery Technology Branch.

Major accomplishments in these studies include the one-dimensional, steady-state modeling of a turbofan and turboshaft engine that incorporate a wave rotor component in place of a conventional combustor. In these studies the wave rotor acts as a burner with a

pressure rise. The pressure rise across the wave rotor is 13 to 20 percent depending on the temperature ratio across the wave rotor and the amount of cooling flow required from the wave rotor. Off-design operating characteristics for the wave rotor were used in calculating engine off-design performance. It was shown that the off-design steady-state behavior of the wave rotor is compatible with these engine types. There are challenges to be overcome, however. The wave rotor adds weight and complexity to an engine, and parts of the wave rotor must withstand extreme temperatures and pressures. Ongoing technology development programs will help further define and solve these limitations.

Results from these studies show that the wave rotor can increase the specific thrust of a high-bypass turbofan by 3 percent. Although this seems minor, when included on a subsonic transport (similar to the Boeing 777), this 3-percent gain in specific thrust reduced aircraft takeoff gross weight by 7 percent. The benefit of the wave rotor in turboshaft engines is even more dramatic: it increased specific power at design and partial power conditions by 15 to 20 percent. Other potential applications for the wave rotor, such as auxiliary power units and ground power units, are also being investigated.

Lewis contact: Scott M. Jones, (216) 977-7015
Headquarters program office: OA



Schematic of high-bypass turbofan with wave rotor component.

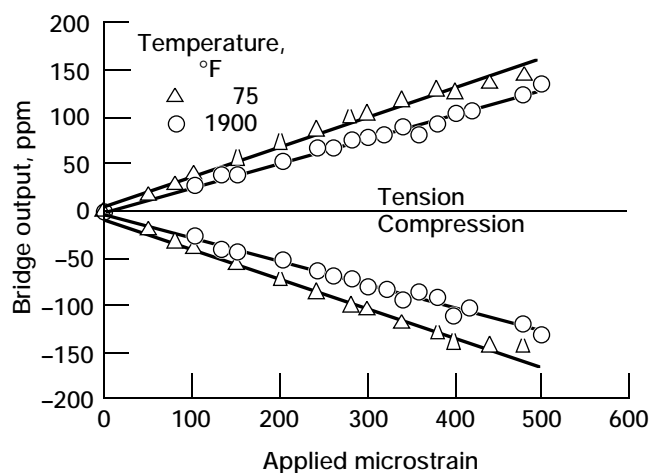
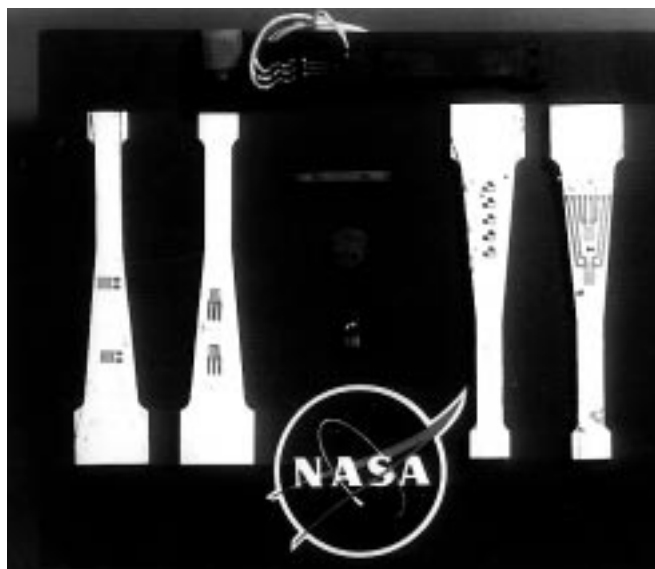
Instrumentation and Control Technology

High-Temperature, Thin-Film Strain Gages Improved

Conventional resistance strain gage technology uses “bonded” strain gages. These foil or wire gages are bonded onto the surface of the test article with glue, ceramic cements, or flame-sprayed ceramics. These bonding agents can, in some instances, limit both the degree of strain transmission from the test structure to the gage and the maximum working temperature of the gage. Also, the bulky, bonded gage normally disrupts aerodynamic gas flow on the surface of the test structure because of its intrusive character.

To respond to the urgent needs in aeronautic and aerospace research where stress and temperature gradients are high, aerodynamic effects need to be minimized, and higher operational temperatures are required, the NASA Lewis Research Center developed a thin-film strain gage. This gage, a vacuum-deposited thin film formed directly on the surface of a test structure, operates at much higher temperatures than commercially available gages do and with minimal disruption of the aerodynamic flow.

The gage uses an alloy, palladium-13 wt % chromium (hereafter, PdCr), which was developed by United Technologies Research Center under a NASA contract. PdCr is structurally stable and oxidation resistant up to at least 1100 °C (2000 °F); its temperature-induced resistance change is linear, repeatable, and not sensitive to the rates of heating and cooling. An early strain gage, which was made of 25- μm -diameter PdCr wire and demonstrated to be useable to 800 °C, won an R&D 100 award in 1991. By further improving the purity of the material and by developing gage fabrication techniques that use sputter-deposition, photolithography patterning, and chemical etching, we have made an 8- to 10- μm PdCr thin-film strain gage that can measure dynamic and static strain to at least 1100 °C. For static strain measurements, a 5- μm -thick Pt element serves as a temperature compensator to further minimize the temperature effect of the gage. These thin-film gages provide the advantage of minimally intrusive surface strain measurements and give highly repeatable readings with low drift at temperatures from ambient to 1100 °C. This is a 300 °C advance in operating temperature over the PdCr wire gage and a 500 °C advance over commercially available gages made of other materials.



Top: PdCr thin-film strain gages for static or dynamic strain measurements. Bottom: Mechanical response of a PdCr thin-film strain gage.

Bibliography

Lei, J.-F.: High Temperature Thin Film Strain Gages. HITEMP Review 1994, NASA CP-10146, Vol. I, 1994, pp. 25-1 to 25-13. (Available to U.S. citizens only. Permission to use this material was granted by Hugh R. Gray, January 1996.)

Lewis contact: Dr. Jih-Fen Lei, (216) 433-3922
Headquarters program office: OA

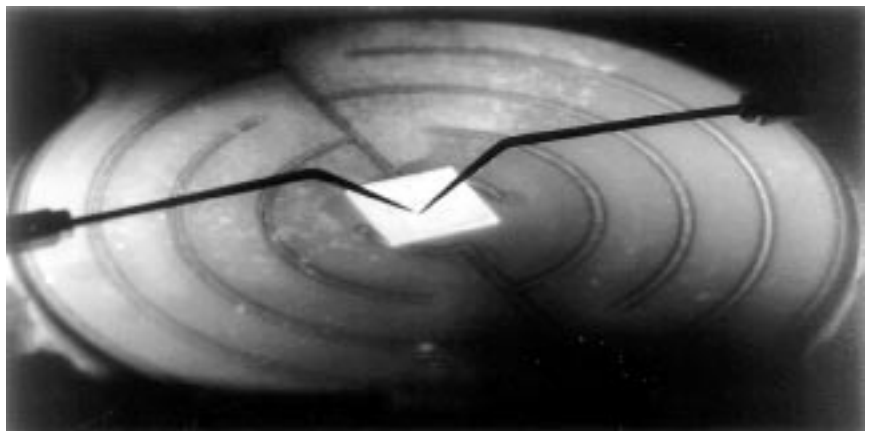
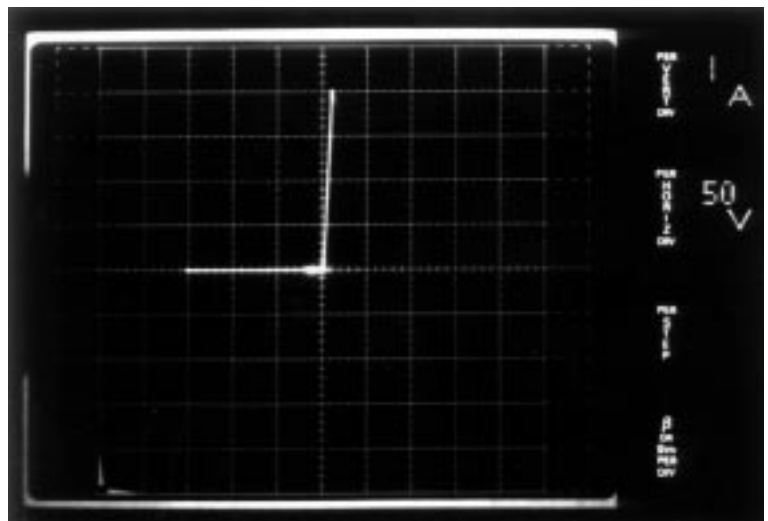
Silicon Carbide High-Temperature Power Rectifiers Fabricated and Characterized

The High Temperature Integrated Electronics and Sensors (HTIES) team at the NASA Lewis Research Center is developing silicon carbide (SiC) for use in harsh conditions where silicon, the semiconductor used in nearly all of today's electronics, cannot function. Silicon carbide's demonstrated ability to function under extreme high-temperature, high-power, and/or high-radiation conditions will enable significant improvements to a far-ranging variety of applications and systems. These improvements range from improved high-voltage switching for energy savings in public electric power distribution and electric vehicles, to more powerful microwave electronics for radar and cellular communications, to sensors and controls for cleaner-burning, more fuel-efficient jet aircraft and automobile engines. In the case of jet engines, uncooled operation of 300 to 600 °C SiC power actuator electronics mounted in key high-temperature areas would greatly enhance system performance and reliability. Because silicon cannot function at these elevated temperatures, the semiconductor device circuit components must be made of SiC.

Lewis' HTIES group recently fabricated and characterized high-temperature SiC rectifier diodes whose record-breaking characteristics represent significant progress toward the realization of advanced high-temperature actuator control circuits. The first figure illustrates the 600 °C probe-testing of a Lewis SiC pn-junction rectifier diode sitting on top of a glowing red-hot heating element. The second figure shows the current-versus-voltage rectifying characteristics recorded at 600 °C. At this high temperature, the diodes were able to "turn-on" to conduct 4 A of current when forward biased, and yet block the flow of current ("turn-off") when reverse biases as high as 150 V were applied. This device represents a new record for semiconductor device operation, in that no previous semiconductor electronic device has ever simultaneously demonstrated 600 °C functionality, and 4-A turn-on and 150-V rectification. The high operating current was achieved

despite severe device size limitations imposed by present-day SiC wafer defect densities. Further substantial increases in device performance can be expected when SiC wafer defect densities decrease as SiC wafer production technology matures.

Lewis contacts: Dr. Philip G. Neudeck, (216) 433-8902; Dr. David J. Larkin, (216) 433-8718; and J. Anthony Powell, (216) 433-3652
Headquarter program office: OA



Top: Current versus voltage-rectifying characteristics of a 4-A, 150-V SiC diode measured at 600 °C. Bottom: SiC rectifier diode being probe-tested at 600 °C. The circular heating element and the square, 5- by 5-mm SiC chip are both glowing red hot.

Automated Hydrogen Gas Leak Detection System

The GenCorp Aerojet Automated Hydrogen Gas Leak Detection System was developed through the cooperation of industry, academia, and the Government. Although the original purpose of the system was to detect leaks in the main engine of the space shuttle while on the launch pad, it also has significant commercial potential in applications for which there are no existing commercial systems. With high sensitivity, the system can detect hydrogen leaks at low concentrations in inert environments. The sensors are integrated with hardware and software to form a complete system. Several of these systems have already been purchased for use on the Ford Motor Company assembly line for natural gas vehicles.

This system to detect trace hydrogen gas leaks from pressurized systems consists of a microprocessor-based control unit that operates a network of sensors. The sensors can be deployed around pipes, connectors, flanges, and tanks of pressurized systems where leaks may occur. The control unit monitors the sensors and provides the operator with a visual representation of the magnitude and locations of the leak as a function of time. The system can be customized to fit the user's needs; for example, it can monitor and display the condition of the flanges and fittings associated with the tank of a natural gas vehicle.

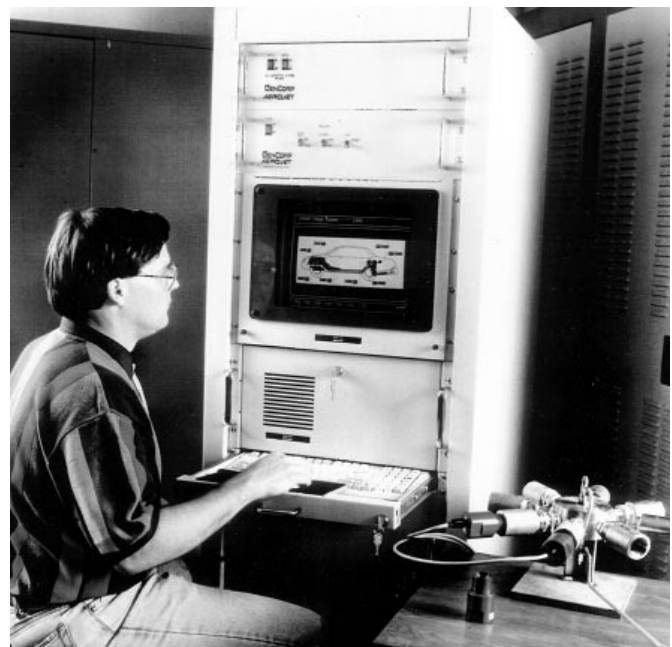
This leak-detection system deploys palladium/silver (PdAg) solid state hydrogen sensors at potential leak sites, such as vehicle fuel-line connections. The hydrogen sensors are the enabling technology and major innovation of the product. They are operated by a microprocessor-based control system that acquires data and uses closed-loop control to maintain the sensors at a constant temperature of approximately 80 °C. The PdAg sensors can detect hydrogen concentrations from 1 to 4000 ppm and do not require an oxygen atmosphere for this detection. Included on the sensor chip are a temperature detector and a heater. These allow temperature control and stable sensor operation in environments with varying temperatures. The PdAg sensors were developed by Case Western Reserve University in cooperation with the NASA Lewis Research Center. The sensor technology has been licensed to GenCorp Aerojet for commercial applications and in-house production.

The microprocessor-based electronics were developed by GenCorp Aerojet for NASA Marshall Space Flight Center for flight applications. Using multiplexing

techniques, these electronics permit operation of up to 128 sensors. Signals are conditioned by hardware located near the sensor, and the resulting signal is fed to a multiplexing unit. Graphical, PC-based software displays the sensor readings and derived values, such as leak rate (e.g., standard cubic centimeters per hour (scm/hr)), as well as a graphical image corresponding to the position and magnitude of the leaks.

A prime application of this system is checking pressurized systems for leaks as a part of safety and quality control. Such leak checking can be done with inert gas mixtures as well as with combustible hydrogen mixtures. Preferably, an inert mixture such as 1% H₂/99% N₂ can be used. The sensors are interfaced to a fuel-line component by a flexible "boot" that surrounds the component to be tested (such as a fitting). When the system is pressurized, a leak causes the detected hydrogen concentration in the boot to increase. The rate of rise of the hydrogen concentration is proportional to the leak rate. The quantitative leak rate is determined by calibration of the sensor boot to account for the free volume of the boot and any leakage of gas out of the boot. The graphical interface displays an image of the boot with the plume of the leak, allowing the operator to pinpoint the leak.

Lewis contact: Gary W. Hunter (216) 433-6459
Headquarters program office: OSAT



Leak-monitoring system with visual display of leak location.

Fuzzy Logic Particle Tracking

A new all-electronic Particle Image Velocimetry technique that can efficiently map high-speed gas flows has been developed in-house at the NASA Lewis Research Center. Particle Image Velocimetry is an optical technique for measuring the instantaneous two-component velocity field across a planar region of a seeded flow field. A pulsed laser light sheet is used to illuminate the seed particles entrained in the flow field at two instances in time. One or more charged coupled device (CCD) cameras can be used to record the instantaneous positions of particles. Using the time between light sheet pulses and determining either the individual particle displacements or the average displacement of particles over a small subregion of the recorded image enables the calculation of the fluid velocity. Fuzzy logic minimizes the required operator intervention in identifying particles and computing velocity.

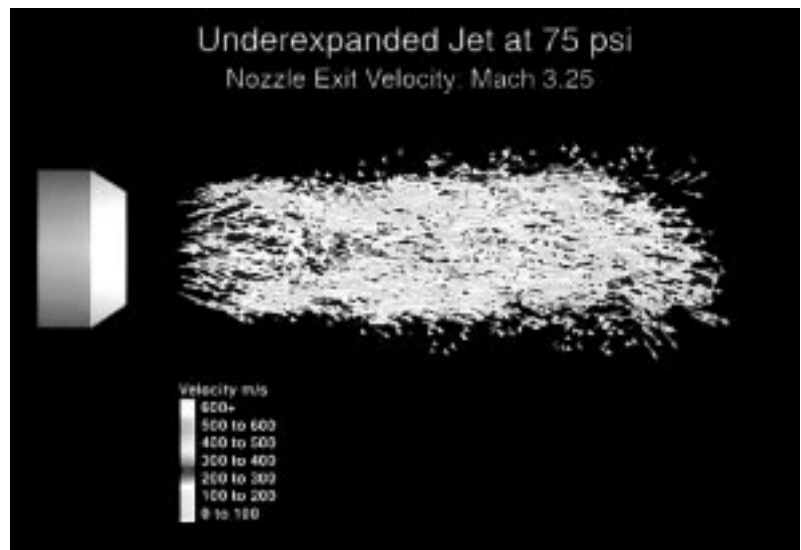
Using two cameras that have the same view of the illumination plane yields two single-exposure image frames. Two competing techniques that yield unambiguous velocity vector direction information have been widely used for reducing the single-exposure, multiple-image frame data: (1) cross-correlation and (2) particle tracking. Correlation techniques yield averaged velocity estimates over subregions of the flow, whereas particle tracking techniques give individual particle velocity estimates.

For the correlation technique, the correlation peak corresponding to the average displacement of particles across the subregion must be identified. Noise on the images and particle dropout result in misidentification of the true correlation peak. The subsequent velocity vector maps contain spurious vectors where the displacement peaks have been improperly identified. Typically these spurious vectors are replaced by a weighted average of the neighboring vectors, thereby decreasing the independence of the measurements.

In this work, fuzzy logic techniques are used to determine the true correlation displacement peak even when it is not the maximum peak, hence maximizing the information recovery from the correlation operation, maintaining the number of independent measurements, and minimizing the number of spurious velocity vectors. Correlation peaks are correctly identified in both high and low seed density cases. The correlation velocity vector

map can then be used as a guide for the particle-tracking operation. Again fuzzy logic techniques are used, this time to identify the correct particle image pairings between exposures to determine particle displacements, and thus the velocity (see figure). Combining these two techniques makes use of the higher spatial resolution available from the particle tracking. Particle tracking alone may not be possible in the high seed density images typically required for achieving good results from the correlation technique. This two-staged velocimetric technique can measure particle velocities with high spatial resolution over a broad range of seeding densities.

The data shown in the figure are from a two-camera setup where each camera records a single exposure of the particle-seeded flow illuminated by a neodymium:yttrium aluminum garnet (Nd:YAG) laser light sheet pulse. The time between exposures was 500 nsec. A convergent nozzle was operated at a plenum pressure of 75 psi, generating an underexpanded jet flow with an exit velocity of Mach 3.25. The effects of the Mach disk can be seen in the flow, approximately 1.5 nozzle diameters downstream of the nozzle exit plane. Approximately 3000 velocity vectors have been identified in the flow. The velocity vector density was so high that a pseudovelocity-contour plot was created by color coding the vector magnitudes. The color figure is included in the World Wide Web version of this report (<http://www.lerc.nasa.gov/WWW/RT1995/2000/2520w.htm>).



Particle-tracking velocity vector map of an underexpanded nozzle flow. Pressure, 75 psi; nozzle exit velocity, Mach 3.25

Bibliography

Wernet, M.P.: Fuzzy Logic Particle-Tracking Velocimetry. Proceedings of the SPIE Conference on Optical Diagnostics in Fluid and Thermal Flow, SPIE, Bellingham, WA, 1993, pp. 701-708.

Wernet, M.P.: Fuzzy Inference Enhanced Information Recovery From Digital PIV Using Cross-Correlation Combined With Particle Tracking. Optical Techniques in Fluid, Thermal, and Combustion. S.S. Cha and J.D. Trolinger, eds., SPIE, vol. 2546, 1995, pp. 54-64.

Find out more about Particle Image Velocimetry on the World Wide Web:

<http://www.lerc.nasa.gov/WWW/OptInstr/piv.html>

Lewis contact: Dr. Mark P. Wernet, (216) 433-3752
Headquarters program office: OA

Fiber Optic Repair and Maintainability (FORM) Program Progresses

Advanced aircraft will employ fiber-optic interconnection components to transmit information from airframe and propulsion sensors to the flight control computers. Although these optical interconnects have been rigorously tested under laboratory conditions to determine their operating and environmental limits, there is concern as to their repairability and maintainability when placed in actual service.

The Fiber Optic Repair and Maintainability (FORM) flight test program will provide data to enable designers to improve these fiber-optic interconnection systems for the next generation of aircraft. FORM is identifying critical problems in installing, maintaining, testing, and repairing fiber-optic interconnection systems in an operational avionics environment. This program is a cooperative Government/industry effort to evaluate optical component acceptability and installation techniques for aircraft.

FORM, which began in 1994, has three phases spanning a 3-year period where approximately 250 flight test hours will be accumulated on experimental fiber-optic components. In Phase I, a total of 60 flight hours were accumulated on fiber-optic harnesses and connectors installed onboard the OV-10 aircraft at the NASA Lewis Research Center. This phase was funded by Lewis and Navy Crane, where several participants from the aerospace industry (Sikorsky Aircraft, Amphenol, and Deutsch) supplied the test hardware.

An additional 90 flight hours were accumulated in Phase II, which was funded by the Fly-by-Light/Power-by-Wire program at Lewis. As part of this effort, additional fiber-optic harnesses, provided by Sikorsky Aircraft and Lockheed Corporation, and optical splices, provided by Aurora Optics, were installed on the aircraft. To date, FORM has flown over 150 hours.

To route the fiber-optic harnesses through the aircraft, we mounted 3/4-in. convoluted conduit through the OV-10 cargo bay, fuselage, wing, boom, and horizontal stabilizer. We compared split and nonsplit conduit installation by running separate segments side-by-side along the cargo bay and fuselage areas. Another run of nonsplit conduit extends through the booms to the horizontal stabilizer and back to the cargo bay. In all installations, the conduit was partially filled with electrical wire to reproduce actual aircraft conditions.

Once the conduit was completely installed and secured, two methods of fiber-optic harness installation were tested. The first method pulls the harnesses through the conduit with a jet line/pull wire that extends the entire length inside the conduit. One end is attached to the fiber-optic harness and then pulled from the other. The second method slips the optical cables into the split conduit. Although split conduit provides easy access to the harnesses, it requires more time to feed fibers through than the nonsplit conduit does. The nonsplit conduit provides more protection to the fibers, as well as ease of installation and removal.

The harnesses were flown unmated for portions of the tests to expose the fiber-optic connectors to contaminants present in normal aircraft environment. Transmissive loss measurements were taken before and after cleaning the connectors during this procedure.

Phase III of FORM will test optical data bus transmission and the electro-optical transmission and reception units. It will demonstrate actual data bus transmission through a 1773 optical data bus segment on the OV-10. The current 1553 data bus on the aircraft will be modified to include the 1773 segment in its data path. All the installation and test information collected in this program will be actively transferred to the private vendors for implementation in their ongoing programs, such as Sikorsky's Comanche program, Lockheed's Red Eye, and the F-22 programs.

The NASA OV-10 aircraft used for this test is a twin-engine, two-crew-member, tandem seating turboprop aircraft. It has a top airspeed of 350 kn, a maximum



NASA OV-10 research aircraft.

altitude of 30,000 ft, and acceleration limits from -1.0 to 4.5g.

The OV-10 flight test profiles for this program follow:

- Profile I: Low-altitude navigation (below 5000 ft) at maximum continuous power with numerous accelerated turns and with 3.0 to 4.5g maneuvers in turbulent atmospheric conditions
- Profile II: High-altitude navigation (above 21,000 ft)
- Profile III: Multiple takeoffs, approaches, and landings

Lewis contact: Jorge L. Sotomayor, 433-8303
Headquarters program office: OA

Transient Wave Rotor Performance Investigated

The NASA Lewis Research Center is investigating the wave rotor for use as a core gas generator in future gas turbine engines. The device, which uses gas-dynamic waves to transfer energy directly to and from the working fluid through which the waves travel, consists of a series of constant-area passages that rotate about an axis. Through rotation, the ends of the passages are periodically exposed to various circumferentially arranged ports that initiate the traveling waves within the passages. Because each passage of the wave rotor is periodically exposed to both hot and cold flow, the mean temperature of the rotor material can be expected to remain considerably below the peak cycle temperature. Estimates made using numerical simulations indicate that, for a small engine (5 lbm/sec), the mean passage wall temperature is approximately 360 °C below the combustor discharge temperature.

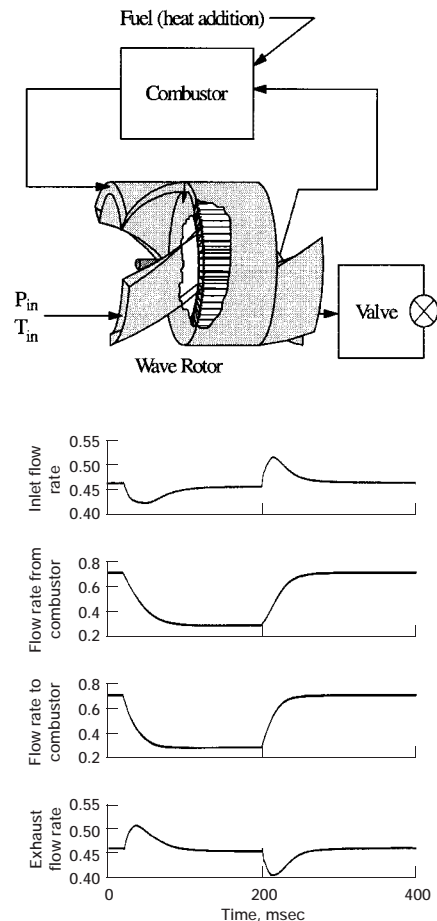
A one-dimensional simulation developed at Lewis was used to generate steady-state performance maps for an optimally designed wave rotor. These maps were used in cycle deck studies to assess steady on-design and

off-design performance in an engine environment (i.e., with surrounding turbomachinery). The results indicate favorable performance throughout the normal operating regime.

A multipassage wave rotor simulation is being used to investigate transient wave rotor behavior. Preliminary results indicate that the wave rotor is stable and well behaved even when subjected to severe transient input. Furthermore, the wave rotor response time is very short when compared with conventional turbomachinery.

Lewis is also investigating the concept of removing the external combustor and allowing the combustion process to occur in the rotor passages (i.e., at constant volume). To study this, we modified the one-dimensional simulation to include simple combustion kinetics. Results indicate that the concept is feasible.

Lewis contact: Daniel E. Paxson, (216) 433-8334
Headquarters program office: OA



Top: Schematic of transient wave rotor simulation. Bottom: Wave rotor response to a 50-percent step change in fuel flow rate; nondimensional port mass flow rate.

Concept Designed and Developed for Distortion-Tolerant, High-Stability Engine Control

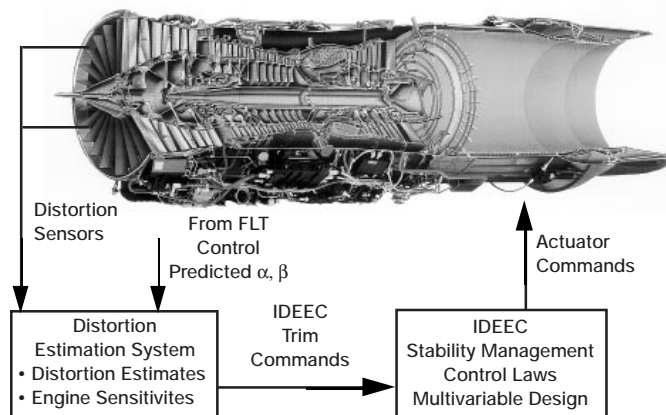
Future aircraft turbine engines, both commercial and military, must be able to successfully accommodate expected increased levels of steady-state and dynamic engine-face distortion. Advanced tactical aircraft are likely to use thrust vectoring to enhance their maneuverability. As a result, the engines will see more extreme aircraft angles-of-attack and sideslip levels than are currently encountered with present-day aircraft. Also, the mixed-compression inlets needed for the High Speed Civil Transport will likely encounter disturbances similar to those seen by tactical aircraft, in addition to planar pulse, inlet buzz, and high distortion levels at low flight speed and off-design operation.

The current approach of incorporating a sufficient component design stall margin to tolerate these increased levels of distortion would significantly reduce performance. The objective of the High Stability Engine Control (HISTEC) program is to design, develop, and flight demonstrate an advanced, high-stability, integrated engine-control system that uses measurement-based, real-time estimates of distortion to enhance engine stability. The resulting distortion-tolerant control reduces the required design stall margin, with a corresponding increase in performance and decrease in fuel burn. The HISTEC concept has been designed and developed, and the software implementing the concept has successfully accommodated time-varying distortion. The NASA Lewis Research Center is currently overseeing the development and validation of the hardware and software necessary to flight test the HISTEC concept. HISTEC is a contracted effort with Pratt & Whitney of West Palm Beach, Florida.

The HISTEC approach includes two major systems: A Distortion Estimation System (DES) and Stability Management Control (SMC) (see figure). DES is an aircraft-mounted, high-speed processor that estimates the amount and type of distortion present and its effect on the engine. It uses high-response pressure measurements at the engine face to calculate indicators of the type and extent of distortion in real time. From these indicators, DES determines the effects of distortion on the propulsion systems and the corresponding engine match point necessary to accommodate it. DES output consists of fan and compressor pressure ratio trim commands that are passed to the SMC. In addition, DES uses maneuver information, consisting of angle-of-attack and sideslip from the flight control, to anticipate high inlet distortion conditions. The SMC, which is contained in the engine-mounted, Improved Digital

Electronic Engine Control (IDEEC), includes advanced control laws to directly control the fan and compressor transient operating line (pressure ratio). These advanced control laws, with a multivariable design, have the potential for higher bandwidth and the resulting more precise control of engine match. The ability to measure and assess the distortion effects in real time coupled with a high-response controller improves engine stability at high levels of distortion.

The software algorithms implementing DES have been designed, developed, and demonstrated, and integration testing of the DES and SMC software has been completed. The results show that the HISTEC system will be able to sense inlet distortion, determine the effect on engine stability, and accommodate distortion by maintaining an adequate margin for engine surge. The Pratt & Whitney Comprehensive Engine Diagnostic Unit was chosen as the DES processor. An instrumented inlet case for sensing distortion was designed and fabricated. HISTEC is scheduled for flight test on the ACTIVE F-15 aircraft at the NASA Dryden Flight Research Center in Edwards, California, in late 1996.



Distortion Tolerant Control. (Copyright Pratt & Whitney; used with permission.)

Bibliography

Ouzts, P.J.; Lorenzo, C.F.; and Merrill, W.C.: Screening Studies of Advanced Control Concepts for Airbreathing Engines. NASA TM-106042, 1993.

Southwick, R.D., et al.: High Stability Engine Control (HISTEC) Phase I: Algorithm Development, Volume I: Final Report and Appendix A. NASA CR-198399, 1995. (Permission to use this material was granted by Sanjay Garg, February 1996.)

Lewis contact: John C. DeLaat, (216) 433-3744
Headquarters program office: OA

Internal Fluid Mechanics

Coupled Monte Carlo Probability Density Function/SPRAY/CFD Code Developed for Modeling Gas-Turbine Combustor Flows

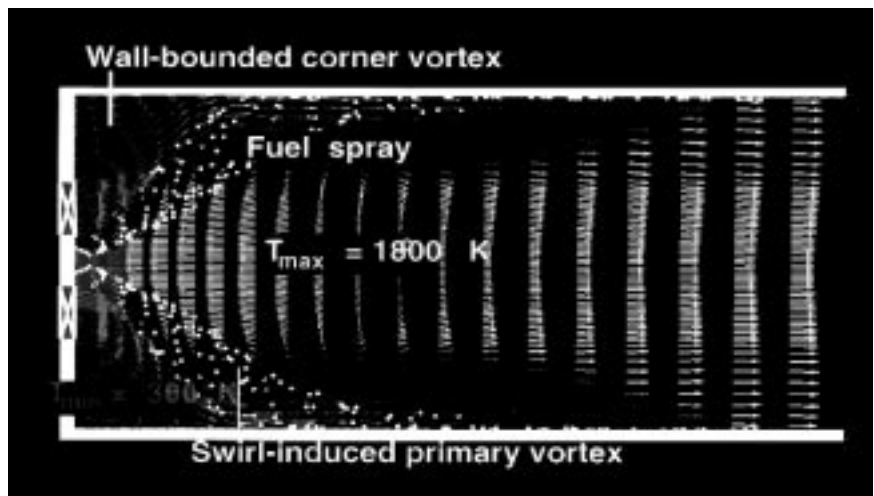
The success of any solution methodology for studying gas-turbine combustor flows depends a great deal on how well it can model various complex, rate-controlling processes associated with turbulent transport, mixing, chemical kinetics, evaporation and spreading rates of the spray, convective and radiative heat transfer, and other phenomena. These phenomena often strongly interact with each other at disparate time and length scales. In particular, turbulence plays an important role in determining the rates of mass and heat transfer, chemical reactions, and evaporation in many practical combustion devices. Turbulence manifests its influence in a diffusion flame in several forms depending on how turbulence interacts with various flame scales. These forms range from the so-called wrinkled, or stretched, flamelets regime, to the distributed combustion regime. Conventional turbulence closure models have difficulty in treating highly nonlinear reaction rates.

A solution procedure based on the joint composition probability density function (PDF) approach holds the promise of modeling various important combustion phenomena relevant to practical combustion devices such as extinction, blowoff limits, and emissions predictions because it can handle the nonlinear chemical reaction rates without any approximation. In this approach, mean and turbulence gas-phase velocity fields are determined from a standard turbulence model; the joint composition field of species and enthalpy are determined from the solution of a modeled PDF transport equation; and a Lagrangian-based dilute spray model is used for the liquid-phase representation with appropriate consideration of the exchanges of mass, momentum, and energy between the two phases. The PDF transport equation is solved by a Monte Carlo method, and existing state-of-the-art numerical representations (refs. 1 and 2) are used to solve the mean gas-phase velocity and turbulence fields together with the liquid-phase equations.

The joint composition PDF approach was extended in our previous work to the study of compressible reacting flows (refs. 3 and 4). The application of this method to several supersonic diffusion flames associated with scramjet combustor flow fields provided favorable comparisons with the available experimental data.

A further extension of this approach to spray flames, three-dimensional computations, and parallel computing was reported in a recent paper (ref. 5). The recently developed PDF/SPRAY/computational fluid dynamics (CFD) module combines the novelty of the joint composition PDF approach with the ability to run on parallel architectures. This algorithm was implemented on the NASA Lewis Research Center's Cray T3D, a massively parallel computer with an aggregate of 64 processor elements. The calculation procedure was applied to predict the flow properties of both open and confined swirl-stabilized spray flames. The figure shows the global flow characteristics of a ducted-axisymmetric spray flame, showing the velocity field, temperature contours, and droplet trajectories.

Preliminary estimates indicate that it is well within today's modern parallel computer's reach to do a realistic gas-turbine combustor simulation within a reasonable turnaround time. This work was conducted



Global flow characteristics of a ducted-axisymmetric swirl-stabilized spray flame.

in collaboration with Dr. M.S. Raju of NYMA, Inc., whose journal article with A.T. Hsu and Y.-L.P. Tsai (ref. 3) received NYMA, Inc.'s, best technical paper of the year award for 1994.

References

1. Raju M.S.: Heat Transfer and Performance Characteristics of a Dual-Ignition Wankel Engine. SAE Paper 920303, SAE Tech. Lit. Abstr., 1992.
2. Shyy, W.; Correa, S.M.; and Braaten, M.E.: Computation of Flow in a Gas Turbine Combustor. Combust. Sci. Tech., vol. 58, 1988, pp. 97-117.
3. Hsu, A.T.; Tsai Y.-L.P.; and Raju M.S.: Probability Density Function Approach for Compressible Turbulent Reacting Flows. AIAA Journal, vol. 32, no. 7, pp. 1407-1415, 1994.
4. Hsu A.T.; Raju M.S.; and Norris A.T.: Application of a pdf Method to Compressible Turbulent Reacting Flows. AIAA Paper 94-0781, 1994.
5. Raju, M.S.: Coupled Monte-Carlo-PDF/SPRAY/CFD Computations of Swirl-Stabilized Flames. AIAA Paper 95-2442, 1995.

Lewis contact: Dr. D.R. Reddy, (216) 433-8133
Headquarters program office: OA

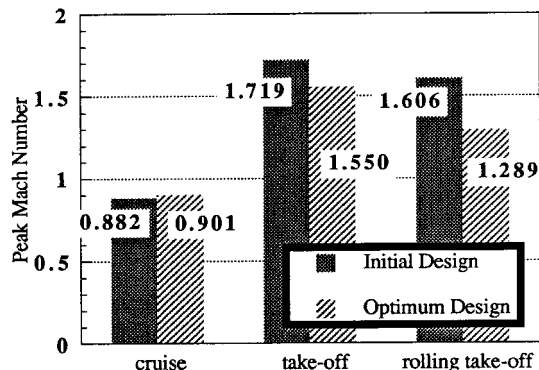
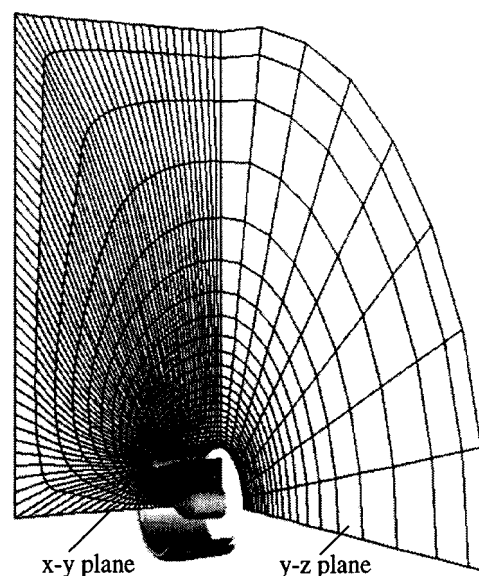
CFD-Based Design Optimization Tool Developed for Subsonic Inlet

The traditional approach to the design of engine inlets for commercial transport aircraft is a tedious process that ends with a less-than-optimum design. With the advent of high-speed computers and the availability of more accurate and reliable computational fluid dynamics (CFD) solvers, numerical optimization processes can effectively be used to design an aerodynamic inlet lip that enhances engine performance. The designers' experience at Boeing Corporation showed that for a peak Mach number on the inlet surface beyond some upper limit, the performance of the engine degrades excessively. Thus, our objective was to optimize efficiency (minimize the peak Mach number) at maximum cruise without compromising performance at other operating conditions.

Using the CFD code NPARC, the NASA Lewis Research Center, in collaboration with Boeing, developed an integrated procedure at Lewis to find the optimum shape of a subsonic inlet lip and a numerical optimization code, ADS. We used a GRAPE-based

three-dimensional grid generator to help automate the optimization procedure.

The inlet lip shape at the crown and the keel was described as a super-ellipse, and the super-ellipse exponents and radii ratios were considered as design variables. Three operating conditions: cruise, takeoff, and rolling takeoff, were considered in this study. Three-dimensional Euler computations were carried out to obtain the flow field. At the initial design, the peak Mach numbers for maximum cruise, takeoff, and rolling takeoff conditions were 0.88, 1.772, and 1.61, respectively. The acceptable upper limits on the takeoff and rolling takeoff Mach numbers were 1.55 and 1.45. Since the initial design provided by Boeing was found to be optimum with respect to the maximum cruise condition, the sum of the peak Mach numbers at takeoff and rolling takeoff were minimized in the current study while the maximum cruise Mach number was constrained to be close to that at the existing design.



Top: Inlet and sample three-dimensional grid in two planes. Alternate grid lines shown along the radial direction. Bottom: Comparison of peak Mach numbers at initial and optimum designs.

With this objective, the optimum design satisfied the upper limits at takeoff and rolling takeoff while retaining the desirable cruise performance. Further studies are being conducted to include static and cross-wind operating conditions in the design optimization procedure. This work was carried out in collaboration with Dr. E.S. Reddy of NYMA, Inc.

Bibliography

Mason, J.G., et al.: Inlet Design Using a Blend of Experimental and Computational Techniques. Proceedings of the 18th ICAS Congress, AIAA, Washington, DC, 1992, pp. 445-454.

Reddy, E.S.; and Reddy, D.R.: Aerodynamic Shape Optimization of a Subsonic Inlet Using 3-D Euler Computation. AIAA Paper 95-2757, 1995.

Sorenson, R.L.: A Computer Program to Generate Two-Dimensional Grids About Airfoils and Other Shapes by the Use of Poisson's Equation. NASA TM-81198, 1980.

Vanderplaats, G.N.: ADS: A Fortran Program for Automated Design Synthesis: Version 1.10. Final Report. NASA CR-177985, 1985.

Lewis contact: Dr. D.R. Reddy, (216) 433-8133
Headquarters program office: OA

User Interface Developed for Controls/CFD Interdisciplinary Research

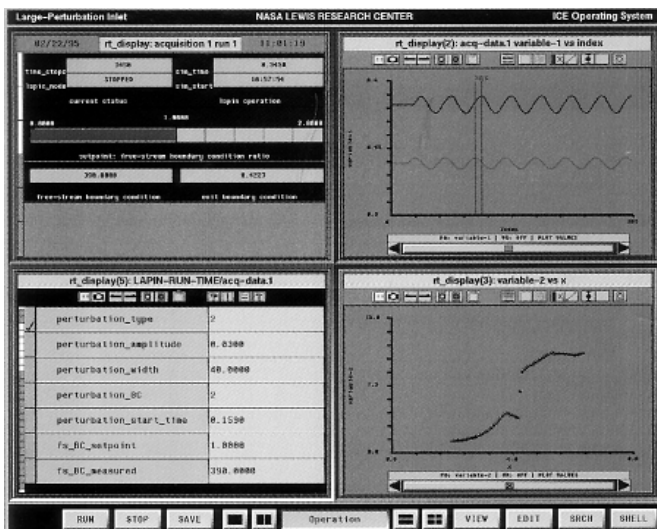
The NASA Lewis Research Center, in conjunction with the University of Akron, is developing analytical methods and software tools to create a cross-discipline "bridge" between controls and computational fluid dynamics (CFD) technologies (ref. 1). Traditionally, the controls analyst has used simulations based on large lumping techniques to generate low-order linear models convenient for designing propulsion system controls. For complex, high-speed vehicles such as the High Speed Civil Transport (HSCT), simulations based on CFD methods are required to capture the relevant flow physics. The use of CFD should also help reduce the development time and costs associated with experimentally tuning the control system. The initial application for this research is the High Speed Civil Transport inlet control problem.

A major aspect of this research is the development of a controls/CFD interface for non-CFD experts, to facilitate the interactive operation of CFD simulations and the extraction of reduced-order, time-accurate models from CFD results. A distributed computing

approach for implementing the interface is being explored. Software being developed as part of the Integrated CFD and Experiments (ICE) project provides the basis for the operating environment, including run-time displays and information (data base) management. Message-passing software is used to communicate between the ICE system and the CFD simulation, which can reside on distributed, parallel computing systems. Initially, the one-dimensional Large-Perturbation Inlet (LAPIN) code is being used to simulate a High Speed Civil Transport type inlet. LAPIN can model real supersonic inlet features, including bleeds, bypasses, and variable geometry, such as translating or variable-ramp-angle centerbodies. Work is in progress to use parallel versions of the multidimensional NPARC code.

The figure shows a snapshot of one display configuration of the Controls/CFD user interface during interactive operation of LAPIN. The CFD code execution mode is controlled by the **RUN** and **STOP** buttons at the lower left of the screen. The **RECORD** button permits the user to start or stop recording flow field information at any time. The **SAVE** button enables users to save the recorded information as a permanent file in the ICE data base. With LAPIN, execution and display updates both occur in near-real time. The upper left quadrant shows the code execution status and slider bars for interactively controlling the inlet and exit boundary conditions (only the slider bar for the free-stream temperature set point is visible in this screen).

In this case, LAPIN is simulating the response of the inlet without control, while operating at a free-stream Mach number of 2.35 and an exit Mach number operating-point value of 0.4223. The inlet is being perturbed by a 40-Hz sinusoid in the exit Mach number with a 3.0-percent zero-to-peak amplitude. The lower left quadrant shows some of the variables that can be changed interactively to affect the LAPIN execution (e.g., variables specifying the inlet perturbation). The upper right quadrant shows time histories of two inlet variables—Mach number at the exit (lower curve) and Mach number at a location downstream of, but near, the normal shock. Phase shift between the two signals can be measured by the two vertical lines, which are manually positioned by clicking on the horizontal axis. (Horizontal lines for determining amplitude response can be positioned by clicking on the vertical axis.) The lower right plot shows the "instantaneous" axial static-pressure distribution in the inlet. The nearly discontinuous jump in pressure indicates the location of the normal shock.



Controls/CFD user interface.

Reference

1. Cole, G.L., et al.: Computational Methods for HSCT-Inlet Controls/CFD Interdisciplinary Research. AIAA Paper 94-3209, 1994.

For more information about Controls/CFD and ICE research, visit our World Wide Web sites:

<http://www.lerc.nasa.gov/WWW/IFMD/2620/homepage.html>

<http://controls.lerc.nasa.gov:8080/projects/cntrlcfd/index.htm>

Lewis contact: Gary L. Cole, (216) 433-3655

Headquarters program office: OA

Wavelet Techniques Applied to Modeling Transitional/Turbulent Flows in Turbomachinery

Computer simulation is an essential part of the design and development of jet engines for the aeropropulsion industry. Engineers concerned with calculating the flow in jet engine components, such as compressors and turbines, need simple engineering models that accurately describe the complex flow of air and gases and that allow them to quickly estimate loads, losses, temperatures, and other design parameters. In this ongoing collaborative project, advanced wavelet analysis techniques are being used to gain insight into the complex flow phenomena. These insights, which cannot be achieved by commonly used methods, are being used to develop innovative new flow models and to improve existing ones.

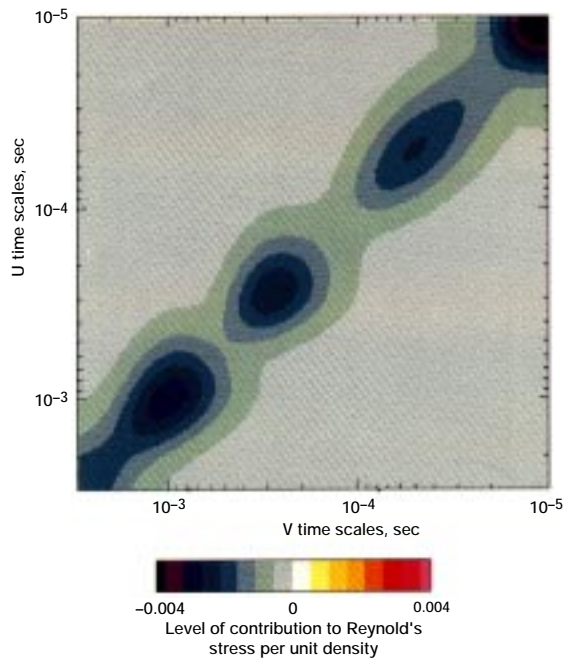
Wavelet techniques are very suitable for analyzing the complex turbulent and transitional flows pervasive in jet engines. These flows are characterized by intermittency and a multitude of scales. Wavelet analysis results in information about these scales and their locations. The distribution of scales is equivalent to the frequency spectrum provided by commonly used Fourier analysis techniques; however, no localization information is provided by Fourier analysis. In addition, wavelet techniques allow conditional sampling analyses of the individual scales, which is not possible by Fourier methods.

The NASA Lewis Research Center developed various wavelet-based algorithms for post-processing the time-trace signals of transitional and turbulent flows (ref. 1). The techniques were demonstrated by analysis of the experimental hot-wire data from the bypass transition experiments conducted at Lewis by Sohn and Reshotko (ref. 2). The figure displays the stress map, a plot exclusively constructed by wavelet processing of two simultaneous signals of the velocity components. It shows the contributions of the various scales to the Reynolds stress at a point in the flow. The structure of this map indicates that dominant scales contribute to the momentum transport—an important conclusion. Conditional sampling showed that the scales that contribute to the transport in the turbulent parts of the signals do not contribute to the energy transport. This information will be used in modeling bypass transition, which is prevalent in turbomachinery flow.

The techniques were developed at Lewis, in collaboration with Dr. Jacques Lewalle of Syracuse University, under a contract funded by the Lewis Director's discretionary fund. The software developed is available for collaborative work with industry and academia. One collaborative project is currently underway with Dr. D. Wisler and D. Halstead of GE Aircraft Engines in Evandale, Ohio. Under this project, data from turbine and compressor experiments performed at the General Electric Company (ref. 3) are being analyzed at Lewis with wavelet techniques as part of Lewis' Low Pressure Turbine Flow Physics Program.

References

1. Lewalle, J.; and Ashpis, D.E.: Demonstration of Wavelet Techniques in the Spectral Analysis of Bypass Transition Data. NASA TP-3555, 1995.
2. Sohn, K-H.; and Reshotko E.: Experimental Study of Boundary Layer Transition With Elevated Freestream Turbulence on a Heated Flat Plate. NASA CR-187068, 1991.



Wavelet-based stress map. U is the streamwise velocity, and V is the normal velocity. (Data are from ref. 2, grid G1, at $x = 0.9$ in. and $y = 0.030$ in.)

3. Halstead, D.E., et al.: Boundary Layer Development in Axial Compressors and Turbines. Parts 1-4, ASME Papers 95-GT-461, 462, 463, and 464, 1995.

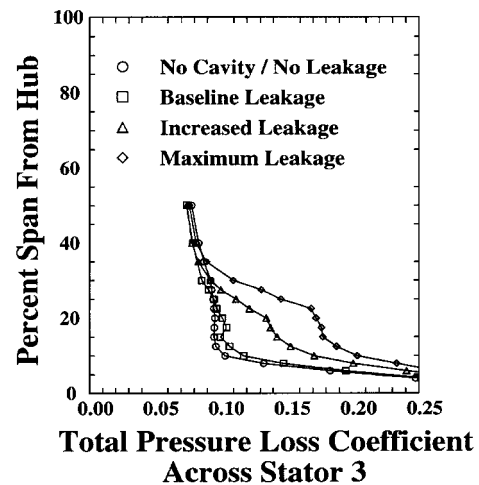
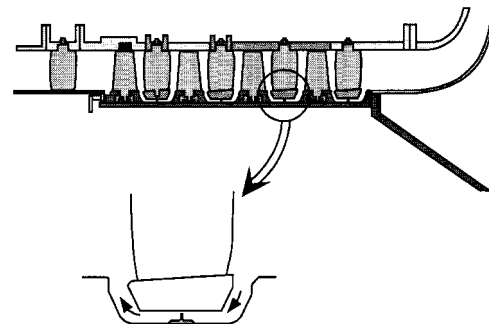
Lewis contact: Dr. David E. Ashpis, (216) 433-8317
Headquarters program office: OA

Effect of Shrouded Stator Leakage Flows on Core Compressor Studied

Efforts to improve core compressor technology have traditionally focused on improving the power stream aerodynamics. During core compressor design and numerical simulation, the effects of leakage flows have been modeled with relatively simple approximations. A combined experimental/numerical research program aimed at studying the effects of the leakage flow under core compressor shrouded stators was therefore undertaken to improve our ability to predict the effects of this leakage flow on power stream aerodynamics. The experimental effort involves detailed measurements in both the seal cavity and power stream in the 4-ft-diameter, four-stage NASA Low-Speed Compressor. The numerical simulation effort involves three-dimensional Navier-Stokes simulations of the Low-Speed Compressor (performed in-house at the NASA Lewis Research Center) and simulations of a representative high-speed core exit stage (performed under contract by Allison Engine Company).

The Low-Speed Compressor features shrouded stator seal cavities with a single labyrinth seal tooth. Measurements of the power stream aerodynamics have been made for a range of seal tooth clearances. In the initial series of tests, the seal tooth clearances were changed in all four stages. In a second series of tests, the seal clearance was changed in only the third stage. Results from both test series indicate that significant changes in the power stream aerodynamics occur with different seal leakage rates. For example, the change in total pressure loss across the third stator is shown in the figure for a range of seal tooth clearances. The measured results indicate that the power stream aerodynamics are influenced across the lower 40 percent of the blade span by the leakage flow. The measured results will be compared with computational fluid dynamics simulations in which the seal cavity is included in the computational domain. The results will also be used to develop a simple leakage flow model for future computational fluid dynamics simulations so that the actual seal cavity will not have to be included in the computational domain.

Lewis contact: Dr. Michael D. Hathaway, (216) 433-6250
Headquarters program office: OA



Investigation of leakage effects on the aerodynamic performance of shrouded compressor stators. Top: Meridional view of NASA's low-speed axial-flow compressor. Bottom: Pressure loss coefficient as function of percent span from hub.

Stable Lobed Mixer With Combustion Demonstrated and Measured

The NASA Lewis Research Center collaborated with the Massachusetts Institute of Technology (MIT) on an experiment to study the use of lobed mixers to improve the fuel-air mixing process and increase combustion intensity in combustors with minimal pressure loss. This experiment is the first known stable combustor flow studied for this device, and the data show a much faster and much more uniform combustion process than for flat-plate mixers. Several potential benefits may be realized from this study in future combustors, including a reduction in NO_x emissions because of the more uniform temperature distribution.

The experiment was done in Lewis' Planar Reacting Shear Layer facility, which was adapted to accept a lobed mixer in addition to the original planar tip. A graduate student at MIT provided the mixer design concept, and Lewis provided the engineering, operations, and research expertise.

The experiment used hydrogen-nitrogen mixtures to react with vitiated hot air at 920 K. A flow speed of about 120 m/sec and a speed ratio of 0.5 were used. Flow diagnostics consisted of traversing fine-wire thermocouples and pitot probes for flow mapping. Supplementary fluorescence images were taken with a charged coupled device (CCD) camera to show the location and temporal behavior of the reaction zone.

The data showed that the lobed mixer consumed the reactants between 3 to 10 times faster than a corresponding planar shear layer. The figure shows the dramatic difference in the measured temperature distribution with and without the lobed mixer. The increased mixing rate was due to a larger interfacial area as well as to the secondary flow from the streamwise vortices off the tips of the lobes. In addition, the fluorescence images showed that the lobes acted as flame stabilizers.

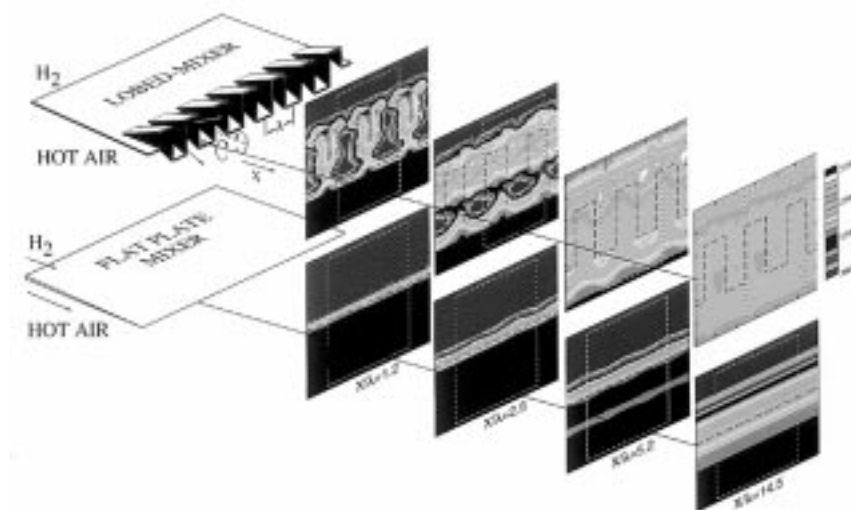
This Lewis-funded program (funded through a cooperative agreement), which resulted in a Masters' thesis, was conducted over 3 years and was finished at the end of June 1995. The series of experiments showed that the reacting shear layer is a potential combustion device for high-speed combustors where low pressure loss is required. It would be applicable to ramjets, afterburners, or combustors of complex cycles.

Bibliography

Underwood, D.S.: Effect of Heat Release on Streamwise Vorticity Enhanced Mixing, MIT Thesis, Aug. 1995.

Waitz, I.A.; and Underwood, D.S.: Effect of Heat Release on Streamwise Vorticity Enhanced Mixing. AIAA Paper 95-2471, 1995.

Lewis contact: Dr. Clarence T. Chang, (216) 433-8561
Headquarters program office: OA



Stable lobed mixer with combustion.

Effect of Tabs on a Rectangular Nozzle Studied

In a continuing research program, jets from nozzles of different geometries are being investigated with the aim of increasing mixing and spreading in those flows. Flow fields from nozzles with elliptic, rectangular, and other more complex cross-sectional shapes are being studied in comparison to circular nozzles over a wide Mach number range. As noted by previous researchers, noncircular jets usually spread faster than circular jets.

Another technique being investigated to increase jet spreading even further for a given nozzle is the use of “tabs” to generate vortices. A typical tab is a triangular-shaped protrusion placed at the nozzle exit, with the base of the triangle touching the nozzle wall and the apex leaning downstream at 45° to the stream direction. This geometry was determined by a parametric study to produce the optimum effect for a given area blockage. The tabs can increase jet spreading significantly. The underlying mechanism traces to a pair of counter-rotating streamwise vortices originating from each tab. These vortex pairs persist in the flow; and with the appropriate number and strength, they can increase spreading.

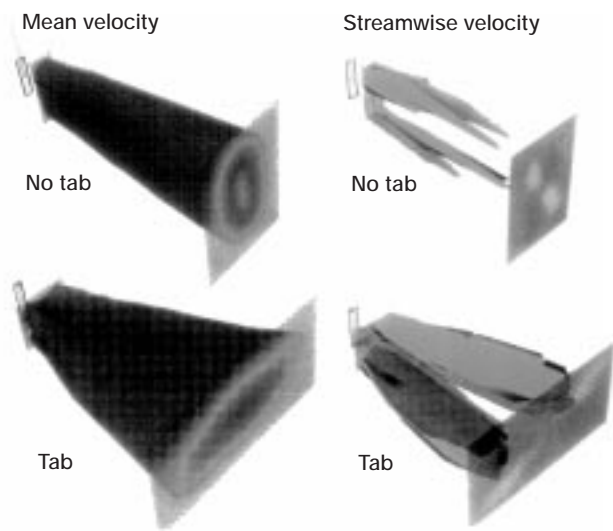
With jets from noncircular nozzles, the effect of the tabs is relatively more complex. Such flows usually contain streamwise vortices, even without any tabs, because of the tortuous flow paths within the nozzle. When tabs are applied, the resulting vortex pairs interact with the already existing vortices. Thus, depending on the location, size, and orientation of the tabs, the

vortex interaction can be either beneficial, increasing spreading, or detrimental, actually reducing spreading.

With a suitable choice of the tabs, a large increase in jet spreading can be achieved with noncircular nozzles. An example is shown in the figure. Here, the nozzle is rectangular with an aspect ratio of 3:1. The Reynolds number is 450,000, and the Mach number is 0.3. The data are obtained by hot-wire anemometry. Each figure in the left column shows an “isosurface” of the mean velocity, $U/U_{JET} = 15$ percent, providing a perspective view of the jet spreading. It can be seen that the jet cross section for the no-tab case has become essentially round by the last measurement station, $x/D_{EQUIVALENT} = 8$. For the case in the lower figure, two relatively large tabs are used, one each on the narrow edges of the nozzle. The tabs cause an enormous increase in the jet spreading. The increase in the amount of entrained ambient air at $x/D_{EQUIVALENT} = 8$ is about 100 percent. Note also that the tabs cause “axis switching”; that is, whereas the long dimension of the nozzle is aligned vertically, that of the jet cross section becomes horizontal shortly downstream of the nozzle.

The two figures on the right show the corresponding distributions of streamwise vorticity. Looking from downstream, the darker and lighter isosurfaces represent regions of anticlockwise and clockwise rotation, respectively. In the no-tab case, as mentioned earlier, two pairs of vortices occur because of secondary flow within the nozzle. It should be evident that the tabs produce very strong vortex pairs with opposite rotation directions. These vortex pairs completely dominate the flow field, and are responsible for the observed increase in the jet spreading as well as the axis switching. The effect of the tabs in this configuration has also been found to be persistent and, in fact, more pronounced at supersonic conditions.

Current effort in the research includes testing with more practical nozzles relevant to the High Speed Civil Transport (HSCT) and the Advanced Subsonic Technology (AST) programs. Efforts are also under way to address fundamental issues: for example, vorticity dynamics, mixedness, and small-scale mixing, as affected by the tabs, relevant to combustor flows and jet noise. In a parallel computational study, the flow field was also simulated successfully by a three-dimensional Navier-Stokes analysis. Currently, a parametric study is being carried out in the computational work by varying the tab size, orientation, and other factors—complementing and guiding the experimental work.



Distributions of mean velocity and streamwise vorticity with and without the tabs. Nozzle exit is shown on the left of each figure; flow is from left to right.

Bibliography

Steffen, C.J.; Reddy, D.R.; and Zaman, K.B.M.Q.: Analysis of Flowfield From a Rectangular Nozzle With Delta Tabs. AIAA Paper 95-2146, 1995.

Zaman, K.B.M.Q.; Reeder, M.F.; and Samimy, M.: Control of an Axisymmetric Jet Using Vortex Generators, *Phys. Fluids*, vol. 6, no. 2, Feb. 1993, pp. 778-793.

Zaman, K.B.M.Q.: Axis Switching and Spreading of an Asymmetric Jet—Role of Vorticity Dynamics. AIAA Paper 95-0889, 1995.

Lewis contacts: Dr. Khairul Zaman, (216) 433-5888; Christopher J. Steffen, Jr., (216) 433-8508; and Dr. Judith K. Foss, (216) 433-3587
Headquarters program office: OA

Propulsion Systems

Spherical Joint Piston and Connecting Rod Developed

Under an interagency agreement with the Department of Energy, the NASA Lewis Research Center manages a Heavy-Duty Diesel Engine Technology (HDET) research program. The overall program objectives are to reduce fuel consumption through increased engine efficiency, reduce engine exhaust emissions, and provide options for the use of alternative fuels. The program is administered with a balance of research contracts, university research grants, and focused in-house research.

The Cummins Engine Company participates in the HDET program under a cost-sharing research contract. Cummins is researching and developing in-cylinder component technologies for heavy-duty diesel engines. An objective of the Cummins research is to develop technologies for a low-emissions, 55-percent thermal efficiency (LE-55) engine. The best current-production engines in this class achieve about 46-percent thermal efficiency. Federal emissions regulations are driving this technology. Regulations for heavy-duty diesel engines were tightened in 1994, more demanding emissions regulations are scheduled for 1998, and another step is planned for 2002. The LE-55 engine emissions goal is set at half of

the 1998 regulation level and is consistent with plans for 2002 emissions regulations.

LE-55 engine design requirements to meet the efficiency target dictate a need to operate at higher peak cylinder pressures. A key technology being developed and evaluated under the Cummins Engine Company LE-55 engine concept is the spherical joint piston and connecting rod. Unlike conventional piston and connecting rod arrangements which are joined by a pin forming a hinged joint, the spherical joint piston and connecting rod use a ball-and-socket joint. The ball-and-socket arrangement enables the piston to have an axisymmetric design allowing rotation within the cylinder. The potential benefits of piston symmetry and rotation are reduced scuffing, improved piston ring sealing, improved lubrication, mechanical and thermal load symmetry, reduced bearing stresses, reduced running clearances, and reduced oil consumption.

The spherical joint piston is a monolithic, squeeze-cast, fiber-reinforced aluminum piston. The connecting rod has a ball end that seats on a spherical saddle within the piston and is retained by a pair of aluminum bronze holder rings. The holder rings are secured by a threaded ring that mates with the piston.

As part of the ongoing research and development activity, the Cummins Engine Company successfully completed a 100-hr test of the spherical joint piston and connecting rod at LE-55 peak steady-state engine conditions. In addition, a 100-hr transient cycle test that varied engine conditions between LE-55 no-load and LE-55 full-load was successfully completed.

Lewis contact: Dr. Mark J. Valco, (216) 433-3717
Headquarters program office: OA



Spherical joint piston and connecting rod—exploded assembly.

Mach 6 Integrated Systems Tests of Lewis' Hypersonic Tunnel Facility

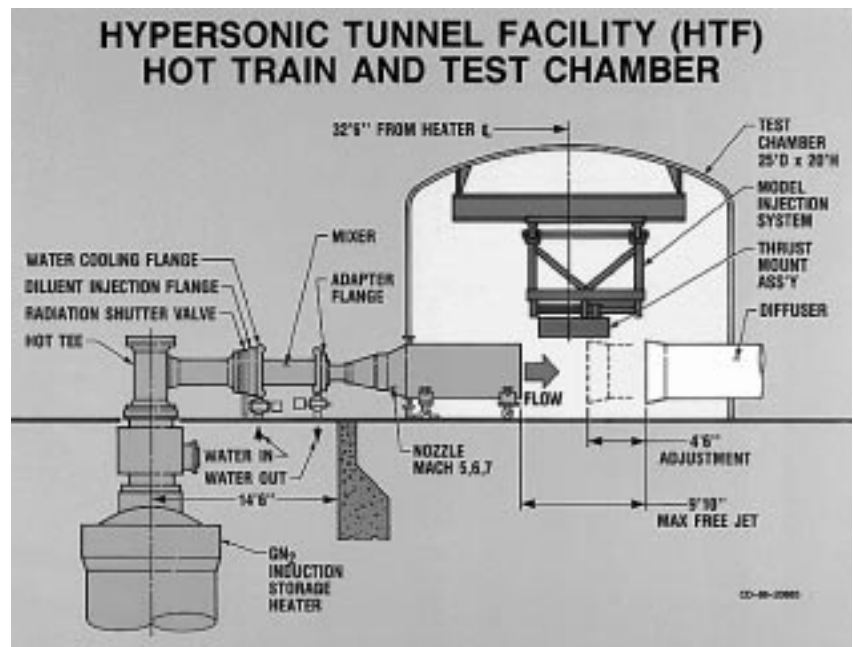
A series of 15 integrated systems tests were conducted at the NASA Lewis Research Center's Hypersonic Tunnel Facility (HTF) with test conditions simulating flight up to Mach 6. Facility stagnation conditions up to 3050 °R and 1050 psia were obtained with typical test times of 20 to 45 sec.

The HTF is a free-jet, blowdown propulsion test facility that can simulate up to Mach 7 flight conditions with true air composition. Mach 5, 6, and 7 facility nozzles, each with a 42-in. exit diameter, are available. The facility, without modifications, can accommodate models approximately 10-ft long. (Major HTF components are illustrated in the figures.) Nitrogen is heated by a graphite core induction heater, and oxygen is added downstream to produce simulated air. The combination of clean-air, large scale, and Mach 7 capabilities is unique to the HTF.

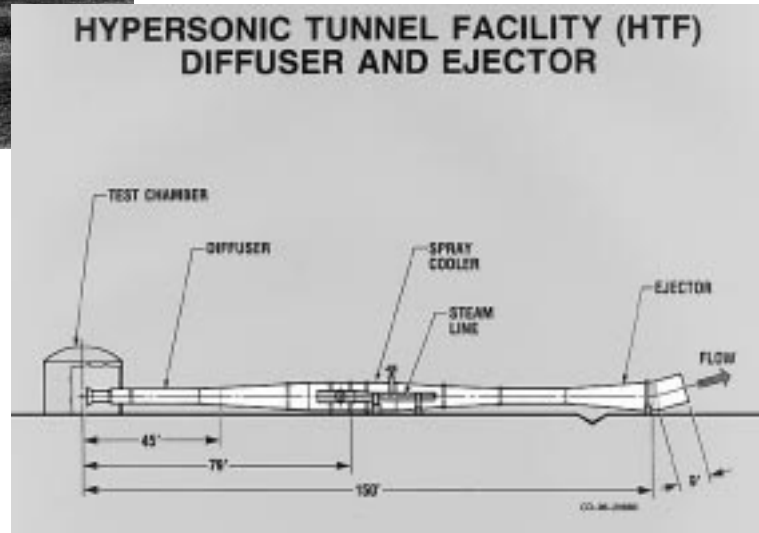
The HTF was reactivated between 1990 and May 1994. This activity included refurbishing the graphite heater, the steam generation plant, the gaseous oxygen system, and all control systems. All systems were checked out and recertified, and environmental systems were upgraded to meet current standards. The data systems also were upgraded to current standards, and a communication link with NASA-wide computers was added.

In May 1994 a short-duration integrated systems test (approximately 2 sec) was conducted to verify facility operability. This test identified several modifications and corrections to the HTF that were required to improve overall facility performance. From the end of 1994 to April 1995, these modifications were completed, and the 3000-ft-long, 30-in.-diameter steam supply line was insulated to improve system efficiency and allow operation in all weather conditions. Through May 1995 the integrated systems were tested. The photo shows the facility steam ejector in operation during an integrated systems test.

During this activity, significant test experience was gained, the graphite storage heater was used at up to the maximum operating temperature of 5000 °R, several improvements were made to various facility systems and test procedures, and some operational problems experienced in the past were resolved (e.g., elimination of water backflow during shutdown). The HTF was operated with significant run times for the first time since being reactivated and for the first time in more than 20 years. Overall, this test program resulted in smooth, relatively trouble-free facility operation and served to successfully demonstrate the operating capability and reliability of the HTF.



HTF hot train and test chamber.



Left: HTF steam ejector in operation during integrated systems testing. Right: HTF diffuser and ejector. All dimensions are in feet.

Bibliography

Thomas, S.R.; Woike, M.R.; and Pack, W.D.: Mach 6 Integrated Systems Tests of the NASA Lewis Research Center Hypersonic Tunnel Facility. NASA TM-107083, 1996.

Find out more about the Hypersonic Tunnel Facility on the World Wide Web:

<http://www.lerc.nasa.gov/WWW/AFED/facilities/htf.htm>

Lewis contact: Scott R. Thomas, (216) 433-8713
Headquarters program office: OA

Capabilities Enhanced for Researching the Reduction of Emissions in Future Aircraft

Future aircraft jet engines will run at higher pressures to obtain greater fuel efficiency and performance. This will require new combustor designs to keep the nitrogen oxide and carbon monoxide emissions at environmentally acceptable levels.

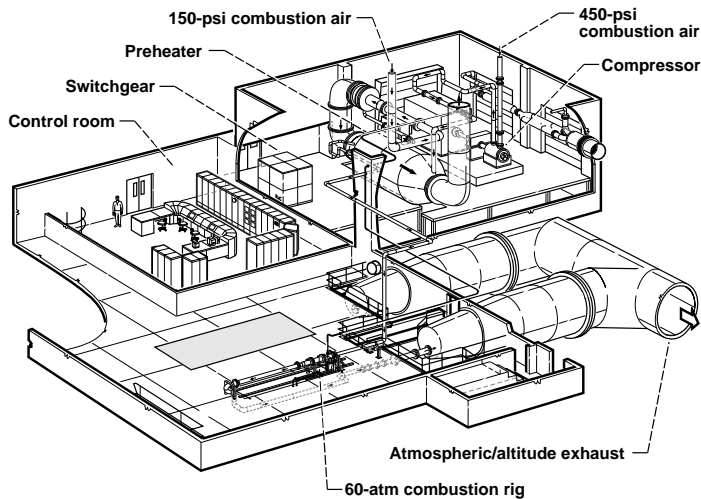
The actual pressures and temperatures found in gas turbine combustors must be duplicated in a laboratory to verify the emissions characteristics of gas turbine engines. Recognizing this, the U.S. aircraft gas turbine industry identified a need for a national facility that could duplicate the severe inlet conditions of future combustors.

Because of our expertise in combustion emissions reduction research and in the design and operation of high-pressure test facilities, the NASA Lewis Research Center was seen as the natural location for such a facility. As a national laboratory, Lewis could provide these facilities to all U.S. gas turbine engine manufacturers while protecting their proprietary interests.

Called the Advanced Subsonic Combustion Rig (see figure), the facility will provide up to 60-atm pressures at inlet temperatures up to 1300 °F and air flow rates up to 38 lb/sec. Furthermore, it will offer state-of-the-art diagnostic methods for characterizing advanced combustor concepts.

Aeronautical combustion research at Lewis provided several significant accomplishments recently in support of both the High Speed Research (HSR) and Advanced Subsonic Technology (AST) programs. For example, in the High Speed Research Program, NO_x reductions of up to 90 percent were achieved in prototype combustor hardware. Advanced computational analysis, gas sampling, and laser diagnostic techniques were critical to this success.

Working closely with the gas turbine industry, we have successfully transferred this low-emissions combustor technology into engine prototype hardware. This hardware is now being tested at the engine



The Advanced Subsonic Combustor Rig will provide actual gas turbine combustor inlet temperatures and pressures for future emissions reduction research.

manufacturer's facilities. Complementary tests in Lewis' currently available 30-atm test facilities are also underway, taking advantage of Lewis' unique diagnostic capabilities. By utilizing test facilities belonging to both NASA and its industry partners, we have tested multiple combustor concepts in a shorter period of time.

Having screened these concepts in the 30-atm facilities (which simulate aircraft cruise conditions), the most promising concepts will undergo further testing at actual takeoff and advanced cycle cruise conditions in the new 60-atm rig. This new facility was ready in the fall of 1995.

Lewis contact: Richard W. Niedzwiecki, (216) 433-3407
Headquarters program office: OA

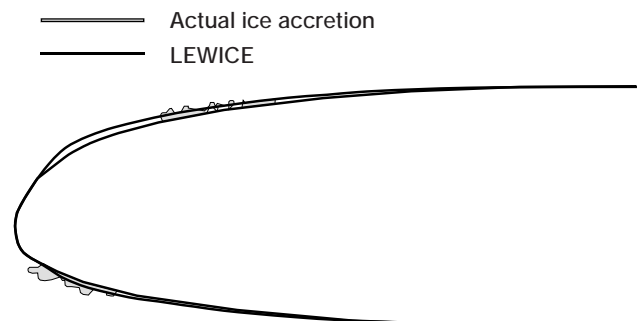
Aircraft Ice Accretion Due to Large-Droplet Icing Clouds

Studies of aircraft icing due to clouds consisting of individual droplets 10 times larger than those normally found in icing conditions are being carried out by members of the NASA Lewis Research Center's Icing Technology Branch. When encountered by an aircraft in freezing conditions, clouds consisting of large water droplets have a significantly different effect than those with normal droplets. A large-water-droplet cloud has been suggested as the cause of a commuter airplane

accident in the late fall of 1994. As a result, studies of what happens to aircraft flying in these rare, but potentially very hazardous, conditions have been reemphasized.

Atmospheric clouds are defined by factors such as water droplet size, liquid water content, and air temperature. In natural clouds, droplets are not all the same size, but rather are of various diameters. A statistical factor called median volume diameter is used to describe the relative droplet size distribution for a particular cloud. Typically, individual droplets range from 2 to 50 μm in diameter, and clouds usually have median volume diameters of less than 35 μm . Generally, it is thought that droplets tend to precipitate out as they reach 100 μm in diameter. However, under certain conditions, icing clouds with median volume diameters as high as 170 μm , with individual droplet diameters as large as 400 μm , may exist.

Large-droplet icing tests are being conducted in the Icing Research Tunnel with aircraft wing models of various lift profiles and element configurations—both with and without ice protection devices. Very peculiar ice shapes and ice types have been observed in Lewis' Icing Research Tunnel studies. On models with no ice-protection equipment, thin ice forms and breaks into pieces. These pieces then slide around slowly over a film of water on the airfoil. On the ice-protected models, small water rivulets flow aft from the leading edge to an ice ridge that forms aft of the ice protection. Here, some of the water freezes while some of it gets blown off the edge of the ridge, subsequently impinging on the model further aft, creating strange ice nodules that grow normal to the model surface. All these tests are being supported by an analytical effort including computational studies using LEWICE, a Lewis-developed code that simulates aircraft icing.



Comparison of LEWICE ice accretion prediction to actual ice accretion on an airfoil model in the Icing Research Tunnel under large droplet conditions.

In addition, Icing Technology Branch members have been involved in Air Force and Federal Aviation Administration (FAA) icing tanker flight testing at Edwards Air Force Base and in hearings and investigations being conducted by the National Transportation Safety Board concerning the commuter aircraft accident of 1994. We are working to increase understanding of the large-droplet ice-accretion phenomenon as well as helping the aerospace industry to address the situation.

Lewis contacts: Dean R. Miller, (216) 433-5349, and Gene Addy, (216) 977-7467
Headquarters program office: OA

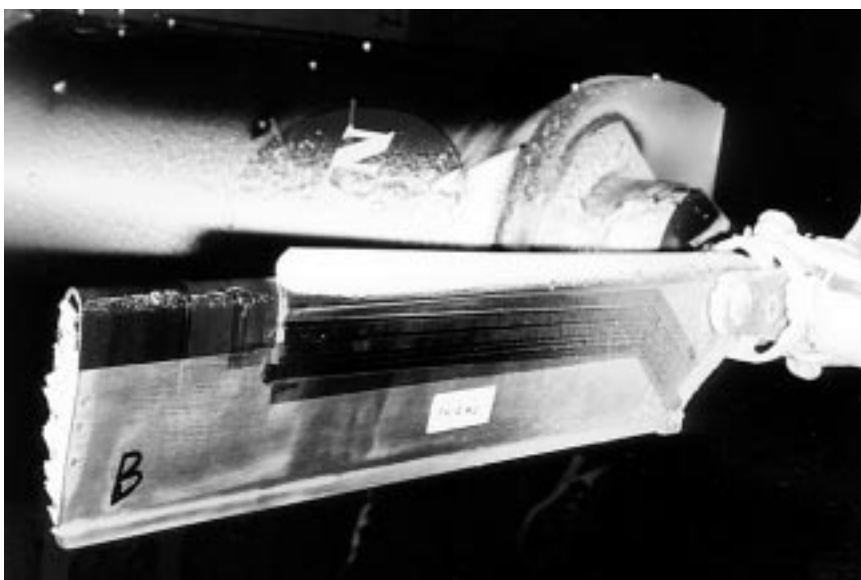
Shape-Memory-Alloy-Based Deicing System Developed

Ice buildup on aircraft leading edge surfaces has historically been a problem. Most conventional deicing systems rely either on surface heating to melt the accreted ice or pneumatic surface inflation to mechanically debond the ice. Deicers that rely solely on surface heating require large amounts of power. Pneumatic deicers usually cannot remove thin layers of ice and lack durability. Thus, there is a need for an advanced, low-power ice-protection system.

As part of the NASA Small Business and Innovation Research (SBIR) program, Innovative Dynamics, Inc., developed an aircraft deicing system that utilizes the properties of Shape Memory Alloys (SMA). The SMA-based system has achieved promising improvements in energy efficiency and durability over more conventional deicers. When they are thermally activated, SMA materials change shape; this is analogous to a conventional thermal expansion. The thermal input is currently applied via conventional technology, but there are plans to implement a passive thermal input that is supplied from the energy transfer due to the formation of the ice itself.

The actively powered deicer was tested in the NASA Lewis Icing Research Tunnel on a powered rotating rig in early 1995. The system showed promise, deicing both rime and glaze ice shapes as thin as 1/8 in. The first prototype SMA deicer reduced power usage by 45 percent over existing electrothermal systems. This prototype system was targeted for rotorcraft system development. However, there are current plans underway to develop a fixed-wing version of the deicer.

Lewis contacts: Thomas H. Bond, (216) 433-3414, and Randall K. Britton, (216) 977-1064
Headquarters program office: OA



SMA-based deicer mounted on powered rotating rig in Lewis' Icing Research Tunnel.

Laser Sheet Flow Visualization Developed for Lewis' Icing Research Tunnel

A new flow-visualization technique has been developed for use in the NASA Lewis Research Center's Icing Research Tunnel (IRT). This technique uses a sheet of light shining across the wind tunnel to illuminate a mist of water droplets in the air and display any organized flow patterns. Since the IRT already has the special water spray system required for aircraft icing experiments, no special visualization seeding material is required. The system has been used to visualize the changes in tip and leading edge vortices caused by ice accretion. Because the IRT's icing spray is used as part of the visualization technique, changes in the flow patterns about a wing can be observed and measured during the ice accretion process.

A 15-W argon-ion laser coupled with sheet-generating optics allows flow to be visualized in the IRT. Fiber-optic cables transport light from the remotely located laser into the tunnel test section. The laser rests on a vibration isolation table that floats on a layer of air. The intensity of the light is controlled by a local controller, and the laser is cooled by circulating water. An optical box made of wavelength-limiting tinted acrylic material is attached to the laser housing. This filtered Plexiglas allows observers to see the optics inside the box, but not the laser beam itself. The box has an interlocked hinged top so that only qualified operators can open it to align the laser.

The sheet-generating optics allow the thickness and the fanning of the sheet to be controlled very easily. The optics are mounted on remotely controlled traverses to aid in positioning the laser sheet in the test section.

Cameras can be placed on up to three sides of the tunnel test section to record flow-visualization images. The most common views are an overhead view and a side view of the model. Because both areas have exposed laser light, they are isolated from nonqualified personnel with interlocks. The windows to the IRT control room are covered with wavelength-limiting, tinted acrylic material to protect the tunnel operators and researchers from the laser light. High-speed, low-light digital cameras, low-light video cameras, 35-mm cameras, and intensified, digital still cameras are used to image the flow. For most tests, the laser power is limited to 3 to 4 W to prevent blooming in the imaging.

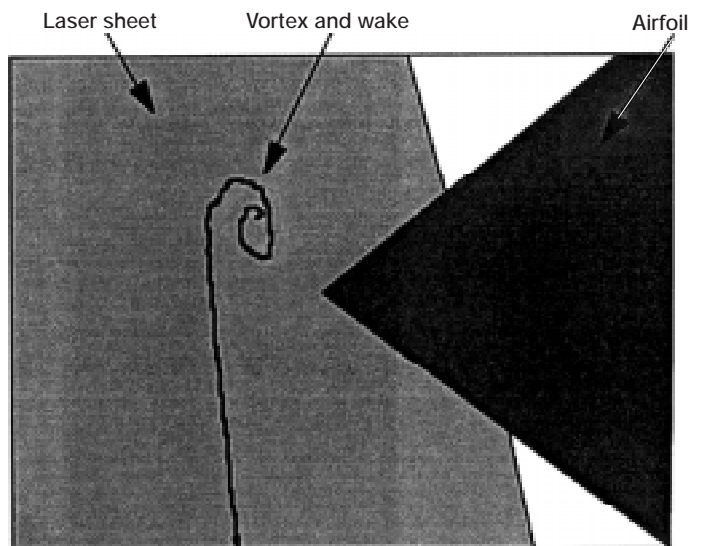
As just mentioned, the IRT's spray system generates the seed for the flow visualization. The most commonly used spray condition was selected to produce frozen ice particles in the 10- to 15- μm range. This spray

condition is used because the resultant particles do not produce any significant ice accretion on the model.

The photograph and drawing depict the wing tip vortex and wake produced by a swept-wing model. The dark bands correspond to regions where the water droplets have been swept away by the vortex or wake. The bright regions correspond to areas where the water droplets have accumulated.

Find out more about Lewis' IRT on the World Wide Web:
<http://www.lerc.nasa.gov/WWW/AFED/facilities/irt.html>

Lewis contacts: Victor A. Canacci, (216) 433-2697, and Dr. Mark G. Potapczuk, (216) 433-3919
Headquarters program office: OA



Laser sheet image (top) of wing tip vortex from IRT and description of laser sheet image (bottom).

Gear Crack Propagation Investigation

Reduced weight is a major design goal in aircraft power transmissions. Some gear designs incorporate thin rims to help meet this goal. Thin rims, however, may lead to bending fatigue cracks. These cracks may propagate through a gear tooth or into the gear rim. A crack that propagates through a tooth would probably not be catastrophic, and ample warning of a failure could be possible. On the other hand, a crack that propagates through the rim would be catastrophic. Such cracks could lead to disengagement of a rotor or propeller from an engine, loss of an aircraft, and fatalities.

To help create and validate tools for the gear designer, the NASA Lewis Research Center performed in-house analytical and experimental studies to investigate the effect of rim thickness on gear-tooth crack propagation. Our goal was to determine whether cracks grew through gear teeth (benign failure mode) or through gear rims (catastrophic failure mode) for various rim thicknesses. In addition, we investigated the effect of rim thickness on crack propagation life. A finite-element-based computer program simulated gear-tooth crack propagation. The analysis used principles of linear elastic fracture mechanics, and quarter-point, triangular elements were used at the crack tip to represent the stress singularity. The program had an automated crack propagation option in which cracks were grown numerically via an automated remeshing scheme. Crack-tip stress-intensity factors were estimated to determine crack-propagation direction. Also, various fatigue crack-growth models were used to estimate crack-propagation life.

Experiments were performed in Lewis' Spur Gear Fatigue Rig to validate predicted crack-propagation results. Gears with various backup ratios were tested to validate crack-path predictions. Also, test gears were installed with special crack-propagation gages in the tooth fillet region to measure bending-fatigue crack growth.

From both predictions and tests, gears with backup ratios (rim thickness divided by tooth height) of 3.3 and 1.0 produced tooth fractures, whereas a backup ratio of 0.3 produced rim fractures. For a backup ratio of 0.5, the experiments produced rim fractures and the predictions produced both rim and tooth fractures, depending on the initial geometry of the crack. Good correlation between predicted and measured crack growth was achieved when the fatigue crack-closure concept was introduced into the analysis. As the gear rim thickness decreased, the compressive cyclic stress in the gear-tooth fillet region increased. This retarded

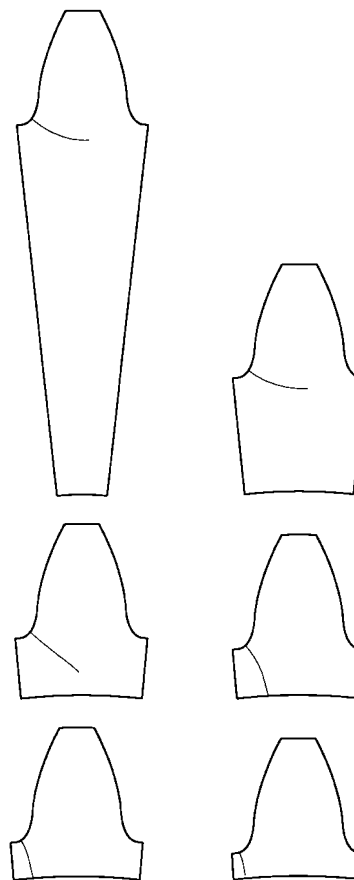
crack growth and increased the number of crack-propagation cycles to failure.

All studies to date have been two-dimensional analyses; validation has been with narrow-face-width spur gears. In the current analysis, which is being investigated for three-dimensional applications of spiral-bevel gears, data are being compared in a full-scale OH-58 helicopter main rotor transmission application.

Bibliography

Lewicki, D.G.: Crack Propagation Studies to Determine Benign or Catastrophic Failure Modes for Aerospace Thin-Rim Gears, Ph.D. Thesis, Case Western Reserve University, 1995.

Lewis contact: Dr. David G. Lewicki, (216) 433-3970
Headquarters program office: OA

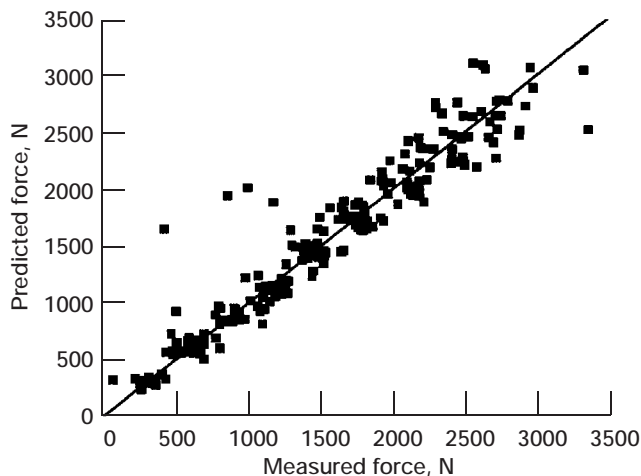


Effect of rim thickness on gear-tooth crack-propagation path for various backup ratios (rim thickness divided by tooth height). Backup ratios, 3.3 (top left), 1.0 (top right), 0.5 (center left), 0.4 (center right), 0.3 (bottom left), and 0.2 (bottom right).

Study of Gear Dynamic Forces Completed

Gearbox-generated noise and vibration is objectionable in many vehicles, particularly helicopters. This noise excitation is caused by the load fluctuation as gear teeth enter and leave mesh. In high-quality gears, a common technique to reduce gear noise and vibration is to modify the tooth profile. Gear noise reduction is a NASA and U.S. Army goal, and a NASA/U.S. Army research project sponsored development of gear dynamics computer codes to help design quiet gears. As part of this project, a series of experiments was performed in the NASA Lewis Research Center's Gear Noise Rig to develop a data base of dynamic test data and to validate the predictions of the codes for several gear designs under a variety of test conditions.

A method was developed to use dynamic strain gage measurements performed on Lewis' Gear Noise Rig to determine the forces acting between the gear teeth. Then, these dynamic force data were compared with predictions of DANST-PC, a NASA gear dynamics code. Tests were performed on six sets of low-contact-ratio spur gears that were identical except for different tooth profile modifications. The figures compare measured and predicted dynamic tooth force under several load conditions. They demonstrate that the analysis code successfully simulates the dynamic behavior of the gears under most conditions.



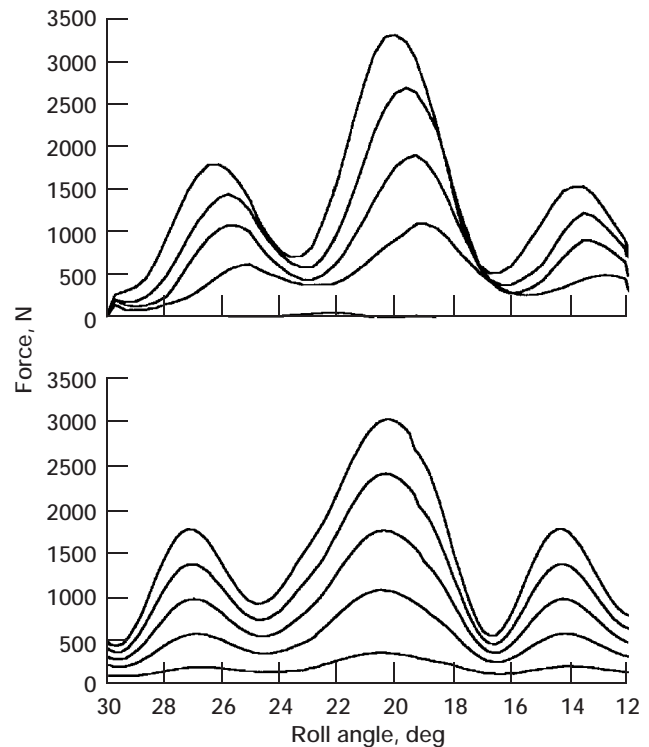
This analysis code can be used by gear designers to develop improved tooth profiles for quieter gears. Experiments continue to extend the data base to include high-contact-ratio gears and nonstandard tooth profiles. These promise further improvements in gear performance.

Bibliography

Oswald, F.B.; and Townsend, D.P.: Influence of Tooth Profile Modification on Spur Gear Dynamic Tooth Strain. AIAA Paper 95-3050 (NASA TM-106952), 1995.

Oswald, F.B., et al.: Measuring Dynamic Forces in Spur Gears to Validate a Gear Dynamics Code. To be published as a NASA TM, 1996.

Lewis contact: Fred B. Oswald, (216) 433-3957
Headquarters program office: OA



Left: Comparison of measured and predicted maximum dynamic tooth force for 6 gear designs and at 36 test conditions. Right: Measured (top) and predicted (bottom) dynamic tooth force for unmodified gear (4000 rpm and 5 different torque levels).

Code to Optimize Load Sharing of Split-Torque Transmissions Applied to the Comanche Helicopter

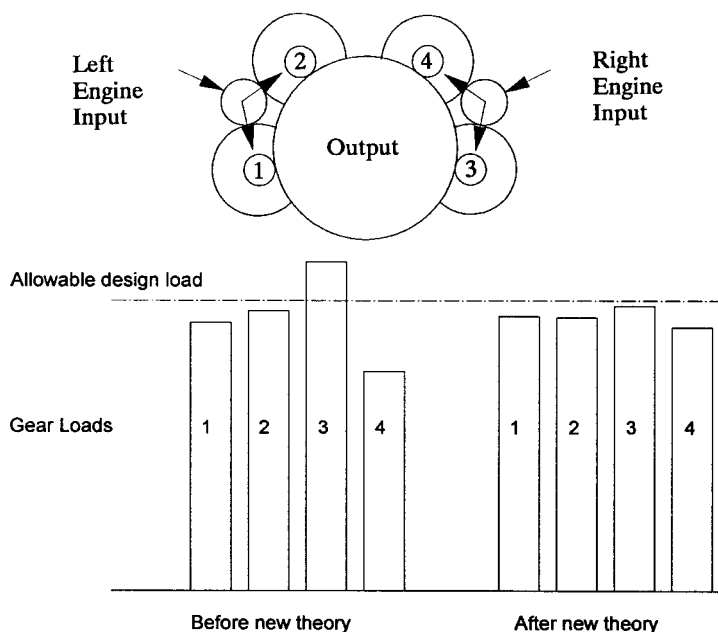
Most helicopters now in service have a transmission with a planetary design. Studies have shown that some helicopters would be lighter and more reliable if they had a transmission with a split-torque design instead. However, a split-torque design has never been used by a U.S. helicopter manufacturer because there has been no proven method to ensure equal sharing of the load among the multiple load paths. The Sikorsky/Boeing team has chosen to use a split-torque transmission for the U.S. Army's Comanche helicopter, and Sikorsky Aircraft is designing and manufacturing the transmission. To help reduce the technical risk of fielding this helicopter, NASA and the Army have done the research jointly in cooperation with Sikorsky Aircraft. A theory was developed that equal load sharing could be achieved by proper configuration of the geartrain, and a computer code was completed in-house at the NASA Lewis Research Center to calculate this optimal configuration.

The prototype split-torque transmission for the Comanche helicopter was designed and built before the new theory and computer code were available, and the measured loads on the four final drive gears of the prototype were not equal. In fact, one of the gears was loaded beyond the allowable design load. The new theory and computer code correctly predicted the trend of the loads for the prototype design, and the code was

applied to calculate small, but important, design changes to theoretically balance the loads on all four gears. The code calculates how elastic deformations affect the relative amount of load carried in each load path. The deformations that were considered in the analysis were tooth bending, gearshaft twist, gearshaft bowing, housing deflections, and the Hertzian deformations at bearing rolling element and raceway contacts. The design changes calculated to accommodate the deformations were manufactured, and the test of the redesigned transmission proved that the load sharing was greatly improved. As shown in the figure, the loads on the four final drive gears are now nearly equal, and all loads are less than the allowable design load. A significant amount of development time and money was saved by applying the analysis to achieve good load sharing with only one design iteration.

The new theory and computer code have been validated, and a patent application has been submitted for this technology with Government and Sikorsky personnel as coinventors. We plan to continue to support Sikorsky Aircraft with transmission technology from Lewis and the Army as needed to bring the Comanche gearbox design to maturity.

Lewis contact: Timothy L. Krantz, (216) 433-3580
Headquarters program office: OA



Measurements of loads on the four final drive gears prove the new theory to ensure load sharing.

Face Gear Technology for Aerospace Power Transmission Progresses

The use of face gears in an advanced rotorcraft transmission design was first proposed by the McDonnell Douglas Helicopter Company during their contracted effort with the U.S. Army under the Advanced Rotorcraft Transmission (ART) program. Face gears would be used to turn the corner between the horizontal gas turbine engine and the vertical output rotor shaft—a function currently done by spiral bevel gears. This novel gearing arrangement would substantially lower the drive system weight partly because a face gear mesh would be used to split the input power between two output gears. However, the use of face gears and their ability to operate successfully at the speeds and loads required for an aerospace environment was unknown. Therefore a proof-of-concept phase with an existing test stand at the NASA Lewis Research Center was pursued. Hardware was designed that could be tested in Lewis' Spiral Bevel Gear Test Rig.

The initial testing indicated that the face gear mesh was a feasible design that could be used at high speeds and load. Surface pitting fatigue was the typical failure mode, and that could lead to tooth fracture. An interim project was conducted to see if slight modifications to the gear tooth geometry or an alternative heat treating process could overcome the surface fatigue problems. From the initial and interim tests, it was apparent that for the surface fatigue problems to be overcome the manufacturing process used for this component would have to be developed to the level used for spiral bevel gears. The current state of the art for face gear manufacturing required using less than optimal gear materials and manufacturing techniques because the surface of the tooth form does not receive final finishing after heat treatment as it does for spiral bevel gears. This resulted in less than desirable surface hardness and manufacturing tolerances.

An Advanced Research and Projects Agency (ARPA) Technology Reinvestment Project has been funded to investigate the effects of manufacturing process improvements on the operating characteristics of face gears. The program is being conducted with McDonnell Douglas Helicopter Co.,

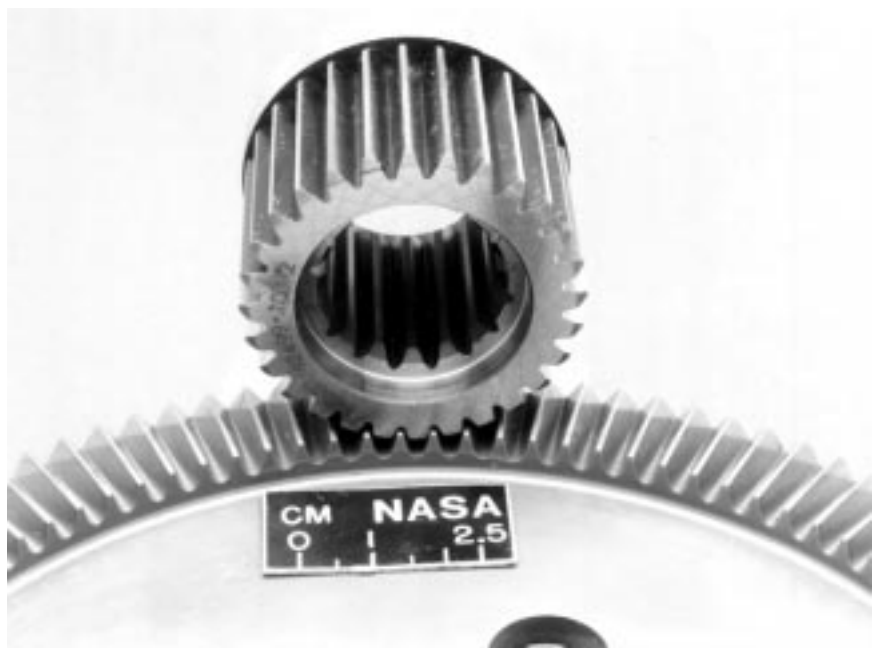
Lucas Western Inc., the University of Illinois at Chicago, and a NASA/U.S. Army team. The goal of the project is to develop the grinding process, experimentally verify the improvement in face gear fatigue life, and conduct a full-scale helicopter transmission test. The theory and methodology to grind face gears has been completed, and manufacture of the test hardware is ongoing. Experimental verification on test hardware is scheduled to begin in fiscal 1996.

Bibliography

Handschuh, R.; Lewicki, D.; and Bossler, R.: Experimental Testing of Prototype Face Gears for Helicopter Transmissions. NASA TM-105434, 1992.

Heath, G.F.; and Bossler, R.B.: Advanced Rotorcraft Transmission (ART) Program. Final Report. NASA CR-191057, 1993.

Lewis contacts: Dr. David G. Lewicki, (216) 433-3970, and Dr. Robert F. Handschuh, (216) 433-3969
Headquarters program office: OA



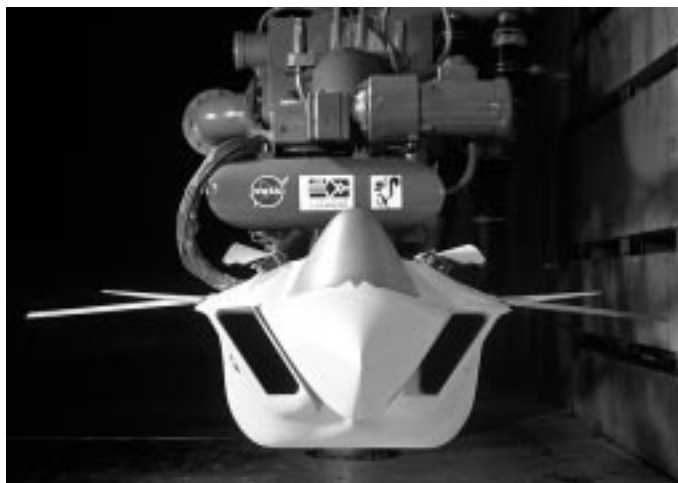
Face gear test hardware.

Advanced Short Takeoff and Vertical Landing (ASTOVL) Concepts Tested

In this cooperative program between NASA, Lockheed Corporation, and the Advanced Research and Projects Agency (ARPA), an advanced short takeoff and vertical landing (ASTOVL) model was tested in the 9- by 15-Foot Low-Speed Wind Tunnel at the NASA Lewis Research Center. The 10-percent scaled model was tested over a range of headwind velocities from 25 to 120 kn. This inlet/forebody test was a key part of an important Department of Defense program investigation enabling technologies for future high-performance ASTOVL aircraft.

The Lockheed concept is focused on a shaft-coupled lift fan system centered around Pratt & Whitney's F119 power plant. As envisioned, a conventional takeoff and landing version (CTOL) would replace the U.S. Air Force's F-16's. The ASTOVL version would eventually replace Marine and, possibly, British Harrier aircraft. The ASTOVL and CTOL versions are scheduled to begin their manufacturing development phases in 2000.

The purpose of this test was to acquire data pertinent to the inlet-forebody model. The test was very successful. Both steady-state and dynamic data were obtained. This small-scale testing, which is directed at reducing risks, may greatly reduce the risks on a full-scale aircraft.



Front view of ASTOVL model.

Lewis contacts: Albert L. Johns, (216) 433-3972, and George H. Neiner, (216) 433-5661
Headquarters program office: OA

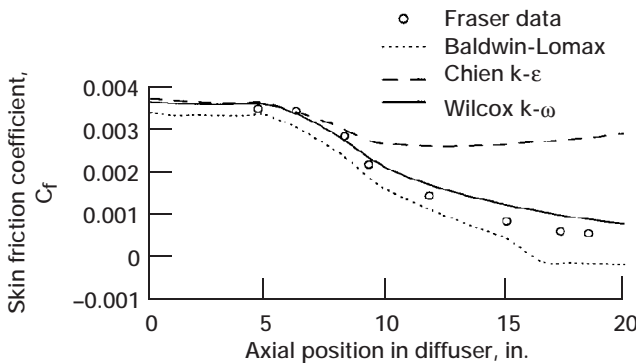
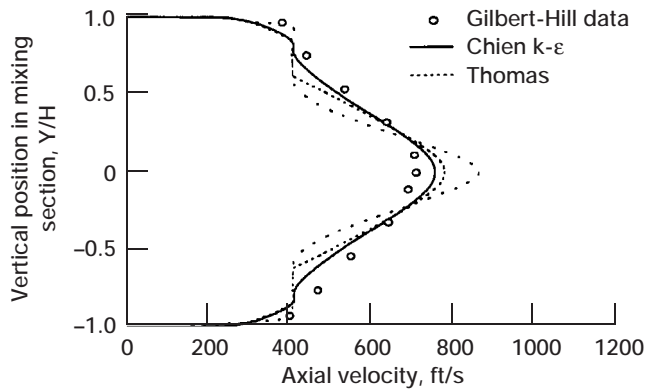
NPARC Code Upgraded With Two-Equation Turbulence Models

The National PARC (NPARC) Alliance was established by the NASA Lewis Research Center and the Air Force Arnold Engineering Development Center to provide the U.S. aeropropulsion community with a reliable Navier-Stokes code for simulating the nonrotating components of propulsion systems. Recent improvements to the turbulence model capabilities of the NPARC code have significantly improved its capability to simulate turbulent flows. Specifically, the Chien $k-\epsilon$ and Wilcox $k-\omega$ turbulence models were implemented at Lewis.

Lewis researchers installed the Chien $k-\epsilon$ model into NPARC to improve the code's ability to calculate turbulent flows with attached wall boundary layers and free shear layers (ref. 1). Calculations with NPARC have demonstrated that the Chien $k-\epsilon$ model provides more accurate calculations than those obtained with algebraic models previously available in the code. Grid sensitivity investigations have shown that computational grids must be packed against the solid walls such that the first point off of the wall is placed in the laminar sublayer (ref. 2). In addition, matching the boundary layer and momentum thicknesses entering mixing regions is necessary for an accurate prediction of the free shear-layer growth.

Because algebraic and two-equation $k-\epsilon$ turbulence models have been found to be deficient in predicting flows with adverse pressure gradients or separations, the Wilcox $k-\omega$ model was also installed into NPARC (ref. 3). Calculations with NPARC for the Fraser diffuser (adverse pressure gradient flow) and Sajben diffuser (separated flow) have shown that the $k-\omega$ model provides the most accurate calculations among turbulence models available in NPARC for such flows.

The Chien $k-\epsilon$ and Wilcox $k-\omega$ two-equation turbulence models were installed in production versions of NPARC and are being used by the aeropropulsion community for inlet, nozzle, and propulsion-airframe integration flow problems. Additional turbulence model upgrades, including an algebraic Reynolds stress model, are planned for NPARC to make the code a state-of-the-art solver for complex turbulent flows.



Top: Velocity profiles for an ejector nozzle flow. Bottom: Skin friction for the Fraser subsonic diffuser.

References

1. Georgiadis, N.J.; Chitsomboon, T.; and Zhu, J.: Modification of the Two-Equation Turbulence Model in NPARC to a Chien Low Reynolds Number $k-\epsilon$ Formulation. NASA TM-106710, 1994.
2. Georgiadis, N.J.; Dudek, J.C.; and Tierney, T.P.: Grid Resolution and Turbulent Inflow Boundary Condition Recommendations for NPARC Calculations. AIAA Paper 95-2613 (NASA TM-106959), 1995.
3. Yoder, D.; Georgiadis, N.J.; and Orkwis, P.: Implementation of a Two-Equation $k-\omega$ Turbulence Model in NPARC. AIAA Paper 96-0383, 1995.

For more information about the NPARC Alliance, visit their site on the World Wide Web:

<http://info.arnold.af.mil/nparc/index.html>

Lewis contact: Nicholas J. Georgiadis, (216) 433-3958
Headquarters program office: OA

Mixing Process in Ejector Nozzles Studied at Lewis' Aero-Acoustic Propulsion Laboratory

The NASA Lewis Research Center has been studying mixing processes in ejector nozzles for its High Speed Research (HSR) Program. This work is directed at finding ways to minimize the noise of a future supersonic airliner. Much of the noise such an airplane would generate would come from the nozzle, where a hot, high-speed jet exits the engine.

Several different nozzle configurations were used to produce nozzle systems with different acoustical and aerodynamic characteristics. The acoustical properties were measured by an array of microphones in an anechoic chamber, and the aerodynamics were measured by traditional pressure and temperature instruments as well as by Laser Doppler Velocimetry (LDV), a technique for visualizing the airflow pattern without disturbing it. These measurements were put together and compared for different configurations to examine the relationships between mixing and noise generation.

Shown in the photo is the mixer-ejector nozzle with the installed flow-visualization windows (foreground), the optical equipment and the supporting structure for the Laser Doppler Velocimetry flow visualization (midfield), and the sound-absorbing wedges used to create an anechoic environment for acoustic testing (background).

The High Speed Research Program is a NASA-funded effort, in cooperation with the U.S. aerospace industry, to develop enabling technologies for a future supersonic airliner. One of the technological barriers being addressed is noise generated during near-airport operation. The mixer-ejector nozzle concept is being examined as a way to reduce jet noise while maintaining thrust. Ambient air is mixed with the high-velocity engine exhaust to reduce the jet velocity and hence the noise generated by the jet.

The model was designed and built by Pratt & Whitney under NASA contract. The test, completed in June 1995, was conducted in Lewis' Aero-Acoustic Propulsion Laboratory.



Ejector nozzle being used to study mixing processes for noise reduction.

For more information about Lewis' Aero-Acoustic Propulsion Laboratory and the High Speed Research Program, visit our sites on the World Wide Web:

<http://www.lerc.nasa.gov/WWW/AFED/facilities/aapl.html>

<http://www.lerc.nasa.gov/WWW/HSR/>

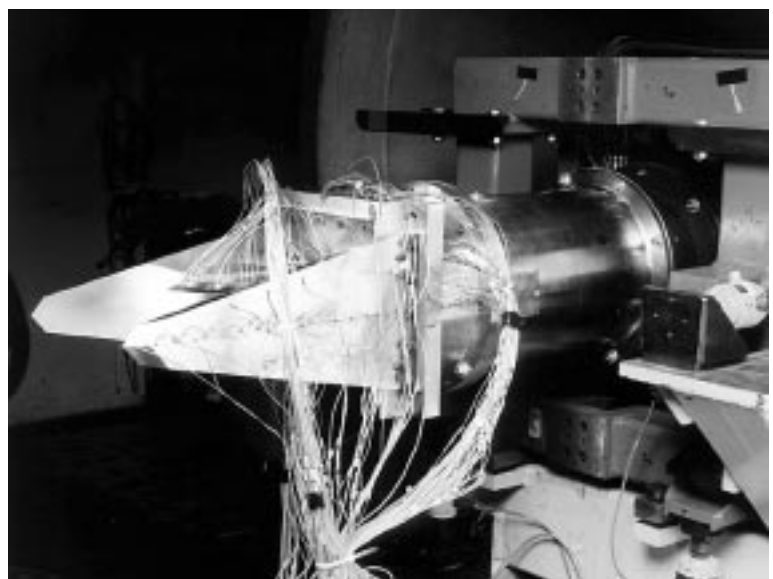
**Lewis contact: John D. Wolter, (216) 433-3941
Headquarters program office: OA**

F119 Nozzle Flaps Tested at Lewis' CE-22 Facility

The next generation of aircraft fighters requires higher engine performance and enhanced stealth characteristics for air superiority. A Lockheed-Martin/Boeing aircraft with a Pratt & Whitney F119 engine was selected by the Air Force for the next advanced tactical fighter (ATF). As part of this program, the NASA Lewis Research Center entered into a cooperative test program with Pratt & Whitney along with the Air Force to study the performance for various advanced nozzle concepts for the F119 engine. The area of interest was to measure the internal performance (both thrust and flow coefficients) of nozzle flaps redesigned for low observability with minimal performance loss.

The experimental program was successfully completed May 1995 in Lewis' CE-22 facility. The models were tested over a wide range of geometric variations and nozzle pressure ratios. Results confirmed that the redesigned nozzle flaps had an insignificant effect on the thrust performance and that the resulting flow patterns should not be a problem in the cooling flow design. The results also agreed well with Pratt & Whitney's computational fluid dynamics analysis. The data obtained from this test were added to the current data base to help validate other performance prediction methodology.

**Lewis contact: David W. Lam, (216) 433-8875
Headquarters program office: OA**



F119 nozzle in CE-22 test facility.

Prediction Capability for Transonic Nozzle Afterbodies Improved

Under the High Speed Research (HSR) Program, the NASA Lewis Research Center, the NASA Langley Research Center, and the aerospace industry have been developing exhaust nozzle concepts for a future High Speed Civil Transport (HSCT). This 300-passenger aircraft, which is envisioned for the year 2005, would cruise supersonically at speeds of Mach 2.4. For such an aircraft to be both economically viable and environmentally acceptable, the exhaust nozzles must combine highly efficient operation throughout the flight envelope with low noise levels at takeoff.

The initial phase of the HSR Program focused on environmental challenges, with nozzle-related research emphasizing the reduction of takeoff noise. The effort produced nozzle designs that not only meet but surpass HSR noise-reduction goals. The next step in the design process is to address the nozzle's performance throughout the aircraft's mission and integrate it with the rest of the propulsion system. To evaluate nozzle concepts for all flight conditions, engineers rely on empirical data bases obtained through extensive wind tunnel tests. However, the current HSR nozzles are a rectangular (two-dimensional) design, and this type of nozzle is not well represented in the existing data base. Therefore, the current methods for predicting nozzle performance are inadequate. This is especially troublesome at transonic (near Mach 1) conditions where the drag on the nozzle afterbody (boattail) can be as high as 25 percent of the thrust produced.

For a more accurate analysis at transonic speeds, a two-dimensional afterbody data base was needed. Because of the expense, time requirements, and difficulties in testing at these Mach numbers, wind tunnel tests were not feasible. A team composed of researchers from Lewis, Langley, and McDonnell Douglas created a two-dimensional data base using computational fluid dynamics. First, each group validated their computational fluid dynamics code against existing experimental data to gain confidence in the code's results. Next, the organizations analyzed several configurations, and the results were used to create the new data base. Then, the analysis methods

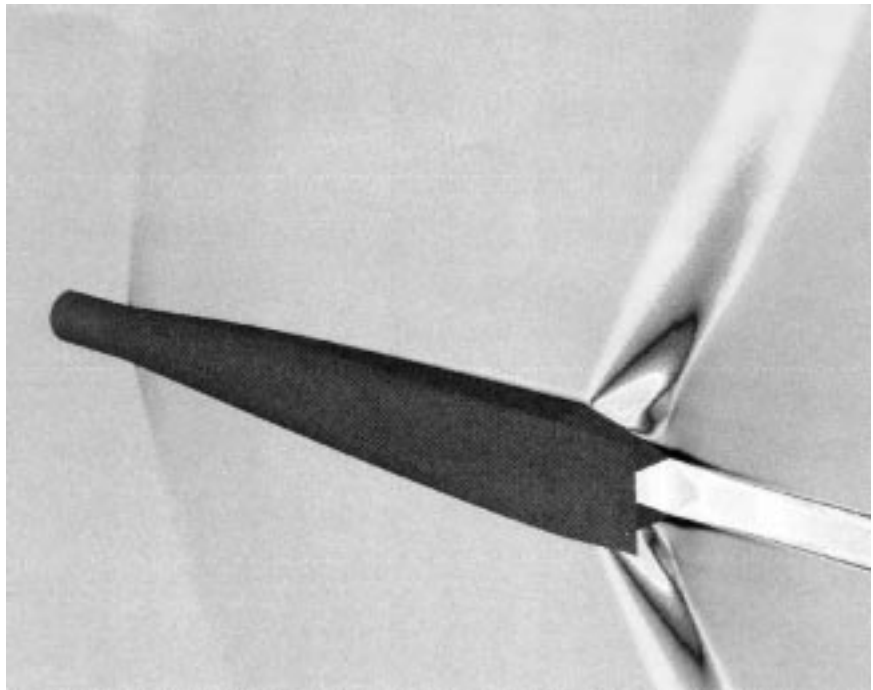
were updated to account for the effects of two-dimensional nozzles. This will result in a more accurate analysis of the propulsion system for the High Speed Civil Transport.

Researchers at Lewis used the NPARC computational fluid dynamics code in their portion of the analysis. This code is a general-purpose, full Navier-Stokes solver that is supported through a joint effort between Lewis and the Air Force's Arnold Engineering Development Center. The analyses were run on both Lewis' Cray Y-MP and the Aeronautics Consolidated Supercomputing Facility's Cray C-90 located at the NASA Ames Research Center. Lewis produced seven calculations for the data base. Results of the Government-industry team correlated well with each other as well as with the accepted theory.

For more information about the HSR Program and NPARC, visit their sites on the World Wide Web:

<http://www.lerc.nasa.gov/WWW/HSR/>
<http://info.arnold.af.mil/nparc/index.html>

Lewis contact: James R. DeBonis, (216) 433-6581
Headquarters program office: OA



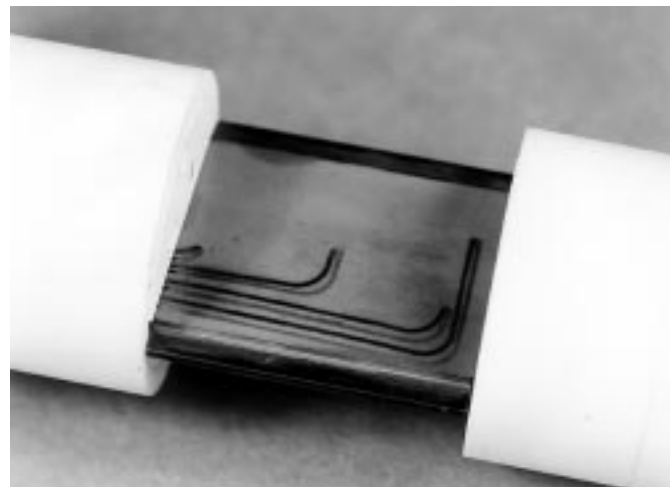
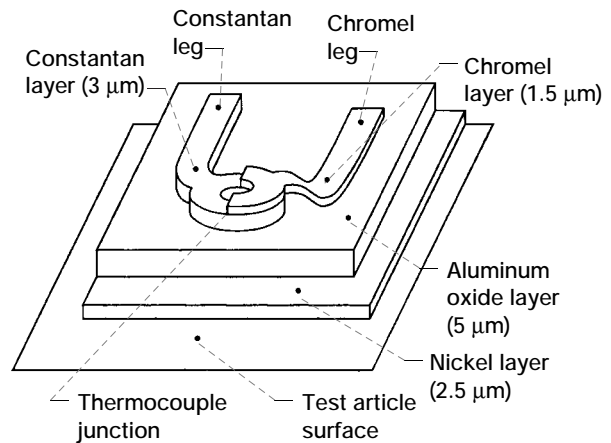
NPARC code prediction of Mach number contours about a transonic nozzle afterbody.

Thin-Film Thermocouple Technology Demonstrated for Reliable Heat Transfer Measurements

Exploratory work is in progress to apply thin-film thermocouples to localized heat transfer measurements on turbine engine vanes and blades. The emerging thin-film thermocouple technology shows great potential to improve the accuracy of local heat transfer measurements. With conventional imbedded thermocouples, heat-transfer measurements on the thin walls of cooled turbine blades have a high uncertainty because of unavoidable flow and heat-path perturbations caused by the bulky thermocouples and lead wires. Thin-film thermocouples offer an ideal solution for blade and vane surface temperature measurements because they guarantee virtually no perturbation of the heat path and blade wall thickness or of the coolant and gas flow patterns. However, early attempts to use thin-film sensors were not fully successful mainly because of problems with the thin-film-to-lead-wire connections.

To verify and master the experimental methodology of thin-film thermocouples, the NASA Lewis Research Center conducted a proof-of-concept experiment in a controlled environment before applying the thin-film sensors to turbine tests. The test article consisted of a flat plate with an internally cooled narrow passage submerged into a stream of heated air. Both the externally heated side and the internally cooled side were instrumented with thin-film sensors. A typical thin-film thermocouple sensor and the instrumented test article are shown in the figures. A major problem with applying thin films to electrically conducting metal surfaces is the necessity to insulate the sensor from the substrate. We accomplished this by modifying the aluminum oxide layer. Another crucial aspect of thin-film sensor reliability is the connection between the thin-film thermocouple legs and the lead wires that link the sensors with data-acquisition equipment. In our approach, the sputtered thermocouple legs were first connected to bare 25- μm thermocouple alloy wires, which were then connected to 0.25-mm insulated thermocouple lead wires. This approach proved highly reliable; no thermocouple was lost during testing.

Initial tests were conducted at Mach 0.4 and at a static temperature of 425 K on the heated side and at Mach 0.5 and a static temperature of 280 K on the cooled side; the heat flow rate was 200 kW/m². Lewis is preparing work with partners from industry on applying the thin-film thermocouples to turbine blades for temperature measurements up to 700 K and to turbine vanes for temperatures up to 1000 K.



Top: Thin-film thermocouple (type E). Bottom: Test article instrumented with four thin-film thermocouples.

Bibliography

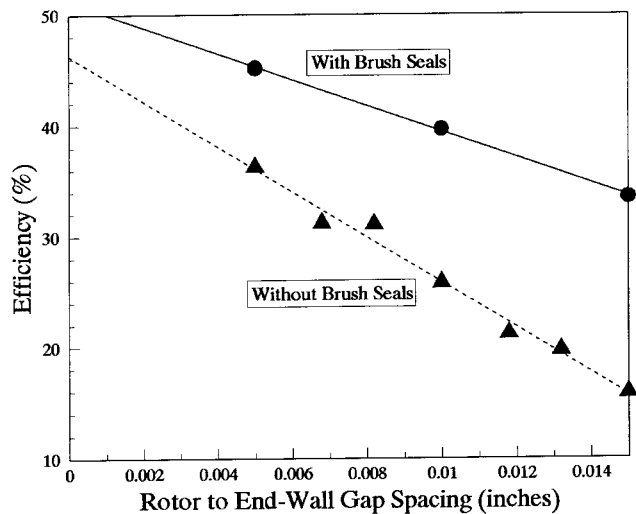
Lepicovsky, J.; Bruckner, R.J.; and Smith, F.A.: Application of Thin-Film Thermocouples to Localized Heat Transfer Measurements. AIAA Paper 95-2834 (NASA TM-107045), 1995.

Lewis contact: Dr. Jan Lepicovsky, (216) 977-1402
Headquarters program office: OA

Effect of Brush Seals on Wave Rotor Performance Assessed

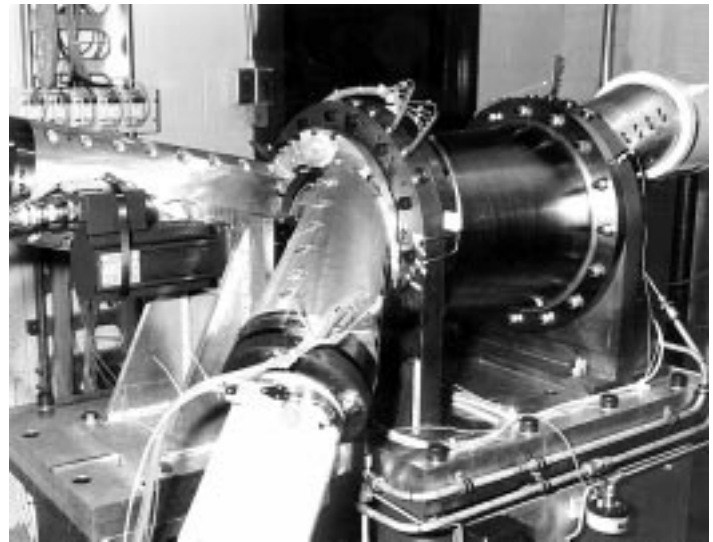
The NASA Lewis Research Center's experimental and theoretical research shows that wave rotor topping can significantly enhance gas turbine engine performance levels. Engine-specific fuel consumption and specific power are potentially enhanced by 15 and 20 percent, respectively, in small (e.g., 400 to 700 hp) and intermediate (e.g., 3000 to 5000 hp) turboshaft engines. Furthermore, there is potential for a 3- to 6-percent specific fuel consumption enhancement in large (e.g., 80,000 to 100,000 lbf) turbofan engines (ref. 1). This wave-rotor-enhanced engine performance is accomplished within current material-limited temperature constraints.

The completed first phase of experimental testing involved a three-port wave rotor cycle in which medium total pressure inlet air was divided into two outlet streams, one of higher total pressure and one of lower total pressure. The experiment successfully provided the data needed to characterize viscous, partial admission, and leakage loss mechanisms. Statistical analysis indicated that wave rotor product efficiency decreases linearly with the rotor to end-wall gap, the square of the friction factor, and the square of the passage of nondimensional opening time. Brush seals were installed to further minimize rotor passage-to-cavity leakage. The graph shows the effect of brush seals on wave rotor product efficiency.



For the second-phase experiment, which involves a four-port wave rotor cycle in which heat is added to the Brayton cycle in an external burner, a one-dimensional design/analysis code (ref. 2) is used in conjunction with a wave rotor performance optimization scheme (ref. 3) and a two-dimensional Navier-Stokes code (ref. 4). The purpose of the four-port experiment is to demonstrate and validate the numerically predicted four-port pressure ratio versus temperature ratio at pressures and temperatures lower than those that would be encountered in a future wave rotor/demonstrator engine test. Lewis and the Allison Engine Company are collaborating to investigate wave rotor integration in an existing turboshaft engine.

Recent theoretical efforts include simulating wave rotor dynamics (e.g., startup and load-change transient analysis, see ref. 5), modifying the one-dimensional wave rotor code to simulate combustion internal to the wave rotor, and developing an analytical wave rotor design/analysis tool based on macroscopic balances for parametric wave rotor/engine analysis.



Left: Brush seals have been added to the three-port rotor experiment. These seals prevent leakage from the passages to the surrounding cavity but do not affect circumferential (i.e., passage to passage) leakage. The seals improved the performance significantly at large values of the rotor to end-wall gap spacing, but they had less of an effect at small values of gap spacing. Right: Three-port wave rotor rig.

References

1. Welch, G.E.; Jones, S.M.; and Paxson, D.E.: Wave Rotor-Enhanced Gas Turbine Engines. AIAA Paper 95-2799 (NASA TM-106998 and ARL-TR-806), 1995.
2. Paxson, D.E.: A Comparison Between Numerically Modelled and Experimentally Measured Loss Mechanisms in Wave Rotors. AIAA Paper 93-2522 (NASA TM-106279), 1993.
3. Wilson, J.; and Paxson, D.E.: Optimization of Wave Rotors for Use as Gas Turbine Engine Topping Cycles. NASA TM-106951, 1995.
4. Welch, G.E.; and Chima, R.V.: Two-Dimensional CFD Modeling of Wave Rotor Flow Dynamics. AIAA Paper 93-3318 (NASA TM-106261), 1993.
5. Paxson, D.E.: A Numerical Model for Dynamic Wave Rotor Analysis. AIAA Paper 95-2800 (NASA TM-106997), 1995.

Lewis contacts: Dr. Jack Wilson, (216) 977-1204, and Dr. Gerard E. Welch, (216) 433-8003
Headquarters program office: OA

Scale-Model, Low-Tip-Speed Turbofan Tested at Simulated Takeoff and Approach Conditions

Tests are currently being performed in the NASA Lewis Research Center's 9- by 15-Foot Low-Speed Wind Tunnel on a Pratt & Whitney designed low-tip-speed fan. The test objectives are to determine the acoustic, aerodynamic, and aeromechanical performance of this low-speed, high-bypass-ratio fan stage. Noise reductions from various combinations of engine nacelle acoustic treatments are also being obtained.

The test rig simulates full-scale engine components in scale-model size. The complete engine fan module (engine nacelle, bypass fan stage, and nozzle), a throughflow core duct, and engine acoustic treatment within the nacelle are all simulated. During the testing, fan model performance is obtained from force balances mounted internally in the model as well as by airflow measurements taken with duct wall and rake instrumentation. The internal force balances consist of a two-component rotating balance to measure thrust and torque and a six-component static balance to measure the drag and torque forces of the bypass stator and nacelle. Far-field acoustic measurements are obtained

by a track-mounted, axially translating microphone. The microphone makes equal-angle stops along the traverse to obtain the noise at simulated takeoff and approach conditions. A rotating microphone array is used in the inlet and exhaust to obtain induct noise measurements for source diagnostic research.

The data obtained during this test will be used by NASA and Pratt & Whitney research engineers to ascertain the benefits of this lower tip speed, high-bypass-ratio fan stage. They will validate computer design and analysis codes used for both fan stage components and acoustic treatment. Comparison of the data with predictions from the computer codes will indicate where these codes can be improved for better performance predictions, lower noise, and better engine designs.



Low-tip-speed fan installed in wind tunnel.

Lewis contacts: Dr. James H. Dittmar, (216) 433-3921, and Robert J. Jeracki, (216) 433-3917
Headquarters program office: OA

First Test of Fan Active Noise Control (ANC) Completed

With the advent of ultrahigh-bypass engines, the space available for passive acoustic treatment is becoming more limited, whereas noise regulations are becoming more stringent. Active noise control (ANC) holds promise as a solution to this problem. It uses secondary (added) noise sources to reduce or eliminate the offending noise radiation.

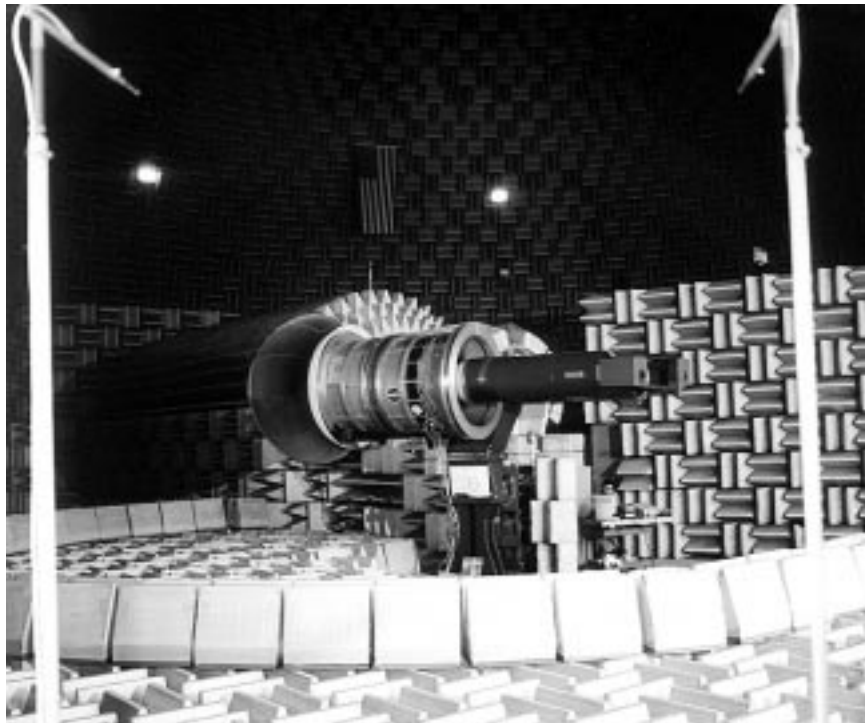
The first active noise control test on the low-speed fan test bed was a General Electric Company system designed to control either the exhaust or inlet fan tone. This system consists of a “ring source,” an induct array of error microphones, and a control computer. Fan tone noise propagates in a duct in the form of spinning waves. These waves are detected by the microphone array, and the computer identifies their spinning structure. The computer then controls the “ring source” to generate waves that have the same spinning structure and amplitude, but 180° out of phase with the fan noise. This computer-generated tone cancels the fan tone before it radiates from the duct and is heard in the far field.

The “ring source” used in these tests is a cylindrical array of 16 flat-plate acoustic radiators that are driven by thin piezoceramic sheets bonded to their back surfaces. The resulting source can produce spinning waves up to mode 7 at levels high enough to cancel the fan tone. The control software is flexible enough to work on spinning mode orders from -6 to 6. In this test, the fan was configured to produce a tone of order 6.

The complete modal (spinning and radial) structure of the tones was measured with two built-in sets of rotating microphone rakes. These rakes provide a measurement of the system performance independent from the control system error microphones. In addition, the far-field noise was measured with a semicircular array of 28 microphones.

This test represents the first in a series of tests that demonstrate different active noise control concepts, each on a progressively more complicated modal structure. The tests are in preparation for a demonstration on a flight-type engine.

**Lewis contact: Larry J. Heidelberg, (216) 433-3859
Headquarters program office: OA**



General Electric Company's active noise control system installed on the 4-ft low-speed fan in Lewis' Aero-Acoustic Propulsion Laboratory.

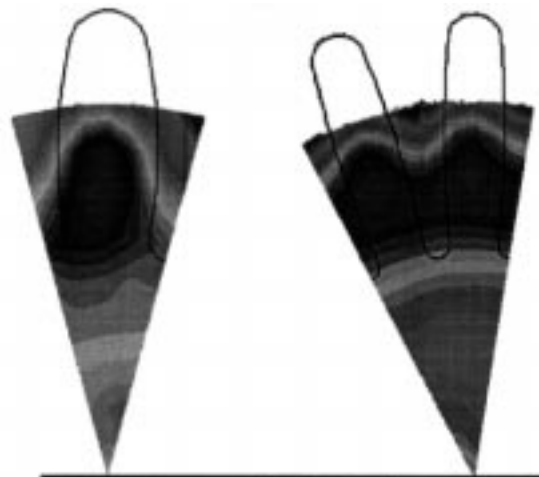
Subsonic Jet Noise Reduced With Improved Internal Exhaust Gas Mixers

Aircraft noise pollution is becoming a major environmental concern for the world community. The Federal Aviation Administration (FAA) is responding to this concern by imposing more stringent noise restrictions for aircraft certification than ever before to keep the U.S. industry competitive with the rest of the world. At the NASA Lewis Research Center, attempts are underway to develop noise-reduction technology for newer engines and for retrofitting existing engines so that they are as quiet as (or quieter than) required. Lewis conducted acoustic and Laser Doppler Velocimetry (LDV) tests using Pratt & Whitney's Internal Exhaust Gas Mixers (IEGM). The IEGM's mix the core flow with the fan flow prior to their common exhaust.

All tests were conducted in Lewis' Aero-Acoustic Propulsion Laboratory—a semihemispheric dome open to the ambient atmosphere. This was the first time Laser Doppler Velocimetry was used in such a facility at Lewis. Jet exhaust velocity and turbulence and the internal velocity fields were detailed. Far-field acoustics were also measured. Pratt & Whitney provided 1/7th scale model test hardware (a 12-lobe mixer, a 20-lobe mixer, and a splitter) for 1.7 bypass ratio engines, and NASA provided the research engineers, test facility, and test time. The Pratt & Whitney JT8D-200 engine power conditions were used for all tests.

The Laser Doppler Velocimetry measurements at the common exhaust nozzle showed the presence of high-velocity regions at the nozzle exit which directly corresponded to the mixer lobes (see figure). The 12-lobe mixer had 12 high-velocity regions, and the 20-lobe mixer had 20. The radial mean velocity between the mixers was nearly equivalent, but it was approximately 300 ft/sec slower than the radial mean velocity with the splitter. The turbulence intensity, with respect to the centerline velocity, reached about 12 percent between the core and the fan shear layer for the splitter. The 20-lobe mixer had about the same intensity, but the 12-lobe mixer had about 16-percent turbulence intensity.

The acoustic data showed that both mixers were quieter than the splitter nozzle. This is a direct consequence of reductions in the mean jet exhaust velocities. The mixing between the core and the fan within the IEGM created the high-frequency noise. The mixing noise for the 12-lobe mixer was higher than that for the splitter, and the 20-lobe mixer had the quietest mixing noise.



Laser Doppler Velocimetry data from the subsonic jet noise program.

When scaled to constant full-scale thrust, the 20-lobe mixer was approximately 7.5 effective perceived noise decibels (EPNdB) quieter than the splitter and approximately 2 EPNdB quieter than the 12-lobe mixer. Efforts are continuing to make these IEGM's reach the Federal Aviation Administration's noise limits. Lewis, in cooperation with industry, is continuing to advance the research and technology to quiet U.S. aircraft engines.

For more information about Laser Doppler Velocimetry and Lewis' Aero-Acoustic Propulsion Laboratory, visit Lewis on the World Wide Web:

<http://www.lerc.nasa.gov/WWW/OptInstr/ldv.html>

<http://www.lerc.nasa.gov/WWW/AFED/facilities/aapl.html>

Lewis contact: Naseem H. Saiyed, (216) 433-6736

(E-Mail: scnasn@lims01.lerc.nasa.gov)

Headquarters program office: OA

Aeropropulsion Facilities and Experiments

Drive Motor Improved for 8- by 6-Foot Supersonic Wind Tunnel/9- by 15-Foot Low-Speed Wind Tunnel Complex

An operational change made recently in the drive motor system for the 8- by 6-Foot Supersonic Wind Tunnel (8x6 SWT)/9- by 15-Foot Low-Speed Wind Tunnel (9x15 LSWT) complex resulted in dramatic power savings and expanded operating range.

The 8x6 SWT/9x15 LSWT complex offers a unique combination of wind tunnel conditions for both high- and low-speed testing. Prior to the work discussed in this article, the 8- by 6-ft test section offered airflows ranging from Mach 0.36 to 2.0. Subsonic testing was done in the 9-ft high, 15-ft wide test area in the return leg of the facility. The air speed in this test section can range from 0 to 175 mph (Mach 0.23).

In the past, we varied the air speed by using a combination of the compressor speed and the position of the tunnel flow-control doors. When very slow speeds were required in the 9x15 LSWT, these large tunnel flow-control doors might be very nearly full open, bleeding off large quantities of air, even with the drive system operating at its previous minimum speed of about 510 rpm. Power drawn during this mode of operation varied between 15 and 18 MW/hr, but clearly much of this power was not being used to provide air that would be used for testing in the test section. The air exiting these large doors represented wasted power.

Early this year, the facility's tunnel drive system was run on one motor instead of three to see if lower drive speeds could be achieved that would, in turn, result in large power savings because unnecessary air would not be blown out of the flow-control doors unnecessarily. In addition, if the drive could be run slower, then slower speeds would also be possible in the 8x6 SWT test section as an added benefit.

Results of the first tests performed early last year showed that in fact the drive, when operating on only one motor, actually reached a steady-state speed of only 337 rpm and drew an amazingly small 6 MW/hr of electrical power. During daytime operation of the drive, this meant that it would be possible to save as much as 10 MW/hr, or nearly \$600 per hour of operation, for many of the 9x15 LSWT's testing regimes.

An added benefit of this power-saving venture was that since the 8x6 SWT and 9x15 LSWT are indeed on a common loop, if the compressor is slowed down to benefit the 9x15 LSWT, then the air moving through the 8x6 SWT is also moving slower than ever before. In fact, testing has proven that the 8x6 SWT can now achieve Mach 0.25, whereas its previous lower limit was Mach 0.36. This added benefit has attracted additional customers.

Find out more about the 8- by 6-Foot Supersonic Wind Tunnel and the 9- by 15-Foot Low-Speed Wind Tunnel on the World Wide Web:

<http://www.lerc.nasa.gov/WWW/AFED/facilities/8x6.html>
<http://www.lerc.nasa.gov/WWW/AFED/facilities/9x15.html>

Lewis contact: Robert R. Smalley, (216) 433-5743
Headquarters program office: OA

Testing Efficiency Improved by Addition of Remote Access Control Room

Because researchers need prompt access to test data and information from testing in aeropropulsion facilities, offsite research engineers usually travel to be present in the facility control room during testing. These travel costs can become quite high for extended test entries. The NASA Lewis Research Center's Remote Access Control Room (RACR) uses off-the-shelf video conferencing software integrated with existing facility data systems to provide access to the test data by networking from virtually anywhere in the country. The system allows research engineers in remote locations to participate in tests and monitor data in real time just as if they were present in the control room.

The concept of remote access to test data is not a new one at Lewis, and access to data has been provided in many different ways. The objective of each solution was to get the data to researchers as quickly as possible to expedite testing. The RACR set out to provide the remote location with all the real-time tools available in the control room. Unlike other implementations, the RACR displays the data as it is being acquired (once per second updates). This includes tabular and graphical data from the steady-state and dynamic data systems. In addition, video data from schlieren, pressure-sensitive paint, or sheet laser systems are included, as well as a video conferencing system to facilitate communications between the two locations. By integrating all these tools on a single workstation, the engineer at the remote location can participate in the test in the same manner as the engineers at the facility.

RACR has already reduced the travel required to support a test. This is increasingly important when budgets are shrinking and the number of industry customers participating is increasing, such as in the High Speed Research (HSR) Program. An added benefit of such a system is that additional engineers, who would not have traveled to the test site, can participate at the remote location. This could increase the level of support and improve testing efficiency for tests that use the Remote Access Control Room. Lewis is planning to expand this capability and provide the service in several other aeropropulsion facilities.

Lewis contact: Robert R. Smalley, (216) 433-5743
Headquarters program office: OA



Remote Access Control Room being used in a recent test at the Abe Silverstein 10- by 10-Foot Supersonic Wind Tunnel.

Interdisciplinary Technology Office

Lewis/ACTS/Boeing Experiment Demonstrates Gigabit Application Using ACTS

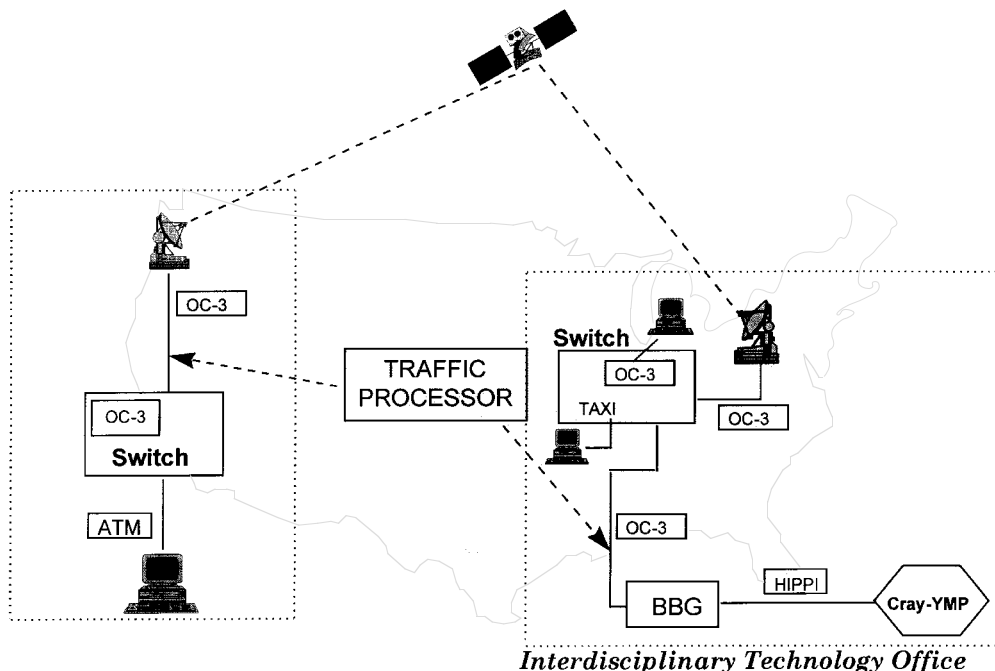
The objective of this project was to demonstrate a satellite-based gigabit application using the Advanced Communications Technology Satellite (ACTS).

To achieve this objective, a series of numerical experiments were conducted to develop an engine inlet control system for the High Speed Research (HSR) Program. An inlet simulator was run on the NASA Lewis Research Center's Cray YMP supercomputer but was controlled by Boeing Corporation in Seattle, Washington. Flow visualization information was transported via ACTS to the remote site for display on a high-performance, three-dimensional graphics workstation. This enabled control system design parameters to be varied for rapid evaluation of the integrated inlet/control system performance. The experimental ACTS network allowed remote access of NASA's distributed engine simulation application to aerospace manufacturers.

Synchronous optical networks (SONET)/asynchronous transfer mode (ATM) traffic studies were performed on this unique experimental network to evaluate the network performance. The experimental SONET/ATM network's performance for this and other applications was characterized experimentally.

Accomplishments

- This was the first high-data-rate experiment to use ACTS.
- It was the first experiment to provide end-to-end ATM connectivity across the United States.
- Computational fluid dynamics simulation results were used to validate experimental data from Lewis' 10- by 10-Foot Supersonic Wind Tunnel. Computational fluid dynamics simulations and windtunnel tests at Lewis were evaluated and controlled simultaneously from the same room at Boeing Corporation in Seattle.
- Reportedly, Lewis was the first site in the United States to deploy the high-performance gigabit router ("GigaRouter") from NETSTAR.
- Lewis was the first site to use the Bus Based Gateway (BBG) developed by Cray Research, Inc. The BBG, which was designed and developed for this experiment, is now commercially available from Cray Research, Inc., as a high-performance parallel interface (HiPPI)-ATM/SONET adapter.
- Bellcore designed and developed the traffic processor for this experiment. This processor can collect ATM cell-level statistics and shape traffic on the basis of



Layout of Lewis/ACTS/Boeing experiment.

specific algorithms. A more refined version that supports OC48 speeds is being built for the NECTAR project.

Significance of the Work

The Lewis/ACTS/Boeing experiment

- Reduced the amount of wind tunnel test time required to develop inlet control systems for high-speed engines
- Supported the High Speed Research Project inlet downselect milestone at the end of 1995
- Assessed the effect of the propagation delay on the performance of distributed computing applications
- Identified key issues in developing reliable, high-speed communication transfer protocols for aerospace applications

For more information about this experiment, visit our site on the World Wide Web:

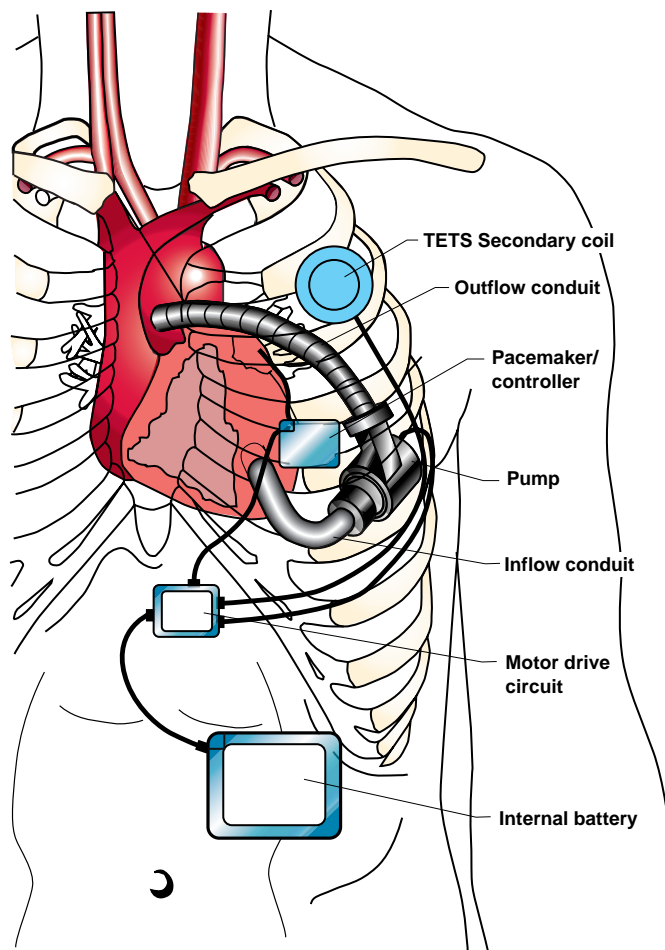
http://www.lerc.nasa.gov/WWW/NPSS/html/nps_bellcore.html

Lewis contact: Isaac López, (216) 433-5893
Headquarters program office: OA (HPCCO)

Heart Pump Design for Cleveland Clinic Foundation

Through a Lewis CommTech Program project with the Cleveland Clinic Foundation, the NASA Lewis Research Center is playing a key role in the design and development of a permanently implantable, artificial heart pump assist device. Known as the Innovative Ventricular Assist System (IVAS), this device will take on the pumping role of the damaged left ventricle of the heart. The key part of the IVAS is a nonpulsatile (continuous flow) artificial heart pump with centrifugal impeller blades, driven by an electric motor. Lewis is part of an industry and academia team, led by the Ohio Aerospace Institute (OAI), that is working with the Cleveland Clinic Foundation to make IVAS a reality. This device has the potential to save tens of thousands of lives each year, since 80 percent of heart attack victims suffer irreversible damage to the left ventricle, the part of the heart that does most of the pumping.

Impeller blade design codes and flow-modeling analytical codes will be used in the project. These codes were developed at Lewis for the aerospace industry but will be applicable to the IVAS design project. The



"Published with permission of The Cleveland Clinic Foundation"

Lewis/Cleveland Clinic Foundation heart pump. Top: photo, Bottom: sketch showing placement.

analytical codes, which currently simulate the flow through the compressor and pump systems, will be used to simulate the flow within the blood pump in the artificial heart assist device. The Interdisciplinary Technology Office heads up Lewis' efforts in the IVAS project. With the aid of numerical modeling, the blood pump will address many design issues, including some fluid-dynamic design considerations that are unique to the properties of blood. Some of the issues that will be addressed in the design process include hemolysis, deposition, recirculation, pump efficiency, rotor thrust balance, and bearing lubrication. Optimum pumping system performance will be achieved by modeling all the interactions between the pump components. The interactions can be multidisciplinary and, therefore, are influenced not only by the fluid dynamics of adjacent components but also by thermal and structural effects.

Lewis-developed flow-modeling codes to be used in the pump simulations will include a one-dimensional code (ref. 1) and an incompressible three-dimensional Navier-Stokes flow code (ref. 2). These codes will analyze the prototype pump designed by the Cleveland Clinic Foundation. With an improved understanding of the flow phenomena within the prototype pump, design changes to improve the performance of the pump system can be verified by computer prior to fabrication in order to reduce risks. The use of Lewis flow modeling codes during the design and development process will improve pump system performance and reduce the number of prototypes built in the development phase.

The first phase of the IVAS project is to fully develop the prototype in a laboratory environment that uses a water/glycerin mixture as the surrogate fluid to simulate blood. A later phase of the project will include testing in animals for final validation. Lewis will be involved in the IVAS project for 3 to 5 years.

References

1. Veres, J.P.: Centrifugal and Axial Pump Design and Off-Design Performance Prediction. NASA TM-106745, 1995.
2. Hah, C.: Calculation of Three-Dimensional Viscous Flows in Turbomachinery With an Implicit Relaxation Method. *J. Propulsion*, Sept.-Oct., vol. 3, no. 5, 1987.

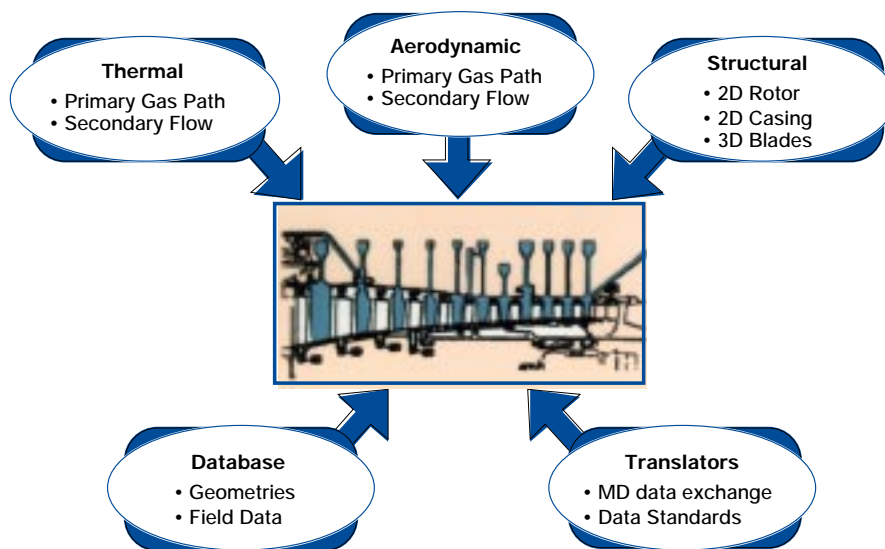
Lewis contact: Joseph P. Veres, (216) 433-2436
Headquarters program office: OA (HPCCO)

Coupled Aerodynamic-Thermal-Structural (CATS) Analysis

Coupled Aerodynamic-Thermal-Structural (CATS) Analysis is a focused effort within the Numerical Propulsion System Simulation (NPSS) program to streamline multidisciplinary analysis of aeropropulsion components and assemblies. Multidisciplinary analysis of axial-flow compressor performance has been selected for the initial focus of this project. CATS will permit more accurate compressor system analysis by enabling users to include thermal and mechanical effects as an integral part of the aerodynamic analysis of the compressor primary flowpath. Thus, critical details, such as the variation of blade tip clearances and the deformation of the flowpath geometry, can be more accurately modeled and included in the aerodynamic analyses. The benefits of this coupled analysis capability are (1) performance and stall line predictions are improved by the inclusion of tip clearances and hot geometries, (2) design alternatives can be readily analyzed, and (3) higher fidelity analysis by researchers in various disciplines is possible. The goals for this project are a 10-percent improvement in stall margin predictions and a 2:1 speed-up in multidisciplinary analysis times.

Working cooperatively with Pratt & Whitney, the Lewis CATS team defined the engineering processes and identified the software products necessary for streamlining these processes. The basic approach is to integrate the aerodynamic, thermal, and structural computational analyses by using data management and Non-Uniform Rational B-Splines (NURBS) based data mapping. Five software products have been defined for this task: (1) a primary flowpath data mapper, (2) a two-dimensional data mapper, (3) a database interface, (4) a blade structural pre- and postprocessor, and (5) a computational fluid dynamics code for aerothermal analysis of the drum rotor.

Thus far (1) a cooperative agreement has been established with Pratt & Whitney, (2) a Primary Flowpath Data Mapper has been prototyped and delivered to General Electric Aircraft Engines and Pratt & Whitney for evaluation, (3) a collaborative effort has been initiated with the National Institute of Standards and Testing to develop a Standard Data Access Interface, and (4) a blade tip clearance capability has been implemented into the Structural Airfoil Blade Engineering Routine (SABER) program.



CATS system components.

We plan to continue to develop the data mappers and data management tools. As progress is made, additional efforts will be made to apply these tools to propulsion system applications.

More information about the CATS analysis is available on the World Wide Web:

<http://www.lerc.nasa.gov/WWW/NPSS/CATS/Requirements/requirements.book.html>

Lewis contact: Dr. Charles Lawrence, (216) 433-6048
Headquarters program office: OA (HPCCO)

NASA Lewis IITA Kindergarten to 12th Grade Program

Objectives

The NASA Lewis Research Center's Information Infrastructure Technology and Applications for Kindergarten to 12th Grade (IITA K-12) Program is designed to introduce into school systems computing and communications technology that benefits math and science studies. By incorporating this technology into K-12 curriculums, we hope to increase the proficiency and interest in math and science subjects by K-12 students so that they continue to study technical subjects after their high school careers are over.

Approach

To accomplish this, we give K-12 teachers hands-on instruction on Macintosh software applications and

Internet navigation. We offer formal 2-week training during the summer and other workshops throughout the school year.

Lewis' IITA K-12 Program includes research on the most cost-effective means to connect schools to the Internet. Radio frequency datalink and integrated services digital network (ISDN) technologies have been deployed in area schools as prototypes. Data such as reliability, capacity, and scalability of the technologies are being collected to determine the overall efficiency of the connections.

Thirteen schools have been identified as partner schools with Lewis' IITA K-12 Program. These schools have received Macintosh workstations, software, and network connections. In return, the teachers from these schools are developing instructional materials that use computer technology. This material will be disseminated to other K-12 schools.

Fiscal 1995 Accomplishments

- A Classroom of Excellence equipped with eight Macintosh workstations was built at the NASA Lewis Visitors Center, the location for all the teacher training.
- Sixty people attended the K-12 Technology Forum. Speakers from Government agencies, educational institutions, and industry gave presentations on their technical K-12 programs.

- The IITA K-12 Summer Teacher Training was held from July 24 to August 4. Thirteen teachers from ten different schools were trained on Macintosh software applications and Internet access and navigation. In the summer, the K-12 program ran its first Student Summer Camp where students attended workshops on various computer-related topics and completed a project using the skills they had learned.
- Three schools were connected to the Internet via a radiofrequency datalink and three via an ISDN line.
- The Lewis IITA K-12 Program sponsors a wind tunnel project, where with teacher guidance, students construct a small-scale wind tunnel. Two schools are currently participating in this program—Barberton High School and General Benjamin O. Davis Jr. Aviation High School.

Lewis' IITA K-12 Program was a catalyst for many of the teachers who were in the program to implement technology into their schools and classrooms in various ways. Barberton High School now has a supercomputing class that was developed and implemented by the Barberton teacher in our program. Two schools have established local area networks within their schools; these were set up by teachers in our programs and paid for by matching funds. General Benjamin O. Davis Jr. Aviation High School is using the wind tunnel project to help them develop a new technology curriculum.

Future Plans

The Classroom of Excellence will be opened in the Winter of 1996. There, teachers will be able to attend various computer-related workshops, preview new software and technologies, and develop classroom projects during open lab time.

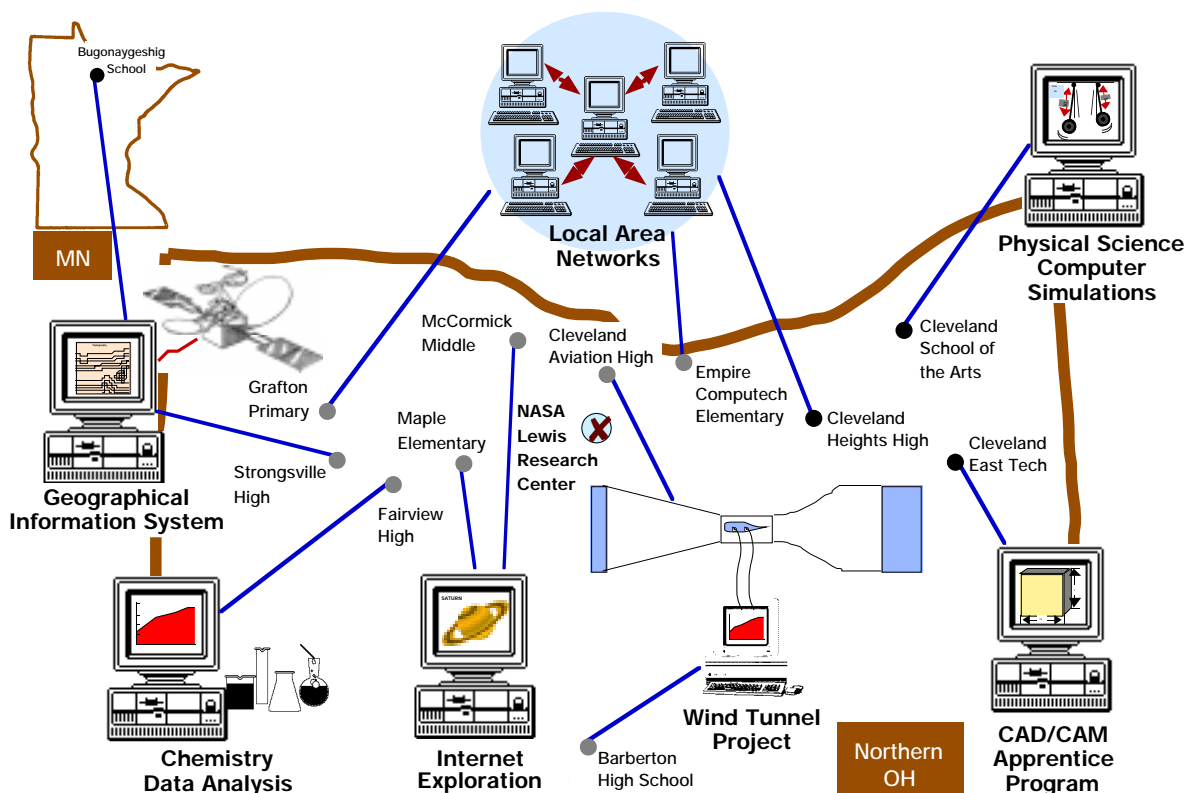
Five area schools will participate in a networking collaboration. These schools will be identified as Internet hubs, and a teacher from each school will be trained as a system administrator.

This year, the wind tunnel project will focus on developing classroom projects and experiments that use the wind tunnel to demonstrate aerodynamic principles.

For more information about Lewis' IITA K-12 Program, visit our site on the World Wide Web:

http://www.lerc.nasa.gov/WWW/K-12/K-12_homepage.html

**Lewis contact: Beth Lewandowski, (216) 433-8873
Headquarters program office: OA (HPCCO)**



Lewis' IITA K-12 Program.

1995 R&T Aerospace Technology

Materials

Advanced High Temperature Engine Materials Technology Progresses

The objective of the Advanced High Temperature Engine Materials Technology Program (HITEMP) is to generate technology for advanced materials and structural analysis that will increase fuel economy, improve reliability, extend life, and reduce operating costs for 21st century civil propulsion systems. The primary focus is on fan and compressor materials (polymer-matrix composites—PMC's), compressor and turbine materials (superalloys, and metal-matrix and intermetallic-matrix composites—MMC's and IMC's) and turbine materials (ceramic-matrix composites—CMC's). These advanced materials are being developed by in-house researchers and on grants and contracts.

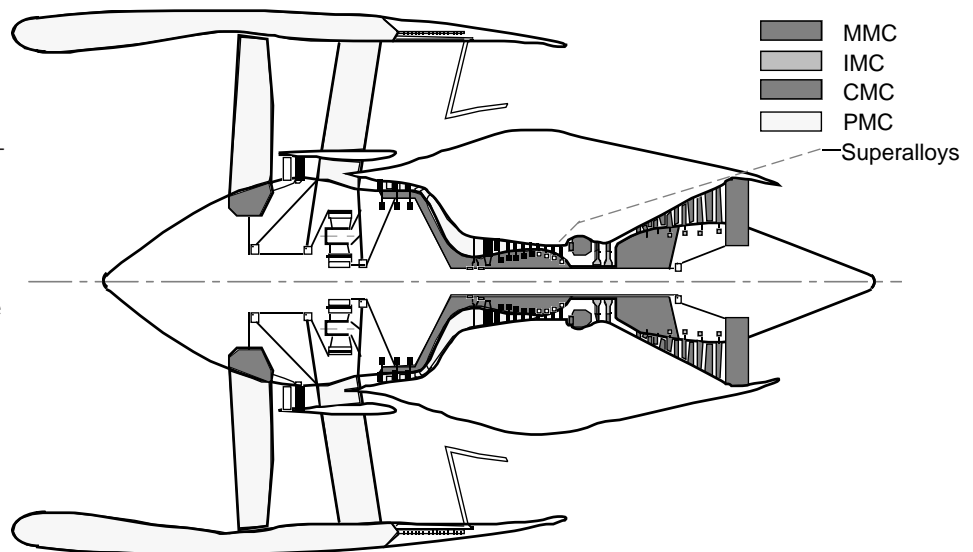
NASA considers this program to be a focused materials and structures research effort that builds on our base research programs and supports component-development projects. HITEMP is coordinated with the Advanced Subsonic Technology (AST) Program and the Department of Defense/NASA Integrated High-Performance Turbine Engine Technology (IHPTET) Program. Advanced materials and structures technologies from HITEMP may be used in these future applications.

Recent technical accomplishments have not only improved the state-of-the-art but have wide-ranging applications to industry. A high-temperature thin-film strain gage was developed to measure both dynamic and static strain up to 1100 °C (2000 °F). The gage's unique feature is that it is minimally intrusive. This technology, which received a 1995 R&D 100 Award, has been transferred to AlliedSignal Engines, General Electric Company, and Ford Motor Company. Analytical models developed at the NASA Lewis Research Center were used to study Textron Specialty

Materials' manufacturing process for titanium-matrix composite rings. Implementation of our recommendations on tooling and processing conditions resulted in the production of defect-free rings. In the Lincoln Composites/AlliedSignal/Lewis cooperative program, a composite compressor case is being manufactured with a Lewis-developed matrix, VCAP. The compressor case, which will reduce weight by 30 percent and costs by 50 percent, is scheduled to be engine tested in the near future.

The annual review of the HITEMP program was held October 24 to 25, 1995. Details of research accomplishments are published in the conference report HITEMP Review 1995, NASA CP-10178. (Available to U.S. citizens only. Permission to use this material was granted by Hugh R. Gray, January 1996.)

Lewis contacts: Dr. Hugh R. Gray, (216) 433-3230, and Carol A. Ginty, (216) 433-3335
Headquarters program office: OA



Advanced materials for 21st century civil propulsion systems with greatly increased fuel economy, improved reliability, extended life, and reduced operating costs.

Stereo Imaging Velocimetry

Stereo imaging velocimetry (SIV) will permit the collection of quantitative, three-dimensional flow data from any optically transparent fluid that can be seeded with tracer particles. This includes such diverse experiments as the study of multiphase flow, bubble nucleation and migration, pool combustion, and crystal growth. This technique will be useful to the microgravity science community as our investigations of fluid behavior in reduced-gravity environments enhance our knowledge of heat transfer, surface tension, concentration-gradient-driven anomalies, and residual effects from g-jitter.

In its proposed configuration, the NASA Lewis Research Center's Stereo Imaging Velocimeter will consist of at least two charged coupled device (CCD) cameras, oriented at some relative angle with respect to each other. The cameras will observe a fluid experiment that has been seeded with tracer particles that are neutrally buoyant to permit accurate flow tracking. Except for the tracer particles, this measurement technique will be nonintrusive. Velocity accuracies will be on the order of 1 to 5 percent of full field. Each camera will make a two-dimensional record of the motion of the seed particles in the observation volume. Three-dimensional data will be obtained by computationally combining the two-dimensional information.

Stereo imaging velocimetry subdivides into several problems:

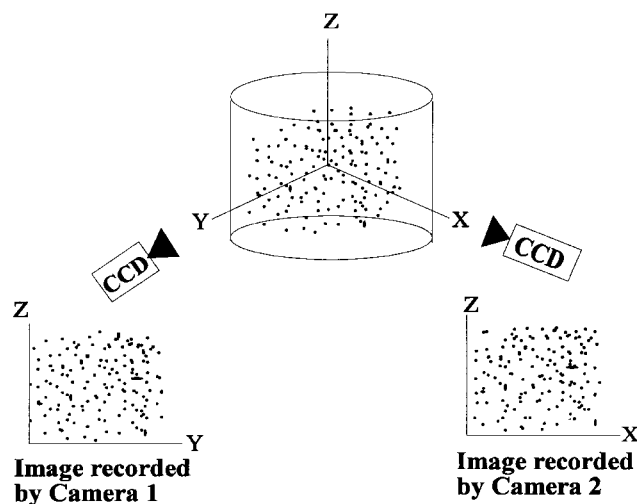
- Camera calibration
- Centroid determination with overlap decomposition
- Particle tracking
- Stereo matching
- User interface
- Testing and error analysis

Benefits

- Stereo imaging velocimetry provides a diagnostic tool for quantitative and qualitative characterization of fluid flows.
- Stereo imaging velocimetry permits direct comparison between computed and experimentally measured three-dimensional flows.
- A PC-based stereo imaging velocimetry applications package is available for incorporation into fluid experiments.

Technology Transfer Highlight

LTV Steel company has requested Lewis' assistance in measuring velocities and flow patterns in a scaled-water model of a submerged entry nozzle and mold of a continuous casting machine. Velocity measurement is being pursued in an attempt to better understand the effects of the submerged entry nozzle design, throughput, depth, and mold width. LTV's ultimate goal is to develop new nozzle designs and casting practices to optimize flow in the mold and reduce defects in as-cast slabs.



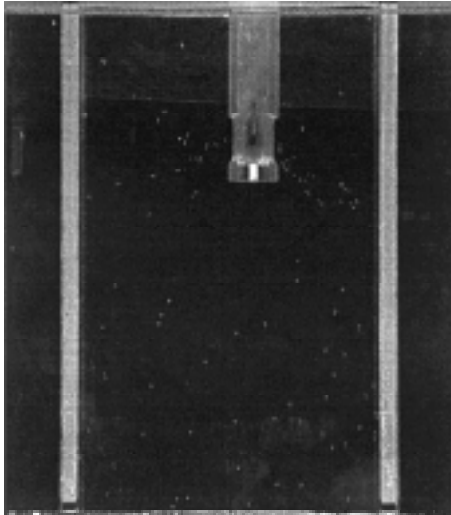
Top: Fluid experiment seeded with tracer particles. Bottom: SIV three-dimensional velocity vectors.

Source of Scatter in the Creep Lives of NiAl(Hf) Single Crystals Revealed

In recent years, there has been an increased emphasis in developing NiAl-based alloys for high-temperature applications in aircraft engines (ref. 1). In comparison to commercial superalloys, binary NiAl has a higher melting temperature, lower density, larger thermal conductivity, and better oxidation resistance. These properties make it a desirable material to replace superalloys as blades and vanes in aircraft engines. Despite this attractive combination of properties, binary NiAl cannot be used as a reliable structural material because of its low-temperature brittleness and poor high-temperature creep strength.

GE Aircraft Engines in Cincinnati, Ohio, has recently developed NiAl(Hf) alloys that have creep strengths comparable to commercial superalloys while maintaining the other desirable properties of binary NiAl. The microstructures of these alloys consist of finely distributed G-phase ($\text{Ni}_{16}\text{f}_6\text{Si}_7$) precipitates, which strengthen the NiAl matrix. However, while the creep properties of these alloys were being evaluated, considerable scatter was observed in the creep lives of specimens tested under identical stress and temperature conditions. Although these alloys had nominally the same composition, the test specimens were obtained from four different ingots (A, B, C, and D) that had been heat treated under similar conditions. The NASA Lewis Research Center began the present study at the request of GE Aircraft Engines under a Space Act Agreement to identify the source of this scatter.

Detailed fracture and microstructural analyses of the failed specimens and the original ingots were conducted in this study. The fracture analysis revealed that, except in one instance, the failure could not be traced to any extrinsic defects, such as shrinkage porosity, machining cracks, or large particles. Instead, an analysis of the creep data revealed an inverse linear correlation between the creep ductility and creep life (see figure), thereby suggesting that the source of the scatter was somehow related to factors affecting the deformation behavior of the material rather than any random occurrence. In addition, the geometry of the fracture surfaces of the specimens with shorter creep lives were more elliptical than those with longer creep lives. This observation suggested that specimens with shorter creep lives had deformed by single slip, whereas those with longer lives had deformed by normal multiple slip. Evidence for the latter slip morphology was confirmed by scanning electron microscopy. Another important clue was provided by the creep data, which revealed that the two specimens

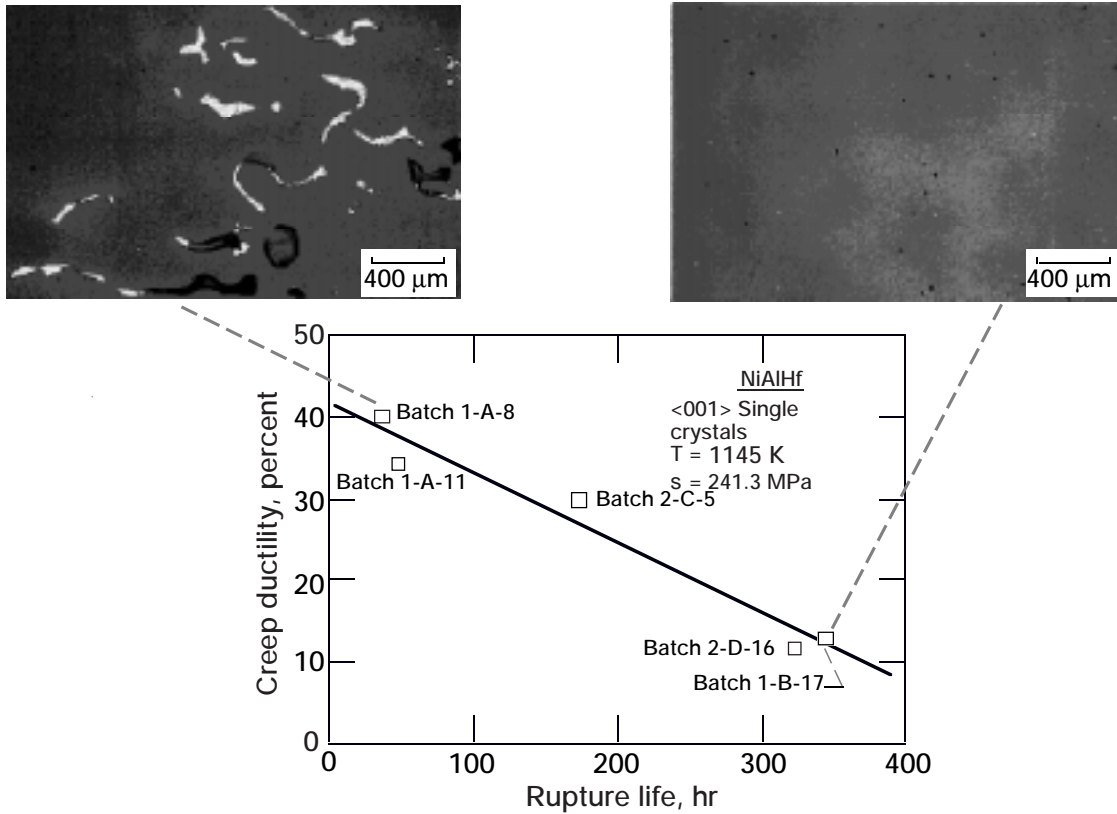


Continuous casting model showing raw vectors (top) and SIV vectors (bottom).

SIV will give LTV advantages over previous qualitative analyses of mold flow (dye injection and video taping). It will provide vector maps of the mold flow which show the direction and magnitude of the flow; these parameters have never been seen with dye injection. In addition, SIV-generated flow-field data will provide more data points for verification and for mathematical models.

Find out more about SIV on the World Wide Web:
<http://sarah.lerc.nasa.gov/~msbeth/siv1.html>

Lewis contact: Mark D. Bethea, (216) 433-8161
(E-Mail: msbeth@bomani.lerc.nasa.gov)
Headquarters program office: OLMSA (MSAD)



Scatter in the creep rupture lives and creep ductility between four batches of a NiAl(Hf) alloy after deformation at 1145 K under an initial stress of 241.3 MPa.

with the shortest lives had been machined from the same ingot. Therefore, it became clear that the scatter in the creep lives resulted from differences in the microstructure probably due to differences in melting and heat-treatment practices.

Transmission electron microscopy revealed that specimens with short creep lives contained large amounts of undissolved Hf-rich particles segregated in the interdendritic regions. In contrast, the densities of these particles were much smaller in specimens with longer creep lives. The presence of these Hf-rich particles appeared to influence the creep behavior of these alloys in two ways. First, the particles depleted the surrounding matrix of Hf, and possibly Si, which in turn resulted in a lower density of the strengthening G-phase precipitates in comparison to the portions of the matrix that were far away from the particles.

Second, the large particles appeared to significantly bias the stress fields around them, which in extreme cases resulted in a deviation from multiple slip behavior to single slip behavior. Therefore, we concluded that the scatter in the creep lives was due to improper heat-treatment conditions that left undissolved Hf-rich particles in some of the ingots. In response to these findings, GE Aircraft Engines is modifying their heat treatment and processing schedules to reduce scatter in the creep lives of these alloys to within acceptable limits.

Lewis contacts: Dr. Sai V. Raj, (216) 433-8195, and Dr. Anita Garg, (216) 433-8908
Headquarters program office: OA

Creep Testing of High-Temperature Cu-8 Cr-4 Nb Alloy Completed

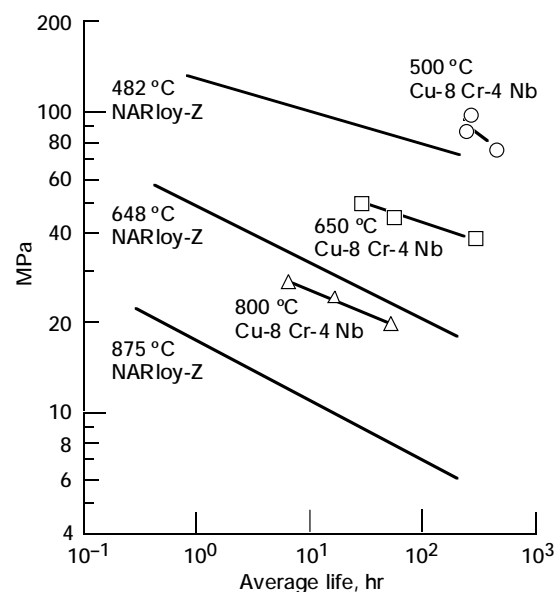
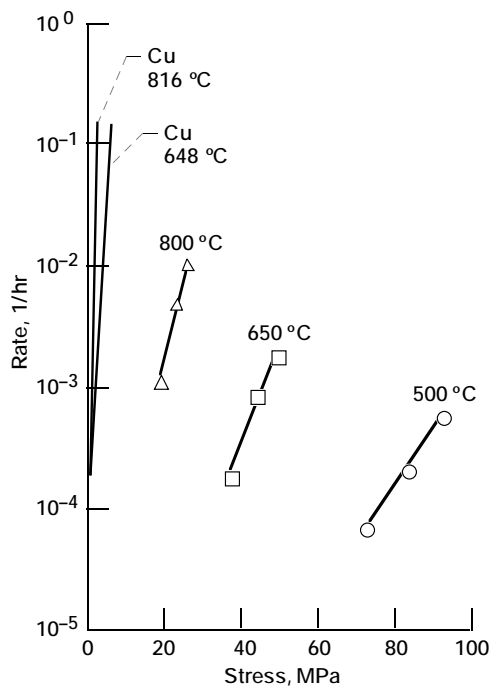
A Cu-8 at.% Cr-4 at.% Nb (Cu-8 Cr-4 Nb) alloy is under development for high-temperature, high-heat-flux applications, such as actively cooled, hypersonic vehicle heat exchangers and rocket engine combustion chambers. Cu-8 Cr-4 Nb offers a superior combination of strength and conductivity. It has also shown exceptional low-cycle fatigue properties. Following preliminary testing (ref. 1) to determine the best processing route, a more detailed testing program was initiated to determine the creep lives and creep rates of Cu-8 Cr-4 Nb alloy specimens produced by extrusion.

Testing was conducted at the NASA Lewis Research Center with constant-load vacuum creep units. Considering expected operating temperatures and mission lives, we developed a test matrix to accurately determine the creep properties of Cu-8 Cr-4 Nb between 500 and 800 °C. Six bars of Cu-8 Cr-4 Nb were extruded. From these bars, 54 creep samples were machined and tested.

The figure on the left shows the steady-state, or second-stage, creep rates for the samples. Comparison data for NARloy-Z (Cu-3 wt % Ag-0.5 wt % Zr), the alloy currently used in combustion chamber liners, were not available. Therefore the steady-state creep rates for Cu at similar temperatures are presented (ref. 2). As expected, in comparison to pure Cu, the creep rates for

Cu-8 Cr-4 Nb are much lower. The lives of the samples are presented in the figure on the right. As shown, Cu-8 Cr-4 Nb at 800 °C is comparable to NARloy-Z at 648 °C. At equivalent temperatures, Cu-8 Cr-4 Nb enjoys a 20 to 50 percent advantage in stress for a given life and 1 to 3 orders of magnitude greater life at a given stress. The improved properties allow for design tradeoffs and improvements in new and existing heat exchangers such as the next generation of combustion chamber liners.

Currently, two companies are interested in the commercial usage of the Cu-8 Cr-4 Nb alloy. The Rocketdyne Division of Rockwell International is conducting independent testing to analyze the properties for their projected needs in advanced rocket engine applications. Metallamics, a company based in Traverse City, Michigan, is entering into a Space Act Agreement to evaluate and test Cu-Cr-Nb alloys as materials for welding electrodes that are used in robotic welding operations. Creep rate is one of the alloy properties that determines the degree to which a welding electrode will mushroom or expand at the tip. A material with a low creep rate will resist mushrooming and give the electrode a longer life, minimizing downtime. This application holds the potential for large-scale usage of the alloy in the automotive and other industries. Success here would dramatically decrease the cost of the alloy and increase availability for aerospace applications.



Left: Average creep rates for Cu-8 Cr-4 Nb and pure Cu. Right: Average creep lives for Cu-8 Cr-4 Nb and NARloy-Z.

References

1. Ellis, D.L.; Michal, G.M.; and Dreshfield, R.L.: A New Copper-Based Alloy for High-Temperature Applications. *Matls. Tech.*, vol. 10, no. 5/6, May-June, 1995, pp. 92-93.
2. McDanel, D.L.; Signorelli, R.A.; and Weeton, J.W.: NASA TN D-4173, 1967.

Lewis contact: Dr. David L. Ellis, (216) 433-8736
Headquarters program office: OA

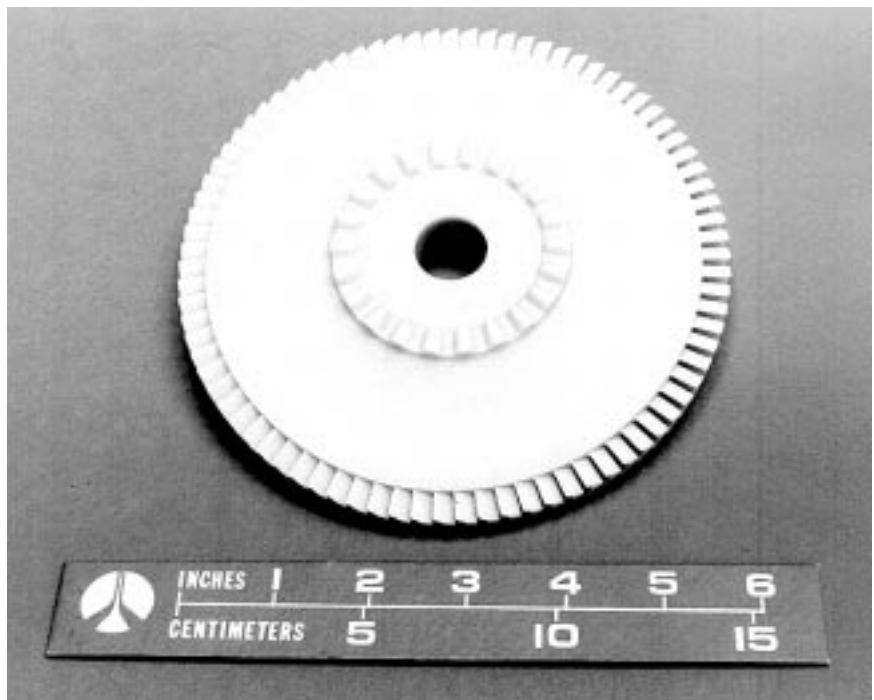
Ceramic Composites Used in High-Speed Turbines for Rocket Engines

Ceramic matrix composite (CMC) technology offers many benefits for liquid-fueled rocket engines. Analyses show that components made from fiber-reinforced ceramic matrix composites (FRCMC's) offer the opportunity for revolutionary gains in turbomachinery performance. In addition, they offer reduced weight and the potential for longer life and lower operating costs. A NASA-sponsored turbopump development effort, conducted at Rocketdyne with parallel material characterization at the NASA Lewis Research Center, confirmed the potential to use FRCMC's for complex turbomachinery components.

The selected FRCMC, C/SiC, is a two-dimensional carbon-fiber-reinforced silicon carbide prepared by chemical vapor infiltration. Results to date on two-dimensional C/SiC coupons and airfoil shapes are encouraging and support the eventual application of FRCMC in advanced rocket engines. Resistance of test coupons to thermal and mechanical fatigue is outstanding, and their ability to survive in a hydrogen-rich steam environment is very good. However, several issues require resolution. Fatigue tests were conducted on representative specimens, but these were limited to a maximum of 10^6 cycles versus a baseline operating life of 10^9 cycles. Also, tests were run independently, and the effects of simultaneous application of thermal and mechanical loads within the combustion environment need to be evaluated.

Available coupon test facilities are limited in their ability to evaluate these combined effects. Subelement tests of stator vanes show the ability of a complex fabricated FRCMC shape to endure severe combined thermal and mechanical loads. Modeling of these subelements validated the ability to analyze these complex materials. However, full-scale turbopump testing will ultimately be required to provide fully representative conditions.

The fabrication and test of a full-scale turbopump component (stator) are the subject of a current program. The stator test is scheduled for early in fiscal 1996 at the Air Force Phillips Laboratory. Pretest and post-test characterizations are being done by the Air Force Wright Laboratories. An unbladed turbine rotor was successfully spun to burst. Burst occurred at 76,889 rpm (128 percent of rated speed) at a projected stress 64 percent greater than the nominal operating stress. The final design of an FRCMC rotor is complete. A selected laser-sintered prototype of this rotor is shown in the figure. Future full-scale component tests of fully bladed rotors will provide the final demonstration of material capability. The next logical step is to fabricate and test a bladed rotor and insert the technology into a flight-scale turbopump.



Selective laser sintered (rapid prototype model) of a fully bladed rotor.

Bibliography

Brockmeyer, J.W.; and Schnittgrund, G.D.: Fiber-Reinforced Ceramic Composites for Earth-to-Orbit Rocket Engine Turbines. Final Report. NASA CR-185264, 1996.

Brockmeyer, J.W.: Ceramic Matrix Composite Applications in Advanced Liquid Fuel Rocket Engine Turbomachinery. ASME, J. Eng. Gas Turbines Power, vol. 115, no. 1, 1993, pp. 58-63.

Eckel, A.J., et al.: Thermal Shock Fiber-Reinforced Ceramic Matrix Composites. Ceram. Eng. Sci. Proc., vol. 13, no. 7-8, 1991, pp. 1500-1508.

Herbell, T.P.; Eckel, A.J.; and Brockmeyer, J.W.: Composites in High Speed Turbines for Rocket Engines. High Temperature High Performance Materials for Rocket Engines and Aerospace Applications. TMS, 1995, pp. 13-20.

Lewis contact: Dr. Thomas P. Herbell, (216) 433-3246
Headquarters program office: OA

Affordable Fiber-Reinforced Ceramic Composites Win 1995 R&D 100 Award

Affordable fiber-reinforced ceramic matrix composites (AFReCC) with high strength and toughness, good thermal conductivity, thermal shock resistance, and oxidation resistance are needed for high-temperature structural applications. AFReCC materials will have various applications in advanced high-efficiency and high-performance engines: that is, the High Speed Civil Transport (HSCT), space propulsion components, and land-based systems. For example, silicon-carbide-fiber-reinforced silicon carbide matrix composites show promise for meeting the criteria of high strength, thermal conductivity, and toughness required for the HSCT combustor liner. AFReCC received R&D Magazine's prestigious R&D 100 Award in 1995.

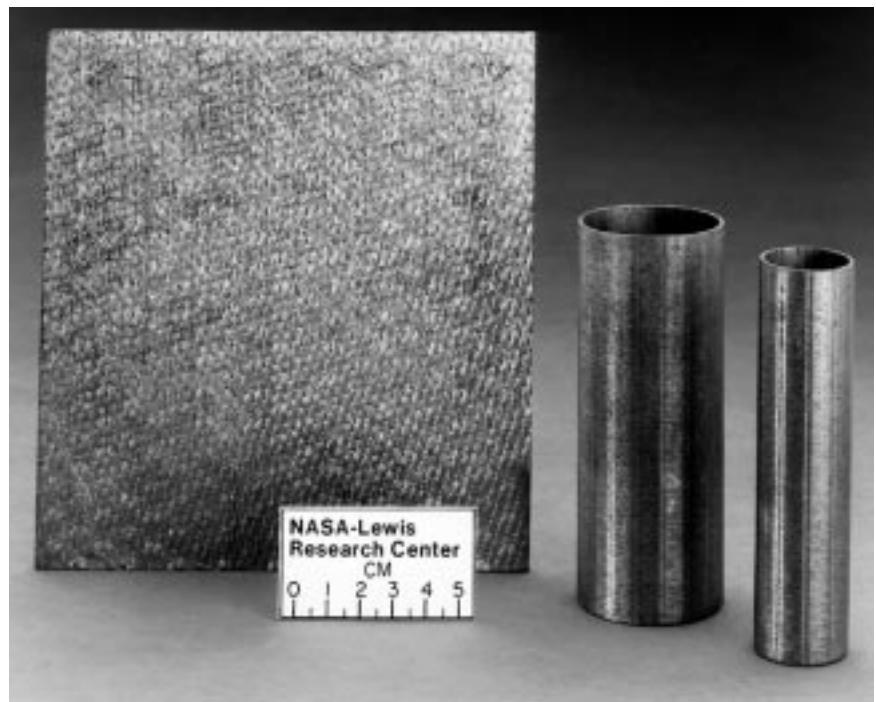
The fabrication process for these composites has three steps. In the first step, fiber preforms are made and chemical vapor infiltration is used to apply the desired interface coating on the fibers. This step also rigidizes the preform. The second step consists of

resin infiltration, which after pyrolysis, yields an interconnected network of porous carbon as the matrix. In the final step of the process, the carbon-containing preform is infiltrated with molten silicon or silicon alloys in a furnace. This converts the carbon to silicon carbide leaving as little as 5 percent residual free silicon or refractory disilicide phase. This process is suitable for any type of small-diameter fiber (e.g., carbon, alumina, or silicon carbide) woven into a two- or three-dimensional architecture. This processing approach leads to dense composites where matrix microstructure and composition can be tailored for optimum properties. It has much lower processing cost (<50 percent) in comparison to other approaches to fabricating silicon-carbide-based composites. The photograph shows the various AFReCC components. Thermomechanical and thermochemical characterization of these composites under the hostile environments that will be encountered in engine applications is underway.

Find out more about the High Speed Civil Transport on the World Wide Web:

<http://www.lerc.nasa.gov/WWW/HSR/hsct.html>

Lewis contact: Dr. Mrityunjay Singh, (216) 433-8883
Headquarters program office: OA



Various AFReCC components.

Thermomechanical Property Data Base Developed for Ceramic Fibers

A key to the successful application of metal and ceramic composite materials in advanced propulsion and power systems is the judicious selection of continuous-length fiber reinforcement. Appropriate fibers can provide these composites with the required thermomechanical performance. To aid in this selection, researchers at the NASA Lewis Research Center, using in-house state-of-the-art test facilities, developed an extensive data base of the deformation and fracture properties of commercial and developmental ceramic fibers at elevated temperatures. Lewis' experimental focus was primarily on fiber compositions based on silicon carbide or alumina because of their oxidation resistance, low density, and high modulus. Test approaches typically included tensile and flexural measurements on single fibers or on multifilament tow fibers in controlled environments of air or argon at temperatures from 800 to 1400 °C. Some fiber specimens were pretreated at composite fabrication temperatures to simulate in situ composite conditions, whereas others were precoated with potential inter-phase and matrix materials.

For application conditions under which the fibers display time-dependent mechanical behavior, tests measured fiber creep, rupture, and stress relaxation properties under constant temperature and stress (or strain) for up to ~100 hr (ref. 1). Because of the many test variables in such studies, mechanism-based analytical models (ref. 2) were developed for these properties. Such models not only allow accurate interpolation of time, temperature, and stress effects within the data set, but also permit prediction of fiber behavior outside the data set (see figure). This modeling capability is particularly important for the time variable because fiber test times are generally much shorter than the service lives required for some advanced heat engine components ($>10^4$ hr).

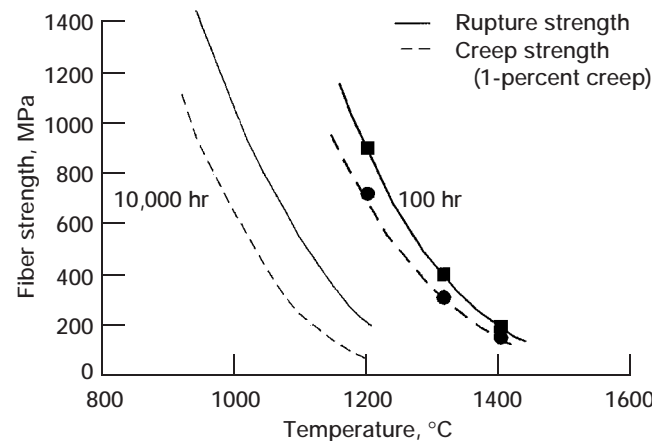
Currently, the thermomechanical property data base and models for a variety of ceramic fibers are publicly available in numerous reports, publications, and review papers (refs. 3 and 4). For component developmental programs outside and within NASA (Enabling Propulsion Materials (EPM) and the Advanced High Temperature Engine Materials Technology Program (HITEMP)), these results are being used by composite designers and fabricators to select the optimum fiber for each application and also by the fiber manufacturers to understand and improve fiber performance. Research at Lewis is continuing in order to expand the

data base and improve the property models, particularly for those fiber types with the most technical potential.

References

1. DiCarlo, J.A.: Property Goals and Test Methods for High Temperature Ceramic Fiber Reinforcement. *Adv. Sci. Tech.* 1995, vol. 7, 1995.
2. DiCarlo, J.A., et al.: Models for the Thermostructural Properties of SiC Fibers. *High Temperature Ceramic-Matrix Composites I*, A.G. Evans and R. Naslain, eds. *Ceramic Trans.*, vol. 57, American Ceramic Society, 1995, pp. 343-348.
3. Tressler, R.E.; and DiCarlo, J.A.: Creep and Rupture of Advanced Ceramic Reinforcements. *High Temperature Ceramic-Matrix Composites II*, A.G. Evans and R. Naslain, eds. *Ceramic Transactions*, vol. 57, American Ceramic Society, 1995, pp. 141-155.
4. DiCarlo, J.A.; and Dutta, S: Continuous Ceramic Fibers for Ceramic Composites. *Handbook on Continuous Fiber-Reinforced Ceramic Matrix Composites*, chapter 4, R.L. Lehman, S.K. El-Rahaiby, and J.B. Wachtman, eds. *Ceramics Information Analysis Center, Purdue University (West Lafayette, IN)*, 1995.

Lewis contact: Dr. James A. DiCarlo, (216) 433-5514
Headquarters program office: OA



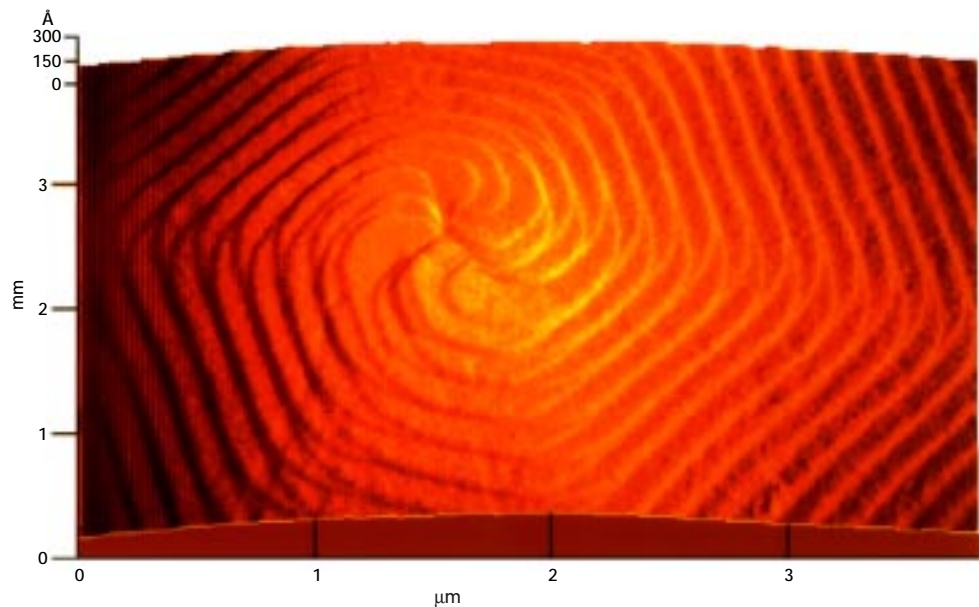
Creep and rupture strengths of Hi-Nicalon silicon carbide fibers for service lives of 10^2 and 10^4 hr. Symbols indicate actual data points and lines indicate predictions from property models.

Silicon Carbide Epitaxial Films Studied by Atomic Force Microscopy

Silicon carbide (SiC) holds great potential as an electronic material because of its wide band gap energy, high breakdown electric field, thermal stability, and resistance to radiation damage. Possible aerospace applications of high-temperature, high-power, or high-radiation SiC electronic devices include sensors, control electronics, and power electronics that can operate at temperatures up to 600° C and beyond. Commercially available SiC devices now include blue light-emitting diodes (LED's) and high-voltage diodes for operation up to 350 °C, with other devices under development (ref. 1). At present, morphological defects in epitaxially grown SiC films limit their use in device applications. Research geared toward reducing the number of structural inhomogeneities can benefit from an understanding of the type and nature of problems that cause defects. The Atomic Force Microscope (AFM) has proven to be a useful tool in characterizing defects present on the surface of SiC epitaxial films.

The in-house High-Temperature Integrated Electronics and Sensors (HTIES) Program at the NASA Lewis Research Center not only extended the dopant concentration range achievable in epitaxial SiC films, but it reduced the concentration of some types of defects (ref. 2). Advanced structural characterization using the AFM was warranted to identify the type and structure of the remaining film defects and morphological inhomogeneities. The AFM can give quantitative information on surface topography down to molecular scales. Acquired, in part, in support of the Advanced High Temperature Engine Materials Technology Program (HITEMP), the AFM had been used previously to detect partial fiber debonding in composite material cross sections (ref. 3).

Atomic force microscopy examination of epitaxial SiC film surfaces revealed molecular-scale details of some unwanted surface features. Growth pits propagating from defects in the substrate, and hillocks due,



Atomic force microscopy image of spiral steps propagating from the peak of a 6H-SiC hillock. Steps, which are produced by a super screw dislocation, evidence anisotropic step-bunching.

presumably, to existing screw dislocations in the substrates, were imaged. Away from local defects, step bunching was observed to yield step heights of hundreds of angstroms, with possible implications for the uniformity of dopants incorporated in SiC devices during fabrication. The quantitative topographic data from the AFM allow the relevant defect information to be extracted, such as the size and distribution of step bunching and the Burgers vector of screw dislocations (ref. 4).

These atomic force microscopy results have furthered the understanding of the dynamic epitaxial SiC growth process. A model describing the observed hillock step bunching has been proposed. This cooperation between researchers involved in crystal growth, electronic device fabrication, and surface structural characterization is likely to continue as atomic force microscopy is used to improve SiC films for high-temperature electronic devices for NASA's advanced turbine engines and space power devices, as well as for future applications in the automotive industry.

References

1. Powell, J.A., et al.: Progress in Silicon Carbide Semiconductor Technology, Mater. Res. Soc. Symp. Proc. vol. 242, 1992, pp. 495-505.

2. Neudeck, P.G., et al.: Greatly Improved 3C-SiC p-n Junction Diodes Grown by Chemical Vapor Deposition, IEEE Electron. Device. Lett., vol. 14, no. 3, 1993, pp. 136-139.
3. Eldridge, J.I.; Abel, P.B.; and Ghosn, L.J.: The Effect of Fiber/Matrix Thermal Expansion Mismatch on Fiber Debond Initiation During Fiber Push-Out. HITEMP Review 1994, NASA CP-10146, Vol. III, 1994, pp. 82-1 to 82-11. (Available to U.S. citizens only. Permission to use this material was granted by Hugh R. Gray, January 1996.)
4. Powell, J.A., et al.: Effect of Tilt Angle on the Morphology of SiC Epitaxial Films Grown on Vicinal (0001) SiC Substrates. Accepted for publication in the Proceedings of the 6th International Conference on Silicon Carbide and Related Materials—1995, Kyoto, Japan, Sept. 18-22, 1995.

Find out more about the AFM on the World Wide Web:
http://www.lerc.nasa.gov/WWW/SurfSci/ssb_siac.html

**Lewis contacts: Phillip B. Abel, (216) 433-6063, and
 J. Anthony Powell, (216) 433-3652
 Headquarters program office: OA**

Self-Lubricating, Wear-Resistant Diamond Films Developed for Use in Vacuum Environment

Diamond's outstanding properties—extreme hardness, chemical and thermal inertness, and high strength and rigidity—make it an ideal material for many tribological applications, such as the bearings, valves, and engine parts in the harsh environment found in internal-combustion engines, jet engines, and space propulsion systems.

It has been demonstrated that chemical-vapor-deposited diamond films have low coefficients of friction (on the order of 0.01) and low wear rates ($<10^{-7}$ mm³/N-m) both in humid air and dry nitrogen but that they have both high coefficients of friction (>0.4) and high wear rates (on the order of 10^{-4} mm³/N-m) in vacuum. It is clear that surface modifications that provide acceptable levels of friction and wear properties will be necessary before diamond films can be used for tribological applications in a spacelike, vacuum environment. Previously, it was found that coatings of amorphous, nondiamond carbon can provide low friction in vacuum. Therefore, to reduce the friction and wear of diamond film in vacuum, carbon ions were

implanted in an attempt to form a surface layer of amorphous carbon phases on the diamond films.

Diamond films with grain sizes ranging from 20 to 3300 nm were deposited on silicon, silicon carbide, and silicon nitride by microwave-plasma-assisted chemical vapor deposition. Carbon ions were implanted into the as-deposited diamond films at an accelerating energy of 60 keV and a current density of 50 $\mu\text{A}/\text{cm}^2$ for approximately 6 min, resulting in a dose of 1.2×10^{17} carbon ions/cm². The substrate temperatures during ion implantation did not exceed 200 °C. The as-deposited and ion-implanted diamond films were characterized at the NASA Lewis Research Center through the use of a variety of techniques—such as scanning and transmission electron microscopy, surface profilometry, and Raman spectroscopy. The friction and wear properties of these films in contact with a natural bulk diamond pin at a mean hertzian contact pressure of 2 GPa were examined in an ultrahigh vacuum of 7×10^{-7} Pa at room temperature.

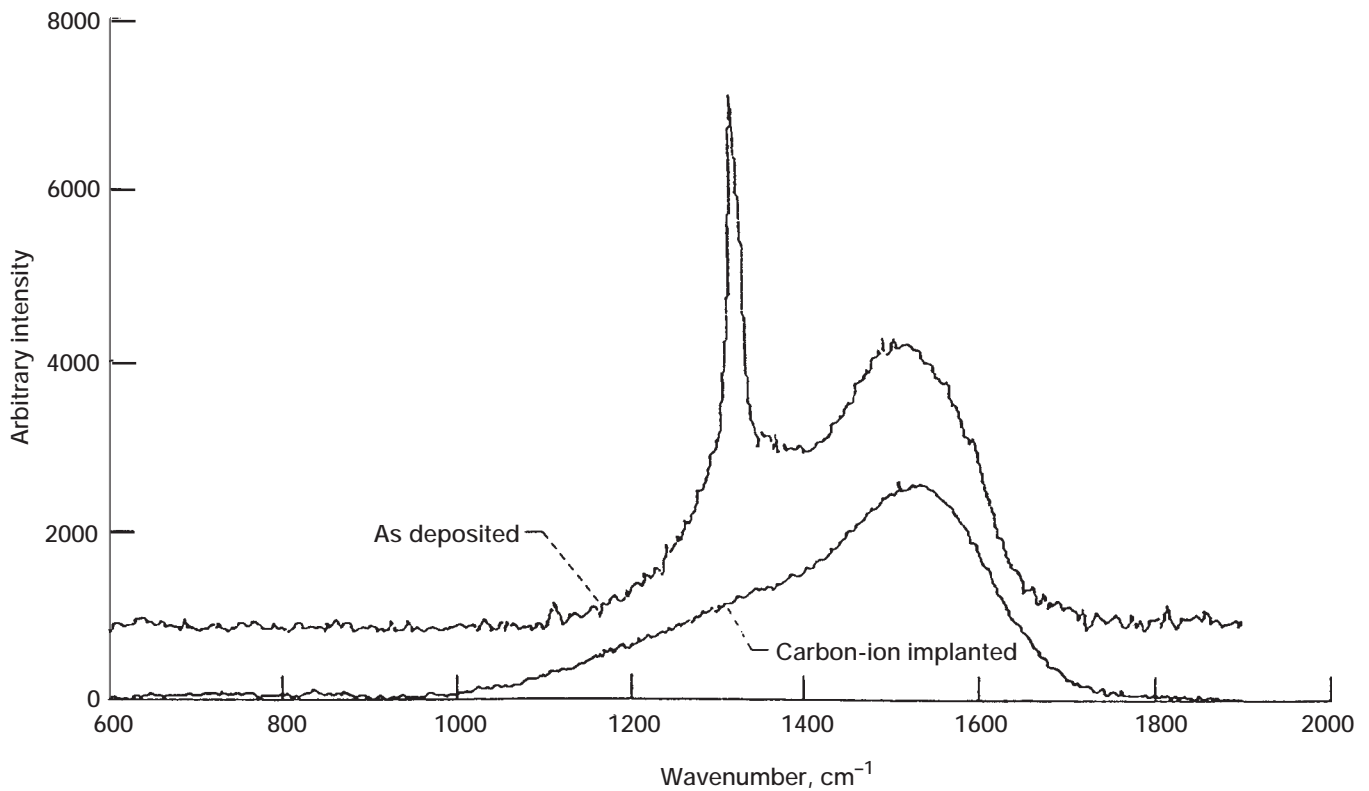
The results indicate that carbon ion implantation structurally modified the diamond lattice and produced a thin surface layer of amorphous, nondiamond carbon (as verified by the Raman data in the figure). The amorphous, nondiamond carbon greatly decreased both the friction and wear of the diamond films. The coefficients of friction for the carbon-ion-implanted, fine-grain diamond films were less than 0.1, factors of 20 to 30 lower than those for the as-deposited, fine-grain diamond films. The coefficients of friction for the carbon-ion-implanted, coarse-grain diamond films were approximately 0.35, a factor of 5 lower than those for the as-deposited, coarse-grain diamond films. The wear rates for the carbon-ion-implanted diamond films were on the order of 10^{-6} mm³/N-m, factors of 30 to 80 lower than those for the as-deposited diamond films, regardless of grain size.

The friction of the carbon-ion-implanted diamond films was greatly reduced because the amorphous, nondiamond carbon, which exhibited a low shear strength, was restricted to the surface layers ($<0.1\text{-}\mu\text{m}$ thick) and because the underlying diamond materials retained their high hardness. The size and morphological characteristics of the wear debris particles were related to the wear rates. Much finer wear particles were generated on the surfaces of the carbon-ion-implanted diamond films than were generated on the surfaces of the as-deposited diamond films. Thus, the carbon-ion-implanted, fine-grain diamond films can be used effectively as wear-resistant, self-lubricating coatings for ceramics, such as silicon nitride and silicon carbide, in ultrahigh vacuum.

Bibliography

Miyoshi, K., et al.: Physical and Tribological Characteristics of Ion-Implanted Diamond Films, NASA TM-106682, Nov. 1994.

Lewis contacts: Dr. Kazuhisa Miyoshi, (216) 433-6078, and Dr. Susan L. Heidger, (216) 433-6057
Headquarters program office: OA



Raman spectra of as-deposited and carbon-ion-implanted, coarse-grain diamond film on an α -SiC substrate. Spectra are vertically displaced for viewing purposes.

Lubricous Deposit Formed In Situ Between Wearing Surfaces at High Temperatures

Many components of future aircraft will be constructed from novel high-temperature materials, such as super-alloys and ceramic composites, to meet expected operating temperatures in excess of 300 °C. There are no known liquid lubricants that can lubricate above 300 °C without significant decomposition. Solid lubricants could be considered, but problems caused by the higher friction coefficients and wear rates of the solid lubricant film make this an undesirable approach. An alternative method of lubrication is currently being investigated: vapor phase lubrication.

In vapor phase lubrication, an organic liquid (in our studies a thioether was used) is vaporized into a flowing air stream that is directed to sliding surfaces where lubrication is needed. The organic vapor reacts at the concentrated contact sliding area generating a lubricous deposit. This deposit has been characterized as a thin polymeric film that can provide effective lubrication at temperatures greater than 400 °C.

Initial tribological studies were conducted at the NASA Lewis Research Center and Cleveland State University with a high-temperature friction and wear tribometer. A cast iron rod was loaded (a 4-kg mass was used to generate a contact pressure of 1.2 MPa) against a reciprocating, cast iron plate at 500 °C. This system

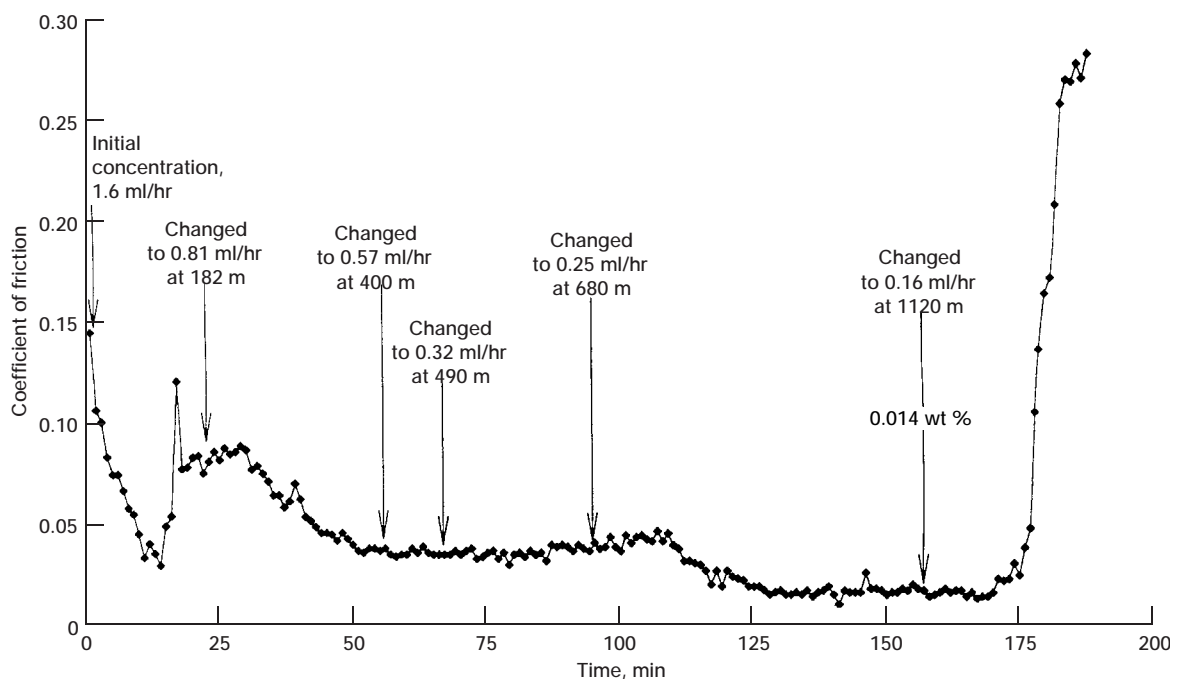
was then lubricated with the vapor phase of thioether. The following results were obtained:

- The deposited film resulted in friction coefficients as low as 0.01.
- Cast iron wear was not detectable.
- The system could self-recover: when the vapor flow was stopped and the system allowed to go into failure (a friction coefficient greater than 0.3), renewal of the vapor flow reduced the friction coefficient back to 0.01.
- The amount of thioether used was 0.014 wt % in air (1.2 ml/hr of lubricant in 2000 ml/min air).

These results were so promising that Cleveland State University filed a patent application listing Dr. Earl Graham (Cleveland State University) and Dr. Wilfredo Morales (NASA Lewis Research Center) as coinventors.

Vapor phase lubrication will not only allow operation at higher temperatures, but it will produce a net savings in weight aboard aircraft because no large oil reservoirs will be needed.

Lewis contact: Dr. Wilfredo Morales, (216) 433-6052
Headquarters program office: OA



Coefficient of friction versus time for various concentrations of thioether in air. Thioether on cast iron; plate temperature, 500 °C; vapor temperature, 400 °C; load, 4 kg.

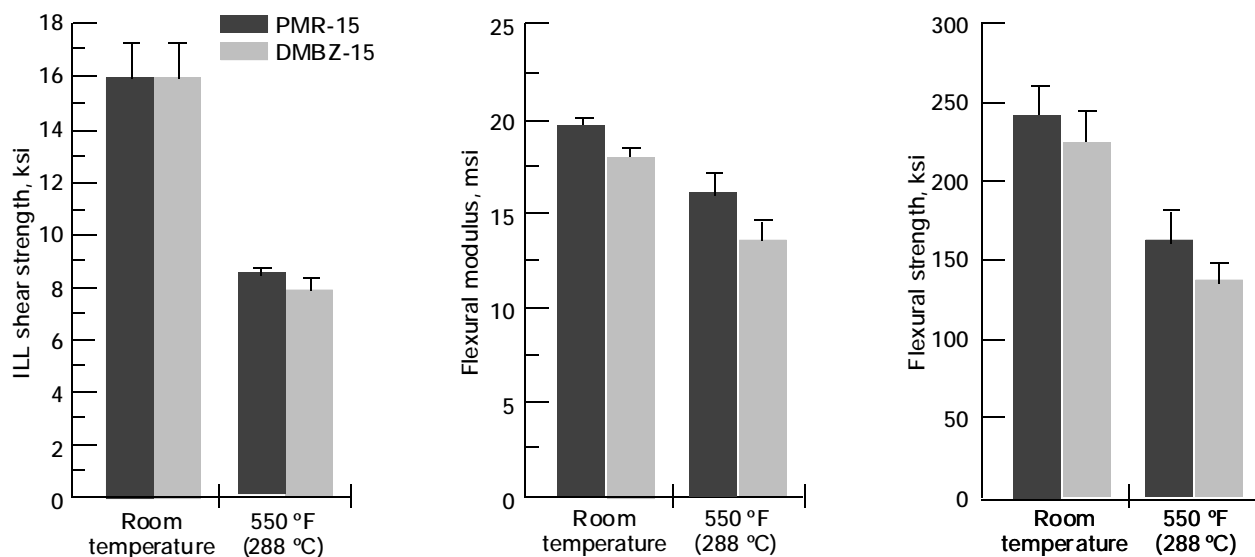
DMBZ Polyimides Provide an Alternative to PMR-15 for High-Temperature Applications

PMR-15, a high-temperature polyimide developed in the mid-1970's at the NASA Lewis Research Center, offers the combination of ease of processing, low cost, and good stability and performance at temperatures up to 288 °C (500 °F). This material is widely regarded as one of the leading high-temperature matrix resins for polymer-matrix-composite aircraft engine components. PMR-15 is widely used in both military and civilian aircraft engines. The current worldwide market for PMR-15 is on the order of 50,000 lb, with a total sales of around \$5 to \$10 million.

However, PMR-15 is made from methylene dianiline (MDA), a known animal mutagen and a suspected human mutagen. Recent concerns about the safety of workers involved in the manufacture and repair of PMR-15 components have led to the implementation of costly protective measures to limit worker exposure and ensure workplace safety. In some cases, because of safety and economic concerns, airlines have eliminated PMR-15 components from engines in their fleets.

Current efforts at Lewis are focused on developing suitable replacements for PMR-15 that do not contain mutagenic constituents and have processability, stability, and mechanical properties comparable to that of PMR-15. A recent development from these efforts is a new class of thermosetting polyimides based on 2,2'-dimethylbenzidine (DMBZ). Autoclave processing developed for PMR-15 composites was used to prepare low-void-content T650-35 carbon-fiber-reinforced laminates from DMBZ-15 polyimides. The glass transition temperatures of these laminates were about 50 °C higher than those of the T650-35/PMR-15 composites (400 versus 348 °C). In addition, DMBZ-15 polyimide composites aged for 1000 hr in air at 288 °C (500 °F) had weight losses close to those of comparable PMR-15 laminates (0.9 versus 0.7 percent). The elevated (288 °C) and room-temperature mechanical properties of T650-35-reinforced DMBZ-15 polyimide and PMR-15 laminates were comparable (see figure). Standard Ames tests are being conducted on this diamine to assess its mutagenicity.

Lewis contact: Dr. Kathy C. Chuang, (216) 433-3227
Headquarters program office: OA



Elevated and room-temperature mechanical properties of DMBZ and PMR-15 composites. Left: Interlaminar strength. Center: Flexural modulus. Right: Flexural strength.

Low-Cost Resin Transfer Molding Process Developed for High-Temperature Polyimide Matrix Composites

The use of high-temperature polymer matrix composites (PMC's) in aircraft engine applications can significantly reduce engine weight and improve performance and fuel efficiency. High-temperature PMC's, such as those based on the PMR-15 polyimide matrix resin developed by the NASA Lewis Research Center, have been used extensively in military applications where performance improvements have justified their use regardless of the cost involved in producing the component. However, in commercial engines cost is a primary driver, and PMC components must be produced at costs comparable to those of the metal components that they will replace.

Current production methods used to manufacture components from high-temperature PMC's are fairly labor intensive. Although less labor intensive, more efficient processing techniques such as resin transfer molding (RTM) have been developed to process PMC's; these methods are not suitable for use with high-temperature PMC's. RTM involves infiltrating a fiber preform with molten resin. To process good quality parts via RTM, one must use a resin with a low enough viscosity and sufficiently long pot-life to completely infiltrate the preform. Although high-temperature polymers such as PMR-15 melt, the viscosity of the molten resin is too high to be successfully processed by RTM.

One of the goals of the Advanced Subsonic Technology program is to develop new processing methods that enable the low-cost production of high-temperature PMC engine hardware. A recent development of this program is a modification of the RTM process to allow complete infiltration of the fiber preform by monomers prior to processing. A demonstration of this technique, developed jointly by GE Aircraft Engines, Fiber Innovations, Inc., and Lewis, was successfully completed, leading to the production of a center vent tube for the GE-90 engine using a Lewis-developed high-temperature polyimide, AMB-21. It is estimated that this process could reduce manufacturing costs by 30 to 50 percent in comparison to costs for a comparable part produced by hand layup and autoclave processing. Furthermore, this technique should be applicable to a variety of high-temperature PMC's as well as to a

number of engine components. Engine testing of this RTM-processed center vent tube is currently underway.

Find out more about the Advanced Subsonic Technology program on the World Wide Web:

<http://bearcat.lerc.nasa.gov/ast.html>

**Lewis contact: Raymond D. Vannucci, (216) 433-3202
Headquarters program office: OA**



Resin transfer molded AMB-21 Center Vent Tube for the GE-90 engine.

Nuclear Magnetic Resonance Used to Quantify the Effect of Pyrolysis Conditions on the Oxidative Stability of Silicon Oxycarbide Ceramics

This work was undertaken in support of the Low Cost Ceramic Composite Virtual Company, (LC³), whose members include Northrop Grumman Corporation, AlliedSignal Inc., and Allison Advanced Development Company. LC³ is a cost-shared effort funded by the Advanced Research Projects Agency (ARPA) and the LC³ participants to develop a low-cost fabrication methodology for manufacturing ceramic matrix composite structural components. The program, which is being administered by the U.S. Air Force Wright Laboratory Materials Directorate, is focused on demonstrating a ceramic matrix composite turbine seal for a regional aircraft engine. This part is to be fabricated by resin transfer molding of a siloxane polymer into a fiber preform that will be transformed into a ceramic by pyrolytic conversion.

Pyrolysis conditions are known to have a profound effect on the silicon redistribution reactions involved in converting the polymer into a ceramic (refs. 1 and 2). Different relative amounts of silicon carbide, silicon oxide, and silicon oxycarbides are produced, depending on the structure of the starting polymer and the pyrolysis path. These variations directly affect the oxidative stability. The purpose of this study was to quantify the effect of pyrolysis variables, namely time and temperature, on the redistribution reactions and, hence, on the oxidative stability.

Solid sample ²⁹Si nuclear magnetic resonance spectroscopy (NMR) can distinguish between various silicon species. For that reason, ²⁹Si NMR was used in this study to directly measure the percent peak areas of silicon carbide, silicon oxide, and silicon oxycarbides in ceramic test samples. Samples were produced under different pyrolysis conditions and were analyzed both before and after oxidation for 500 hr at 600 °C. The pyrolysis temperature was varied between 900 and 1100 °C, and the pyrolysis time was varied from 1 to 5 hr.

Ceramic samples were prepared by AlliedSignal and analyzed by NMR at the NASA Lewis Research Center. The experiments were carried out under a statistical design in a randomized run order. In this way, the data could be analyzed by multiple linear least squares regression to give models predicting the effect of the variables on the NMR peak areas. A three-dimensional graph of the predictive model for percent silicon carbide peak plotted versus pyrolysis

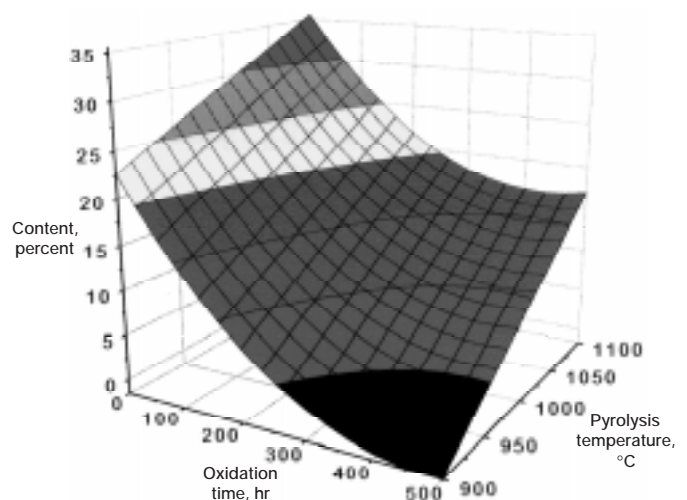
temperature and oxidation time is shown. The shaded bands represent silicon carbide contours in 5-percent intervals. This graph clearly demonstrates that increasing pyrolysis temperature significantly increases the amount of silicon carbide produced during pyrolysis. This increased silicon carbide production greatly improved oxidative stability, as evidenced by the greater retention of silicon carbide after oxidation. Pyrolysis time had little effect on percent silicon carbide.

We concluded that pyrolysis at 1100 °C produces the most oxidatively stable ceramic matrix. Furthermore, for samples like these with large surface-to-volume ratios, there is no benefit in pyrolyzing for more than 1 hr. Shorter pyrolysis cycles can greatly reduce the cost of producing the ceramic part.

References

1. Hurwitz, F.I., et al.: Characterization of the Pyrolytic Conversion of Polysilsesquioxanes to Silicon Oxycarbides. *J. Mater. Sci.*, vol. 28, 1993, pp. 6622-6630.
2. Hurwitz, F.I.; Heimann, P.J.; and Kacik, T.A.: Redistribution Reactions in Blackglas™ During Pyrolysis and Their Effect on Oxidative Stability. *Ceram. Eng. and Sci. Proc.*, vol. 16, no. 4, 1995, pp. 217-224.

Lewis contacts: Dr. Mary Ann Meador, (216) 433-3221, and Dr. Frances I. Hurwitz, (216) 433-5503
Headquarters program office: OA

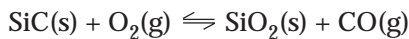


Predictive model for percent silicon carbide peak area plotted versus pyrolysis temperature and oxidation time.

Thermochemical Degradation Mechanisms for Reinforced Carbon/Carbon Panels on the Space Shuttle

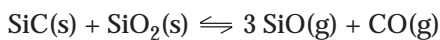
The wing leading edge and nose cone of the space shuttle are fabricated from a reinforced carbon/carbon material (RCC). This material attains its durability from a diffusion coating of silicon carbide (SiC) and a glass sealant (ref. 1). During reentry, this material is subjected to an oxidizing high-temperature environment. Joint work between the Ohio State University and the NASA Lewis Research Center led to a survey of potential degradation mechanisms of the reinforced carbon/carbon (RCC) material at high temperatures (ref. 2).

These mechanisms include oxidation of the SiC to form a silica scale (SiO₂), reaction of the SiC with SiO₂ to generate gaseous products, viscous flow of the glass, vaporization of the glass, and salt-induced (NaCl) corrosion, which may lead to pinholes. Continued thermal oxidation of the SiC coating occurs as



This adds silica to the glass coating and slows the oxidation rate. Under the extreme conditions of very low oxygen partial pressures and high temperatures, active oxidation may occur leading to SiO(g) instead of SiO₂(s) and rapid material consumption.

The reaction of SiC and SiO₂ occurs as follows:

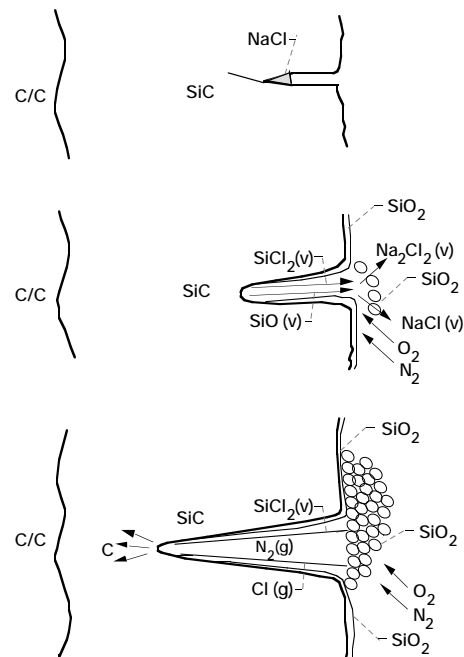


This leads to gas formation at the SiC/SiO₂ interface. Total vapor pressure calculations for carbon-rich SiC, silicon-rich SiC, and SiC, which forms SiO and CO in the 3-to-1 ratio of the above reaction, indicate that it is very desirable to keep the SiC silicon-rich to minimize this gas generation. This is currently done with the reinforced carbon/carbon material on the space shuttle.

Degradation of the glass sealant was also discussed. This is primarily a sodium silicate glass. At elevated temperatures, the glass sealant flows. This is beneficial since the sealant fills the cracks in the SiC that were formed because of the thermal expansion mismatch between the SiC and the carbon/carbon. However, under extreme conditions the glass may be blown off the surface by viscous drag, exposing the SiC and possibly the carbon/carbon to attack. The sodium component of the glass also vaporizes preferentially. This is suppressed to some degree by the oxygen in the reentry environment.

After many missions, the leading-edge wing surfaces have exhibited small pinholes. A mechanism based on NaCl deposits is proposed to explain this. Before launch, the shuttle is exposed to the sea-salt-laden air of Florida for periods of up to a month. This salt can deposit in the cracks and crevices of the reinforced carbon/carbon material on the wings and is likely to remain trapped there during launch and reentry. A cyclical chlorination/oxidation mechanism, which was proposed to explain this, is shown schematically in the figure. The trapped NaCl releases chlorine, which forms SiCl₂(g) with the SiC. This SiCl₂(g) migrates to the top of the pinhole and oxidizes to form SiO₂. This reaction leads to the silica fume observed near the top of the pinhole and releases chlorine that returns to the silicon carbide and forms more SiCl₂(g). Thus the pinhole grows. Diffusion calculations give results consistent with the observed pinhole depths.

Current work focuses on further verification of this mechanism and prediction of damage to the carbon/carbon after a pinhole is formed.



Schematic representation of chloridation/oxidation reaction mechanism. Top: Contamination of surface cracks. Center: Transient passive reaction in a pinhole. Bottom: Steady-state active reaction with pinhole growth and fume deposition at external surface.

References

1. Williams, S.D., et al.: Ablation Analysis of the Shuttle Orbiter Oxidation Protected Reinforced Carbon-Carbon. AIAA Paper 94-2084, 1994.
2. Jacobson, N.S.; and Rapp, R.A.: Thermochemical Degradation Mechanisms for the Reinforced Carbon/Carbon Panels on the Space Shuttle. NASA TM-106793, 1995.

Lewis contact: Dr. Nathan S. Jacobson, (216) 433-5498
Ohio State University contact: Prof. Robert A. Rapp, (614) 292-6178
Headquarters program office: OA

Structures

Cascade Optimization Strategy Maximizes Thrust for High-Speed Civil Transport Propulsion System Concept

The design of a High-Speed Civil Transport (HSCT) air-breathing propulsion system for multimission, variable-cycle operations was successfully optimized through a soft coupling of the engine performance analyzer NASA Engine Performance Program (NEPP) to a multidisciplinary optimization tool COMETBOARDS that was developed at the NASA Lewis Research Center. The design optimization of this engine was cast as a nonlinear optimization problem, with engine thrust as the merit function and the bypass ratios, r -values of fans, fuel flow, and other factors as important active design variables. Constraints were specified on factors including the maximum speed of the compressors, the positive surge margins for the compressors with specified safety factors, the discharge temperature, the pressure ratios, and the mixer extreme Mach number.

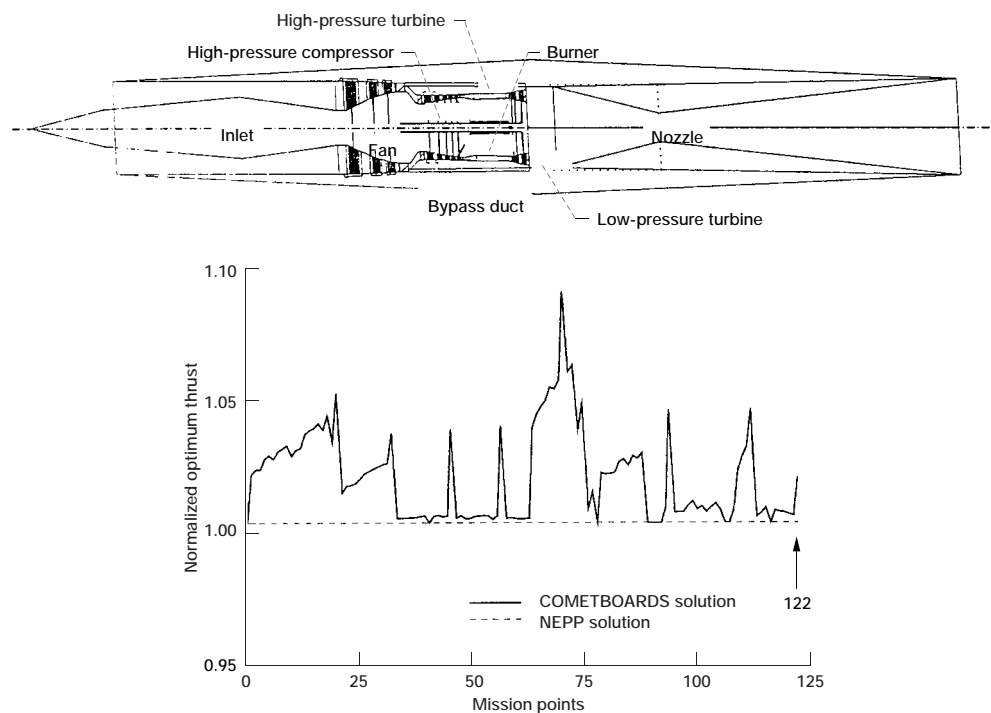
Solving the problem by using the most reliable optimization algorithm available in COMETBOARDS would

provide feasible optimum results only for a portion of the aircraft flight regime because of the large number of mission points (defined by altitudes, Mach numbers, flow rates, and other factors), diverse constraint types, and overall poor conditioning of the design space. Only the cascade optimization strategy of COMETBOARDS, which was devised especially for difficult multidisciplinary applications, could successfully solve a number of engine design problems for their flight regimes. Furthermore, the cascade strategy converged to the same global optimum solution even when it was initiated from different design points. Multiple optimizers in a specified sequence, pseudorandom damping, and reduction of the design space distortion via a global scaling scheme are some of the key features of the cascade strategy.

The figure depicts a COMETBOARDS solution for an HSCT engine (Mach-2.4 mixed-flow turbofan) along with its configuration. The optimum thrust is normalized with respect to NEPP results. COMETBOARDS added value in the design optimization of the HSCT engine.

Find out more about the HSCT on the World Wide Web:
<http://www.lerc.nasa.gov/WWW/HSR/hscet.html>

Lewis contact: Dale A. Hopkins, (216) 433-3260
Headquarters program office: OA



HSCT engine concept, optimized solution for HSCT engine concept.

Impact Properties of Metal Fan Containment Materials Being Evaluated for the High-Speed Civil Transport (HSCT)

Under the Enabling Propulsion Materials (EPM) program—a partnership between NASA, Pratt & Whitney, and GE Aircraft Engines—the Materials and Structures Divisions of the NASA Lewis Research Center are involved in developing a fan-containment system for the High-Speed Civil Transport (HSCT). The program calls for a baseline system to be designed by the end of 1995, with subsequent testing of innovative concepts. Five metal candidate materials are currently being evaluated for the baseline system in the Structures Division's Ballistic Impact Facility.

This facility was developed to provide the EPM program with cost-efficient and timely impact test data. At the facility, material specimens are impacted at speeds up to 350 m/sec by projectiles of various sizes and shapes to assess the specimens' ability to absorb energy and withstand impact. The tests can be conducted at either room or elevated temperatures. Posttest metallographic analysis is conducted to improve understanding of the failure modes. A dynamic finite element program is used to simulate the events and both guide the testing as well as aid in designing the fan-containment system.

To date, four of the five candidates for the baseline system have been tested. We plan to test the fifth material at Lewis as soon as it is available. Tests on more innovative materials and designs are currently

being initiated. Results of these tests will be used to select materials for further large-scale testing, and to help engine designers in the design of the fan-containment system.

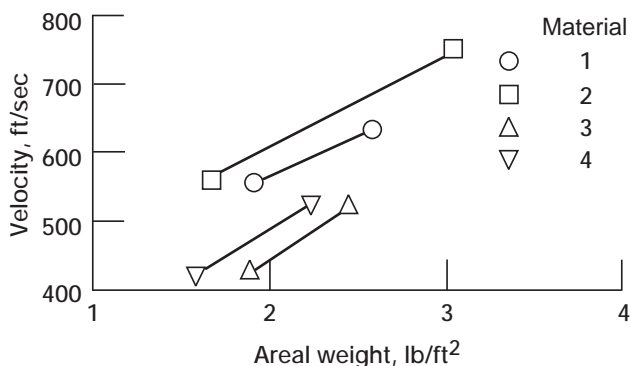
Find out more about the HSCT on the World Wide Web:
<http://www.lerc.nasa.gov/WWW/HSR/hsct.html>

Lewis contact: J. Michael Pereira, (216) 433-6738
Headquarters program office: OA (HSRD)

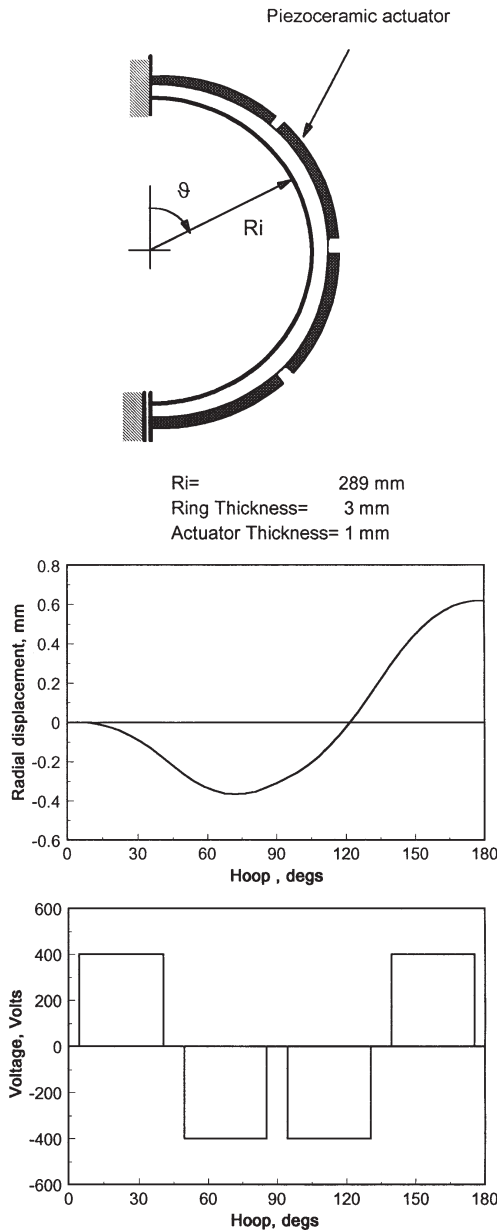
Active Piezoelectric Structures for Tip Clearance Management Assessed

Managing blade tip clearance in turbomachinery stages is critical to developing advanced subsonic propulsion systems. Active casing structures with embedded piezoelectric actuators appear to be a promising solution. They can control static and dynamic tip clearance, compensate for uneven deflections, and accomplish electromechanical coupling at the material level. In addition, they have a compact design. To assess the feasibility of this concept and assist the development of these novel structures, the NASA Lewis Research Center developed in-house computational capabilities for composite structures with piezoelectric actuators and sensors, and subsequently used them to simulate candidate active casing structures.

The simulations indicated the potential of active casings to modify the blade tip clearance enough to improve stage efficiency. They also provided valuable design information, such as preliminary actuator configurations (number and location) and the corresponding voltage patterns required to compensate for uneven casing deformations. The figure illustrates an active ovalization of a casing with four discrete piezoceramic actuators attached on the outer surface. The center figure shows the predicted radial displacements along the hoop direction that are induced when electrostatic voltage (bottom figure) is applied at the piezoceramic actuators. This work, which has demonstrated the capabilities of in-house computational models to analyze and design active casing structures, is expected to contribute toward the development of advanced subsonic engines.



Velocity required for a standard projectile to penetrate four candidate materials at 370 °C (700 °F).



Active ring structures with piezoelectric actuators. Top: Typical configuration. Center: Induced radial deflections. Bottom: Applied electric voltage at actuators.

Bibliography

Heyliger, P.; Ramirez, G.; and Saravanos, D.: Coupled Discrete-Layer Finite Elements for Laminated Piezoelectric Plates. *Commun. Numer. Meth. Eng.*, vol. 10, 1994, pp. 971-981.

Saravanos, D.A., et al.: On Smart Composite Structures for Active Tip Clearance Control. *Adaptive Structures and Composite Materials Analysis and Application*. E. Garcia, H. Cudney, and A. Dasgupta, eds., ASME, New York, 1994.

Lewis contact: Dale A. Hopkins (216) 433-3260
 Headquarters program office: OA

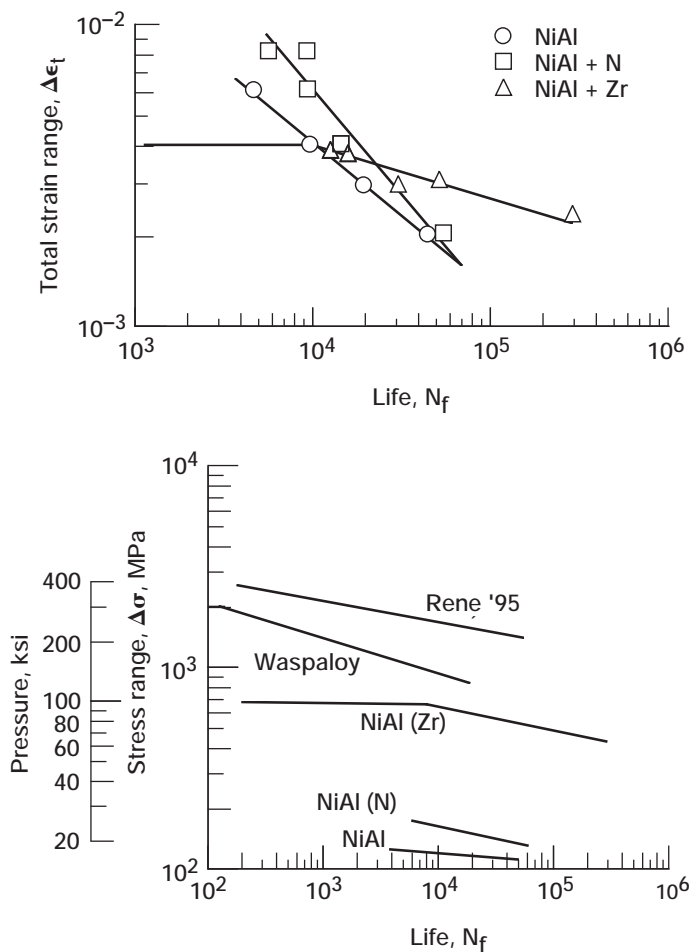
Microalloying Improves the Low-Cycle Fatigue Behavior of Powder-Extruded NiAl

There is considerable interest in developing new structural materials in which high use temperatures and strength, coupled with low density, are the minimum requirements. The goal for these new materials is to provide operation well beyond the working range of conventional superalloys. Of the many intermetallics under consideration, NiAl is one of the few systems that has emerged as a promising candidate for further development. This is because of a number of property advantages—including low density, high melting temperature, high thermal conductivity, and excellent environmental resistance. However, binary NiAl lacks strength and creep resistance at elevated temperatures. Also, its poor high-temperature strength results in worse-than-predicted low-cycle fatigue (LCF) lives at low strain ranges at 727 °C (1341 °F) because of accelerated creep damage mechanisms that result in significant intergranular cracking (refs. 1 and 2). One approach for improving these properties involves microalloying NiAl with either Zr or N. As an integral part of this alloy-development program at the NASA Lewis Research Center, the low-cycle fatigue behavior of Zr- and N-doped nickel aluminides produced by extrusion of prealloyed powders was investigated and compared with similarly processed binary NiAl.

The fatigue-life behavior of the various NiAl alloys is plotted in the first figure. Two stages occurred in the total strain-life plot of NiAl(Zr) because the fracture behavior changed from slow and stable intergranular crack growth at strain ranges ≤ 0.38 percent to brittle-cleavage-dominated overload fracture above this value. At strain ranges above 0.38 percent, the peak tensile stress reached the monotonic cleavage fracture stress of the Zr-doped alloy at 1000 K (328 MPa) in less than 100 cycles, enabling fast crack growth by cleavage. At total strain ranges ≤ 0.38 percent, the peak tensile cyclic stresses remained at a much lower level than the tensile cleavage fracture stress. In general, fatigue lives are governed by the ductility of the material at high strains and by its strength at low strains. The longer lives of NiAl(Zr) at low strain ranges result from its basic capacity to resist the applied strains on the basis of high strength. Both the NiAl and NiAl(N) alloys have shorter lives at low strain ranges because of the synergistic interaction between fatigue and creep. For the fatigue resistance of the binary and N-doped alloy to be improved, the grain boundaries need to be strengthened by a suitable means to reduce grain-boundary sliding and associated intergranular wedge cracking. Because Zr segregates to the grain boundaries in NiAl (ref. 3) and apparently strengthens the

boundary regions, preventing grain-boundary sliding, NiAl(Zr) does not suffer from grain-boundary sliding and intergranular wedge cracking as do the other two alloys.

Previously it was shown that binary NiAl materials have fatigue lives superior to conventional superalloys when compared on a plastic strain-range basis (ref. 1). This holds true for the additional NiAl alloys studied here. Conversely, the NiAl alloys compared poorly to superalloys when compared on a stress-range basis. However, the current results show that with even an extremely small Zr addition (approximately 0.1 at.%) fatigue life improved significantly on a stress-range basis, approaching that of the superalloys (see second figure). Furthermore, whereas Ni-based superalloys are highly alloyed materials, the NiAl alloy has a significant potential to improve both strength and fatigue life by the incorporation of higher levels of alloying additions.



Top: Fatigue life of three NiAl alloys tested at 727 °C. Bottom: NiAl alloys compared with typical superalloys tested at a nominal temperature of 727 °C.

References

1. Lerch, B.A.; and Noebe, R.D.: Low-Cycle Fatigue Behavior of Polycrystalline NiAl at 1000 K. Metall. Mater. Trans. A, vol. 25A, Feb. 1994, pp. 309-319.
2. Rao, K.B.S.; Lerch, B.A.; and Noebe, R.D.: Effect of Processing Route on Strain Controlled Low Cycle Fatigue Behavior of Polycrystalline NiAl. Fatigue and Fracture of Ordered Intermetallic Materials II, W.O. Soboyejo, T.S. Srivatsan, and R.O. Ritchie, eds., TMS, 1995, pp. 245-271.
3. Zeller, M.V.; Noebe, R.D.; and Locci, I.E.: Grain Boundary Segregation Studies of NiAl and NiAl(Zr) Using Auger Electron Spectroscopy. HITEMP Review 1990, NASA CP-10051, pp. 21-1 to 21-17. (Available to U.S. citizens only. Permission to use this material was granted by Hugh R. Gray, January 1996.)

Lewis contacts: **Bradley A. Lerch, (216) 433-5522, and Ronald D. Noebe, (216) 433-2093**
Headquarters program office: OA

Effects of Control Mode and R-Ratio on the Fatigue Behavior of a Metal Matrix Composite

Because of their high specific stiffness and strength at elevated temperatures, continuously reinforced metal matrix composites (MMC's) are under consideration for a future generation of aeropropulsion systems. Since components in aeropropulsion systems experience substantial cyclic thermal and mechanical loads, the fatigue behavior of MMC's is of great interest.

Almost without exception, previous investigations of the fatigue behavior of MMC's have been conducted in a tension-tension, load-controlled mode. This has been due to the fact that available material is typically less than 2.5-mm thick and, therefore, unable to withstand high compressive loads without buckling. Since one possible use of MMC's is in aircraft skins, this type of testing mode may be appropriate. However, unlike aircraft skins, most engine components are thick. In addition, the transient thermal gradients experienced in an aircraft engine will impose tension-compression loading on engine components, requiring designers to understand how the MMC will behave under fully reversed loading conditions. The increased thickness of the MMC may also affect the fatigue life.

Traditionally, low-cycle fatigue (LCF) tests on MMC's have been performed in load control. For monolithic alloys, low-cycle fatigue tests are more typically

performed in strain control. Two reasons justify this choice: (1) the critical volume from which cracks initiate and grow is generally small and elastically constrained by the larger surrounding volume of material, and (2) load-controlled, low-cycle fatigue tests of monolithics invariably lead to unconstrained ratcheting and localized necking—an undesired material response because the failure mechanism is far more severe than, and unrelated to, the fatigue mechanism being studied. It is unknown if this is the proper approach to composite testing. However, there is a lack of strain-controlled data on which to base any decisions. Consequently, this study (ref. 1) addresses the isothermal, LCF behavior of a $[0]_{32}$ MMC tested under strain- and load-controlled conditions for both zero-tension and tension-compression loading conditions. These tests were run at 427 °C on thick specimens of SiC-reinforced Ti-15-3.

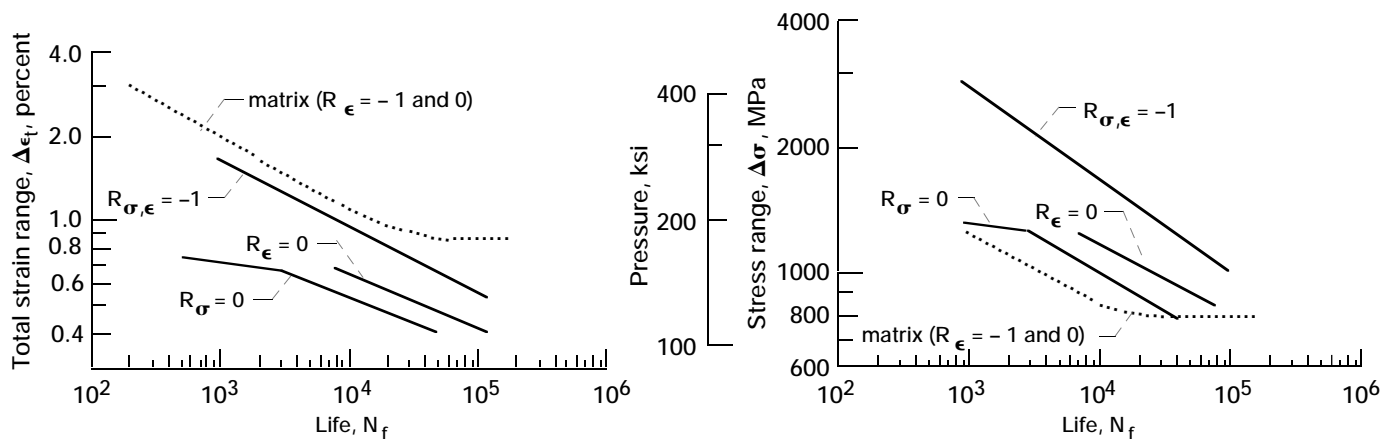
For the fully-reversed tests, no difference was observed in the lives between the load- and strain-controlled tests. However, for the zero-tension tests, the strain-controlled tests had longer lives by a factor of 3 in comparison to the load-controlled tests. This was due to the fact that under strain-control the specimens cyclically softened, reducing the cracking potential. In contrast, the load-controlled tests ratcheted toward larger tensile strains leading to an eventual overload of the fibers.

Fatigue tests revealed that specimens tested under fully-reversed conditions had lives approximately an order of magnitude longer than for those specimens tested under zero tension. When examined on a strain-range basis, the fully reversed specimens had similar, but still shorter lives than those of the unreinforced matrix material. However, the composite had a strain limitation at short lives because of the limited strain capacity of the brittle ceramic fiber. The composite also suffered at very high lives because of the lack of an apparent fatigue limit in comparison to the unreinforced matrix. The value of adding fibers to the matrix is apparent when the fatigue lives are plotted as a function of stress range. Here, the composite is far superior to the unreinforced matrix because of the additional load-carrying capacity of the fibers.

Reference

1. Lerch, B.; and Halford, G.: Effects of Control Mode and R-Ratio on the Fatigue Behaviour of a Metal Matrix Composite. Proceedings of the TMS/ASM Symposium on Mechanisms and Mechanics of MMC Fatigue, H. Herman, B.S. Majumdar, and B.A. Lerch, eds., Mater. Sci. Eng., vol. A200, nos. 1-2, Sept. 1995, pp. 47-54.

Lewis contacts: **Bradley A. Lerch, (216) 433-5522, and Dr. Gary R. Halford, (216) 433-3265**
Headquarters program office: OA



Summary of fatigue lives on a strain-range (left) and stress-range (right) basis for the SiC/Ti-15-3 composite and the unreinforced matrix tested at 427 °C.

Thermomechanical Fatigue Behavior of Coated and Uncoated Enhanced SiC/SiC Studied

Thermomechanical fatigue (TMF) testing provides a method of evaluating candidate continuous-fiber-reinforced ceramic composites under thermal and mechanical loading conditions. Although these tests are complicated, they provide a reasonable approximation of the combined thermal and mechanical loads that will be experienced by the material in service. The resulting data will be used to develop life-prediction models as well as to aid materials development.

Previous TMF testing of the SiC/SiC composite at the NASA Lewis Research Center demonstrated that enhancing the oxidation resistance of the matrix by a proprietary process increased the TMF lives (ref. 1). The improvement allowed the continued application of maximum cyclic stresses at or above the level where microcracking occurs (ref. 2)—in contrast to the unenhanced composite where the development of microcracks led to rapid failure. This indicates that the enhanced composite has improved damage tolerance. Further improvements in TMF life were realized with the use of an oxidation-resistant coating, which also permitted an increase in the maximum temperature by at least 100 °C (ref. 3).

Cracks developed in the composite with the enhanced matrix (both coated and uncoated) through the formation of periodic microcracks. These cracks initiated on the edge of the sample at interbundle regions where only matrix material (which also contained uninfiltreated regions) existed. The interbundle regions are weak, unreinforced areas and are very susceptible

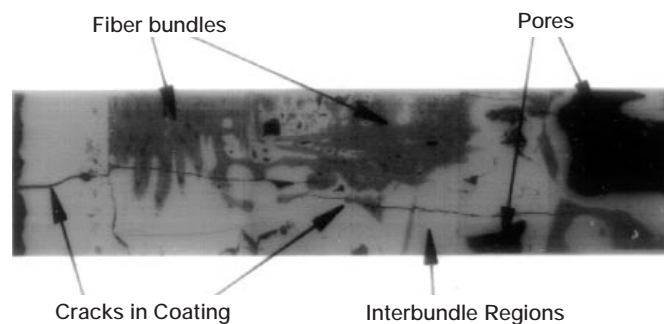
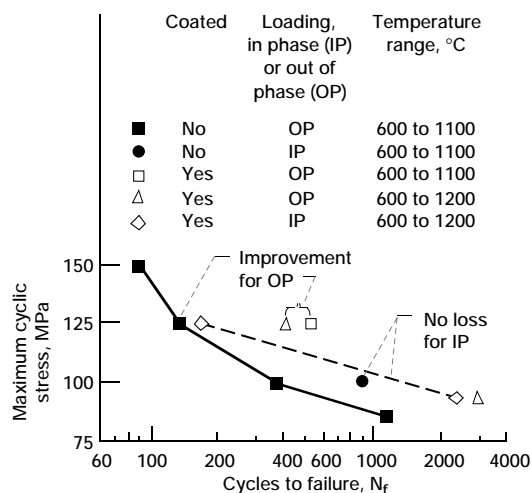
to crack formation. The cracking subsequently allowed oxygen to penetrate into the interior of the composite, leading to the formation of a glasslike phase, which was intended to seal the cracks. However, this phase also formed at the fiber/matrix interface and is suspected of degrading fiber strength.

These results indicate that the TMF behavior of SiC/SiC composites can be improved by an improvement in the oxidation resistance of the matrix and an application of an oxidation-resistant coating. However, these improvements may only be marginal, because the material still suffered from the weak interbundle regions. These regions are manifestations of the woven character of the material. Also, the matrix enhancements and the oxidation-resistant coating may be chemically incompatible with the fibers, leading to strength degradation during long-term tests.

References

1. Worthem, D.W.: Thermomechanical Fatigue of Three Ceramic-Matrix Composites. HITEMP Review 1993, NASA CP-19117, Vol. III, 1993, pp. 79-1 to 79-11. (Available to U.S. citizens only. Permission to use this material was granted by Hugh R. Gray, January 1996.)
2. Marshall, D.B.; and Evans, A.G.: Failure Mechanisms in Ceramic-Fiber/Ceramic-Matrix Composites. J. Am. Ceram. Soc., vol. 68, 1985, pp. 225-231.
3. Worthem, D.W. : Thermomechanical Fatigue Behavior of Coated and Uncoated Enhanced SiC/SiC[PW]. HITEMP Review 1994, NASA CP-10146, Vol. III, 1994, pp. 66-1 to 66-12. (Available to U.S. citizens only. Permission to use this material was granted by Hugh R. Gray, January 1996.)

Lewis contact: Dennis W. Worthem, (216) 977-1041
Headquarters program office: OA



Right: Maximum cyclic stress versus cycles to failure. Left: Optical micrograph showing the composite microstructure and the propagation of cracks from the edge of the sample.

Micromechanics Analysis Code (MAC) Developed

The ability to accurately predict the thermomechanical deformation response of advanced composite materials continues to play an important role in the development of these strategic materials. Analytical models that predict the effective behavior of composites are used not only by engineers in performing structural analysis of large-scale composite components but also by material scientists in developing new material systems.

For an analytical model to fulfill these two distinct functions, it must be based on a micromechanics approach that uses physically based deformation and life constitutive models, and it must allow one to generate the average (macro) response of a composite material given the properties of the individual constituents and their geometric arrangement. Only then can such a model be used by a material scientist to investigate the effect of different deformation mechanisms on the overall response of the composite and, thereby, identify the appropriate constituents for a given application.

However, if a micromechanical model is to be used in a large-scale structural analysis it must be (1) computationally efficient, (2) able to generate accurate displacement and stress fields at both the macro and micro level, and (3) compatible with the finite element method. In addition, new advancements in processing and fabrication techniques now make it possible to engineer the architectures of these advanced composite systems. Full utilization of these emerging manufacturing capabilities require the development of a computationally efficient micromechanics analysis tool that can accurately predict the effect of microstructural details on the internal and macroscopic behavior of composites. Computational efficiency is required because (1) a large number of parameters must be varied in the course of engineering (or designing) composite materials and (2) the optimization of a material's microstructure requires that the micromechanics model be integrated with optimization algorithms. From this perspective, analytical approaches that produce closed-form expressions which describe the effect of a material's internal architecture on the overall material behavior are preferable to numerical methods such as the finite element or finite difference schemes.

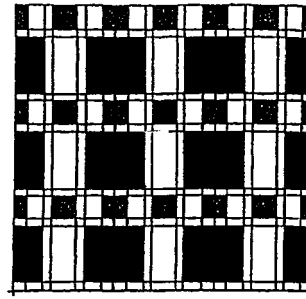
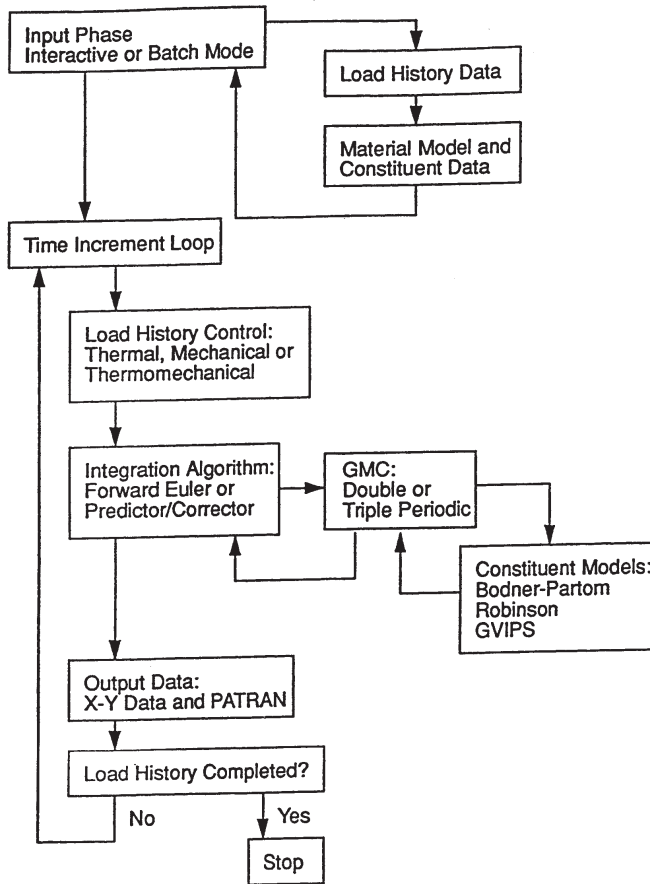
A number of existing models can fulfill some aspect of the aforementioned tasks. However, very few working models are both computationally efficient and

sufficiently accurate at the micro and macro level. One such micromechanics model with the potential of fulfilling both tasks is the method of cells (ref. 1) and its generalization (ref. 2). The comprehensive capabilities and efficiency of this method are documented (refs. 3 to 5). Consequently, a computationally efficient and comprehensive micromechanics analysis code (MAC)—whose predictive capability rests entirely on the fully analytical micromechanics model herein referred to as the generalized method of cells (GMC) (refs. 2 and 3) was recently developed. MAC is a versatile form of research software that “drives” the double or triple periodic micromechanics constitutive models on the basis of GMC. GMC can predict the response of both continuous and discontinuous multiphased composites with an arbitrary internal microstructure and reinforcement shape. It is a continuum-based micromechanics model that provides closed-form expressions for the macroscopic composite response in terms of the properties, size, shape, distribution, and response of the individual constituents or phases that make up the material. GMC also uses physically based viscoplastic deformation and life models for each constituent.

MAC enhances the basic capabilities of GMC by providing a modular framework wherein (1) various thermal, mechanical (stress or strain control), and thermomechanical load histories can be imposed, (2) different integration algorithms can be selected, (3) a variety of constituent constitutive models can be utilized or implemented, and (4) a variety of fiber architectures can be easily accessed through their corresponding representative volume elements. The first figure illustrates the basic flow diagram for this modular framework, and the second figure illustrates MAC's ability to describe the influence of hybrid architectures on the transverse inelastic response of metal matrix composites.

References

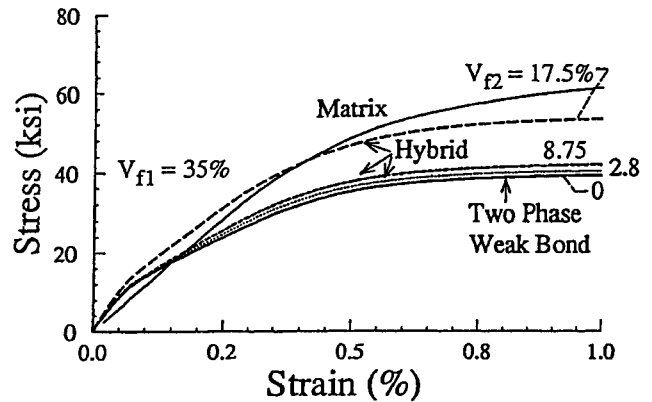
1. Aboudi, J.: *Mechanics of Composite Materials: A Unified Micromechanical Approach*, Elsevier, Amsterdam, 1991.
2. Paley, M.; and Aboudi, J.: *Micromechanical Analysis of Composites by the Generalized Cells Model*. *Mech. Mater.*, vol. 14, 1992, pp. 127-139.
3. Arnold, S.M., et al.: *An Investigation of Macro and Micromechanical Approaches for a Model MMC System*. *HITEMP Review 1993*. NASA CP-19117, Vol. II, 1993, pp. 52-1 to 52-12. (Available to U.S. citizens only.)



Large Fiber (weak)
 $R = 70\mu\text{m}; V_{f1} = 35\%$

Small Fiber (strong)

| $R_2 (\mu\text{m})$ | $V_{f2} (\%)$ |
|---------------------|---------------|
| 14 | 2.8 |
| 35 | 8.75 |
| 35 | 17.5 |



Left: MAC flowchart. Right: Influence of hybrid architecture and bond strength on transverse inelastic response.

Permission to use this material was granted by
 Hugh R. Gray, January 1996.)

5. Wilt, T.E.; and Arnold, S.M.: Micromechanics Analysis Code
 (MAC). User Guide: Version 1.0. NASA TM-106706, 1994.

4. Arnold, S.M.; Pindera, M.J.; and Wilt, T.E.: Influence of
 Fiber Architecture on the Elastic and Inelastic Response of
 Metal Matrix Composites. NASA TM-106705, 1995.

Lewis contact: Steven M. Arnold, (216) 433-3334
 Headquarters program office: OA

Fully Associative, Nonisothermal, Potential-Based Unified Viscoplastic Model for Titanium-Based Matrices

A number of titanium matrix composite (TMC) systems are currently being investigated for high-temperature air frame and propulsion system applications. As a result, numerous computational methodologies for predicting both deformation and life for this class of materials are under development. An integral part of these methodologies is an accurate and computationally efficient constitutive model for the metallic matrix constituent. Furthermore, because these systems are designed to operate at elevated temperatures, the required constitutive models must account for both time-dependent and time-independent deformations.

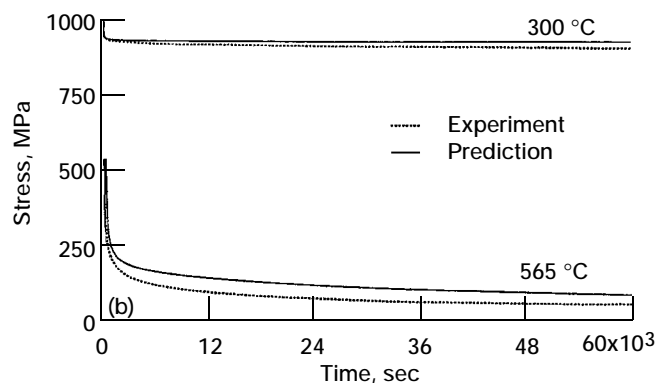
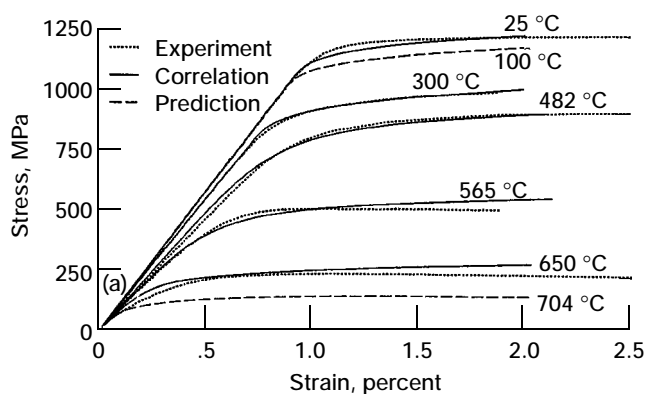
To accomplish this, the NASA Lewis Research Center is employing a recently developed, complete, potential-based framework (ref. 1). This framework, which utilizes internal state variables, was put forth for the derivation of reversible and irreversible constitutive equations. The framework, and consequently the resulting constitutive model, is termed complete because the existence of the total (integrated) form of the Gibbs complementary free energy and complementary dissipation potentials are assumed a priori. The specific forms selected here for both the Gibbs and complementary dissipation potentials result in a fully associative, multiaxial, nonisothermal, unified viscoplastic model with nonlinear kinematic hardening. This model (refs. 2 and 3) constitutes one of many models in the Generalized Viscoplasticity with Potential Structure (GVIPS) class of inelastic constitutive equations.

A unique aspect of this GVIPS model is its inclusion of nonlinear hardening through the use of a compliance

operator (derived from the Gibb's potential) in the evolution law for the back stress. This nonlinear tensorial operator is significant in that

- It allows both the flow and evolutionary laws to be fully associative (and therefore easily integrated) (ref. 4).
- It greatly influences the multiaxial response under nonproportional loading paths (refs. 1 and 5).
- In the case of nonisothermal histories, it introduces an instantaneous thermal softening mechanism proportional to the rate of change in temperature (ref. 3). In addition to this nonlinear compliance operator, the new consistent, potential preserving, internal unloading criterion (ref. 2) was utilized to prevent abnormalities in the predicted stress-strain curves (which are present with nonlinear hardening formulations) during unloading and reversed loading.

This nonisothermal GVIPS model was characterized for TIMETAL 21S (TIMET, Titanium Metals Corporation, Toronto, Ohio), an advanced titanium-based matrix commonly used in TMC's. The results illustrate the very good overall correlation and predictive capability of the model for a wide range of loading conditions—that is, tensile, cyclic, creep, step creep, step temperature, creep/plasticity interaction, and relaxation tests—that are performed over the temperature range of 23 to 704 °C. Finally, the proposed model also was compared with a commonly accepted and employed Bodner-Partom (BP) viscoplastic model and found to be superior both in its predictive capabilities and numerical performance.



Left: GVIPS correlation with experimental tensile data at 25, 300, 482, 565, and 650 °C, for a total strain rate of 8.33×10^{-5} . Right: Stress-time response of GVIPS prediction given relaxation tests at two temperatures (300 and 365 °C) and 1.9-percent strain.

References

1. Arnold, S.M.; and Saleeb, A.F.: On the Thermodynamic Framework of Generalized Coupled Thermoelastic-Viscoplastic-Damage Modeling. *Int. J. Plasticity*, vol. 10, no. 3, 1994, pp. 263-278 (NASA TM-105349, 1991).
2. Arnold, S.M.; Saleeb, A.F.; and Castelli, M.G.: A Fully Associative, Non-Linear Kinematic, Unified Viscoplastic Model for Titanium Based Matrices. NASA TM-106609, 1994.
3. Arnold, S.M.; Saleeb, A.F.; and Castelli, M.G.: A Fully Associative, Non-Linear Kinematic, Unified Viscoplastic Model for Titanium Based Matrices. NASA TM-106609, 1994.
4. Saleeb, A.F.; and Wilt, T.E.: Analysis of the Anisotropic Viscoplastic-Damage Response of Composite Laminates-Continuum Basis and Computational Algorithms. *Int. J. Eng. Num. Meth.*, vol. 36, no. 10, 1993, pp. 1629-1660.
5. Arnold, S.M.; Saleeb, A.F.; and Wilt, T.E.: A Modeling Investigation of Thermal and Strain Induced Recovery and Nonlinear Hardening in Potential Based Viscoplasticity. *J. Eng. Mater. Technol.*, vol. 117, 1995, pp. 157-167 (NASA TM-106122, 1993).

Lewis contact: Steven M. Arnold, (216) 433-3334
Headquarters program office: OA

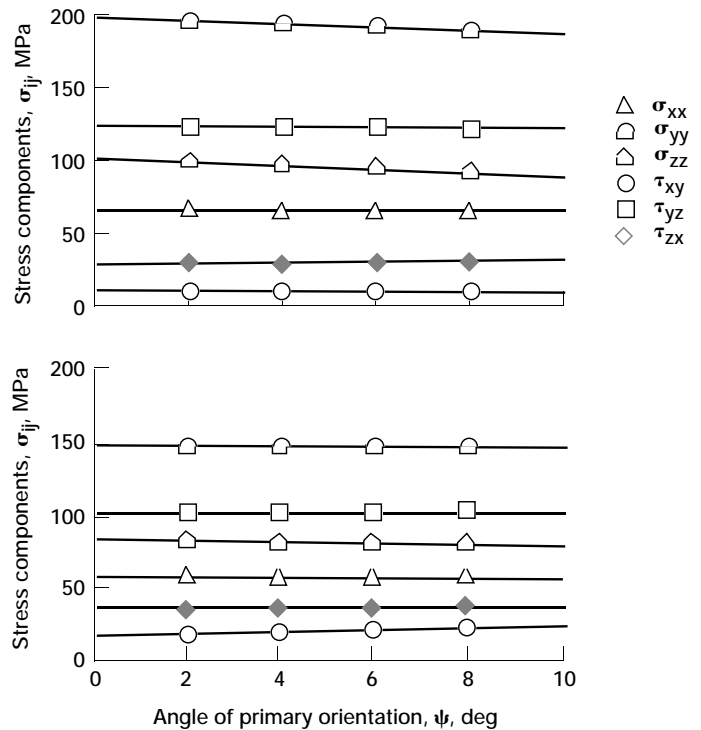
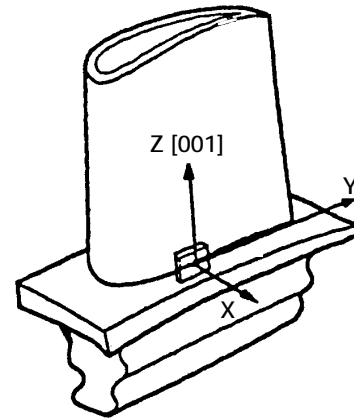
Thermal and Structural Analysis Conducted on Hollow-Core Turbine Blade of the Space Shuttle Main Engine

Hot-section components of spacecraft engines are exposed to severe thermal-structural loading conditions, especially during the startup and shutdown portions of the engine cycle. For instance, the thermal transient during startup within the space shuttle main engine (SSME) can lead to a gas temperatures in excess of 3000 °C, affecting the operating life of key components, such as the turbine blades.

To improve the durability of these components and in particular the turbine blade, single-crystal superalloys have been considered. PWA-1480, a nickel-base superalloy, has been used as the turbine blade material for the Alternate Turbopump Development (ATD) program for the SSME.

Turbine blades made out of single-crystal superalloys, including PWA-1480, are directionally solidified along the low-modulus [001] crystallographic direction. The

directional solidification process usually generates a secondary crystallographic direction, [010], that is randomly oriented with respect to fixed geometric axes in the turbine blade. Moreover, because of the anisotropic nature of the single crystal, the stress-strain response and the dynamic characteristics of any component made out of single crystal (such as the turbine blade) would depend on both the secondary and the primary orientation angles. This work addresses the influence of primary and secondary orientations on the elastic response of an SSME hollow-core, [001]-oriented nickel-base single-crystal superalloy (PWA 1480) turbine blade, under combined thermal and mechanical



Top: Schematic of an SSME hollow-core turbine blade. Bottom: Influence of primary and secondary orientation angles under combined thermal and mechanical loading.

loading conditions. A previous study (ref. 1) involving a flat plate of single-crystal material subjected to thermal loading showed that the influence of the secondary orientation on the elastic stress response is very substantial. Highest stresses occurred at a secondary orientation of 45° , which identified it as the most critical secondary orientation. Also, when the primary orientation angle was constrained between 0° and 10° , its influence on the elastic stresses generated within the turbine blade was much lower than the influence of the secondary orientation angle, which is not usually controlled.

This study consisted of thermal-structural analysis of an SSME-type turbine blade subjected to thermal and mechanical loads characteristic of engine use. The objective was to assess the influence of both the primary and secondary crystallographic orientation on the stresses developed and to compare the results with the conclusions obtained from earlier analyses of simpler structures (ref. 2). The figures show the results, demonstrating that secondary crystallographic orientation has a strong influence on the stresses in the turbine blade, an observation consistent with earlier findings on much simpler structures.

References

1. Kalluri, S.; Abdul-Aziz, A.; and McGaw, M.: Elastic Response of [001]-Oriented PWA 1480 Single Crystal—The Influence of Secondary Orientation. SAE Transactions, vol. 100, SAE Paper 91-1111, 1991.
2. Abdul-Aziz, A.; Kalluri, S.; and McGaw, M.A.: The Influence of Primary Orientation on the Elastic Response of a Nickel-Base Single-Crystal Superalloy. ASME Paper 93-GT-376, 1993.

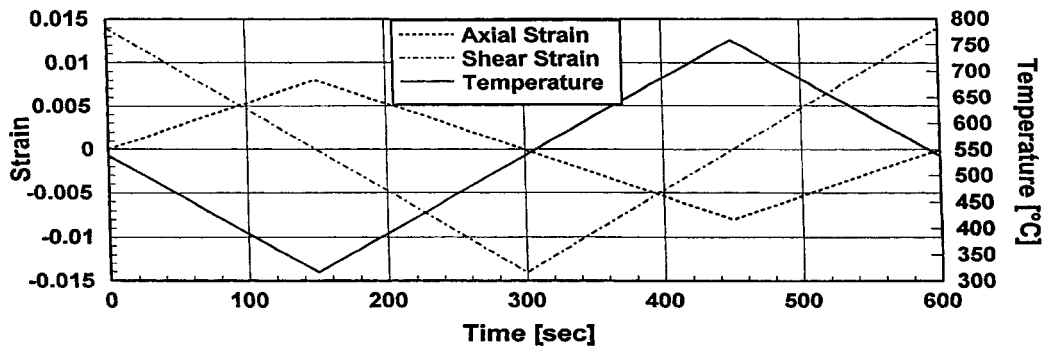
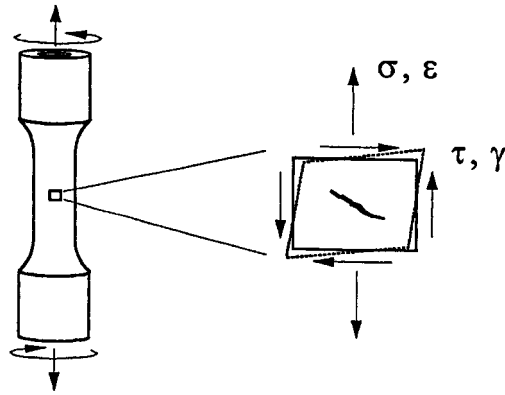
Lewis contacts: Dr. Ali Abdul-Aziz, (216) 433-6729, and Dr. Sreeramesh Kalluri, (216) 433-6727
Headquarters program office: OA

Thermomechanical Multiaxial Fatigue Testing Capability Developed

Structural components in aeronautical gas turbine engines typically experience multiaxial states of stress under nonisothermal conditions. To estimate the durability of the various components in the engine, one must characterize the cyclic deformation and fatigue behavior of the materials used under thermal and complex mechanical loading conditions (refs. 1 and 2). To this end, a testing protocol and associated test control software were developed at the NASA Lewis Research Center for thermomechanical axial-torsional fatigue tests. These tests are to be performed on thin-walled, tubular specimens fabricated from the cobalt-based superalloy Haynes 188. The software is written in C and runs on an MS-DOS based microcomputer.

Innovations incorporated into the test control software include a successive approximation algorithm for constant-rate temperature control, dynamic compensation for $\alpha \cdot \Delta T$ (where α is the coefficient of thermal expansion and ΔT is the temperature change) changes in the specimen dimensions (including the extensometer gage length), synchronization of all command and acquisition events with the microcomputer's 8254 timer chip, high data-acquisition-rate oversampling to reduce noise while minimizing signal time averaging, polynomial interpolation of temperature versus thermal strain, and control of the axial mechanical strain ($\epsilon_{\text{tot}} - (\alpha \cdot \Delta T)$, where ϵ_{tot} is the total strain). In addition, to avoid crack initiation from thermocouple spot welds, the gage section temperature is monitored by a light pipe infrared probe. The test control software allows for arbitrary phasing between the temperature, the axial command waveform signals, and the torsional command waveform signals. Axial and torsional load, strain, and stroke, as well as specimen temperature data, are acquired 1000 times per cycle. Tests are performed in 600-sec cycles (dictated by slowest free-convection cooling rate at the low end of the temperature cycle). Graphical output of axial and torsional stress response, temperatures, and additional pertinent information are displayed on the computer monitor in real time.

The test matrix will include (1) axial in-phase and axial out-of-phase thermomechanical fatigue (TMF) tests, (2) torsional in-phase TMF tests, (3) mechanically in-phase and thermally in-phase tests, (4) mechanically in-phase



Axial-torsional thermomechanical fatigue. Top: Schematic. Bottom: Mechanically out-of-phase and thermally out-of-phase cycles.

and thermally out-of-phase tests, (5) mechanically out-of-phase and thermally in-phase tests, and (6) mechanically out-of-phase and thermally out-of-phase tests. The maximum and minimum temperatures for all tests will be 760 and 316 °C, respectively. Results will be used to assess multiaxial fatigue life models for their applicability to cyclic thermomechanical loading conditions. This program has been preceded by baseline experiments establishing the axial-torsional fatigue and deformation characteristics of Haynes 188 at 760 and 316 °C.

References

1. Kalluri, S.; and Bonacuse, P.J.: Estimation of Fatigue Life Under Axial-Torsional Loading. PVP-Vol. 290, Material Durability/Life Prediction Modeling: Materials for the 21st Century, S.Y. Zamrik and G.R. Halford, eds., ASME, 1994, pp. 17-34.
2. Bonacuse, P.J.; and Kalluri, S.: Cyclic Axial-Torsional Deformation Behavior of a Cobalt-Base Superalloy. NASA TM-106372, 1994, pp. 204-229.

Lewis contacts: Peter J. Bonacuse, (216) 433-3309, and Dr. Sreeramesh Kalluri, (216) 433-6727
Headquarters program office: OA

Fatigue Behavior and Deformation Mechanisms in Inconel 718 Superalloy Investigated

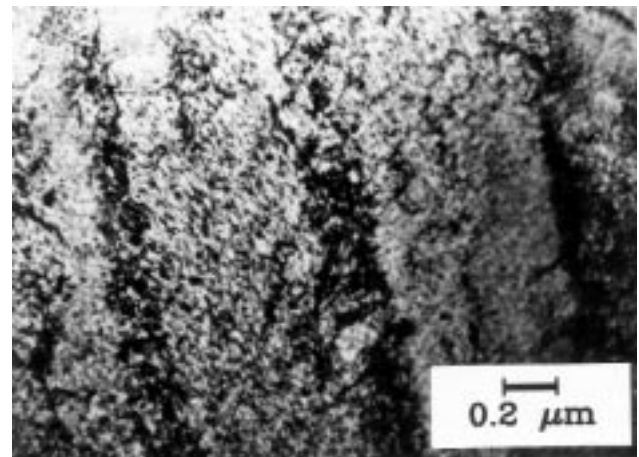
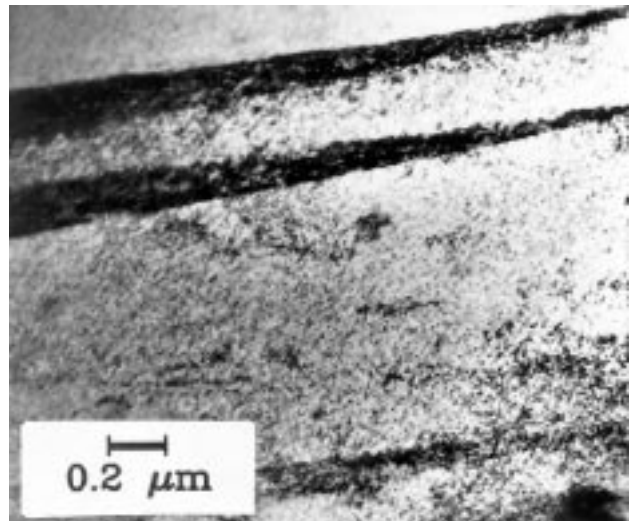
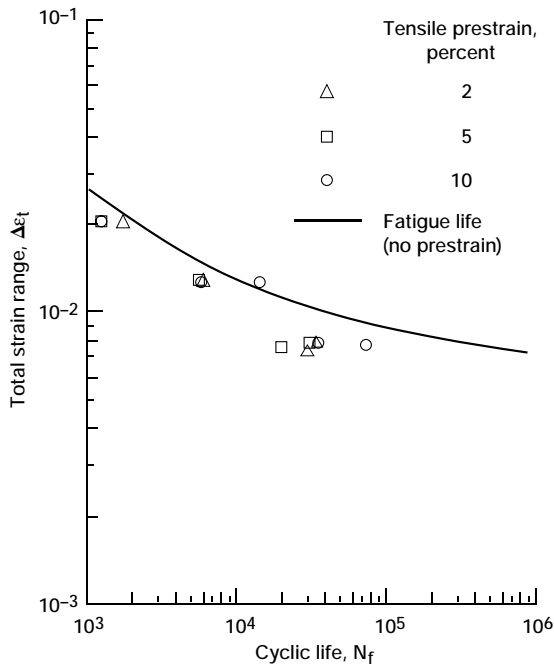
The nickel-base superalloy Inconel 718 (IN 718) is used as a structural material for a variety of components in the space shuttle main engine (SSME) and accounts for more than half of the total weight of this engine. IN 718 is the bill-of-material for the pressure vessels of nickel-hydrogen batteries for the space station. In the case of the space shuttle main engine, structural components are typically subjected to startup and shutdown load transients and occasional overloads in addition to high-frequency vibratory loads from routine operation. The nickel-hydrogen battery cells are proof-tested before service and are subjected to fluctuating pressure loads during operation. In both of these applications, the structural material is subjected to a monotonic load initially, which is subsequently followed by fatigue. To assess the life of these structural components, it is necessary to determine the influence of a prior monotonic load on the subsequent fatigue life of the superalloy. An insight into the underlying deformation and damage mechanisms is also required to properly account for the interaction between the prior monotonic load and the subsequent fatigue loading.

An experimental investigation was conducted to establish the effect of prior monotonic straining on the subsequent fatigue behavior of wrought, double-aged, IN 718 at room temperature (ref. 1). First, monotonic strain tests and fully-reversed, strain-controlled fatigue tests were conducted on uniform-gage-section IN 718 specimens. Next, fully reversed fatigue tests were conducted under strain control on specimens that were monotonically strained in tension. Results from this investigation indicated that prior monotonic straining reduced the fatigue resistance of the superalloy particularly at the lowest strain range. Some of the tested specimens were sectioned and examined by transmission electron microscopy to reveal typical microstructures as well as the active deformation and damage mechanisms under each of the loading conditions (ref. 2). In monotonically strained specimens, deformation during the subsequent fatigue loading was mainly confined to the deformation bands initiated during the prior monotonic straining. This can cause dislocations to move more readily along the previously activated deformation bands and to pile up near grain boundaries, eventually making the grain boundaries susceptible to fatigue crack initiation. The mechanisms inferred from the microstructural investigation were extremely valuable in interpreting the influence of prior monotonic straining on the subsequent fatigue life of Inconel 718 superalloy.

References

1. Kalluri, S.; Halford, G.R.; and McGaw, M.A.: Pre-Straining and Its Influence on Subsequent Fatigue Life. NASA TM-106881, 1995.
2. Kalluri, S., et al.: Deformation and Damage Mechanisms in Inconel 718 Superalloy. Superalloys 718, 625, 706 and Various Derivatives. E.A. Loria, ed., The Minerals, Metals & Materials Society, Warrendale, PA, 1994, pp. 593-606.

Lewis contacts: Dr. Sreeramesh Kalluri, (216) 433-6727, and Dr. Gary R. Halford, (216) 433-3265
 Headquarters program office: OA



Left: Influence of prior monotonic straining on the subsequent fatigue of IN 718 superalloy. Top right: Heavy localization of deformation in planar slip bands. IN 718 tested under a monotonic tensile strain of 10 percent followed by fatigue at a strain range of 2 percent. Bottom right: Dislocation tangles within planar slip bands. IN 718 tested under a monotonic tensile strain of 10 percent followed by fatigue at a strain range of 0.8 percent.

High-Temperature Extensometry and PdCr Temperature-Compensated Wire Resistance Strain Gages Compared

A detailed experimental evaluation is underway at the NASA Lewis Research Center to compare and contrast the performance of the PdCr/Pt dual-element temperature-compensated wire resistance strain gage with that of conventional high-temperature extensometry (ref. 1). The advanced PdCr gage, developed by researchers at Lewis, exhibits desirable properties and a relatively small and repeatable apparent strain to 800 °C (refs. 2 and 3). This gage represents a significant advance in technology because existing commercial resistance strain gages are not reliable for quasi-static strain measurements above ≈ 400 °C. Various thermal and mechanical loading spectra are being applied by a high-temperature thermomechanical uniaxial testing system to evaluate the two strain-measurement systems. This is being done not only to compare and contrast the two strain sensors, but also to investigate the applicability of the PdCr strain gage to the coupon-level specimen testing environment typically employed when the high-temperature mechanical behavior of structural materials is characterized. Strain measurement capabilities to 800 °C are being investigated with a nickel-base superalloy, Inconel 100 (IN 100), substrate material and application to TMC's is being examined with the model system, SCS-6/Ti-15-3. Furthermore, two gage application techniques are being investigated in the comparison study: namely, flame-sprayed and spot welding.

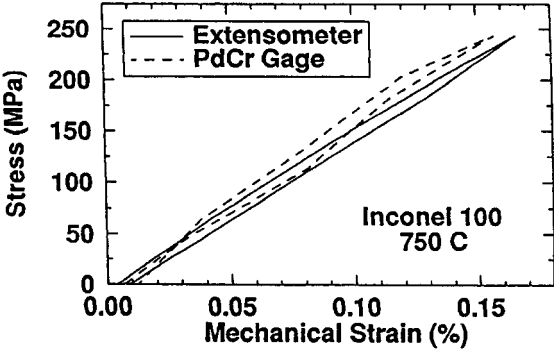
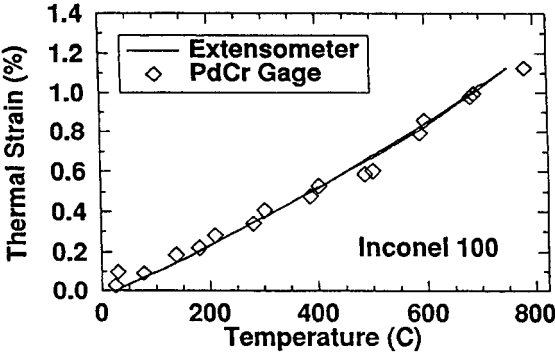
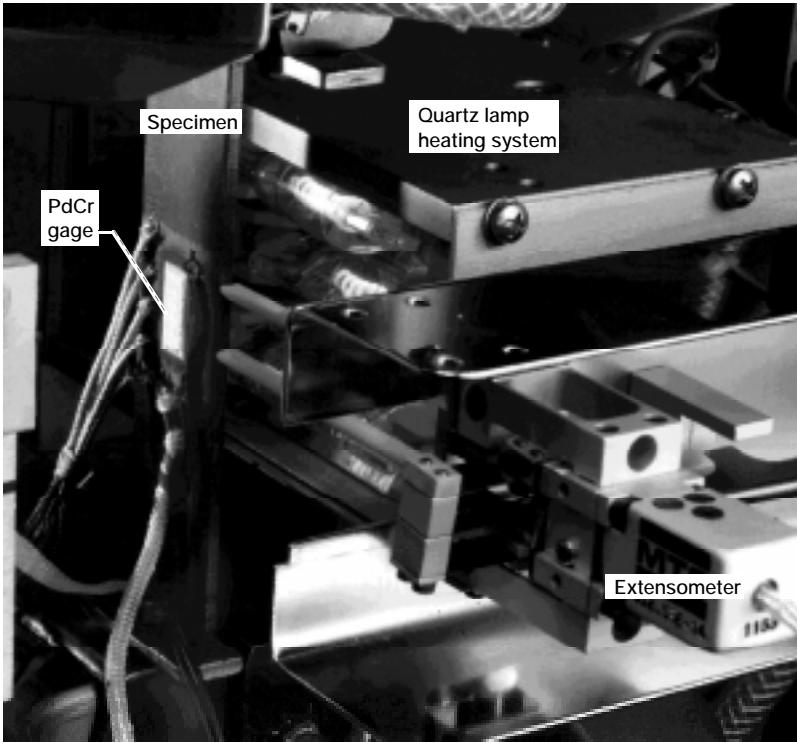
The apparent strain responses of both the weldable and flame-sprayed PdCr wire strain gages were found to be cyclically repeatable on both IN 100 and SCS-6/Ti-15-3 [0]₈. In general, each gage exhibited some uniqueness with respect to apparent strain behavior. Gages mounted on the IN 100 specimens tended to show a repeatable apparent strain within the first few cycles, because the thermal response of IN 100 was stable. This was not the case, however, for the TMC specimens, which typically required several thermal cycles to stabilize the thermal strain response. Thus, progressive changes in the apparent strain behavior were corroborated by the extensometer, which unlike the mounted gage can distinguish quantitative changes in the material's thermal strain response. One specimen was instrumented with both a fixed and floating gage. From the difference in output of these two gages, the thermal expansion strains were calculated. These data, which are given in the figure, show excellent agreement with the values measured by the high-temperature extensometry.

In general, the mechanical strain measurements from the gages and extensometer on both the IN 100 (to 800 °C) and TMC (to 600 °C) were in relatively good agreement (within 10 percent) to 2000 $\mu\epsilon$ (microstrain). However, a slightly larger variation was found in the low-temperature measurements on the IN 100 specimen with the weldable gage. The weldable gage mounted on the TMC effectively failed with the initial loading. This failure was caused by a crack in the TIMETAL 21S shim at a spot-weld location. Data obtained from this gage were, therefore, erroneous since poor contact existed between the shim and the substrate composite. Subsequent to mechanical loading cycles, the specimens were subjected to thermal cycles to measure changes in the apparent strain responses. In general, the apparent strain responses of both the weldable and flame-sprayed gages were repeatable. As a final aspect of mechanical performance in the present work, the specimens are being subjected to progressively increasing mechanical loads to measure the maximum mechanical strain threshold of the gages at room temperature. Preliminary results indicate that the gages tended to lose reliable strain-measurement capabilities at approximately 4500 $\mu\epsilon$.

References

1. Castelli, M.G.; and Lei, J.-F.: A Comparison Between High Temperature Extensometry and PdCr Based Resistance Strain Gages With Multiple Application Techniques. HITEMP Review 1994, NASA CP-10146, Vol. II, Oct. 1994, pp. 36-1 to 36-12. (Available to U.S. citizens only. Permission to use this material was granted by Hugh R. Gray, January 1996.)
2. Lei, J.-F.: A Resistance Strain Gage With Repeatable and Cancellable Apparent Strain for Use to 800 °C. NASA CR-185256, 1990.
3. Lei, J.-F.: Palladium-Chromium Static Strain Gages for High Temperatures. The 1992 NASA Langley Measurement Technology Conference Proceedings, NASA CP-3161, 1992, pp. 189-209.

Lewis contacts: Michael G. Castelli, (216) 433-8464, and Dr. Jih-Fen Lei, (216) 433-3922
Headquarters program office: OA



Gage and extensometer output show excellent agreement under thermal and mechanical loadings. Top: PdCr gage and high-temperature extensometry on specimen in thermomechanical loading system. Bottom: Comparison of extensometer and PdCr gage.

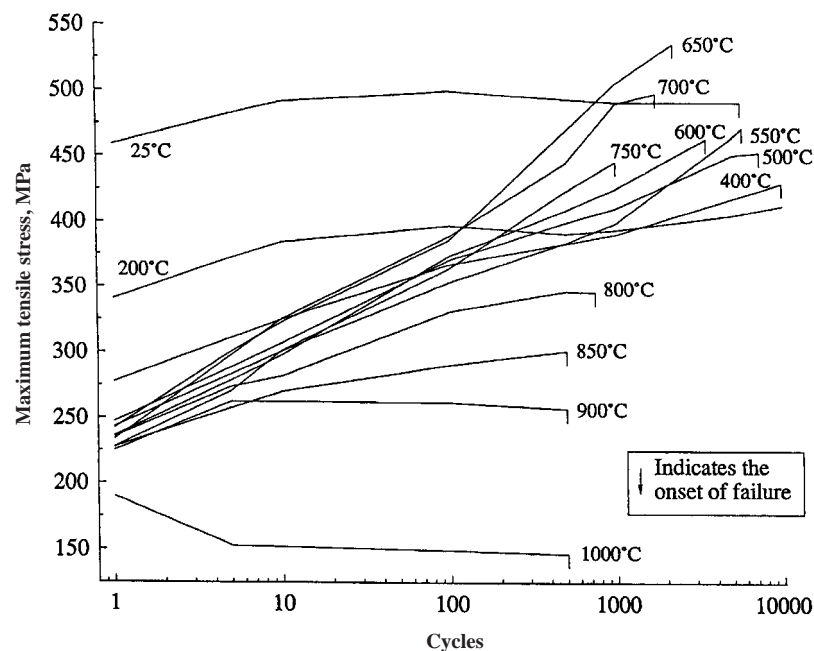
Temperature-Dependent Effects on the Mechanical Behavior and Deformation Substructure of Haynes 188 Under Low-Cycle Fatigue

The mechanical behavior of a cobalt-nickel-chromium-tungsten superalloy, Haynes 188, is being critically examined at the NASA Lewis Research Center. This dynamic, strain-aging (DSA) alloy is used for combustor liners in many military and commercial aircraft turbine engines and for the liquid oxygen posts in the main injectors of the space shuttle main engine. Its attractive features include a good combination of high monotonic yield and tensile strength, and excellent fabricability, weldability, and resistance to high-temperature oxidation for prolonged exposures.

One of the current research activities on Haynes 188 is investigating the effects of temperature on the mechanical behavior and deformation substructure under low-cycle fatigue (LCF) conditions over a range of temperatures between 25 and 1000 °C at a constant strain rate of 10^{-3} sec^{-1} . Particular attention is being given to the effects of DSA on the stress-strain response and the low-cycle fatigue life. Although DSA occurs over a wide temperature range between 300 and 750 °C, the microstructural characteristics and the deformation mechanisms responsible for DSA vary considerably and depend on temperature. Furthermore, DSA is not consistently evidenced by serrated yielding or jerky

flow, as is commonly exhibited in DSA alloys; however, specialized tests where the strain rate is changed at specific cycles reveal a negative strain rate sensitivity, which is indicative of DSA. A correlation between the cyclic deformation behavior and the microstructural processes is shown by detailed transmission electron microscopy investigations on material tested at various temperatures.

As shown in the figure, Haynes 188 exhibits a relatively complex temperature-dependent stress response. At temperatures below 300 °C, the material exhibited a slight period of cyclic hardening followed by an extended period of essentially stable stress response until the onset of failure. Here, cyclic deformation occurred by simultaneous activation of two slip systems. In the midtemperature regime from 400 to 750 °C where DSA occurs, the material exhibited marked cyclic hardening prior to the onset of failure. In this regime, two slip systems were also activated, with the deformation substructure exhibiting much higher dislocation densities than those revealed at 300 °C and below. Between 650 and 750 °C, dislocations were distributed more homogeneously and were pinned by fine chromium-rich carbides, leading to enhanced cyclic



Cyclic stress response of Haynes 188 under low-cycle fatigue conditions with a strain range of ± 0.4 percent and a strain rate of 10^{-3} sec^{-1} .

hardening. Above approximately 800 °C, the tendency for cyclic hardening declined, displaying cyclic softening at temperatures above 900 °C. At 900 °C and above, dynamic recovery by thermally activated climb became prominent and led to the formation of cells and subgrains.

The crack initiation and propagation modes also were temperature dependent in Haynes 188 under low-cycle fatigue conditions. At temperatures lower than 600 °C, crack initiation and propagation occurred in a transgranular mode. In the range between 650 and 750 °C, crack propagation occurred by a mixed transgranular plus intergranular mode, despite the fact that the crack initiation occurred by transcrystalline mechanisms. For specimens fatigued above approximately 800 °C, the fracture surfaces were covered with a thick oxidation layer. At these relatively high temperatures, the apparent predominant mechanism for crack initiation and propagation was environmentally assisted intergranular cracking.

Lewis contact: Michael G. Castelli (216) 433-8464
Headquarters program office: OA

New Method Developed for Aeroelastic Stability Analysis

The development of advanced-design ultrahigh bypass ratio engines has led to renewed interest in the study of the flutter of bladed disks. Previously, two fundamental approaches were used in flutter calculations: frequency domain analysis and time-domain analysis. With the development of time-marching computational fluid dynamics (CFD) flow solvers, both approaches have been used with equal ease. In the present work at the NASA Lewis Research Center, substantial computational savings have been achieved by applying a numerical eigensolver to a nonlinear, time-marching fluid-structure interaction system solver for flutter prediction.

The numerical eigensolver works with the steady-flow solution to determine the eigenvalues and eigenmodes corresponding to the fluid-structure interaction system directly. It does not require a time history of forces on blades and subsequent Fourier transformation to determine stability. Also, it avoids computationally expensive time-domain simulations of small perturbation responses, where several cycles of oscillation are required to determine the growth or decay of perturbations. With this new method, the computational savings over the existing frequency and time-domain nonlinear methods are of the order of 100 to 10,000. However,

note that fundamentally this is a small perturbation (linear) aeroelastic analysis, although steady-flow nonlinearities are taken into account (e.g., blade thickness, blade camber, and shock waves).

In the present work, a numerical eigensystem solver, based on a Lanczos procedure, is applied to a two-dimensional, full-potential, cascade aeroelastic solver. Calculations are performed for a cascade geometry used in previous research. Frequency- and time-domain flutter calculations were previously performed for this configuration. The steady solution is first obtained, as required in all such calculations. Then, the numerical eigensystem solver is used to calculate eigenvalues.

The eigenvalues obtained from this new approach indicate whether the aeroelastic system is stable or unstable. A comparison of the results from this approach with those from existing flutter determination methods shows that the new approach predicts the correct flutter condition. It shows good agreement in flutter speed and flutter mode.

The numerical eigensystem analysis results in substantial computer time savings in comparison to the frequency- and time-domain solutions. It will allow the use of nonlinear, time-marching solvers in routine aeroelastic design analysis. Because of the modular nature of the numerical eigensystem solver, it can be readily adapted to other time-marching aeroelastic solvers with minimal additional effort required on the researchers' part.

SAMPLE FLUTTER RESULTS FROM
 FULL-POTENTIAL AEROELASTIC CODE^a

| Flutter parameter | Frequency domain | Time domain | New method |
|-------------------|------------------|-------------|------------|
| Frequency | 0.265 | 0.262 | 0.239 |
| Velocity | 13.35 | 13.45 | 13.65 |

^a All values are nondimensional

Bibliography

Mahajan, A.J.; Bakhle, M.A.; and Dowell, E.H.: A New Method for Aeroelastic Stability Analysis of Cascades Using Nonlinear, Time-Marching CFD Solvers. AIAA Paper 94-4396, 1994.

Lewis contacts: George L. Stefko, (216) 433-3920, and Milind A. Bakhle, (216) 433-6037
Headquarters program office: OA

High-Temperature Magnetic Bearings for Gas Turbine Engines

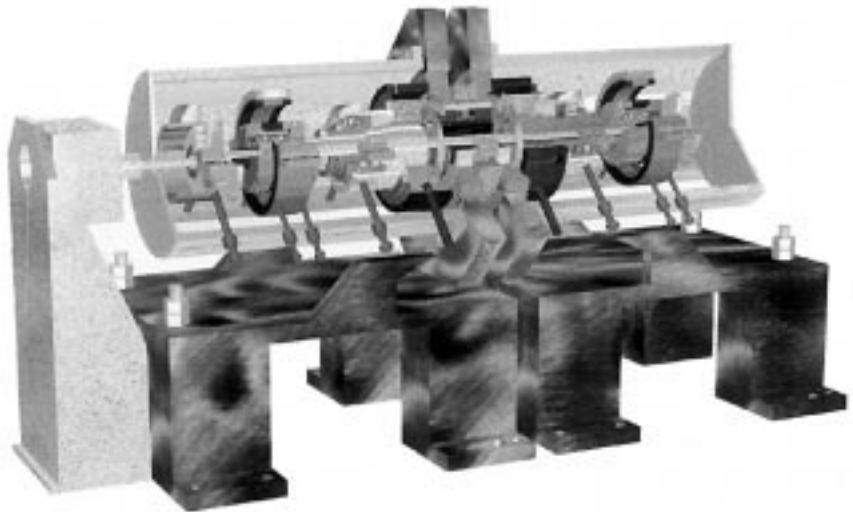
Magnetic bearings are the subject of a new NASA Lewis Research Center and U.S. Army thrust with significant industry participation, and coordination with other Government agencies. The NASA/Army emphasis is on high-temperature applications for future gas turbine engines. Magnetic bearings could increase the reliability and reduce the weight of these engines by eliminating the lubrication system. They could also increase the DN (diameter of the bearing times rpm) limit on engine speed and allow active vibration cancellation systems to be used—resulting in a more efficient, “more electric” engine. Finally, the Integrated High-Performance Turbine Engine Technology (IHPTET) Program, a joint Department of Defense/industry program, identified a need for a high-temperature (as high as 1200 °F) magnetic bearing that could be demonstrated in a phase III engine.

This magnetic bearing is similar to an electric motor. It has a laminated rotor and stator made of cobalt steel. Wound around the stator are a series of electrical wire coils that form a series of electric magnets around the circumference. The magnets exert a force on the rotor. A probe senses the position of the rotor, and a feedback controller keeps it in the center of the cavity. The engine rotor, bearings, and case form a flexible structure that contains a large number of modes. The bearing feedback controller, which could cause some of these modes to become unstable, could be adapted to varying flight conditions to minimize seal clearances and monitor the health of the system.

Cobalt steel has a curie point greater than 1700 °F, and copper wire has a melting point beyond that. Therefore, practical limitations associated with the maximum magnetic field strength in the cobalt steel and the stress in the rotating components limit the temperature to about 1200 °F. The objective of this effort is to determine the limits in temperature and speed of a magnetic bearing operating in an engine. Our approach is to use our in-house experience in magnets, mechanical components, high-temperature materials, and surface lubrication to build and test a magnetic bearing in both a rig and an engine. Testing will be done at Lewis or through cooperative programs in industrial facilities.

During the last year, we made significant progress. We have a cooperative program with Allison Engine to work on a high-temperature magnetic thrust bearing. During this program, we uncovered a problem with the conventional design of the magnetic thrust bearing. The thrust bearing is not laminated, causing eddy currents that severely reduce the bandwidth. Also, we worked at Allison to bring their high-temperature magnetic bearing rig to full speed. We predicted both in-house and Allison magnetic bearing rig stability limits, and we tested a high-temperature displacement probe. Our flexible casing rig is being converted to a high-temperature magnetic bearing rig (see figure). Testing should start next year. Our plan is to develop a high-temperature, compact wire insulation and to fiber reinforce the core lamination to operate at higher temperatures and DN values. We plan to modify our stability analysis and controller theory by including a nonlinear magnetic bearing model. We are developing an expert system that adapts the controller to changing flight conditions and that diagnoses the health of the system. Then, we will demonstrate the bearing on our rotor dynamics rig and, finally, in an engine.

Lewis contacts: Albert F. Kascak, (216) 433-6024, and Gerald Brown, (216) 433-6047
Headquarters program office: OA



NASA 1000 °F magnetic bearing test rig.

Lewis-Developed Seals Serve General Electric Technology Needs

Advanced aircraft engines require high-temperature, flexible seals to prevent backflow of high-temperature combustion gases. To meet this critical need, the NASA Lewis Research Center's Structural Dynamics Branch developed a line of hybrid braided-rope seals capable of high-temperature, high-pressure operation, while conforming to and sealing complex engine structures that distort during operation. The seals operate at temperatures several hundred degrees above competing graphite seals. Another benefit is that they do not have the health hazards associated with competing asbestos-based seals that are now banned for most uses.

Being acquainted with Lewis' high-temperature seal development, the General Electric Company (GE) worked with researchers in the Structural Dynamics Branch to determine if the braided rope seals could be used as a high-temperature compliant seal/mount for components in one of GE's advanced Integrated High Performance Turbine Engine Technology (IHPTET) demonstrator tests. These tests were sponsored by the U.S. Air Force Wright Laboratory's Aero Propulsion and Power Directorate and the U.S. Navy. GE researchers asked Lewis for assistance in solving a difficult sealing problem. Within GE's rapid turnaround requirement of 4 months, Lewis successfully developed, tested, and delivered the necessary seals. These seals are fabricated of a high-temperature, flow-resistant core of ceramic fibers overbraided with an abrasion-resistant sheath made of high-temperature superalloy wires.

Advanced Alloy Development

For a number of years, GE has been developing advanced alloys for high-temperature turbine blades and vanes. Through GE's considerable development efforts, complemented by the efforts of Lewis' Materials and Structures Division researchers, these advanced, high-temperature, oxidation-resistant intermetallic alloys have evolved to sufficient technical maturity to be considered for the IHPTET program.

Vane/Seal Tests

Feasibility testing of the vane/seal system demonstrated that the compliant seal/mount showed promise in reducing thermal stresses that develop in the engine components exposed to combustion temperatures, thereby increasing life. The advanced alloy vanes and the compliant seal/mount were then successfully tested (last quarter of 1995) in a Joint

Technology Advanced Gas Generator (JTAGG) engine, meeting stringent IHPTET phase I and temperature goals. The hardware ran at temperatures several hundred degrees Fahrenheit above conventional technology vane/seal-mount systems. These tests confirmed the viability of the vane and compliant seal/mount approach, paving the way for possible use in future advanced military engines.

This project is an example of how, by working with our industry counterparts, Government researchers can successfully transfer Government-developed technology to private industry. It is rewarding to have a major company recognize that Government researchers provide unique capabilities—solving technically challenging problems and developing critical components in short time periods.

Bibliography

Steinetz, B.M., et al.: High Temperature Braided Rope Seals for Static Sealing Applications. To be published as a NASA TM, 1996.

Lewis contact: Dr. Bruce M. Steinetz; (216) 433-3302
Headquarters program office: OA

Lewis' Ultrasonic Imaging Technology Helps American Manufacturer of Nondestructive Evaluation Equipment Become More Competitive in the Global Market

Background

Sonix, Inc., of Springfield, Virginia, has implemented ultrasonic imaging methods developed at the NASA Lewis Research Center. These methods have heretofore been unavailable on commercial ultrasonic imaging systems and provide significantly more sensitive material characterization than conventional high-resolution ultrasonic c-scanning. The technology transfer is being implemented under a cooperative agreement (NCC3-385) between NASA and Sonix, and several invention disclosures have been submitted by Dr. Roth to protect Lewis interests. Sonix has developed ultrasonic imaging systems used worldwide for microelectronics, materials research, and commercial nondestructive evaluation (NDE). In 1993, Sonix won the U.S. Department of Commerce "Excellence in Exporting" award.

Lewis chose to work with Sonix for two main reasons: (1) Sonix is an innovative leader in ultrasonic imaging systems, and (2) Sonix was willing to apply the improvements we developed with our in-house Sonix equipment. This symbiotic joint effort has produced mutual benefits. Sonix recognized the market potential of our new and highly sensitive methods for ultrasonic assessment of material quality. We, in turn, see the cooperative effort as an effective means for transferring our technology while helping to improve the product of a domestic firm.

Significance

The Lewis-developed methods being implemented by Sonix significantly enhance the materials characterization by ultrasonic imaging. Among the benefits of the Lewis methods is that it eliminates the effects of sample thickness variations. This isolates ultrasonic variations due to material microstructure and overcomes quality control problems during materials processing. Cost savings can be realized because the ultrasonic image can be correctly interpreted without additional machining to control sample thickness. Another benefit of our methods is that velocity variations may, in part, be imaged by ultrasound. This allows the quantitative characterization of microstructural factors, density gradients, and associated mechanical properties. These attributes constitute a major improvement over the capabilities of conventional ultrasonic methods.

Status

Sonix' implementation of Lewis-developed methods is currently being beta-tested at Lewis. It is expected to be available for distribution to other Sonix system users by February 1996.

Find out more about Lewis' technology transfer programs on the World Wide Web:

<http://www.lerc.nasa.gov/WWW/TU/techtran.htm>

Lewis contact: Dr. Don J. Roth, (216) 433-6017
Headquarters program office: OA

Integrated Design Software Predicts the Creep Life of Monolithic Ceramic Components

Significant improvements in propulsion and power generation for the next century will require revolutionary advances in high-temperature materials and structural design. Advanced ceramics are candidate materials for these elevated-temperature applications. As design protocols emerge for these material systems, designers must be aware of several innate features, including the degrading ability of ceramics to carry sustained load.

Usually, time-dependent failure in ceramics occurs because of two different, delayed-failure mechanisms: slow crack growth and creep rupture. Slow crack growth initiates at a preexisting flaw and continues until a critical crack length is reached, causing catastrophic failure. Creep rupture, on the other hand, occurs because of bulk damage in the material: void nucleation and coalescence that eventually leads to macrocracks which then propagate to failure. Successful application of advanced ceramics depends on proper characterization of material behavior and the use of an appropriate design methodology. The life of a ceramic component can be predicted with the NASA Lewis Research Center's Ceramics Analysis and Reliability Evaluation of Structures (CARES) integrated design programs. CARES/CREEP determines the expected life of a component under creep conditions,

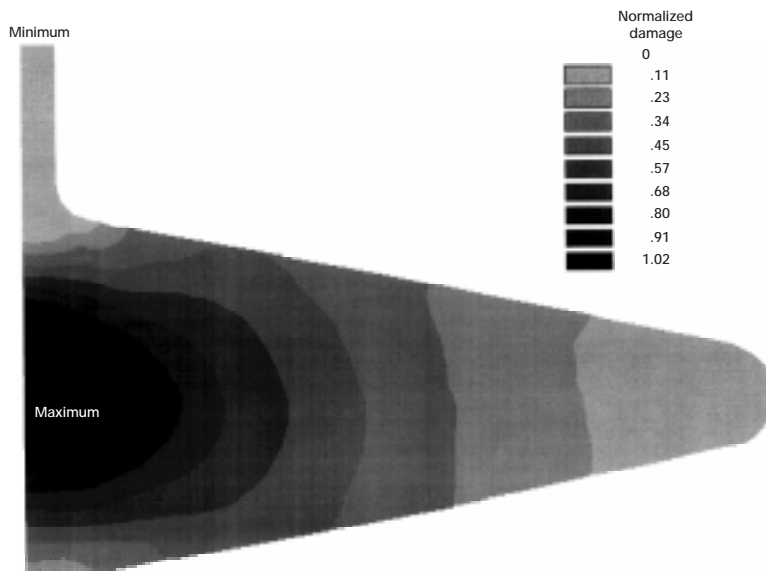
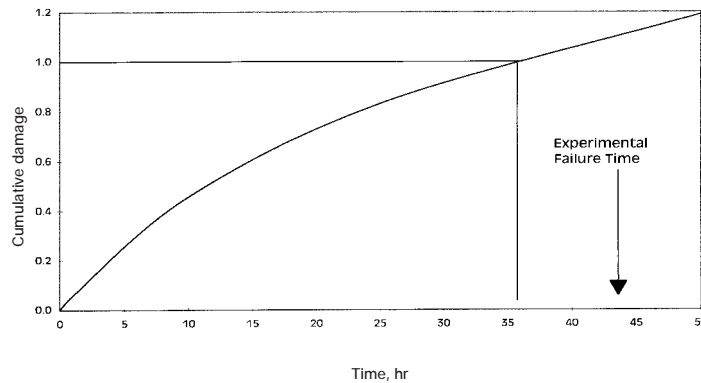
and CARES/LIFE predicts the component life due to fast fracture and subcritical crack growth. The previously developed CARES/LIFE program has been used in numerous industrial and Government applications.

The advent of new techniques in ceramic processing technology has yielded a new class of ceramics that are highly resistant to creep at high temperatures. Such desirable properties have generated interest in using ceramics for turbine engine component applications where the design lives for such systems are on the order of 10,000 to 30,000 hr. These long life requirements necessitate subjecting the components to relatively low stresses. The combination of high temperatures and low stresses typically places failure for monolithic ceramics in the creep and creep-rupture region of a time-temperature-failure mechanism map.

CARES/CREEP, an analytical methodology in the form of an integrated design program, was developed for predicting the life of ceramic structural components subjected to creep rupture conditions. This

methodology employs commercially available finite element packages and takes into account the transient state of stress and creep strain distributions (stress relaxation). The creep life of a component is discretized into short time steps during which the stress distribution is assumed constant. The damage is calculated for each time step on the basis of a modified Monkman-Grant creep rupture criterion. The cumulative damage is subsequently calculated as time elapses in a manner similar to Miner's rule for cyclic fatigue loading. Failure is assumed to occur when the normalized cumulative damage at any point in the component reaches unity. The corresponding time is the creep rupture life for that component.

Benchmark problems of creep life prediction for ceramic components under multiaxial loading have demonstrated the CARES/CREEP program. Analysis of a spin disk, which was a part of an AlliedSignal Inc. program to develop and demonstrate life-prediction methods for ceramic components of advanced vehicular engines, revealed failure mechanisms that



Top: Maximum cumulative damage versus time for a silicon nitride notched tensile specimen. Bottom: Cumulative creep damage distribution for a silicon nitride spin disk.

were a combination of creep and slow crack growth. The second problem was a silicon nitride notched tensile specimen, which was analyzed as a part of the Saint Gobain-Norton advanced heat engines applications program. When the maximum damage in the notched tensile specimen versus time is plotted, failure is expected to occur when the damage is equal to 1. The predicted failure time was 37 hr, whereas the actual failure time was 44 hr, demonstrating a conservative prediction.

The CARES/CREEP code predicts the deterministic life of a ceramic component. Future work involves the role of probabilistic models in this design process. The complete package will predict the life of monolithic ceramic components by using simple uniaxial creep laws to account for multiaxial creep loading. The combination of the CARES/CREEP and CARES/LIFE codes gives the design engineer the tools necessary to predict component life for the two dominant delayed-failure mechanisms.

Lewis contact: Lesley A. Janosik, (216) 433-5160
Headquarters program office: OA

Methodology Developed for Modeling the Fatigue Crack Growth Behavior of Single-Crystal, Nickel-Base Superalloys

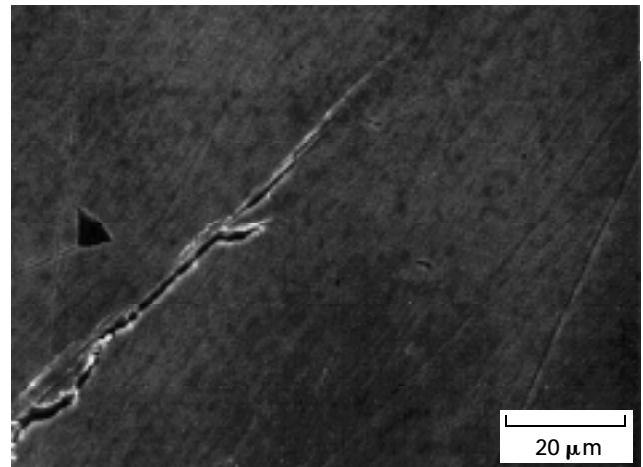
Because of their superior high-temperature properties, gas generator turbine airfoils made of single-crystal, nickel-base superalloys are fast becoming the standard equipment on today's advanced, high-performance aerospace engines. The increased temperature capabilities of these airfoils has allowed for a significant increase in the operating temperatures in turbine sections, resulting in superior propulsion performance and greater efficiencies. However, the previously developed methodologies for life-prediction models are based on experience with polycrystalline alloys and may not be applicable to single-crystal alloys under certain operating conditions. One of the main areas where behavior differences between single-crystal and polycrystalline alloys are readily apparent is subcritical fatigue crack growth (FCG). Whereas in polycrystalline alloys cracks grow perpendicular to the applied load (i.e., mode I cracks), in single-crystal alloys cracks often grow on the operative slip planes that are inclined to the applied load axis.

The NASA Lewis Research Center's work in this area enables accurate prediction of the subcritical fatigue

crack growth behavior in single-crystal, nickel-based superalloys at elevated temperatures. Reference 1 describes the limitations of the currently used mode I crack-driving-force parameter and introduces two new parameters that are based on the resolved shear stresses on the individual slip systems present at the crack tip. The two parameters not only correlate the fatigue crack growth rates as a function of anisotropy but also are able to predict the operative slip system. These parameters can be utilized in life-prediction models, which, when developed, will give a more accurate estimate of the life of the component since they will be based on the actual deformation mechanisms by which progressive failure occurs.

The experimental part of the program was performed in a specially designed, high-temperature, in situ loading stage mounted inside a scanning electron microscope. This allowed for real-time observations of the operative failure modes at high magnifications. The identification of the ongoing failure mechanisms was instrumental in determining the conditions under which a given failure mode was active.

The influence of the environment on the fatigue crack growth behavior of the single-crystal alloy at elevated temperatures was also examined. We determined that oxygen embrittlement at sufficiently low frequencies and high temperatures is responsible for a transition from an octahedral crack growth on the slip planes to the mode I crack growth so prevalent in polycrystalline alloys.



Octahedral mode crack growth process at 427 °C.

Space Propulsion Technology

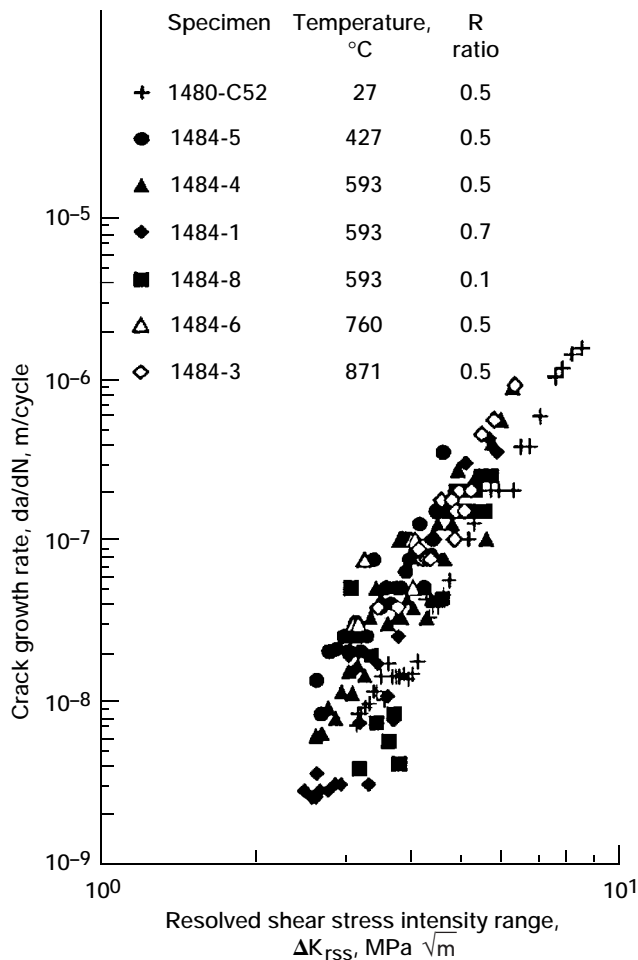
Three Phases of Low-Cost Rocket Engine Demonstration Program Completed

The NASA Lewis Research Center and the TRW Space & Technology Group have successfully completed three phases of testing on the Low-Cost Rocket Engine Demonstration Program. TRW and the McDonnell Douglas Corporation are working, in a joint effort, to quickly develop and produce a highly stable, inexpensive, simple, yet reliable, expendable launch vehicle. Studies have shown that this launch system is required to maintain U.S. viability to space access in the face of growing foreign competition. For the U.S. commercial launch industry to remain competitive, a low-cost launch vehicle must be developed to place payloads into low-Earth orbit. Trade studies performed by McDonnell Douglas and TRW have shown that a low-cost, commercial, expendable launch vehicle could be designed that uses low-pressure turbopumps and rocket combustors. These studies show that expensive high-performance technology can be sacrificed for inexpensive lower performance technology and still meet mission requirements. Because the propulsion system is more than half of a launch vehicle's cost, TRW proposed the pintle injector engine design used in the Apollo Program—the lunar module descent engine.

TRW's pintle injector engine, which runs on liquid hydrogen or RP-1 fuels and liquid oxygen oxidizer, uses modified low-pressure turbopumps to supply the propellants. The engine consists of a centrally located, coaxial injector; an ablative liner for insulating the metal surfaces of the combustion chamber and nozzle; and annular sleeves to throttle the propellant feeds.

Lewis and TRW entered into a Space Act Agreement to demonstrate that the pintle injector can operate at acceptable stable performance levels and to demonstrate the life of a low-cost, combustion chamber with an ablative lining. The test program consisted of three phases: (1) testing a 16,500-lb-thrust liquid oxygen/liquid hydrogen (LOX/LH₂) engine, (2) testing a 40,000-lb-thrust LOX/LH₂ engine, and (3) testing a 13,000-lb-thrust LOX/RP-1 engine. All testing was done at Lewis' Rocket Engine Test Facility (RETF).

The 16,500-lb-thrust engine was tested from December 1991 through March 1992. Results show that the engine delivered 95 to 97 percent characteristic velocity (C^*) efficiency, about 2 to 4 percent higher than expected.



Octahedral fatigue crack growth data plotted in terms of the ΔK_{RSS} parameter at various temperatures and R ratios.

Reference

1. Telesman, J.; and Ghosn, L.: Fatigue Crack Growth Behavior of a PWA 1484 Single Crystal Superalloy at Elevated Temperatures. ASME Paper 95-GT-452, 1995.

Lewis contact: Jack Telesman, (216) 433-3310

(World Wide Web URL:

<http://sdwww.lerc.nasa.gov/people/smteles.html>)

Headquarters program office: OA

No combustion instabilities were exhibited, and the ablative liner showed acceptable levels of ablation.

The 40,000-lb-thrust engine was tested from September 1993 through February 1994 to determine scaling issues and to demonstrate life of the flight-weight ablative liner. The Lewis test results show that the engine delivered 95-percent C^* efficiency. The data indicate no combustion instabilities, and the ablative liner showed acceptable levels of ablation (<0.006 in./sec).

The 13,000-lb-thrust liquid oxygen/RP-1 engine was tested from January 1995 through March 1995. The C^* efficiency demonstrated on this configuration was 95 percent. The engine was stable in general but had low-frequency, rough combustion at startup because of slow manifold filling, a minor design issue. Because of a leaky pintle seal design, TRW's pintle was damaged on several tests. This problem was soon corrected by the Lewis team. During the ablative liner test, half of the throat region ablative liner fell out because it had delaminated from the shell during fabrication. The approximate radius ablation rate was 0.013 in./sec. Using these test results, TRW and McDonnell Douglas are now working on expendable launch vehicle upgrades.

Bibliography

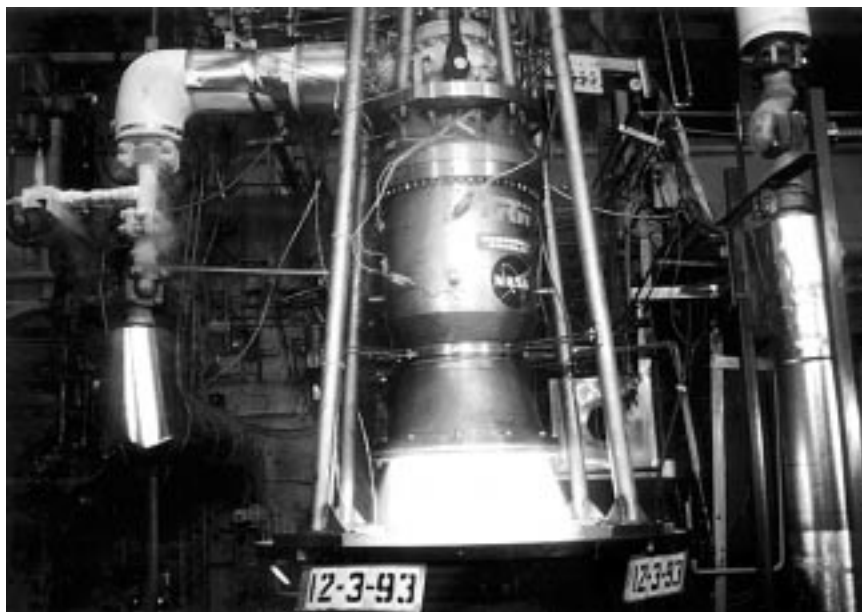
Dressler, G.A., et al.: Test Results from a Simple, Low-Cost, Pressure-Fed Liquid Hydrogen/Liquid Oxygen Rocket Combustor. 1993 JANNAF Propulsion Meeting, Vol. 2, 1992, pp. 51-67.

Henneberry, J.P., et al.: Low-Cost Expendable Launch Vehicles. AIAA Paper 92-3433, 1992.

Klem, M.D.; Jankovsky, A.L.; and Stoddard, F.J.: Results of LOX/RP-1 Pintle Injector Engine Tests. 32nd JANNAF Combustion Subcommittee Meeting, CPIA Publication 631, Vol. II, Oct. 1995.

Klem, M.D.; Wadel, M.F.; and Stoddard, F.J.: Results of 178 KN (40,000 Lbf) Thrust LOX/LH₂ Pintle Injector Engine Tests. 32nd JANNAF Combustion Subcommittee Meeting, CPIA Publication 631, Vol. II, Oct. 1995.

Lewis contact: Mark D. Klem, (216) 977-7473
Headquarters program office: OSAT



Combustion chamber with ablative liner tested with 40,000-lb-thrust liquid oxygen/liquid hydrogen.

High-Aspect-Ratio Cooling Channel Concept Tested in Lewis' Rocket Engine Test Facility

Rocket combustion chamber walls are exposed to the high-temperature environment caused by the combustion of propellants. Even with the walls actively cooled by the fuel, the hot gases can deteriorate the walls severely and limit any possibility for reusing the combustion chamber. For many years, the NASA Lewis Research Center has performed subscale investigations of potential improved cooling concepts to extend the life and reliability of the combustion chamber. Results from previous subscale tests have shown that, by increasing the coolant channel height-to-width aspect ratio, the rocket combustion chamber hot-gas-side wall temperature can be reduced by as much as 28 percent, without an increase in the coolant pressure drop (ref. 1). Recently, a series of experiments were completed in Lewis' Rocket Engine Test Facility (RETF) to validate the benefits of high-aspect-ratio cooling channels with a high-pressure, contoured rocket combustion chamber.

Validation of the high-aspect-ratio cooling channel concept was done with a high chamber pressure, contoured combustion chamber (see photo) to simulate the environment of a flight rocket engine. The combustion chamber had 100 conventional coolant channels outside of the critical heat flux area of the combustion chamber throat. These channels had a nominal aspect ratio of 2.5. High-aspect-ratio cooling channels were used in the critical heat flux area. The 100 conventional cooling channels were bifurcated into 200 channels, and their aspect ratios were increased to a range of 5 to 8. The hot-gas-side wall temperature in the throat region was predicted to be approximately 1200 °R. In comparison, a similar combustion chamber with 100 conventional coolant channels throughout the entire combustion chamber length was predicted to have a hot-gas-side wall temperature of approximately 1475 °R. So that the hot-gas-side wall temperature could be verified experimentally, the combustion chamber was heavily instrumented with 28 skin thermocouples, 9 cooling channel rib thermocouples, and 10 cooling channel pressure taps.

The combustion chamber was tested at chamber pressures from 800 to 1600 psia. The propellants were gaseous hydrogen and liquid oxygen at a nominal mixture ratio of 6, and liquid hydrogen was used as the coolant. A total of 29 thermal cycles, each with 1 sec of steady-state combustion, were completed on the combustion chamber. For 25 thermal cycles, the coolant mass flow rate was equal to the fuel mass flow rate. During the remaining four thermal cycles, the coolant



High-aspect-ratio cooling channel combustion chamber.

mass flow rate was progressively reduced by 6 to 18 percent.

Posttest analysis is being performed on the test data and the combustion chamber. The preliminary results show that the rib thermocouples were cooler than predicted; however, more analysis is required to realize the full effect of this on the hot-gas-side wall temperature. Visual examination of the combustion chamber after testing revealed minimal deterioration in the combustion chamber walls. The final results will be made available so that future rocket engine designers can take advantage of the high-aspect-ratio cooling channel concept.

Bibliography

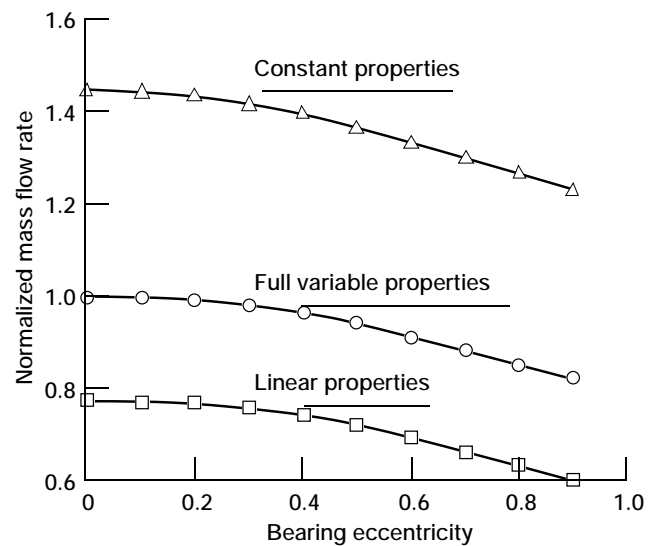
Carlile, J.A.; and Quentmeyer, R.J.: An Experimental Investigation of High-Aspect-Ratio Cooling Passages. AIAA Paper 92-3154 (NASA TM-105679), 1992.

Lewis contacts: Mary F. Wadel, (216) 977-7510, and Michael L. Meyer, (216) 977-7492
Headquarters program office: OSAT

Fluid Film Bearing Code Development

The next generation of rocket engine turbopumps is being developed by industry through Government-directed contracts. These turbopumps will use fluid film bearings because they eliminate the life and shaft-speed limitations of rolling-element bearings, increase turbopump design flexibility, and reduce the need for turbopump overhauls and maintenance. The design of the fluid film bearings for these turbopumps, however, requires sophisticated analysis tools to model the complex physical behavior characteristic of fluid film bearings that are operating at high speeds with low viscosity fluids. State-of-the-art analysis and design tools are being developed at the Texas A&M University under a grant guided by the NASA Lewis Research Center. Originally, Texas A&M was funded by the Rocketdyne Division of Rockwell International and then by Pratt & Whitney to develop the tools; but in 1993, Lewis assumed responsibility for the effort.

The latest version of the code, HYDROFLEXT, is a thermohydrodynamic bulk flow analysis with fluid compressibility, full inertia, and fully developed turbulence models. It can predict the static and dynamic force response of rigid and flexible pad hydrodynamic bearings and of rigid and tilting pad hydrostatic bearings. The Texas A&M code is a comprehensive analysis tool, incorporating key fluid phenomenon pertinent to bearings that operate at high speeds with low-viscosity fluids typical of those used in rocket engine turbopumps. Specifically, the energy equation was implemented into the code to enable fluid properties to vary with temperature and pressure. This is particularly important for cryogenic fluids because their properties are sensitive to temperature as well as pressure. As shown in the figure, predicted bearing mass flow rates vary significantly depending on the fluid model used. In addition, the Texas A&M code accounts for inertia in the thin-film region as well as at the edge of hydrostatic bearing pockets. Because cryogens are semicompressible fluids and the bearing dynamic characteristics are highly sensitive to fluid compressibility, fluid compressibility effects are also modeled. In addition, a turbulence model must be included because of the high operating speeds and low-viscosity fluids encountered in cryogenic turbopumps. The code contains fluid properties for liquid hydrogen, liquid oxygen, and liquid nitrogen as well as for water and air. Other fluids can be handled by the code provided that the user inputs information that relates the fluid transport properties to the temperature.



Predicted mass flow rate versus bearing eccentricity of a liquid hydrogen hydrostatic journal bearing for varying complexity fluid modes.

The Texas A&M bearing code has become the standard analysis and design tool used by the rocket engine community. This code is well accepted for use in designing fluid film bearings because of confidence in its predictions. The code has been validated extensively by Texas A&M and Rocketdyne. In addition, Lewis has joined with the Air Force Phillips Laboratory to validate a key aspect of the analysis through a contracted effort with Texas A&M. Under the direction of the Air Force, Texas A&M is conducting bearing tests using a mixture of water and gaseous nitrogen to verify the code for fluid compressibility effects.

The Phillips Laboratory is interested in the code to support and guide their in-house hydrostatic bearing test program, which will, in turn, provide data to further refine the code. Rocketdyne is presently using a version of the code to design bearings for a low-cost liquid oxygen turbopump being developed under a NASA Marshall Space Flight Center contract. Pratt & Whitney is also using a version of the code to support turbopump development programs including the advanced liquid hydrogen turbopump being developed for the Air Force. In addition, Marshall acquired a copy of HYDROFLEXT to incorporate it into a shaft and bearing kinematic and thermal analysis code, SHABERTH. Previously, SHABERTH was limited to rolling-element bearings.

The collaboration between NASA, the Air Force, and industry resulted in the successful development of a state-of-the-art fluid-film-bearing analysis and design tool. The effort is expected to continue to complete enhancements and validation. Analysis for an angular-injected hydrostatic bearing model and a two-phase flow model are presently being developed.

Bibliography

San Andres, L.: Turbulent Flow, Flexure-Pivot Hybrid Bearings for Cryogenic Applications. Presented at the ASME/STLE Tribology Conference, Orlando, Florida, Oct. 8-11, 1995. ASME Paper 95-TRIB-14, 1995.

**Lewis contact: James F. Walker, (216) 977-7465,
Headquarters program office: OSAT**

Cooperative Testing of Rocket Injectors That Use Gaseous Oxygen and Hydrogen

Gaseous oxygen and hydrogen propellants used in a special engine energy cycle called Full-Flow Staged Combustion are believed to significantly increase the lifetime of a rocket engine's pumps. The cycle can also reduce the operating temperatures of the engine. Improving the lifetime of the hardware reduces its overall maintenance and operations costs, and is critical to reducing costs for the joint NASA/industry Reusable Launch Vehicle (RLV). The work in this project will demonstrate the performance and lifetime of one-element and many-element combustors with gaseous O_2/H_2 injectors. This work supporting the RLV

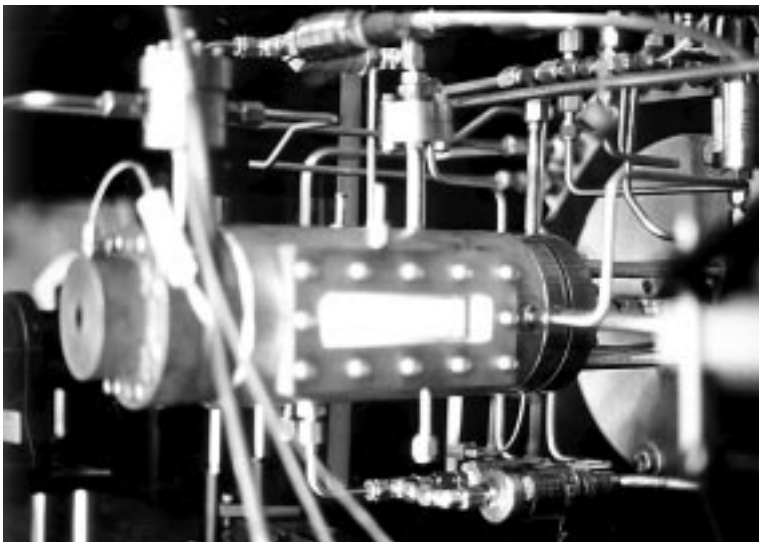
program is a cooperative venture of the NASA Lewis Research Center, the NASA Marshall Space Flight Center, Rocketdyne, and the Pennsylvania State University.

Information about gas-gas rocket injector performance with O_2/H_2 is very limited (ref. 1). Because of this paucity of data, new testing is needed to improve the knowledge base for testing and designing new injectors for the RLV and to improve computer models that predict the combusting gas flows of new injector designs. Therefore, detailed observations and measurements of the combusting flow from many-element injectors in a rocket engine are being sought. These observations and measurements will be done with three different tools: schlieren photography, ultraviolet imaging, and Raman spectroscopy. The schlieren system will take photos of the density differences in combusting flow, the ultraviolet movies will determine the location of the hydroxyl (OH) radical in the combustion flow, and the Raman spectroscopic measurements will provide the combustion temperature and amount of water (H_2O), hydrogen (H_2), and oxygen (O_2) in the combustor.

Marshall is providing overall program management, design and computational fluid dynamics (CFD) analyses, as well as funding for the work at Penn State. An existing, windowed combustor and several injectors will be provided by Rocketdyne—two injectors for the initial screening tests and one with an optimized design based on the best design found in the screening tests.

Lewis will provide a nozzle and several injectors for the screening test program. The configuration of the injectors will be based on a design chosen by all the participants, and their elements will be based on the coaxial and impinging flow. Lewis also will provide the instrumentation for the flow-field measurements: schlieren, ultraviolet imaging, and Raman spectroscopy. In addition, thermocouples will measure heat flow on the injector face. Other traditional measurements of rocket performance will be made as well: chamber pressure, mass flow of each propellant, purge flow, and the barrier cooling gas flow. Penn State will conduct single-element testing with the injector elements from both the Rocketdyne and the jointly designed injectors.

A wide variety of traditional and nontraditional injector designs will be tested in this program. The results will be valuable in computational fluid dynamics code validation and overall rocket combustion efficiency measurements.



Gas-gas windowed combustion chamber during test firing.

Correlations between combustion efficiency, laser measurements of species, and ultraviolet and visible light photography will also be made.

Thus far, several different single-element injectors have been tested at Penn State and Lewis. The figure shows the experimental setup of a rocket engine with a viewing window. The combusting flow is shown in the rectangular window. The results are helping engineers design the many-element injectors.

References

1. Calhoun, D.F.; Ito, J.I; and Kors, D.L.: Investigation of Gaseous Propellant Combustion and Associated Injector-Chamber Design Guidelines. NASA CR-121234, 1973.

Lewis contact: Bryan A. Palaszewski, (216) 977-7493
Headquarters program office: OSAT

Lessons Learned With Metallized Gelled Propellants

During testing of metallized gelled propellants in a rocket engine, many changes had to be made to the normal test program for traditional liquid propellants. The lessons learned during the testing and the solutions for many of the new operational conditions posed with gelled fuels will help future programs run more smoothly. The major factors that influenced the success of the testing were propellant settling, piston-cylinder tank operation, control of self pressurization, capture of metal oxide particles, and a gelled-fuel protective layer.

In these ongoing rocket combustion experiments at the NASA Lewis Research Center, metallized, gelled liquid propellants are used in a small modular engine that produces 30 to 40 lb of thrust. Traditional liquid RP-1 and gelled RP-1 with 0-, 5-, and 55-wt % loadings of aluminum are used with gaseous oxygen as the oxidizer (ref. 1). The figure compares the thrust chamber efficiencies of different engines.

Propellant Settling

After the gelled fuels are mixed and before this mixture is put in the propellant transfer tank, the RP-1/Al must be stirred vigorously. During storage periods of 1 to 10 days, the metal particles in the fuel begin to settle because of gravity, and a thin layer of clear RP-1 forms atop the fuel in its storage can. The fluid layer is about 1-cm thick after about 10 days of storage. Ostwald

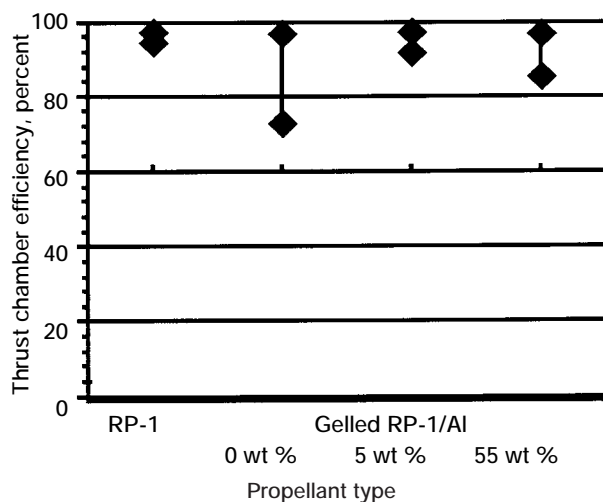
forces (refs. 2 and 3) promote clumping of the propellant during storage.

Using a Piston-Cylinder Tank

In previous testing of gelled fuels (ref. 4), there was some difficulty in feeding the metallized gelled JP-10/Al into the piston-cylinder tank. A manual stirring process was used to reduce the viscosity of the thixotropic fuel until a small pump could feed fuel into the cylinder. To speed up this time-consuming filling process, we fabricated a pressurized transfer tank to fill the piston-cylinder tank. The transfer tank was charged with gelled fuel, and nitrogen pressurant was used to flow the fuel to the cylinder.

Propellant Self Pressurization

Experiments were conducted after we had an unplanned pressurization of the piston-cylinder tank. The propellant had been in the cylinder for several days to several weeks, and the tank pressure had risen from zero to several hundred pounds per square inch (gravimetric). In our testing operations we were unsure as to the fluid interactions, but high-pressure gas is generated when RP-1/Al is exposed to water. To alleviate this problem for the short term, we replaced the "pressurizing" fluid for the gelled propellant with hydraulic fluid. A series of tests that estimate the gas-generation rate from a mixture of RP-1/Al metallized gelled fuel and a test fluid were conducted. The test fluids were water, hydraulic fluid, and Solvent 140. Although Solvent 140 and hydraulic fluid generated little or no pressure, the water exposed to the RP-1/Al created significant pressures in some cases.



Comparison of rocket engine performance for four fuels: RP-1, and 0-, 5-, and 55-wt % RP-1/Al.

Particle Capturing

Rocket testing in Lewis' Cell 21 uses a 9-ft-long tubular diffuser with a series of circumferential water spray nozzles for cooling. This diffuser tube was augmented with an add-on tube (that added 3 ft of length) and a 150-gal plastic tank to capture water from the cooling system and particles from the rocket exhaust. During a firing, the top of the tank was removed and the gaseous exhaust products were vented vertically away from the test cell. The water captured in the tank was run through a 10- μ m filter before the water was exhausted into the laboratory area drain system. A small fraction of the metal particles were exhausted in this manner, but the bulk of the Al_2O_3 and other solid combustion products were captured in the cooling water flow. The filter did foul after a period of several days of testing, and when it fouled, it had to be changed. During the entire 1-year test period, we changed the filter at least 8 to 10 times.

Gelled Propellant Protective Layer

During testing with the gelled RP-1 and the 5-wt % RP-1/Al, some residual propellant was found in the rocket chamber, coating the entire injector face and all the chamber walls. This residual propellant was actually a mix of unburned fuel (with a gray or clear pink color) and some black or combustion products. Although none of the injector ports clogged, there was a potential for the gel to obstruct the ports to a small degree. Once this thin layer was removed with a soft cloth, the metal surfaces exhibited minimal erosion. An improved cooling technique might be derived from this effect. The thickness of the layer is 1 to 2 mm for 0- and 5-wt % RP-1/Al. The layer is easily wiped off with a soft cloth when the face is cleaned after disassembly. The gel layer also coats the injector such that the O_2 and fuel flow form holes in the layer.

References

1. Palaszewski, B.; and Zakany, J.S.: Metallized Gelled Propellants: Oxygen/RP-1/Aluminum Rocket Combustion Experiments. AIAA Paper 95-2435 (NASA TM-107025), 1995.
2. Iler, R.K.: The Chemistry of Silica: Solubility, Polymerization, Colloid and Surface Properties, and Biochemistry, John Wiley and Sons, New York, 1979.
3. Selegny, E.: Charged Gels and Membranes—Part I. D. Reidel Publishing Company, Dordrecht, Holland, 1976.
4. Galecki, D.L.: Ignition and Combustion of Metallized Propellants. AIAA Paper 89-2883, 1989.

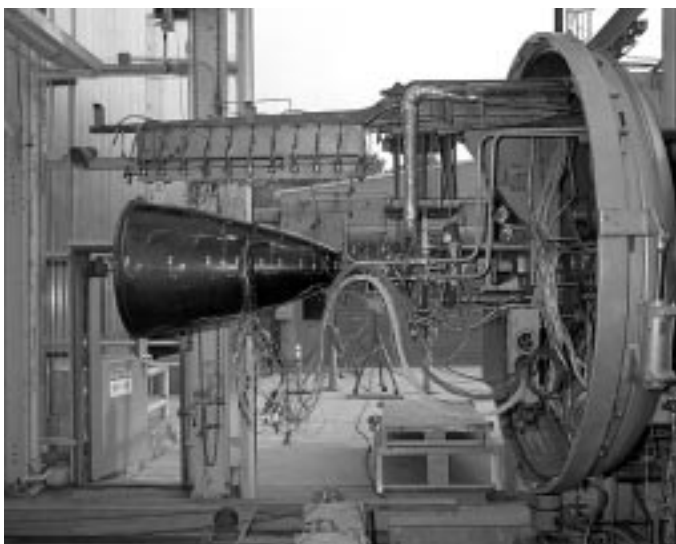
Lewis contact: Bryan A. Palaszewski, (216) 977-7493
Headquarters program office: OSAT

1025:1 Area Ratio Nozzle Evaluated at High Combustion Chamber Pressures

A recently completed experimental test program obtained performance data on an optimally contoured nozzle with an exit-to-throat area ratio ϵ of 1025:1 and on a truncated version of this nozzle with an area ratio of 440:1. The nozzles were tested with gaseous hydrogen and liquid oxygen propellants at combustion chamber pressures of 12.4 to 16.5 mPa (1800 to 2400 psia). Testing was conducted in the altitude test capsule at the NASA Lewis Research Center's Rocket Engine Test Facility (RETF), and results were compared with analytical performance predictions. This testing builds on previous work with this nozzle at Lewis, where testing was completed at a nominal chamber pressure of 350 psia.

High-area-ratio nozzles have long been sought as a means to increase the performance of space-based rocket engines. However, as the area ratio increases, the physical size and weight of the nozzle also increase. As a result, engine and vehicle designers must make trade-offs between nozzle size and performance enhancement. Until this test program, very little experimental data existed on the performance of the high-area-ratio nozzles used in rocket engine designs. The computer codes being used by rocket engine designers rely on data extrapolated from tests of low-area-ratio nozzles, and these extrapolations do not always provide the accuracy needed for a reliable design assessment. Therefore, we conducted this high-area-ratio nozzle testing program to provide performance data for use in rocket engine design and analysis computer codes.

The nozzle had a nominal 2.54-cm- (1-in.-) diameter throat, an exit diameter of 81.3-cm (32.0-in.) at $\epsilon = 1025$, and a length of 128.6 cm (50.6 in.). Testing was conducted in an altitude test capsule to simulate the static pressure at altitude by vacuum pumping. Data such as propellant mass flow, oxidizer-to-fuel mixture, and thrust were measured. These measurements were then used to calculate performance factors such as the thrust coefficient C_F , the characteristic exhaust velocity efficiency ηC^* , and the vacuum specific impulse I_{sp} . In addition, the nozzle temperature was measured to calculate the amount of heat transferred from the combustion gases to the nozzle.



High-area-ratio nozzle on test stand.

References

1. Pavli, A.J.; Kacynski, K.J.; and Smith, T.A.: Experimental Thrust Performance of a High-Area-Ratio Rocket Nozzle. NASA TP-2720, 1987.
2. Smith, T.A.; Pavli, A.J.; and Kacynski, K.J.: Comparison of Theoretical and Experimental Thrust Performance of a 1030:1 Area Ratio Rocket Nozzle at a Chamber Pressure of 2413 kN/m² (350 psia). AIAA Paper 87-2069 (NASA TP-2725), 1987.
3. Kacynski, K.J.; Pavli, A.J.; and Smith, T.A.: Experimental Evaluation of Heat Transfer on a 1030:1 Area Ratio Rocket Nozzle. AIAA Paper 87-2070 (NASA TP-2726), 1987.
4. Jankovsky, R.J.; Kazaroff, J.M.; and Pavli, A.J.: Experimental Performance of a High-Area-Ratio Rocket Nozzle at High Combustion-Chamber-Pressure, NASA TP-3576, 1996.

Lewis contacts: Robert S. Jankovsky, (216) 977-7515, and Timothy D. Smith, (216) 977-7546
Headquarters program office: OSAT

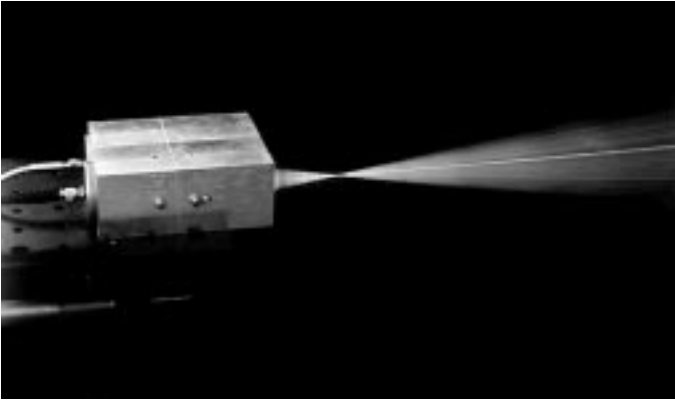
Diagnostics Adapted for Heat-Treating Furnace Environment

Diagnostics developed for the in situ monitoring of rocket combustion environments were adapted for use in heat-treating furnaces. Simultaneous, in situ monitoring of the carbon monoxide, carbon dioxide, methane, water, and hydrogen concentrations in the endothermic gas of a heat-treating furnace were demonstrated under a Space Act Agreement between the NASA Lewis Research Center, the Heat Treating Network, and Akron Steel Treating Company. This endothermic gas, or "endogas," is produced in a catalytic process, where natural gas is "cracked" in the presence of air. Variations in the composition of the natural gas supplied lead to variations in the composition of the endothermic gas. These variations could lead to an unacceptable quality of steel products that are hardened through the carburization process that uses this gas.

Conventional methods of monitoring the endogas include measuring the dew point of the gas and the oxygen concentration. From these data, the carbon monoxide content of the gas can be calculated. This carbon monoxide concentration creates the carbon potential needed for carburization. Several weak links are present in this approach. The oxygen monitor deteriorates over time, and the measurement might be inaccurate by 50 percent. Also, the chemistry equations, which are based on several assumptions, such as secondary species concentrations, provide only an approximate estimate of the carbon monoxide concentration.

To address these weaknesses, we investigated a new method based on ordinary Raman spectroscopy, in which the carbon monoxide concentration is measured directly and in situ. This method measures the laser light scattered from the molecules. Each species interacts with the light and scatters the light at a different frequency. Spectral monitoring of the scattered light intensity at each molecular frequency of interest provides the species concentrations. One advantage over the conventional method is that several species can be monitored simultaneously. A second advantage is that the measurement is direct; there is no need to make assumptions, to filter the gas, or to calibrate the instrument.

An instrument was designed consisting of a laser and a detection system within an enclosure, connected to an optical probe by fibers. For determining carbon monoxide concentration, the probe is mounted on the



Optical diagnostics probe in operation.

endothermic gas line, close to the generator. Optical fibers with a length of 150 ft have been used to transmit laser light from the instrument to the probe. There, the light is focused into the gas, and the scattered light is collected and transmitted back to the instrument where it is analyzed with a photomultiplier and lock-in amplifier. Laboratory tests have shown that with the current system the concentration of carbon monoxide, water, nitrogen, oxygen, and hydrogen in the air can be monitored with an accuracy of 1 percent. The concentration of carbon dioxide in the air can be monitored with an accuracy of 0.5 percent, and the concentration of methane with an accuracy of 0.2 percent.

This instrument was taken to the Akron Steel Treating Plant, where field tests are in progress to verify the system capabilities. Planned developments are improving the accuracy, monitoring multiple locations, and reducing instrument size and cost.

Bibliography

De Groot, W.A.: The Use of Spontaneous Raman Scattering for Hydrogen Leak Detection. AIAA Paper 94-2983 (NASA CP-195373), 1994.

De Groot, W.A.: Fiber-Optic Based Compact Gas Leak Detection System. AIAA Paper 95-2646, 1995.

**Lewis contact: Dr. Wilhelmus A. de Groot,
(216) 977-7485**

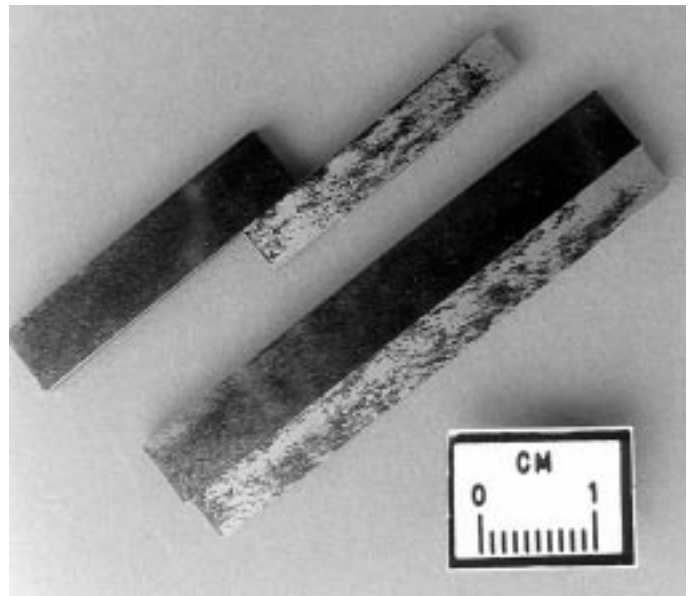
Headquarters program office: OSAT

Rhenium Rocket Manufacturing Technology

The NASA Lewis Research Center's On-Board Propulsion Branch has a research and technology program to develop high-temperature (2200 °C), iridium-coated rhenium rocket chamber materials for radiation-cooled rockets in satellite propulsion systems. Although successful material demonstrations have gained much industry interest, acceptance of the technology has been hindered by a lack of demonstrated joining technologies and a sparse materials property data base.

To alleviate these concerns, we fabricated rhenium to C-103 alloy joints by three methods: explosive bonding, diffusion bonding, and brazing. The joints were tested by simulating their incorporation into a structure by welding and by simulating high-temperature operation. Test results show that the shear strength of the joints degrades with welding and elevated temperature operation but that it is adequate for the application. Rhenium is known to form brittle intermetallics with a number of elements, and this phenomena is suspected to cause the strength degradation. Further bonding tests with a tantalum diffusion barrier between the rhenium and C-103 is planned to prevent the formation of brittle intermetallics.

The rhenium material properties data needed by rocket designers was generated, and low-cycle fatigue tests of powder metallurgy (PM) rhenium specimens were



Rhenium bonded to ClO_3 by the explosive was evaluated and shown to have the necessary strength for the rocket application.

successfully conducted. These specimens passed a 100-cycle test sequence indicating that powder metallurgy rhenium can meet the service requirements of small chemical rockets. Tensile properties of rhenium fabricated by chemical vapor deposition (CVD) and powder metallurgy were evaluated from room temperature to 1900 °C, and evaluations at 2200 °C are planned. These data indicate that either fabrication technique is viable. Rhenium creep tests also indicate that the material is suitable for use in rocket chambers at the pressures and elevated temperatures anticipated. Enhancement of the iridium oxidation resistance also was demonstrated. A ceramic-oxide-coated, iridium-coated rhenium rocket chamber was successfully tested for 32 hr on gaseous hydrogen/gaseous oxygen propellants at a mixture ratio of 4. The oxidizer content in these gases is similar to that of Earth storables, indicating that the oxide coating causes a factor of 5 increase in life over previously tested iridium/rhenium chambers.

Under a Space Act Agreement, the NASA-developed rhenium rocket technology enabled TRW to develop an Advanced Dual Mode rocket with 328 sec of specific impulse. This engine will be baselined on the Lockheed Martin A2100 satellite, if it is flight qualified in the time frame required.

Lewis contact: Dr. Steven J. Schneider, (216) 977-7484
Headquarters program office: OSAT

NSTAR Ion Propulsion System Power Electronics

High-specific-impulse ion propulsion systems (IPS's) have long been targeted as candidates for the primary propulsion systems of both planetary and Earth-space spacecraft, and as auxiliary propulsion systems for geosynchronous communications spacecraft. Major issues with ion propulsion systems are the system cost and complexity, especially in the power processing unit (PPU). In some cases, the PPU's have contained over 4000 discrete parts and 12 power supplies to operate the thruster.

The NASA Solar Electric Propulsion Technology Application Readiness

(NSTAR) program, managed by the Jet Propulsion Laboratory (JPL), is currently developing a high-performance, simplified ion propulsion system. This propulsion system, which is throttleable from 0.5- to 2.3-kW output power to the thruster, targets primary propulsion applications for planetary and Earth-space missions and has been baselined as the primary propulsion system for the first New Millennium spacecraft.

The NASA Lewis Research Center is responsible for the design and delivery of a breadboard PPU and an engineering model thruster (EMT) for this system and will manage the contract for the delivery of the flight hardware to JPL. The PPU requirements, which dictate a mass of less than 12 kg with an efficiency of 0.9 or greater at a 2.3-kW output, forced a departure from the state-of-the-art ion thruster PPU design. Several innovations—including dual-use topologies, simplified thruster control, and the use of ferrite magnetic materials—were necessary to meet these requirements.

To reduce the level of complexity and parts count in the PPU, designers at Lewis employed a dual-use concept for the discharge and neutralizer power supplies. The dual-use topology derives power for the cathode heater and anode from the same power transformer, allowing the construction of a single inverter each for the neutralizer and discharge power supplies. This topology selection reduced the number of power supplies necessary to operate the thruster to four. Further simplifications were realized in the PPU with the application of a single closed loop, implemented in a microcontroller, for thruster control. This loop regulates the beam current, and thus the thrust produced, by varying the discharge current. Completed breadboard power supplies are shown in the photograph.



Three breadboard power-supply modules.

To minimize mass and optimize the efficiency of the breadboard, we set the switching frequency of the power supplies which operate the thruster at 50 kHz. This frequency selection represents a compromise between low mass and high efficiency, and it also allows the power transformers to be designed and fabricated with ferrite (ceramic) cores. If packaging of ferrite components for spaceflight becomes an issue, this frequency is still within the usable range of metallic core transformers that have an extensive heritage in flight designs.

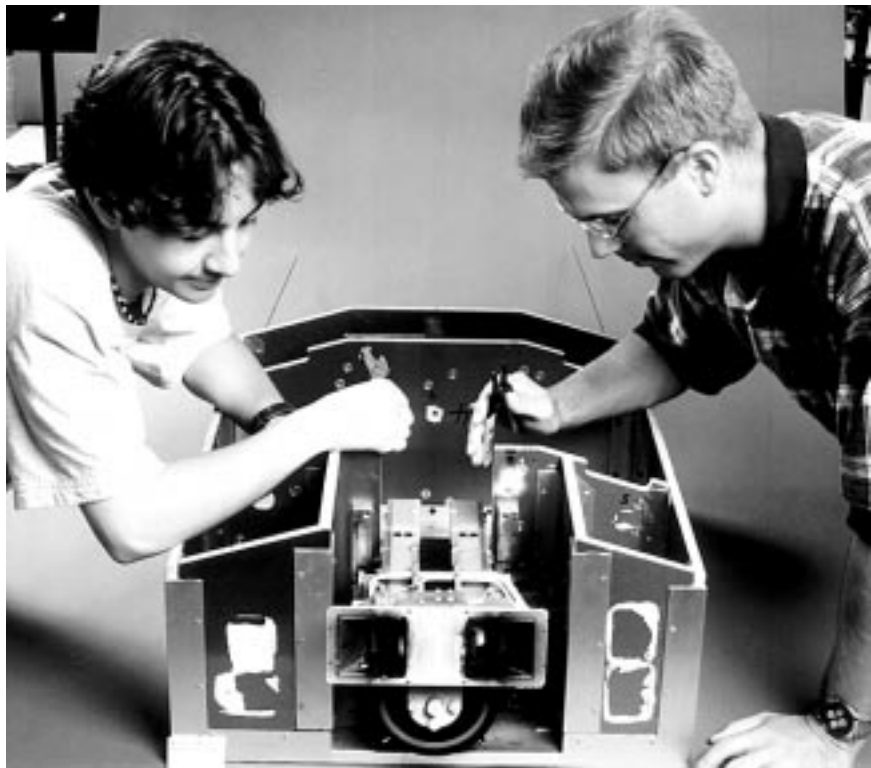
A breadboard version of the PPU was fabricated to validate the dual-use concept and verify closed-loop stability within the individual power supplies and with the thruster. The breadboard, which was integrated with a 30-cm ion thruster, demonstrated autonomous control and stable steady-state operation of the thruster over the full throttling range. The total component mass of the breadboard as built is 6.2 kg, and the efficiency is on the order of 0.9. A simplified user interface facilitates thruster operation via a data terminal, with thruster operations reduced to a single on/off command.

Lewis contact: John A. Hamley, (216) 977-7430
Headquarters program office: OSAT (STD and SSD)

Pulsed Plasma Thruster Technology

The continuing emphasis on reducing costs and downsizing spacecraft is forcing increased emphasis on reducing the subsystem mass and integration costs. For many commercial, scientific, and Department of Defense space missions, onboard propulsion is either the predominant spacecraft mass or it limits the spacecraft lifetime. Electromagnetic-pulsed-plasma thrusters (PPT's) offer the combined benefits of extremely low average electric power requirements (1 to 150 W), high specific impulse (~1000 sec), and system simplicity derived from the use of an inert solid propellant. Potential applications range from orbit insertion and maintenance of small satellites to attitude control for large geostationary communications satellites.

Although PPT's have operated on several spacecraft, there has been no new PPT technology development since the early 1970's. As a result of rapid growth in the small satellite community and the broad range of PPT applications, the NASA Lewis Research Center has initiated a development program to dramatically reduce the PPT dry mass, increase PPT performance, and demonstrate a flight-ready system by October 1997. The flight system is being built under a contract with



LES 8/9 pulsed-plasma thruster mounted on the JAWSAT spacecraft bus in preparation for integration testing at Lewis.

Olin Aerospace. A recent report (ref. 1) summarized the results of a series of near-Earth mission studies, including both primary and auxiliary propulsion and attitude control functions and reviewed the status of NASA's ongoing development program.

The baseline technology for the new development program is the Lincoln Experimental Satellite (LES) 8/9 PPT, which was flight qualified in 1970 with a fueled system mass of 7.0 kg and provides 10,000-N-sec total impulse. The program objectives are to decrease the fueled system mass to 3.5 kg while doubling the total impulse capability to 20,000 N-sec. These objectives are being accomplished via the use of recently developed capacitors, integrated circuit technology for both telemetry and power electronics, new structural materials, and an increase in PPT performance.

Efforts to date have demonstrated a factor of 2 reduction in mass and volume for the power converter, ignition, and logic/telemetry systems. In addition, lightweight capacitors have been selected and are undergoing life testing in a new PPT discharge simulator. Spacecraft integration assessments are also underway, with testing of contamination, electromagnetic interference, and Global Positioning System compatibility. This testing is currently focused on integrating an old LES 8/9 PPT on the Joint Air Force/Weber State University Satellite (JAWSAT), a small educational satellite to be launched in 1997 (see figure). The PPT program is on target to deliver a new, lightweight flight-qualified system in October 1997.

Reference

1. Myers, R., et al.: Pulsed Plasma Thruster Technology for Small Satellite Missions. NASA CR-198427, 1995.

Lewis contact: Dr. Roger M. Myers, (216) 977-7426
Headquarters program office: OSAT

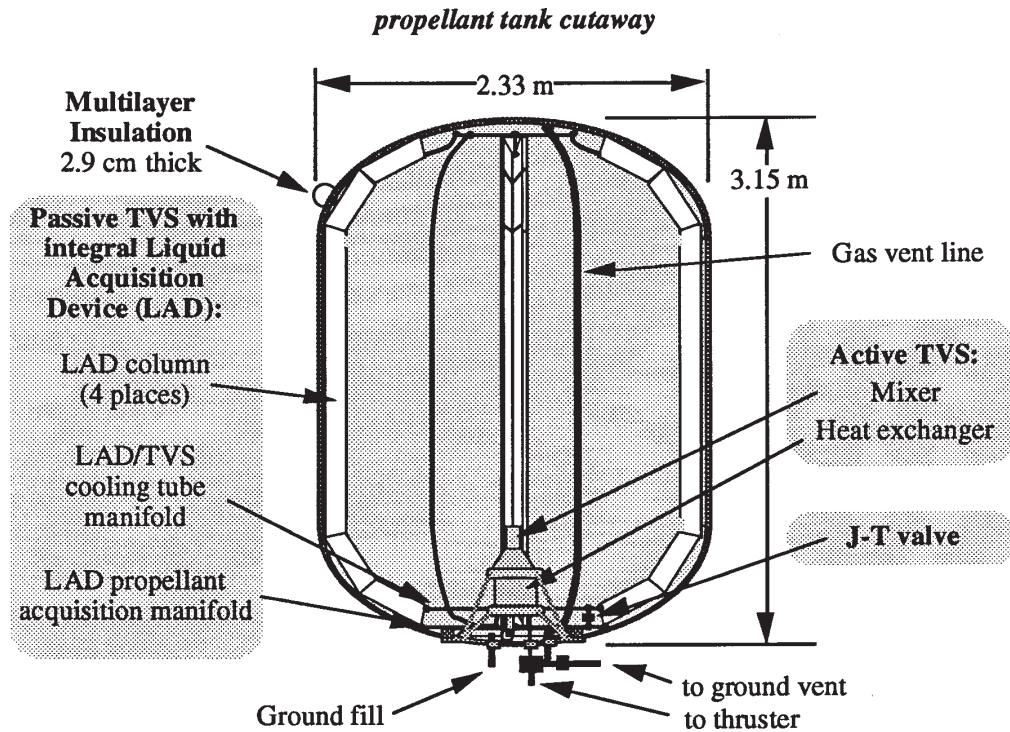
Thermodynamic Vent System Applied as Propellant Delivery System for Air Force

Responding to a request from the Air Force, NASA Lewis Research Center engineers designed a combination pressure control and propellant delivery system based on thermodynamic vent system (TVS) technology. The Air Force is designing a new type of orbit transfer vehicle that uses energy from sunlight to both propel and power the vehicle. Because this vehicle uses propellant at a substantially slower rate than higher-energy rockets, it needed the Lewis-developed TVS technology for long-duration storage of cryogen propellants. Lewis engineers, in conjunction with industry partners, showed how this TVS technology could also be used to deliver propellant to the thruster. The Air Force has now begun the ground test demonstration phase. After successful completion of ground testing, the Air Force plans to use this technology in a space flight as early as 1999.

To reduce satellite operation costs, the Air Force is designing an Integrated Solar Upper Stage (ISUS) to transport communication satellites from low-Earth orbit to higher operational orbits. This vehicle uses solar concentrators for both propulsive heating of the hydrogen propellant and thermionic power generation once the vehicle has reached its operational orbit. Because the payload and spacecraft system are integrated into a common unit and because the propulsion method has a higher specific impulse than conventional upper stages do, the Integrated Solar Upper Stage can use smaller and less-expensive launch vehicles to deliver the same mass as conventional upper stages.

For this application, the Air Force needed a propellant storage and delivery system with the following characteristics: (1) a minimum-volume, cryogenic liquid hydrogen tank, (2) no propellant venting except that which occurs as a part of orbit transfer burns, (3) a 30-day orbit transfer with a nonconstant burn schedule, (4) a high ratio of tank lockup durations to burn durations, and (5) the option to hold the propellants at low orbit for 3 to 7 days before the orbit transfer.

These challenges were met by the Lewis/industry team's conceptual design, shown in the figure. To minimize tank volume, the team used a low-pressure, low-ullage tank (0.3 MPa, 3-percent ullage). A multi-layer insulation system reduces heat leaks into the tank, but it is designed to allow enough background heat into



Thermodynamic vent system applied as propellant delivery system for air force integrated solar upper stage—propellant tank cutaway.

the tank to pressurize the system. A TVS, originally designed for controlling tank pressures for long-duration cryogen storage, simultaneously delivers propellant to the thruster and removes heat from the tank. The resulting pressure drop during each burn is tailored so that the operating pressure will be recovered by background heating before the next burn. Because of the nonconstant burn schedule and uncertainties about the heat rate and corresponding pressure rise in microgravity environments, a TVS incorporating an integral mixer and heat exchanger with an active controller is used. The mixer can also be used between

burns to control tank pressure. A heater included in the system can add heat to the tank if needed.

The next major step of the program is the engine ground demonstration to be conducted in Lewis test facilities (1997). It will demonstrate vehicle operation over a simulated mission profile. Success of the ground testing may lead to a flight mission as early as 1999.

Lewis contact: Marc G. Millis, (216) 977-7535
Headquarters program office: OSAT

Power Technology

SCARLET Solar Array Delivered for METEOR Mission

Solar Concentrator Array with Refractive Linear Element Technology (SCARLET) is a joint NASA Lewis Research Center/Ballistic Missile Defense Organization program to develop advanced photovoltaic array technology for future space missions. This advanced power system technology uses a unique refractive concentrator design to focus sunlight onto a line of photovoltaic cells located below the optical element. The concentrator design is based on previous work conducted at Lewis under a Small Business Innovation Research Program (SBIR) with Entech, Inc.

SCARLET technology offers a number of advantages for future spacecraft systems. In addition to the potential benefits of providing a high-efficiency array at a low cost, its inherent resistance to degradation in a high-radiation environment makes this technology extremely attractive for a number of future Government and commercial missions. The demonstrated benign behavior of concentrator arrays with respect to plasma interactions also makes SCARLET a desired power source for missions involving electric propulsion technology.

Small prototype samples of refractive concentrator technology had flown previously; however, concentrators had not been demonstrated in space at the "array level." When an opportunity to fly a SCARLET array on the first flight of the Multiple Experiments to Earth Orbit and Return (METEOR) spacecraft arose, an industry team led by AEC-Able Engineering, Inc., was contracted to design, build, and test the array. A major problem presented by this flight opportunity was the tight schedule involved. To meet the original launch schedule, we needed to move the SCARLET-METEOR program from the existing prototype component hardware to a new flight-qualified solar array within a 6-month period. Despite the expected problems associated with the development of new technology, a self-contained, fully deployable array was fabricated, flight tested, and delivered for spacecraft integration within the specified time.

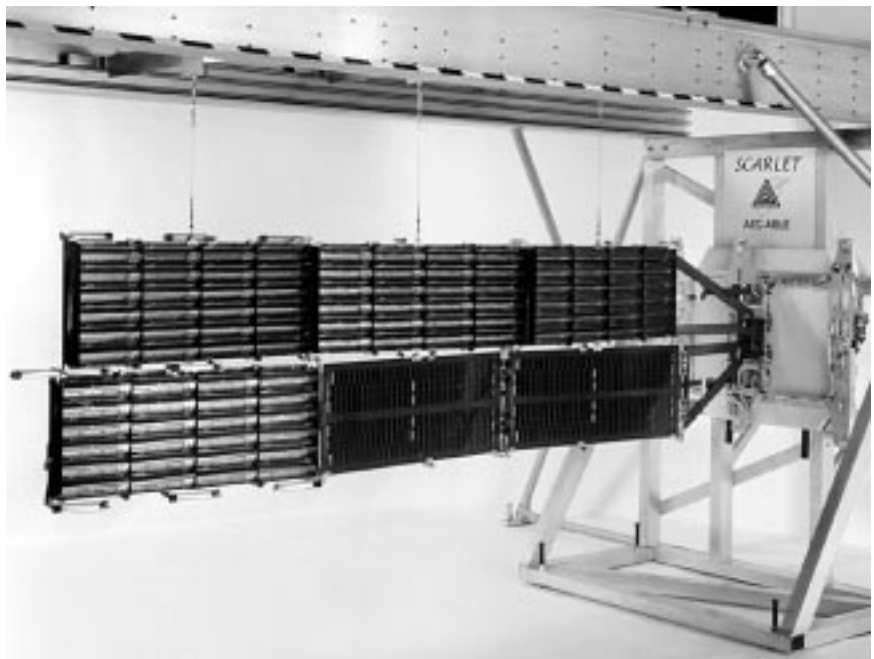
The nominal 200-W array was designed not only to provide valuable in-flight data on SCARLET deployment, performance, and long-term operations, but also to supplement power to the spacecraft bus.

Despite the success of the SCARLET-METEOR hardware development program, failure of the Conestoga launch vehicle on October 23, 1995, prevented actual orbital data from being obtained on this array. However, the development of the METEOR flight hardware provided a basis from which the SCARLET program will continue. The lessons learned and the techniques developed under SCARLET-METEOR will provide invaluable experience as hardware is developed for a variety of future space missions.

For more information about SCARLET, visit our site on the World Wide Web:

<http://powerweb.lerc.nasa.gov/psi/DOC/scarlet.html>

**Lewis contact: Michael F. Piszczor, (216) 433-2237
Headquarters program office: OSAT**



SCARLET-METEOR solar array flight hardware shown in a deployed configuration.

Valuable Data Provided by PASP Plus Flight Experiment After 1 Year in Orbit

Successfully launched on August 3, 1994, the Photovoltaic Array Space Power Plus Diagnostics (PASP Plus) flight experiment is a joint Air Force Phillips Laboratory/NASA Lewis Research Center program designed to test a variety of new and existing photovoltaic (PV) cell and array technologies within the space environment. The experiment consists of 12 different experimental photovoltaic modules, along with numerous diagnostic instruments that measure the space environment and interactions between the experimental modules and that environment. Power Technology Division personnel at Lewis, who had the primary responsibility for integrating the individual photovoltaic module experiments, continue to analyze and interpret the current-voltage characteristics and environmental effects data received back from the spacecraft.

The major goals of the experiment included determining the long-term performance of the photovoltaic modules within a high-radiation environment (PASP Plus was launched into an elliptical, high-radiation orbit) and measuring the interactions between the experimental modules and the space plasma when the modules were biased at high positive and negative voltages. Understanding array interactions within the space plasma is critical to spacecraft power system operations and important to providing higher bus voltage designs in the future.

After 1 year in orbit, a wealth of data has been obtained. Some of the major results show that refractive concentrator arrays provide excellent resistance to space radiation-induced degradation effects. The refractive concentrator optics have shown good survivability within the space environment and the off-pointing performance of this array is consistent with predicted results. Planar cells made from indium phosphide (InP) show less degradation than traditional gallium arsenide (GaAs) and silicon (Si) cells, specifically for this high-radiation, proton-dominated orbit. The light-induced degradation effects of amorphous silicon cell technology have been observed and are consistent with the results predicted by current models. General trends have also been observed for plasma current collection

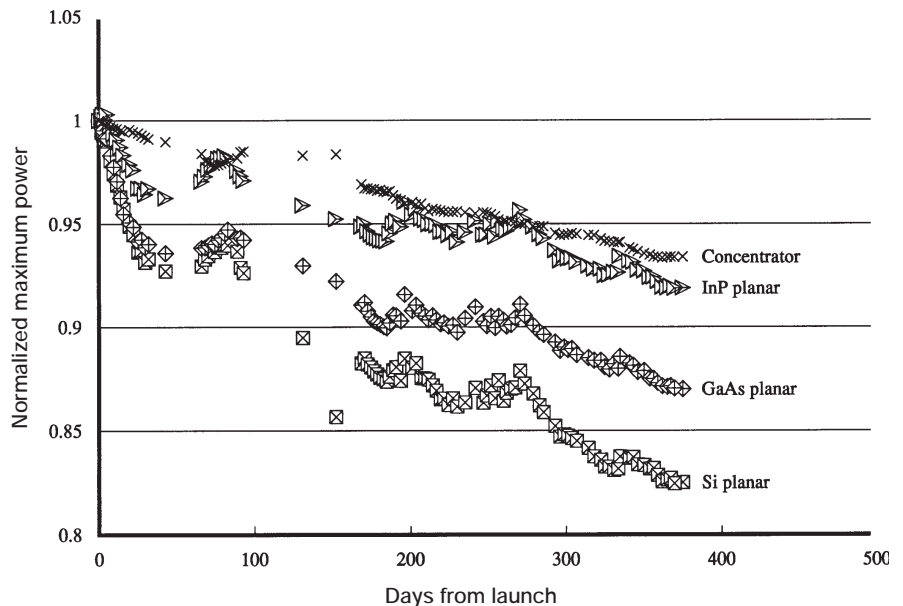
and arcing during the high-voltage biasing experiments. These trends confirm that the cell/array design is critical to the magnitude of the plasma interactions expected for an operational array. The observations noted herein are representative of the invaluable information that PASP Plus has provided to various organizations in NASA, other Government agencies, and industry.

Recent anomalies with the experiment and spacecraft electronics, primarily induced by the high-radiation environment, indicate that PASP Plus may have reached the limit of its useful life. Yet, after just 1 year in orbit, PASP Plus has achieved all its initial objectives. The high-voltage plasma-interaction experiments are complete, and by virtue of the higher orbital apogee attained, the desired cumulative radiation dose was achieved. Although analysis continues on the massive amounts of data obtained over the past year, PASP Plus already has shown itself as "one of the premier experiments with regard to long-term solar cell evaluation and testing in space" (Sal Grisaffe, former Director of Lewis' Aerospace Technology Directorate).

Find out more about Lewis' Power Technology Division on the World Wide Web:

<http://powerweb.lerc.nasa.gov/>

**Lewis contacts: Henry B. Curtis, (216) 433-2231,
Michael F. Piszczor, (216) 433-2237
Headquarters program office: OSAT**



PASP Plus experimental data exhibit performance trends of different cell materials and array types after 1 year in orbit.

Separator Materials Used in Secondary Alkaline Batteries Characterized and Evaluated

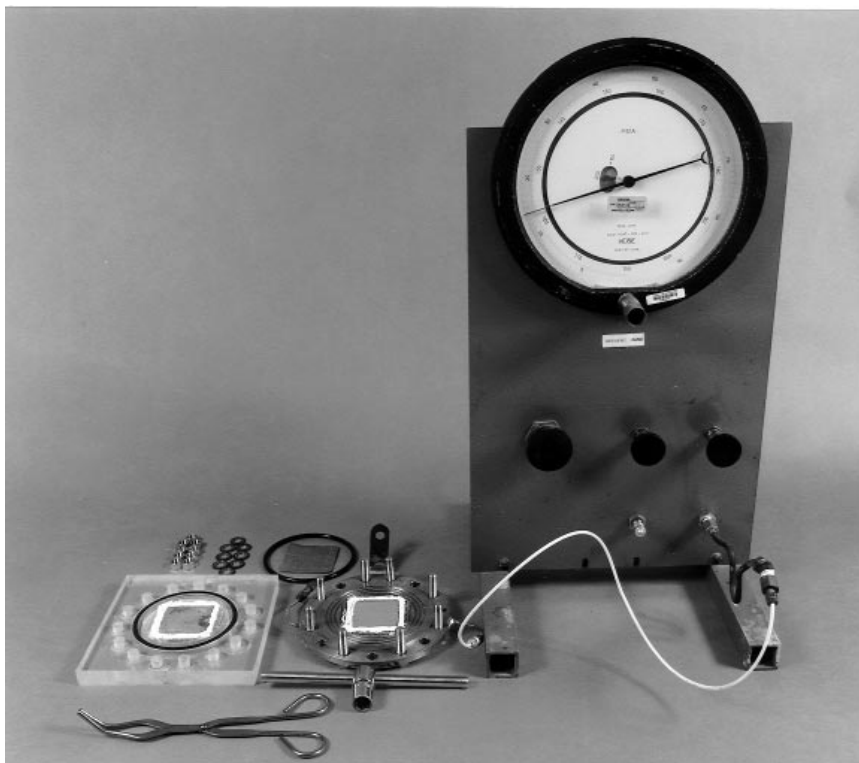
Nickel-cadmium (Ni/Cd) and nickel-hydrogen (Ni/H₂) secondary alkaline batteries are vital to aerospace applications. Battery performance and cycle life are significantly affected by the type of separators used in those batteries. A team from NASA Lewis Research Center's Electrochemical Technology Branch developed standardized testing procedures to characterize and evaluate new and existing separator materials to improve performance and cycle life of secondary alkaline batteries.

Battery separators must function as good electronic insulators and as efficient electrolyte reservoirs. At present, new types of organic and inorganic separator materials are being developed for Ni/Cd and Ni/H₂ batteries. The separator material previously used in the NASA standard Ni/Cd was Pellon 2505, a 100-percent nylon-6 polymer that must be treated with zinc chloride (ZnCl₂) to bond the fibers. Because of stricter Environmental Protection Agency regulation of ZnCl₂ emissions, the battery community has been searching for new separators to replace Pellon 2505. As of today, two candidate separator materials have been identified; however, neither of the two materials have performed

as well as Pellon 2505. The separator test procedures that were devised at Lewis are being implemented to expedite the search for new battery separators.

The new test procedures, which are being carried out in the Separator Laboratory at Lewis, have been designed to guarantee accurate evaluations of the properties that are critical for sustaining proper battery operation. These properties include physical and chemical stability, chemical purity, gas permeability, electrolyte retention and distribution, uniformity, porosity, and area resistivity. A manual containing a detailed description of 12 separator test procedures has been drafted and will be used by the battery community to evaluate candidate separator materials for specific applications. These standardized procedures will allow for consistent, uniform, and reliable results that will ensure that separator materials have the desired properties for long life and good performance in secondary alkaline cells.

Lewis contact: Edwin Guasp, (216) 433-5249
Headquarters program office: OSMA



Bubble Pressure Test Apparatus for determination of gas permeabilities across a battery separator.

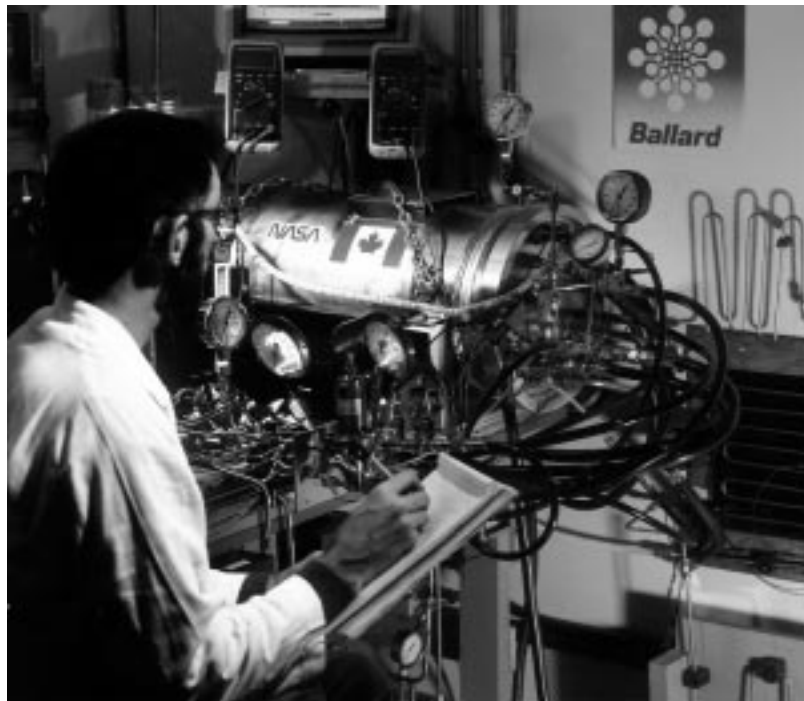
Regenerative Fuel Cell System Testbed Program for Government and Commercial Applications

NASA Lewis Research Center's Electrochemical Technology Branch has led a multiagency effort to design, fabricate, and operate a regenerative fuel cell (RFC) system testbed. Key objectives of this program are to evaluate, characterize, and demonstrate fully integrated RFC's for space, military, and commercial applications. The Lewis-led team is implementing the program through a unique international coalition that encompasses both Government and industry participants. Construction of the 25-kW RFC testbed at the NASA facility at Edwards Air Force Base was completed in January 1995, and the system has been operational since that time.

RFC systems can provide efficient, environmentally benign, highly reliable, renewable energy conversion for a variety of applications. These systems consist of the following subsystems: fuel cells, electrolyzers, photovoltaic arrays, reactant storage, thermal management, and electrical power management. Fuel cells consume hydrogen and oxygen (or air) to produce

electricity, water, and heat. The product water is stored and later dissociated into its hydrogen and oxygen constituents by a solar-powered electrolyzer. The hydrogen and oxygen are then stored for subsequent fuel cell consumption, and the fuel cell waste heat can be utilized in many different ways. If the fuel cell is designed to consume air rather than pure oxygen, then the oxygen from water electrolysis is available for other uses, such as in biological waste purification. For many years, individual RFC subsystem components have been under development for nonregenerative applications. The objectives of the Lewis testbed program are to design, test, and evaluate RFC's to characterize system life, performance, and integration issues for candidate RFC system technologies. The testbed is generic in the sense that it can be used to evaluate the different technologies that are specific to space, military, and commercial needs.

Lewis contact: Dr. Marvin Warshay, (216) 433-6126
Headquarters program office: OSAT (SSD)



High power density fuel cell.

Power-by-Wire Development and Demonstration for Subsonic Civil Transport

During the last decade, three significant studies by the Lockheed Martin Corporation, the NASA Lewis Research Center, and McDonnell Douglas Corporation have clearly shown operational, weight, and cost advantages for commercial subsonic transport aircraft that use all-electric or more-electric technologies in the secondary electric power systems. Even though these studies were completed on different aircraft, used different criteria, and applied a variety of technologies, all three have shown large benefits to the aircraft industry and to the nation's competitive position.

The Power-by-Wire (PBW) program is part of the highly reliable Fly-By-Light/Power-By-Wire (FBL/PBW) Technology Program, whose goal is to develop the technology base for confident application of integrated FBL/PBW systems for transport aircraft. This program is part of the NASA aeronautics strategic thrust in subsonic aircraft/national airspace (Thrust 1) to "develop selected high-leverage technologies and explore new means to ensure the competitiveness of U.S. subsonic aircraft and to enhance the safety and productivity of the national aviation system" (*The Aeronautics Strategic Plan*). Specifically, this program is an initiative under Thrust 1, Key Objective 2, to "develop, in cooperation with U.S. industry, selected high-payoff technologies that can enable significant improvements in aircraft efficiency and cost."

March 17 to 19, 1992, NASA held a requirements workshop at the NASA Langley Research Center which included 95 representatives from many of the companies interested in the FBL/PBW program and representatives from the Government. The PBW panels made recommendations that were incorporated into the PBW program, including (1) complete a system requirements definition study, (2) keep the distribution frequency in the midrange (400 to 1200 Hz), (3) raise the distribution voltage from 110 to 440 V, (4) consider a technology freeze in fiscal 1996, and (5) provide sufficient realistic flight demonstrations.

The objective of this PBW program, which began in 1993, is to develop and demonstrate the technology for a more-electric secondary power system and to provide enough confidence in this technology through testing that the airline industry will begin to transfer this technology into the civil fleet. This more-electric secondary power system will provide all the functions formerly performed by the hydraulic and pneumatic systems. The PBW program also will build a contractor and subcontractor base to support the PBW technology.

In the first phase of the PBW program, power system definitions and requirements will be developed. A power management and distribution (PMAD) architecture that best meets the system requirements will be designed, fabricated, and tested. Several electrical actuators will be designed, fabricated, and demonstrated; and a starter/generator that best meets the system requirements will be designed, fabricated, and demonstrated.

A redundant electrical actuator subsystem developed under the PBW portion of the FBL/PBW program will be delivered to Langley to be integrated into the Transport Systems Research Vehicle (TSRV) 757 for a flight demonstration in 1999. The flight demonstration will consist of a fault-tolerant control subsystem, a fault-tolerant power subsystem, an electrical actuator subsystem, and optic sensors.

A PBW program contract was signed with McDonnell Douglas in September 1993, the specifications and requirements documents were completed and delivered in April 1995, the preliminary flight actuator design was completed in July 1995, and a preliminary design review of the program was completed in November 1995.

Lewis contacts: David D. Renz, (216) 433-5321, and Linda M. Taylor, (216) 433-8478
Headquarters program office: OA (STD)

Advanced Power Regulator Developed for Spacecraft

The majority of new satellites generate electrical power using photovoltaic solar arrays and store energy in batteries for use during eclipse periods. Careful regulation of battery charging during insolation can greatly increase the expected lifetime of the satellite. The battery charge regulator is usually custom designed for each satellite and its specific mission. Economic competition in the small satellite market requires battery charge regulators that are lightweight, efficient, inexpensive, and modular enough to be used in a wide variety of satellites. A new battery charge regulator topology has been developed at the NASA Lewis Research Center to address these needs.

The new regulator topology uses industry-standard dc-dc converters and a unique interconnection to provide size, weight, efficiency, fault tolerance, and modularity benefits over existing systems. A transformer-isolated buck converter is connected such that the high input line is connected in series with the output. This "bypass connection" biases the converter's output onto the solar array voltage. Because of this biasing, the converter only processes the fraction of power necessary to charge the battery above the solar array voltage. Likewise, the same converter hookup can be used to regulate the battery output to the spacecraft power bus with similar fractional power processing.

The advantages of this scheme are

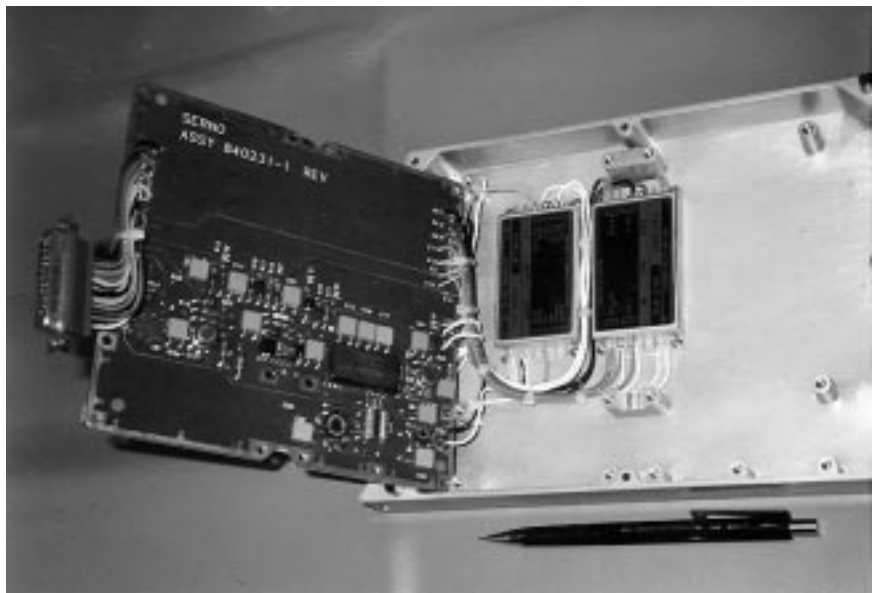
- Because only a fraction of the power is processed through the dc-dc converter, the single-stage conversion efficiency is 94 to 98 percent.
- Costly, high-efficiency dc-dc converters are not necessary for high end-to-end system efficiency.
- The system is highly fault tolerant because the bypass connection will still deliver power if the dc-dc converter fails.
- The converters can easily be connected in parallel, allowing higher power systems to be built from a common building block.

This new technology will be spaceflight tested in the Photovoltaic Regulator Kit Experiment (PRKE) on TRW's Small Spacecraft Technology Initiative (SSTI) satellite scheduled for launch in 1996. This experiment uses commercial dc-dc converters (28 to 15 Vdc) and additional control circuitry to regulate current to a battery load. The 60-W, 87-percent efficiency converters can control 180 W of power at an efficiency of 94 percent in the new configuration. The power density of the Photovoltaic Regulator Kit Experiment is about 200 W/kg.

Find out more about the Photovoltaic Regulator Kit Experiment on the World Wide Web:

<http://powerweb.lerc.nasa.gov/electsys/>

Lewis contact: James F. Soeder, (216) 433-5328
Headquarters program office: OSAT



Photovoltaic Regulator Kit Experiment.

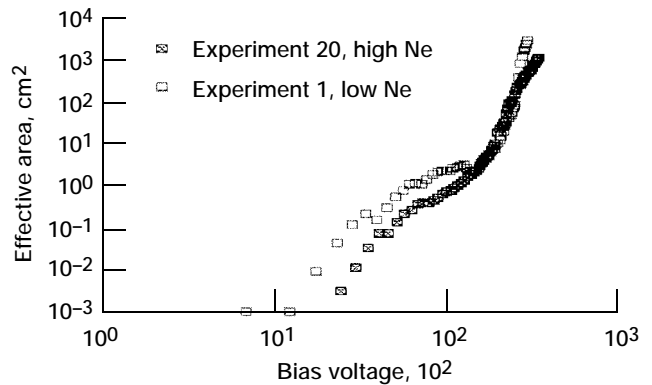
SAMPIE Measurements of the Space Station Plasma Current Analyzed

In March of 1994, STS-62 carried the NASA Lewis Research Center's Solar Array Module Plasma Interactions Experiment (SAMPIE) into orbit, where it investigated the plasma current collected and the arcs from solar arrays and other space power materials immersed in the low-Earth-orbit space plasma. One of the important experiments conducted was the plasma current collected by a four-cell coupon sample of solar array cells for the international space station.

The importance of this experiment dates back to the 1990 and 1991 meetings of the Space Station Electrical Grounding Tiger Team. The Tiger Team determined that unless the electrical potentials on the space station structure were actively controlled via a plasma contactor, the space station structure would arc into the plasma at a rate that would destroy the thermal properties of its surface coatings in only a few years of operation. The space station plasma contactor will control its potentials by emitting electrons into the surrounding low-Earth-orbit plasma at the same rate that they are collected by the solar arrays. Thus, the level at which the space station solar arrays can collect current is very important in verifying that the plasma contactor design can do its job.

The SAMPIE four-cell space station coupon was mounted to the top of the experiment enclosure and oriented in the ram direction by attitude control of the Space Shuttle Columbia. In the electron-collection experiment reported here, the cells were biased at voltages varying from 0 to 300 V, relative to the space shuttle ground. An electrometer measured the electron currents the cells collected from the plasma, and the results were collected on solid state memory. These results were analyzed later when SAMPIE was returned to Earth by Columbia.

Other onboard instruments measured the conditions in the ambient plasma—determining the plasma density and temperature, and the potential of the space shuttle with respect to the surrounding plasma. During the space station measurements, the shuttle potential was never more than about 3 V away from the plasma through which it flew. The data obtained on electron currents to the space station cells were corrected for the plasma conditions and then could be extrapolated to the worst-case conditions expected on the full space station solar array. From this extrapolation, we found that the space station array would at worst collect much less than the 10 A for which the plasma contactor was



Top: Four-cell space station collection expected from SAMPIE.
Bottom: Four-cell coupon sample of space station solar array cells.

designed, so that the plasma contactor should be fully sufficient to control the space station electrical potentials.

For more information about SAMPIE and the results of this experiment, visit our sites on the World Wide Web:

<http://satori2.lerc.nasa.gov/DOC/sample/samplehome.html>

<http://satori2.lerc.nasa.gov/DOC/sample/expres.html>

Lewis contacts: Dr. Barry Hillard, (216) 433-2220, and Dr. Dale C. Ferguson, (216) 433-2298
Headquarters program office: OSAT

Molecular Dynamics Calculations

The development of thermodynamics and statistical mechanics is very important in the history of physics, and it underlines the difficulty in dealing with systems involving many bodies, even if those bodies are identical. Macroscopic systems of atoms typically contain so many particles that it would be virtually impossible to follow the behavior of all of the particles involved. Therefore, the behavior of a complete system can only be described or predicted in statistical ways.

Under a grant to the NASA Lewis Research Center, scientists at the Case Western Reserve University have been examining the use of modern computing techniques that may be able to investigate and find the behavior of complete systems that have a large number of particles by tracking each particle individually. This is the study of molecular dynamics. In contrast to Monte Carlo techniques, which incorporate uncertainty from the outset, molecular dynamics calculations are fully deterministic. Although it is still impossible to track, even on high-speed computers, each particle in a system of a trillion trillion particles, it has been found that such systems can be well simulated by calculating the trajectories of a few thousand particles. Modern computers and efficient computing strategies have been used to calculate the behavior of a few physical systems and are now being employed to study important problems such as supersonic flows in the laboratory and in space.

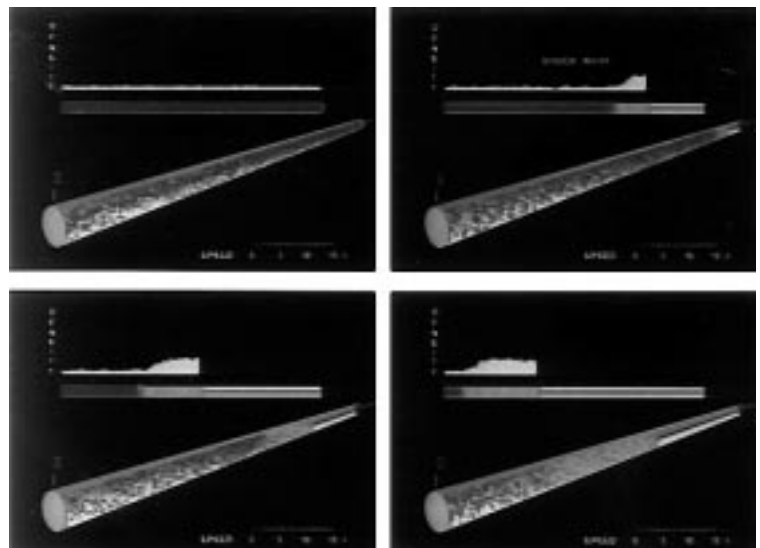
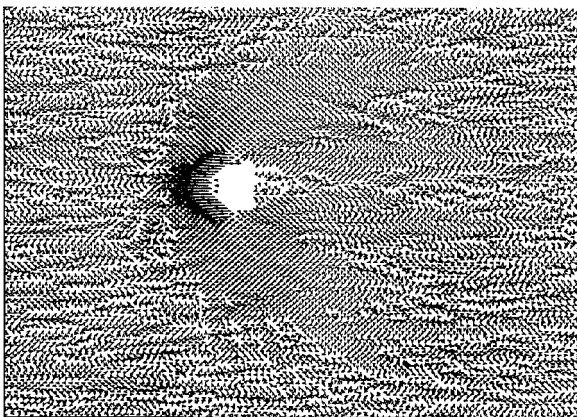
In particular, an animated video was produced by Dr. M.J. Woo, now a National Research Council fellow at Lewis, and the G-VIS laboratory at Lewis. This video

shows the behavior of supersonic shocks produced by pistons in enclosed cylinders by following exactly the behavior of thousands of particles. The major assumptions made were that the particles involved were hard spheres and that all collisions with the walls and with other particles were fully elastic. The animated video was voted one of two winning videos in a competition held at the meeting of the American Physical Society's Division of Fluid Dynamics, held in Atlanta, Georgia, in November 1994. Of great interest was the result that in every shock there were a few high-speed precursor particles racing ahead of the shock, carrying information about its impending arrival.

Most recently, Dr. Woo has been applying molecular dynamics techniques to the problem of determining the drag produced by the space station truss structure as it flies through the thin residual atmosphere of low-Earth orbit. This problem is made difficult by the complex structure of the truss and by the extreme supersonic nature of the flow. A fully filled section of the truss has already been examined, and drag predictions have been made. Molecular dynamics techniques promise to make realistic drag calculations possible even for very complex partially filled truss segments flying at arbitrary angles.

See Dr. Woo's video on the World Wide Web:
<http://www.lerc.nasa.gov/WWW/GVIS/GVIS/MolecularSimulation.mpg>

Lewis contacts: Dr. Myeung J. Woo, (216) 433-8771, and Dr. Dale C. Ferguson, (216) 433-2298
 Headquarters program office: OSAT



Left: Flow field around the truss structure of the international space station. Right: Simulations of shock development.

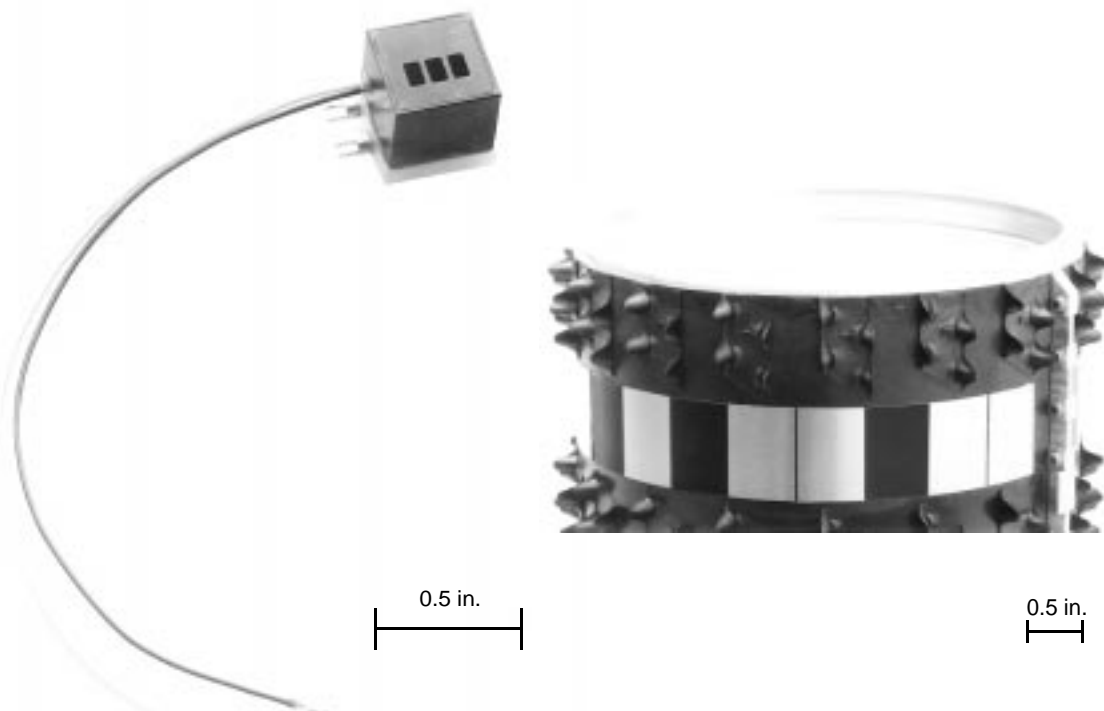
Mars Pathfinder: The Wheel Abrasion Experiment

NASA Lewis Research Center's Wheel Abrasion Experiment (WAE) will measure the amount of wear on wheel surfaces of the Mars Pathfinder rover. WAE uses thin films of Al, Ni, and Pt (ranging in thickness from 200 to 1000 Å) deposited on black, anodized Al strips attached to the rover wheel. As the wheel moves across the martian surface, changes in film reflectivity will be monitored by reflected sunlight. These changes, measured as output from a special photodetector mounted on the rover chassis, will be due to abrasion of the metal films by martian surface sand, dust, and clay. Since fine dust and clay particles are expected to adhere to the wheel and rover surfaces, the first WAE measurements from Pathfinder will provide a baseline against which dust and clay contributions can be calibrated for the remainder of the experiment. All additional changes in reflectivity will be assumed to be due to metal abrasion during martian surface operations.

During surface operations, the rover will move about the landing site on a set of six independently driven wheels. Twice each martian day, all the rover wheels, except the WAE test wheel, will be locked to hold the rover stationary while the test wheel is spun and digs into the martian regolith. These tests will provide wear conditions more severe than simple rolling.

Concomitantly, ground tests will be conducted on Earth with an identical wheel in simulated martian surface conditions. These tests will use different sands and clays to simulate the martian regolith. Slip tests, analogous to those on Mars, will be conducted in these simulations. Statistical analyses of the test results will be compared with similar analyses of Pathfinder data to determine which simulants behave most like the martian surface. Conclusions will be drawn about the likely nature of the martian surface and its effect on wear surfaces.

Initial tests have already been run to demonstrate the feasibility of the concept, and to gain rough estimates of surface abrasion. These initial tests also have produced an interesting result: As the rover moves across the dry martian surface, it will accumulate an electrical charge. This charge appears to be the primary reason for the fine dust and clay adhesion. After making some rough predictions of rover charging, we conducted ground tests using a noncontacting, capacitive probe to monitor wheel electrical potential. These tests have produced surface voltages in excess of 100 V, large enough to cause concern about electrical discharge through the martian atmosphere from rover surfaces. Additional tests with small discharge points have shown that it is



Photodetector for Lewis' Mars Pathfinder Wheel Abrasion Experiment (WAE). Left: Photodetector. Right: Nickel abrasion samples from wheels.

possible to mitigate these charging effects to some extent, and to reduce the probability of unwanted electrical discharge. As a precaution, Lewis recommended a set of discharge points, and these points were included by the Jet Propulsion Laboratory on the Pathfinder rover antenna base. WAE involves a heavy commitment on the part of both the Space Environment Effects Branch and the Photovoltaics Branch at Lewis.

For more information about the Mars Pathfinder, visit the Jet Propulsion Laboratory and Lewis' Space Environment Effects Branch on the World Wide Web:

<http://mpfwww.jpl.nasa.gov/>

<http://www.jpl.nasa.gov/mip/mpf.html>

<http://satori2.lerc.nasa.gov/>

Lewis contacts: Dr. Dale C. Ferguson, (216) 433-2298, and Joseph C. Kolecki, (216) 433-2296

Headquarters program office: OSS (SSED)

EWB: The Environment WorkBench Version 4.0

The Environment WorkBench EWB is a desktop integrated analysis tool for studying a spacecraft's interactions with its environment. Over 100 environment and analysis models are integrated into the menu-based tool. EWB, which was developed for and under the guidance of the NASA Lewis Research Center, is built atop the Module Integrator and Rule-based Intelligent Analytic Database (MIRIAD) architecture. This allows every module in EWB to communicate information to other modules in a transparent manner from the user's point of view. It removes the tedious and error-prone steps of entering data by hand from one model to another. EWB runs under UNIX operating systems (SGI and SUN workstations) and under MS Windows (3.x, 95, and NT) operating systems.

MIRIAD, the unique software that makes up the core of EWB, provides the flexibility to easily modify old models and incorporate new ones as user needs change. The MIRIAD approach separates the computer assisted engineering (CAE) tool into three distinct units:

- A modern graphical user interface to present information
- A data dictionary interpreter to coordinate analysis
- A database for storing system designs and analysis results

The user interface is externally programmable through ASCII data files, which contain the location and type of information to be displayed on the screen. This approach provides great flexibility in tailoring the look and feel of the code to individual user needs. MIRIAD-based applications, such as EWB, have utilities for viewing tabulated parametric study data, XY line plots, contour plots, and three-dimensional plots of contour data and system geometries. In addition, a Monte Carlo facility is provided to allow statistical assessments (including uncertainties) in models or data.

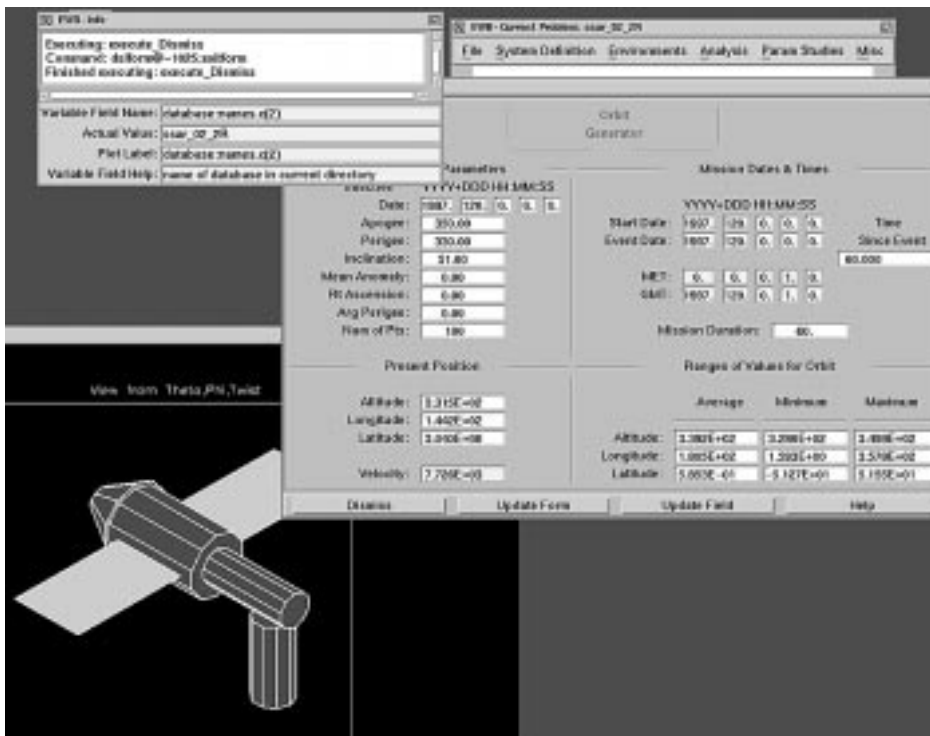
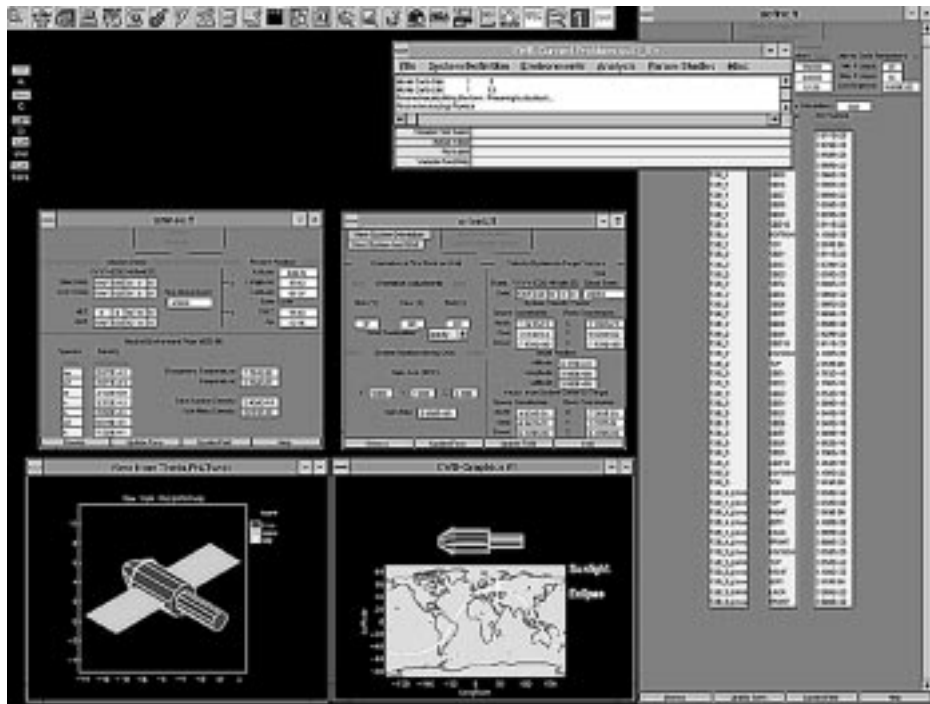
EWB has modeled interactions for several flight experiments, such as the Solar Array Module Plasma Interactions Experiment (SAMPIE) and the Photovoltaic Array for Space Power Plus Diagnostics (PASP Plus). It has been used to interpret and model data obtained from flight experiments as they were occurring. Such was the case with the Space Experiments with Particle Accelerators (SEPAC), the Tethered Satellite System (TSS-1), and the Plasma Motor Generator (PMG) experiments. EWB also has been used extensively in the design and operation of the Plasma Contactor device for the international space station.

With EWB, engineers can get quick answers right on their desktop to "What if?" type design questions related to space environment interactions. Once a spacecraft's geometry has been defined and orbital parameters entered, the user can interact in real time with the tool to obtain answers from the several available models.

More current information about EWB can be found on the World Wide Web:

<http://satori2.lerc.nasa.gov/DOC/EWB/ewbhome.html>

**Lewis contact: Ricaurte Chock, (216) 433-8057
Headquarters program offices: OSF and OSMA**



The user interface for EWB 4.0 provides a consistent look and feel for all its models across all supported platforms.

Protective, Abrasion-Resistant Coatings With Tailorable Properties

Because of their light weight and impact resistance, transparent plastic structures are becoming increasingly desirable for use not only on aircraft but also in terrestrial applications such as automotive windshields and ophthalmic lenses. However, plastics are typically soft and scratch readily, reducing their transparency with use. At the NASA Lewis Research Center, reactively deposited aluminum oxide coatings as thin as 12,000 Å have been demonstrated to provide improved resistance to most scratches encountered during normal use. The properties of the coating can be adjusted to tailor the surface to meet other needs, such as water shedding. These adjustments can be made during the deposition process so that multiple manufacturing steps are eliminated.

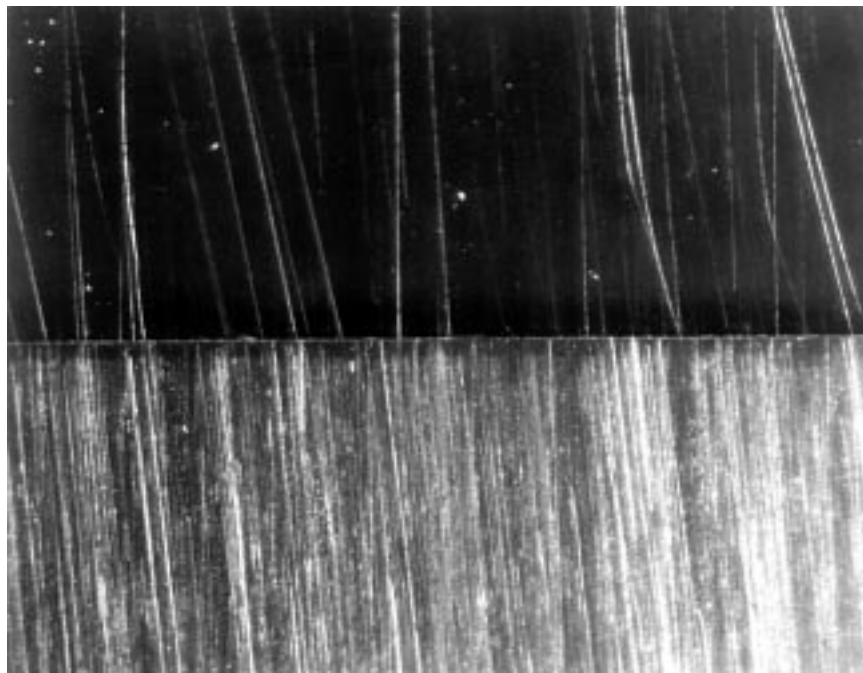
In this reactive deposition, aluminum oxide is sputter deposited from an aluminum target simultaneous with the direction of an atomic oxygen plasma on the surface that is being coated. The aluminum combines with the atomic oxygen at the surface to form a very hard aluminum oxide coating that is under less compressive stress than a coating sputter-deposited from an aluminum oxide target, and this reactively deposited coating can be grown thicker without spalling. Addition of other materials, such as fluoropolymers, during the deposition process can reduce the intrinsic stress of

the coating even further. Reactively deposited aluminum oxide is slightly more hydrophobic (water shedding) than sputter-deposited aluminum oxide, and it can be made hydrophilic (water retaining) with the addition of fluoropolymers. It also is very transparent. An approximately 12,000-Å-thick coating reactively deposited on polycarbonate increases the absolute absorptance by only 1.8 percent. At this thickness, the coating can resist abrasion by small particles that would be present when windows, optical lenses, or other surfaces are cleaned.

The abrasion resistance and transparency of reactively deposited aluminum oxide makes it attractive for a broad range of applications where lightweight and transparent plastics could be effectively used. In addition, the ability to add other materials during the deposition process allows the potential for tailoring the coating to meet the needs of specific use environments.

To find out more about this research, visit our site on the World Wide Web:
<http://www.lerc.nasa.gov/WWW/epbranch/ephome.htm>

Lewis contact: Sharon K. Rutledge, (216) 433-2219
Headquarters program office: OSAT



Polycarbonate with top half coated with reactively deposited aluminum oxide. Surface was abraded with house dust.

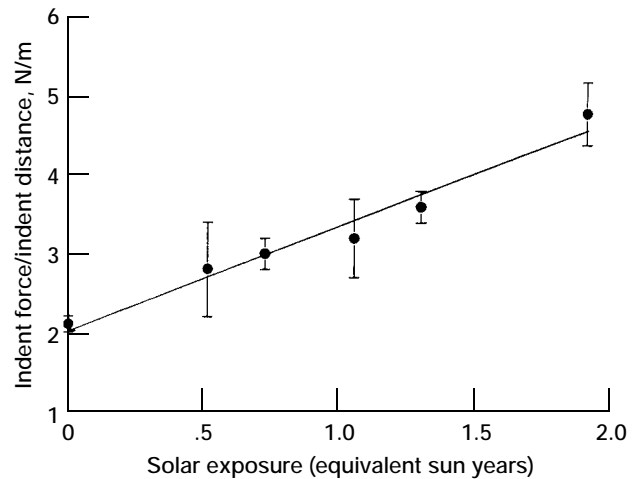
Technique to Predict Ultraviolet Radiation Embrittlement of Polymers in Space

In the low-Earth-orbit environment, solar ultraviolet (UV) radiation embrittles polymer materials through bond breaking and crosslinking. This UV embrittlement increases the surface hardness of the polymer. Before the durability of polymer materials in the low-Earth-orbit environment can be predicted, the extent of UV embrittlement needs to be determined. However, traditional techniques for measuring the microhardness of materials cannot be employed to measure changes in the hardness of UV-embrittled surfaces because traditional techniques measure bulk hardness and are not sensitive enough to surface changes. A unique technique was used at the NASA Lewis Research Center to quantify polymer surface damage that had been induced by UV radiation. The technique uses an atomic force microscope (AFM) to measure surface microhardness.

An atomic force microscope measures the repulsive forces between the atoms in a microscopic cantilevered tip and the atoms on the surface of a sample. Typically, an atomic force microscope produces a topographic image of a surface by monitoring the movement of the tip over features of the surface. The force applied to the cantilevered tip, and the indentation of the tip into the surface, can be measured. The relationship between force and distance of indentation, the quantity force/distance (newtons/meter), provides a measure of the surface hardness. Under identical operating conditions, direct comparisons of surface hardness values can be made.

This technique has been used to evaluate small changes in the surface hardness of fluorinated ethylene-propylene (FEP) Teflon (E.I. du Pont de Nemours & Company, Wilmington, Delaware) samples that received varying solar exposures during 3.6 years on the Hubble Space Telescope. The figure shows the increase in surface hardness (represented as indent force/indent distance) with increasing solar UV radiation of Hubble Space Telescope Teflon.

Because ground test facilities do not exactly simulate the radiation spectrum of the Sun in space, ground-to-space correlation factors need to be determined for in-space durability predictions that are based on ground testing. The force-versus-distance technique can be used to determine the correlation between ground-testing durability predictions and actual in-space durability. This is achieved by determining what ground-test exposure produces the same UV damage as a particular in-space exposure. The Hubble Space



Increase in surface hardness (represented as indent force/indent distance) with increasing solar UV radiation of Hubble Space Telescope Teflon.

Telescope Teflon data will be compared with ground-test-exposed Teflon data to determine the ground-to-space correlation factor of Teflon. Once the ground-to-space correlation factors for materials in a particular facility are determined, long-term, in-space durability can be more accurately predicted on the basis of ground testing.

To find out more about the atomic force microscope and its applications to space durability, visit Lewis on the World Wide Web:

<http://www.lerc.nasa.gov/WWW/epbranch/ephome.htm>
http://www.lerc.nasa.gov/WWW/SurfSci/ssb_siac.html

Lewis contact: Kim K. de Groh, (216) 433-2297
Headquarters program office: OSAT

Transparent, Conductive Coatings Developed for Arc-Proof Solar Arrays

Transparent, conductive thin-film coatings have many potential applications where a surface must be able to dissipate electrical charges without sacrificing its optical properties. Such applications include automotive and aircraft windows, heat mirrors, optoelectronic devices, gas sensors, and solar cell array surfaces for space applications. Many spacecraft missions require that solar cell array surfaces dissipate charges in order to avoid damage such as electronic upsets, formation of pinholes in the protective coatings on solar array blankets, and contamination due to deposition of sputtered products.

In tests at the NASA Lewis Research Center, mixed thin-films of sputter-deposited indium tin oxide (ITO) and magnesium fluoride (MgF_2) that could be tailored to the desired sheet resistivity showed transmittance values of greater than 90 percent. The samples evaluated were composed of mixed, thin-film ITO/ MgF_2 coatings, with a nominal thickness of 650 Å, deposited onto glass substrates. Preliminary results indicated that these coatings were durable to vacuum ultraviolet radiation and atomic oxygen. These coatings show promise for use on solar array surfaces in polar low-Earth-orbit environments, where a sheet resistivity of less than $10^8 \Omega/\square$ is required, and in geosynchronous orbit environments, where a resistivity of less than $10^9 \Omega/\square$ is required. The figures show electrical and optical properties as a function of the estimated volume percent of MgF_2 in the mixed ITO/ MgF_2 coating. Future plans include demonstration of the coating's

durability to atomic oxygen and to vacuum ultraviolet radiation.

Lewis contact: Joyce A. Dever, (216) 433-6294
Headquarters program office: OSAT

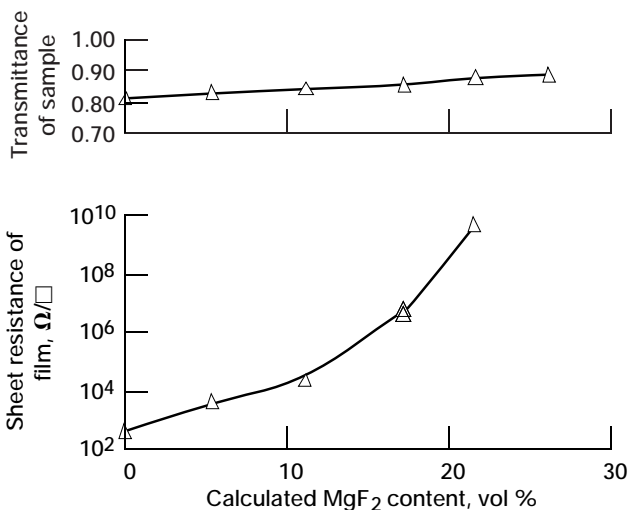
Radiation Protection of New Lightweight Electromagnetic Interference Shielding Materials Determined

Weight savings as high as 80 percent could be achieved by simply switching from aluminum electromagnetic interference (EMI) shielding covers for spacecraft power systems to EMI covers made from intercalated graphite fiber composites. Because EMI covers typically make up about one-fifth of the power system mass, this change would decrease the mass of a spacecraft power system by more than 15 percent.

Intercalated graphite fibers are made by diffusing guest atoms or molecules, such as bromine, between the carbon planes of the graphite fibers. The resulting bromine-intercalated fibers have mechanical and thermal properties nearly identical to pristine graphite fibers, but their resistivity is lower by a factor of 5, giving them better electrical conductivity than stainless steel and making these composites suitable for EMI shielding.

EMI shields, however, must do more than just shield against EMI. They must also protect electrical components from mechanical, thermal, and radiative disturbances. Intercalated graphite fiber composites have a much higher specific strength than the aluminum they would replace, so achieving sufficient mechanical strength and stiffness would not be difficult. Also, the composites absorb and reradiate electromagnetic radiation in the infrared region, so they are actually considerably better at rejecting heat than the very reflective aluminum covers. What had not been characterized was how well these intercalated graphite fiber composites shielded components from ionizing radiation.

The shielding of high-energy radiation generally increases with the total number of electrons in an atom. Thus, carbon, which has 6 electrons per atom, is a poorer shield than aluminum, which has 13. Intercalation with a few percent of bromine (35 electrons/atom) or iodine (53 electrons/atom) was expected to improve



Transmittance (top) and sheet resistivity (bottom) of mixed ITO/ MgF_2 films as a function of the volume percent of MgF_2 .

the radiation shielding, though the average number of electrons per atom would still be below that of aluminum. However, the results of tests done at Manchester College, under a cooperative agreement with the NASA Lewis Research Center, indicated a substantial improvement in the radiation shielding—not only by a factor of 8 over the pristine graphite composite, but actually by a factor of 3 over aluminum. Intercalated graphite composites may well be the EMI cover of choice for spacecraft electronics operating in a high-radiation environment.

MASS ABSORPTION OF EMI MATERIALS

| Material | 46.5-keV γ-ray, cm ² /g | 13.0-keV x-ray, cm ² /g | $\frac{\text{mass abs}}{\text{mass abs Al}}$ |
|-------------------------|--|--|--|
| Aluminum | 0.34 | 0.61 | 1.0 |
| P-100 graphite | .14 | .25 | .4 |
| P-100 + Br ₂ | .61 | .96 | 1.7 |
| P-100 + IBr | 1.0 | 1.8 | 3.0 |

For more information about the work of Lewis' Electro-Physics Branch, visit our site on the World Wide Web: <http://www.lerc.nasa.gov/WWW/epbranch/ephome.htm>

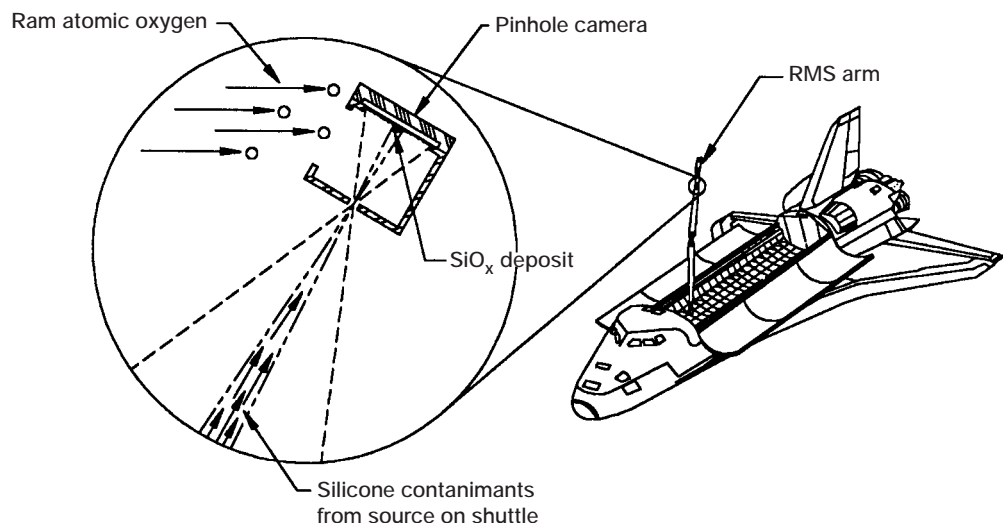
Lewis contact: James R. Gaier, (219) 982-5075 (Feb.-May and Sept.-Dec.) and (216) 433-6686 (Jan. and June-Aug.)
Headquarters program office: OSAT

Silicone Contamination Camera Developed for Shuttle Payloads

On many shuttle missions, silicone contamination from unknown sources from within or external to the shuttle payload bay has been a chronic problem plaguing experiment payloads. There is currently a wide range of silicone usage on the shuttle. Silicones are used to coat the shuttle tiles to enhance their ability to shed rain, and over 100 kg of RTV 560 silicone is used to seal white tiles to the shuttle surfaces. Silicones are also used in electronic components, potting compounds, and thermal control blankets. Efforts to date to identify and eliminate the sources of silicone contamination have not been highly successful and have created much controversy.

To identify the sources of silicone contamination on the space shuttle, the NASA Lewis Research Center developed a contamination camera. This specially designed pinhole camera utilizes low-Earth-orbit atomic oxygen to develop a picture that identifies sources of silicone contamination on shuttle-launched payloads.

The volatile silicone species travel through the aperture of the pinhole camera, and since volatile silicone species lose their hydrocarbon functionalities under atomic oxygen attack, the silicone adheres to the substrate as SiO_x. This glassy deposit should be spatially arranged in the image of the sources of silicone contamination. To view the contamination image, one can use ultrasensitive thickness measurement techniques, such as scanning variable-angle ellipsometry, to map the surface topography of the camera's substrate.



Silicone contamination camera for space shuttle payloads.

The demonstration of a functional contamination camera would resolve the controversial debate concerning the amount and location of contamination sources, would allow corrective actions to be taken, and would demonstrate a useful tool for contamination documentation on future shuttle payloads, with near negligible effect on cost and weight.

Lewis contacts: Bruce A. Banks, (216) 433-2308, and Mark J. Forkapa, (216) 433-2299
Headquarters program office: OSAT

Iron-Containing Carbon Materials Fabricated

Development of high-strength, lightweight materials for electromagnetic interference (EMI) shielding at low frequencies may be possible if the carbon fibers used in these composites can be made to have ferromagnetic properties. One way to obtain such fibers is by inserting small ferromagnetic particles into the fiber structure.

Carbon fibers and carbon powder containing iron oxide, iron metal, or iron alloy have been successfully fabricated at the NASA Lewis Research Center (refs. 1 and 2). These carbon products can be attracted to a regular magnet. Typical samples were estimated to have 1 iron atom per 3.5 to 5 carbon atoms. The sizes of the Fe_3O_4 , iron metal, and iron alloy particles were estimated to be in a wide 10- to 10,000-Å range.

In this fabrication process, first graphite fluoride (CF_x) is exposed to FeCl_3 . Then the product is further heated in a low-oxygen environment, thereby depositing iron oxide, elemental iron, or iron alloy in or on the carbon.

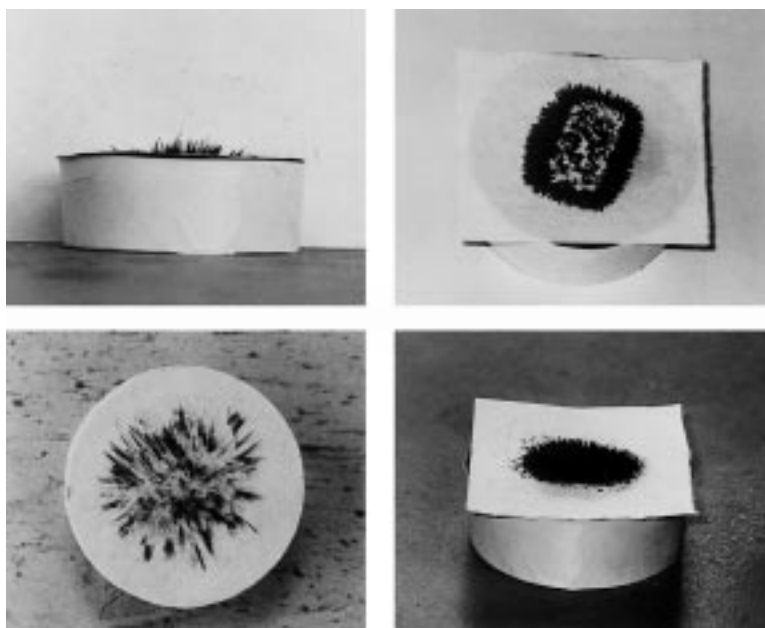
Experiments were conducted to study the kinetics of the fabrication process (ref. 2). At 280 to 295 °C, FeCl_3 can quickly enter the structure of CF_x ; and in 10 to 30 min, it completely converts the CF_x into carbon that has graphite planes between which crystalline FeF_3 and noncrystalline FeCl_2 locate. Further heating this product in a low-oxygen environment converts these iron halides into either a mixture of FeO and Fe_3O_4 , if the temperature is in 750 to 850 °C range, or into elemental iron, if the temperature is at least 900 °C. During the final heat treatment at a temperature of 900 °C or higher, NiO or NiCl_2 could be added to the reaction to produce a carbon material containing nickel-iron alloy, a ferromagnetic material.

In this reaction, a low rate of oxygen supply would cause the iron halide to evaporate before it could be converted to iron oxide, resulting in low iron concentration in the carbon products. On the other hand, a high rate of oxygen supply would cause carbon removal because of the formation of CO and CO_2 . The carbon removal would result in a high iron concentration in structurally damaged carbon products. At an optimum oxygen level, the iron halide in the carbon fibers would be converted to iron oxide or elemental iron without much halide evaporation or carbon structural damage. Potential applications of the iron-containing carbon fibers and powder include spacecraft and aircraft electronic packaging as well as portable, personal-use communication equipment.

References

1. Hung, C.C.: Ferric Chloride-Graphite Intercalation Compounds Prepared From Graphite Fluoride. *Carbon*, vol. 33, no. 3, 1995, pp. 315-322.
2. Hung, C.C.: Fabrication of Iron-Containing Carbon Materials From Graphite Fluoride. Presented at the 22nd Biennial Conference on Carbon, University of California, San Diego, July 1995. *American Carbon Society*, pp. 656-657, 1995.

Lewis contact: Dr. Ching-Cheh Hung, (216) 433-2302
Headquarters program office: OSAT



Iron-containing carbon materials on magnets.

Passive Optical Sample Assembly (POSA-2) Space Flight Experiment

NASA Lewis Research Center's Electro-Physics Branch is participating in the POSA-2 Space Flight Experiment to assess the effects of low Earth orbit and spacecraft environment contamination on power system materials and surfaces. This experiment package will be flown for 1 year in low Earth orbit and will be returned to Earth for subsequent evaluation of optical and thermal properties. Representative samples of solar-array blanket materials, solar dynamic reflector materials, thermal control coatings, and sapphire are included in the experiment package.

Thirty Lewis optical and thermal control coating samples were prepared, characterized, and integrated on the POSA-2 carrier. One-inch-diameter Kapton disks, with and without a protective silicon dioxide coating, were stamped out of stock material, dehydrated, and weighed. Aluminum disks with a proprietary leveling coating were coated by electron-beam evaporation with a reflective coating of either aluminum or silver and with a protective coating of aluminum oxide and/or silicon dioxide.

In addition to mass measurements, total, diffuse, and specular reflectivity values were obtained on these samples through the use of a Perkin-Elmer Lambda-9 spectrophotometer equipped with a 150-mm-diameter integrating sphere.

The optical properties of thermal control coatings provided by the Illinois Institute of Technology Research Institute (IITRI) were evaluated in the visible range with an AZ Technology LPSR-200 reflectometer and in the infrared range with a Gier-Dunkle DB-100 reflectometer. Sapphire contamination monitors also were prepared for flight. Each type of sample was prepared in duplicate to accommodate the unusual opportunity to fly identical samples in both the ram and wake directions simultaneously. The samples were integrated in collaboration with the Boeing Space and Defense Group, Kent, Washington. Vibration testing is scheduled at the NASA Langley Research Center, and launch is expected in early 1996.

POSA-2 should provide important information on the durability of materials to the low-Earth-orbit space environment in the near vicinity of spacecraft. It also should provide information on potential contamination and debris-related issues.

Find out more about the Electro-Physics Branch on the World Wide Web:

<http://www.lerc.nasa.gov/WWW/epbranch/ephome.htm>

Lewis contact: Donald A. Jaworske, (216) 433-2312
Headquarters program office: OSAT



Researchers installing samples in the POSA-2 flight experiment trays.

Aperture Shield Materials Characterized and Selected for Solar Dynamic Space Power System

The aperture shield in a solar dynamic space power system is necessary to prevent thermal damage to the heat receiver should the concentrated solar radiation be accidentally or intentionally focused outside of the heat receiver aperture opening and onto the aperture shield itself. Characterization of the optical and thermal properties of candidate aperture shield materials was needed to support the joint U.S./Russian solar dynamic space power effort for Mir.

The specific objective of testing performed at the NASA Lewis Research Center was to identify a high-temperature material with a low specular reflectance, a low solar absorptance, and a high spectral emittance so that during an off-pointing event, the amount of solar energy reflecting off the aperture shield would be small, the α/ϵ ratio (ratio of solar absorptance to spectral emittance) would provide the lowest possible equilibrium temperature, and the integrity of the aperture shield would remain intact.

An off-pointing event is defined as an event where the focused light from the solar dynamic concentrator moves away from the aperture opening of the heat receiver and onto the aperture shield itself. Such an event would cause a considerable amount of solar energy to impinge on a small area. This area, which is expected to heat rapidly, must be made of a high-temperature material that can withstand temperatures above 2000 °C. The surface finish of the material must be diffuse so it does not reflect energy back to the concentrator. Likewise, the surface must have a low α/ϵ ratio to minimize heating of the structure. Given the low-Earth-orbit application, the surface must also be durable to atomic oxygen exposure.

Over 50 samples of high-temperature materials, including grit-blasted molybdenum, tungsten, and rhenium, were evaluated in collaboration with AlliedSignal Inc. of Torrance, California. Spectral reflectance was obtained with a Perkin-Elmer Lambda-9 spectrophotometer equipped with a 150-mm-diameter integrating sphere. Total and diffuse reflectance were obtained from 250 to 2500 nm, and the data were convoluted into the air mass zero solar spectrum to obtain solar integrated values. Specular reflectance was obtained by subtraction. The solar absorptance was calculated by subtracting the

integrated solar total reflectance from unity. Emittance was estimated from the spectral data with the use of a computer program to integrate the reflectance data into blackbody curves at elevated temperatures.

Only grit-blasted tungsten met all of the optical requirements for the off-pointing event on the aperture shield. Hence, selected samples of the grit-blasted tungsten were further exposed to a simulated atomic oxygen environment in a radiofrequency plasma asher, and to 2000 °C in a high-temperature vacuum furnace. Acceptable optical performance was observed after both of these exposures. As a result of the testing, grit-blasted tungsten foil combined with grit-blasted tungsten screen were identified as the materials of choice and were selected for constructing the aperture shield for the solar dynamic power system to be installed on space station Mir.

Find out more about the Mir Cooperative Solar Array Program and the Joint U.S.-Russian Solar Dynamic Flight Demonstration on the World Wide Web:

<http://godzilla.lerc.nasa.gov/pspo/csa.html>

<http://godzilla.lerc.nasa.gov/pspo/sddemo.html>

Lewis contacts: Donald A. Jaworske, (216) 433-2312, and Kim K. de Groh, (216) 433-2297
Headquarters program office: OSAT



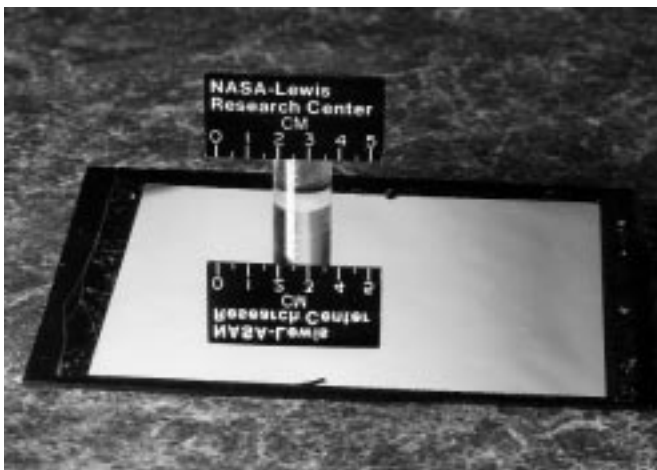
Aperture shield sample being installed in a UV-VIS-NIR (ultraviolet-visible-near infrared) spectrophotometer for optical properties evaluation.

Atomic-Oxygen-Durable Microsheet Glass Reflector

Advanced solar dynamic concentrator concepts being considered by the NASA Lewis Research Center for space power systems include one utilizing microsheet glass coated with silver. For this material, a 5000-Å layer of silver is deposited on the back side of a contoured piece of microsheet glass, 0.2-mm thick. The silvered side is then bonded to a contoured aluminum, magnesium, or graphite epoxy face sheet with a space-qualified, pressure-sensitive thin-film adhesive. Experience gained from the development of this technology suggests that this material may reduce the cost and improve the performance of solar dynamic concentrators. This microsheet glass technology provides an effective barrier to atomic oxygen attack and provides the opportunity to utilize silver-reflective coatings in low-Earth-orbit solar dynamic applications.

Forming the microsheet glass was found to be a challenge. A collaborative effort was initiated with experts in the automotive industry, and a proprietary forming process was developed. The microsheet glass could be formed to the complex curved shapes needed for solar dynamic concentrators, but the degree of curvature had to be gradual.

The second-surface silver mirror created by this technique is lightweight, durable, easily cleaned, and has a total reflectivity of 94 percent. No debonding of



Reflected image in a microsheet glass reflector bonded to a graphite epoxy composite face sheet.

the microsheet glass composite structure was indicated after vacuum exposure and thermal cycling between -80 and 80 °C, and after atomic oxygen exposure, only minor deterioration of the reflective surface, limited to regions near the edges and seams was evident. The overall mass per unit area was 2.5 kg/m².

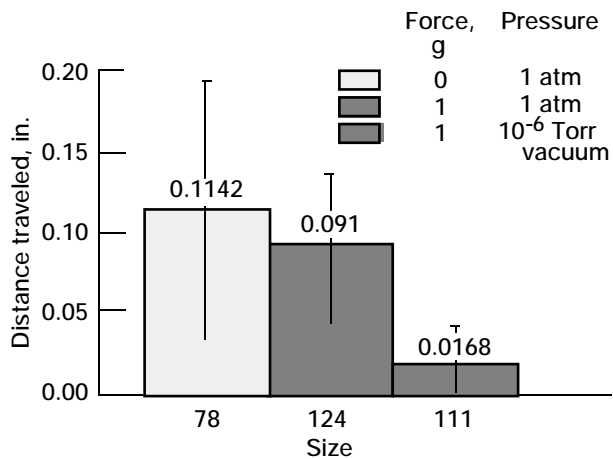
This technology enables the use of silver as a reflective coating in the low-Earth-orbit atomic oxygen environment. Using silver, rather than other materials, as a reflector will increase the overall efficiency of proposed solar dynamic power systems.

Lewis contact: Donald A. Jaworske, (216) 433-2312
Headquarters program office: OSAT

Environmental Influence of Gravity and Pressure on Arc Tracking of Insulated Wires Investigated

Momentary short-circuit arcs between a defective polyimide-insulated wire and another conductor may thermally char (pyrolyze) the insulating material. The charred polyimide, being conductive, can sustain the short-circuit arc, which may propagate along the wire through continuous pyrolyzation of the polyimide insulation (arc tracking). If the arcing wire is part of a multiple-wire bundle, the polyimide insulation of other wires within the bundle may become thermally charred and start arc tracking also (flash over). Such arc tracking can lead to complete failure of an entire wire bundle, causing other critical spacecraft or aircraft failures.

Unfortunately, all tested candidate wire insulations for aerospace vehicles were susceptible to arc tracking. Therefore, a test procedure was designed at the NASA Lewis Research Center to select the insulation type least susceptible to arc tracking. This test procedure addresses the following three areas of concern: (1) probability of initiation, (2) probability of reinitiation (restrike), and (3) extent of arc tracking damage (propagation rate). Item 2 (restrike probability) is an issue if power can be terminated from and reapplied to the arcing wire (by a switch, fuse, or resettable circuit breaker). The degree of damage from an arcing event (item 3) refers to how



Comparison of MIL-W-81381 insulated wire (20 AWG), in each environment of interest, with respect to the distance the arc travels in 16 sec.

easily the arc chars nearby insulation and propagates along the wire pair. Ease of nearby insulation charring can be determined by measuring the rate of arc propagation. Insulation that chars easily will propagate the arc faster than insulation that does not char very easily.

A popular polyimide insulated wire for aerospace vehicles, MIL-W-81381, was tested to determine a degree of damage from an arcing event (item 3) in the following three environments: (1) microgravity (μg) with air at 1-atm pressure, (2) 1g with air at 1 atm, and (3) 1g within a 10^{-6} Torr vacuum.

The microgravity 1-atm air was the harshest environment, with respect to the rate of damage of arc tracking, for the 20 AWG (American Wiring Gauge) MIL-W-81381 wire insulation type. The vacuum environment resulted in the least damage. Further testing is planned to determine if the environmental results are consistent between insulation types and to evaluate the other two parameters associated with arc tracking susceptibility.

Lewis contact: Thomas J. Stueber, (216) 433-2218
(E-Mail: stueber@lerc.nasa.gov)
Headquarters program office: OSMA

Experimental Results From the Thermal Energy Storage-1 (TES-1) Flight Experiment

The Thermal Energy Storage (TES) experiments are designed to provide data to help researchers understand the long-duration microgravity behavior of thermal energy storage fluoride salts that undergo repeated melting and freezing. Such data, which have never been obtained before, have direct application to space-based solar dynamic power systems. These power systems will store solar energy in a thermal energy salt, such as lithium fluoride (LiF) or a eutectic of lithium fluoride/calcium difluoride (LiF-CaF₂) (which melts at a lower temperature). The energy will be stored as the latent heat of fusion when the salt is melted by absorbing solar thermal energy. The stored energy will then be extracted during the shade portion of the orbit, enabling the solar dynamic power system to provide constant electrical power over the entire orbit.

Analytical computer codes have been developed to predict the performance of a space-based solar dynamic power system. However, the analytical predictions must be verified experimentally before the analytical results can be used for future space power design applications. Four TES flight experiments will be used to obtain the needed experimental data. This article focuses on the flight results from the first experiment, TES-1, in comparison to the predicted results from the Thermal Energy Storage Simulation (TESSIM) analytical computer code.

Developed by Dr. David Jacqmin of the NASA Lewis Research Center's Internal Fluid Mechanics Division, TESSIM can predict the migration of voids and the resulting thermal behavior of solar dynamic receiver canisters. It is currently useful as a qualitative design tool but requires further experimental validation before it can be reliably used for critical design decisions. Once thoroughly validated, the code will be invaluable in the detailed design of lighter, more efficient solar dynamic receivers.

An advanced solar dynamic power system with either a Brayton or Stirling Power Conversion System has the potential for high efficiency with lower weight, cost, and area than other solar power systems. When operating in a low Earth orbit, the power system will experience a sun/shade cycle on the order of 60-min sun and 34-min shade. Delivery of continuous electric power over the entire orbit requires a method of storing energy during the sun cycle for use during the shade cycle.

An efficient method of accomplishing this is to utilize the high heat-of-fusion associated with TES phase-change materials. These materials possess physical properties that are desirable in advanced solar dynamic heat receiver designs—including high heat-of-fusion, very low toxicity, and general compatibility with containment materials in a vacuum environment. However, they also have low thermal conductivity, low density, and most significantly, high specific-volume change with phase change. This last characteristic leads to the formation of a void, or voids, that can degrade heat-receiver energy transfer performance by forming local hot spots on the container wall or by distorting the wall locally. Because the formation and location of voids are strongly influenced by gravitational forces, it is necessary to be able to understand and predict this phenomenon in the on-orbit microgravity environment in order to achieve the optimum design for the heat receiver canisters. This is especially important since the canister and heat receiver are significant elements of the overall weight and cost of a solar dynamic power system.

Four experiments are needed to provide the data necessary to validate the TESSIM code. The first two flight experiments, TES-1 and TES-2, were developed to obtain data on TES material behavior in cylindrical canisters. These experiments are identical except for the fluoride salts characterized. TES-1 used lithium fluoride (LiF) salt, which melts at 1121 K; and TES-2 will use a fluoride eutectic salt (LiF/CaF₂), which melts at 1042 K. A postflight tomographic scan of each TES canister will provide data on void location, size, and distribution for comparison with TESSIM predictions.

From the data collected on orbit, the first figure shows some erratic behavior in the first melt cycle in comparison to the remaining three melt-freeze cycles. We believed this to be caused by migration of the void and/or by the gravitational forces present during this period. In general, after the first melt-freeze cycle, the temperatures show repeatability from cycle to cycle at each location.

After the experiment, the canister was scanned by Computer-Aided Tomography (CAT) to record the final location and distribution of the voids in the canister. The second figure (ref. 1) shows the tomographic data taken on the TES-1 canister for nine stations along the length of the canister, along with the predicted results from TESSIM. Salt locations are shown in black. In general, TESSIM appears to have predicted void behavior accurately, as is evidenced by comparing the tomographic images with the TESSIM images. These initial results from TES-1, of high-temperature fluoride

salt melting and freezing under microgravity, do not absolutely validate TESSIM, but the comparison of the predictions with the data establishes a basic confidence in the code. Future experiments, such as TES-2, -3, and -4 will help to further validate TESSIM.

The TES-1 flight experiment provided the first experimental data on the long-duration effects on TES salts used for space-based solar dynamic power systems. Good correlation between the predicted on-orbit characteristics of the salt and the actual flight data indicate that, for the configuration tested, the TESSIM code is basically sound. The additional three flight experiments will provide the opportunity for the TESSIM code to be validated completely. The flight experiments will provide data from different canister configurations and both wetting and nonwetting interfaces for the TES salts. In addition, the effect of heat leakage will be studied more closely.

Find out more about TES on the World Wide Web:

<http://powerweb.lerc.nasa.gov/soldyn/DOC/TESSp.html>

Lewis contacts: Carol M. Tolbert, (216) 433-6167; Lawrence W. Wald, (216) 433-5219; and Dr. David A. Jacqmin, (216) 433-5853

Headquarters program office: OSAT

2-kW Solar Dynamic Space Power System Tested in Lewis' Thermal Vacuum Facility

Working together, a NASA/industry team successfully operated and tested a complete solar dynamic space power system in a large thermal vacuum facility with a simulated sun. This NASA Lewis Research Center facility, known as Tank 6 in building 301, accurately simulates the temperatures, high vacuum, and solar flux encountered in low-Earth orbit. The solar dynamic space power system shown in the first figure in the Lewis facility, includes the solar concentrator and the solar receiver with thermal energy storage integrated with the power conversion unit. Initial testing in December 1994 resulted in the world's first operation of an integrated solar dynamic system in a relevant environment.

Acceptance testing of the solar dynamic system was accomplished in only 3 months, from December 1994 through February 1995, by an industry team led by AlliedSignal Inc. with support from Lewis. Over 2 kW of electrical power was produced on February 17, 1995, while the system was operating at 52,000 rpm with a turbine inlet temperature of 1063.5 K (790.5 °C) and a

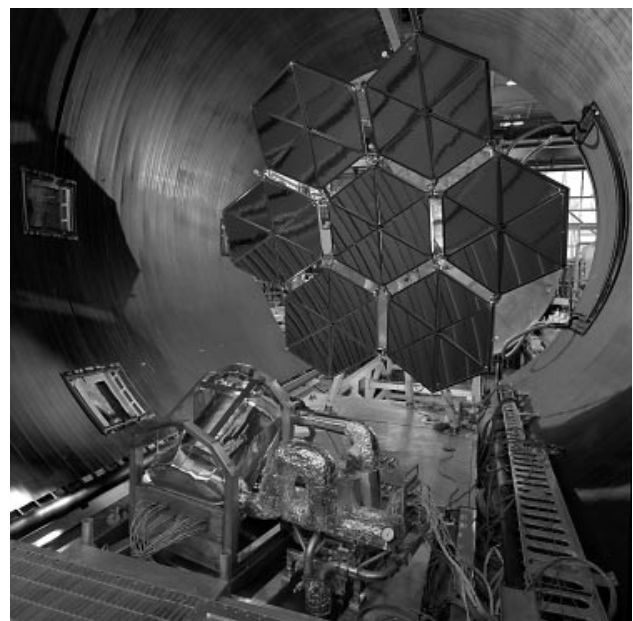
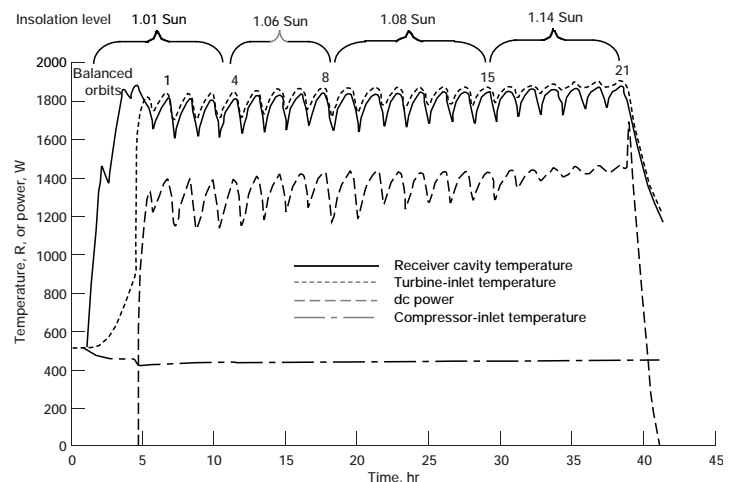
compressor inlet temperature of 270.2 K (-2.8 °C). AlliedSignal's acceptance testing involved about 40 hr of power operation with 10 orbits, including 5 successful ambient starts with 1 hot restart. Operation of the turboalternator-compressor was shown to be within acceptable limits. The 2-kW solar dynamic system was turned over to NASA in March 1995.

The solar dynamic system was tested for over 365 hr of power operation, ranging from 300 W to 2.0 kW, including 187 simulated low-Earth orbits, 16 ambient starts, and 2 hot restarts. NASA characterized the solar dynamic system and evaluated various analytical models over a variety of solar insolation levels, speed conditions, orbit periods, and engine inventories to support the joint U.S./Russian 2-kW Solar Dynamic Flight Demonstration project. System testing showed that an overall system efficiency (conversion of sun into user energy) was in excess of 15 percent, whereas the engine cycle efficiency was over 26 percent. Foil bearing technologies, developed in the 1970's, were successfully demonstrated with 48 start/stops on the turboalternator-compressor. Finally, the solar dynamic space power system demonstrated orbital startup, transient and steady-state orbital operation, and shutdown in a relevant space environment.

The graph shows an example of data from an operational solar dynamic system (receiver and power conversion unit), including the average receiver cavity temperature, the turbine-inlet temperature, the compressor-inlet temperature, and the dc power output. This test was conducted over a 40-hr period with the turboalternator-compressor operating at 48,000 rpm. It illustrates an orbital startup, transient and steady-state orbital operation, and a shutdown. The turboalternator-compressor was operating at 48,000 rpm throughout the test, except for the shutdown at 52,000 rpm. The solar simulator provided four different insolation levels—1.01, 1.06, 1.08, and 1.14 suns ($1.37 \text{ kW/m}^2 = 1 \text{ sun}$)—resulting in four steady-state orbital cases during the 93-min orbit. Balanced orbital operation was achieved on orbits 4, 8, 15, and 21. The first three cases are in a sensible heat receiver (where the canister phase-change material does not melt), which resulted in large temperature (137.2 K) and power (138 W) fluctuations. The fourth case, a latent heat receiver state, resulted in a marked reduction of temperature (19.4 K) and power (49 W) fluctuations during the orbit, which are in good agreement with analytical predictions. For this off-design point, overall "system" efficiency (conversion of sun into

user energy) was in excess of 14 percent and the engine efficiency was about 24 percent.

The collective efforts of the NASA/industry team resulted in the first full-scale demonstration of a complete space-configured solar dynamic system in a large thermal vacuum facility with a simulated sun. Initial operational and performance data have demonstrated a solar dynamic power system with sufficient scale and fidelity to ensure confidence in the availability of solar dynamic technology for space. Studies have shown that solar dynamic power with thermal energy storage can provide continuous electric power in near-Earth orbits with significant savings in life-cycle costs and launch mass when compared with



Top: Data showing startup, multiple orbits, and shutdown of solar dynamic system. Bottom: Solar dynamic system installed in tank 6.

conventional photovoltaic power systems with battery storage for providing continuous electric power in near-Earth orbits. Testing has demonstrated that the solar dynamic technologies developed by NASA programs during the past 30 years are available for near-Earth orbit applications. Applications include potential growth for the international space station, for communication and Earth-observing satellites, and for electric propulsion.

An aerospace Government/industry team worked together to successfully demonstrate solar dynamic power for space in a way that was "cheaper, faster, and better." The solar dynamic ground test demonstration program was completed in early 1995, ahead of schedule and under budget. The Government/industry team delivered the 2-kW solar dynamic system demonstration as promised.

Bibliography

Shaltens, R.K.; and Boyle, R.V.: Update of the 2 kW Solar Dynamic Ground Test Demonstration Program. NASA TM-106730, 1994.

Shaltens, R.K.; and Boyle, R.V.: Initial Results From the Solar Dynamic (SD) Ground Test Demonstration (GTD) Project at NASA Lewis. NASA TM-107004, 1995.

To find out more about the 2-kW Solar Dynamic Space Power System, visit our site on the World Wide Web:
<http://powerweb.lerc.nasa.gov/soldyn/DOC/SDGTD.html>

Lewis contact: Richard K. Shaltens, (216) 433-6138
Headquarters program office: OA

Space Electronics

Digital Audio Radio Broadcast Systems Laboratory Testing Nearly Complete

Radio history continues to be made at the NASA Lewis Research Center with the completion of phase one of the digital audio radio (DAR) testing conducted by the Consumer Electronics Group of the Electronic Industries Association. This satellite, satellite/terrestrial, and terrestrial digital technology will open up new audio broadcasting opportunities both domestically and worldwide. It will significantly improve the current quality of amplitude-modulated/frequency-modulated (AM/FM) radio with a new digitally modulated radio signal and will introduce true

compact-disc-quality (CD-quality) sound for the first time.

Lewis is hosting the laboratory testing of seven proposed digital audio radio systems and modes (see the table). Two of the proposed systems operate in two modes each, making a total of nine systems being tested. The nine systems are divided into the following types of transmission: in-band on-channel (IBOC), in-band adjacent-channel (IBAC), and new bands. The laboratory testing was conducted by the Consumer Electronics Group of the Electronic Industries Association. Subjective assessments of the audio recordings for each of the nine systems was conducted by the Communications Research Center in Ottawa, Canada, under contract to the Electronic Industries Association. The Communications Research Center has the only CCIR-qualified (Consultative Committee for International Radio) audio testing facility in North America.

DESCRIPTIONS OF LABORATORY-TESTED SYSTEMS

| System | Source coding | Data rate tested, kbs | System type | Proposed band, MHz |
|------------------|------------------|-----------------------|-------------------|--------------------|
| USA Digital FM-1 | MUSICAM | 256 | ¹ IBOC | 88 to 108 |
| USA Digital FM-2 | MUSICAM | 256 | ¹ IBOC | 88 to 108 |
| AT&T/AMATILSB | ² PAC | 128 | ¹ IBOC | 88 to 108 |
| AT&T/AMATILSB | ² PAC | 160 | ¹ IBOC | 88 to 108 |
| USA Digital AM | MUSICAM | 92 | ¹ IBOC | 525 to 1705 |
| AT&T | ² PAC | 160 | ³ IBAC | 88 to 108 |
| EUREKA 147 | MUSICAM | 224 | New band | 1452 to 1492 |
| EUREKA 147 | MUSICAM | 192 | New band | 1452 to 1492 |
| VOA/JPL | ² PAC | 160 | ⁴ DBS | 2310 to 2360 |

¹ In-band on-channel.

² The AT&T-developed source-coding scheme called Perceptual Audio Coding (PAC) is derived from the notion of distortion-masking in the human auditory system, the phenomenon whereby one signal can completely mask a sufficiently weaker signal in its frequency or time vicinity.

³ In-band adjacent channel.

⁴ Direct Broadcast Satellite.

Proponents delivered their proposed systems to Lewis in January and February of 1994. Laboratory testing began in March 1994 and concluded in June 1995. Following the laboratory testing, the systems will be installed in a van for field testing in San Francisco, California.

The main goals of the U.S. testing process are to (1) provide technical data to the Federal Communication Commission (FCC) so that it can establish a standard for digital audio receivers and transmitters and (2) provide the receiver and transmitter industries with the proper standards upon which to build their equipment. In addition, the data will be forwarded to

the International Telecommunications Union to help in the establishment of international standards for digital audio receivers and transmitters, thus allowing U.S. manufacturers to compete in the world market.

The overall testing procedures were developed by the Electronics Industries Association in cooperation with the National Radio Standards Committee, all system proponents, equipment manufacturers, and other interested parties. The basic goals of the laboratory tests were to determine the digital audio quality produced by each system, the reception reliability, the ability to coexist with other receivers and broadcast stations (including, in the case of in-band on-channel, the host analog station), and the repeatability of all tests. System testing was conducted with digital audio radio encoders and receivers supplied by the proponents. Other test gear was either provided by interested third parties or purchased by the Electronics Industries Association.

The laboratory tests conducted at Lewis were done in two phases: digital and in-band compatibility. Some tests were conducted on all systems, and others were designed for specific system types. The digital tests (conducted on all systems) included evaluation of quality and characterization of signal failure and of multipath, co-channel, and adjacent channel impairments. The in-band tests (conducted on specific systems) included tests to measure possible interference to the existing analog transmission caused by the introduction of in-band digital audio radio. Tests also were conducted to assess the compatibility of the analog and digital ancillary service channels with the in-band on-channel and in-band adjacent channel signals.

Onsite testing specialists conducted threshold-of-audibility and point-of-failure tests at Lewis. Results of all transmission tests were digitally recorded on digital audio tapes and sent to the Communications Research Center for assessment by listening specialists.

Laboratory test results were announced by the Electronics Industry Association on September 24, 1995, in Monterey, California. Their Digital Audio Radio Subcommittee indicated that these results by themselves reflect only half of the picture. The second half of the picture will come from the field testing to be conducted in San Francisco, California. These tests, which are equally critical, will determine how well each proponent's system will perform under real-world, uncontrollable conditions.

The field test data plus the laboratory test data will complete the testing process for establishing standards. The United States will be able to establish realistic domestic digital audio radio standards based on hard data. The United States will also be a key player in establishing future international digital audio radio service standards.

Lewis contact: James E. Hollansworth, (216) 433-3458
Headquarters program office: OSAT

Role of Communications Satellites in the National and Global Information Infrastructure

Early in 1995, the Satellite Industry Task Force (SITF) was initiated by executives of the satellite industry to define the role for communication satellites in the National and Global Information Infrastructure (NII/GII). Satellites are essential to this information network because they offer ubiquitous coverage and less time to market. SITF, which was chaired by Dr. Thomas Brackey of the Hughes Space and Communication Division, grew out of a series of workshops held during the summer of 1994 by the communication industry, NASA, and the Defense Information Systems Agency (DISA). Experts were convened from 20 companies representing satellite and terrestrial network builders, operators, and users. For 8 months they worked to identify challenges for the satellite industry to play a pivotal role in the National and Global Information Infrastructure. NASA Lewis Research Center personnel helped out with technical and policy matters.

After collecting significant amounts of data and analysis on various issues, SITF participants reached a consensus on five key challenges. Three of the challenges are policy related: access to the communications sector of the electromagnetic spectrum, trade and security, and access to markets. The remaining two are technical: seamless interoperability and technology advancement. SITF also recommended various actions to be taken by the U.S. Government and industry to meet these challenges.

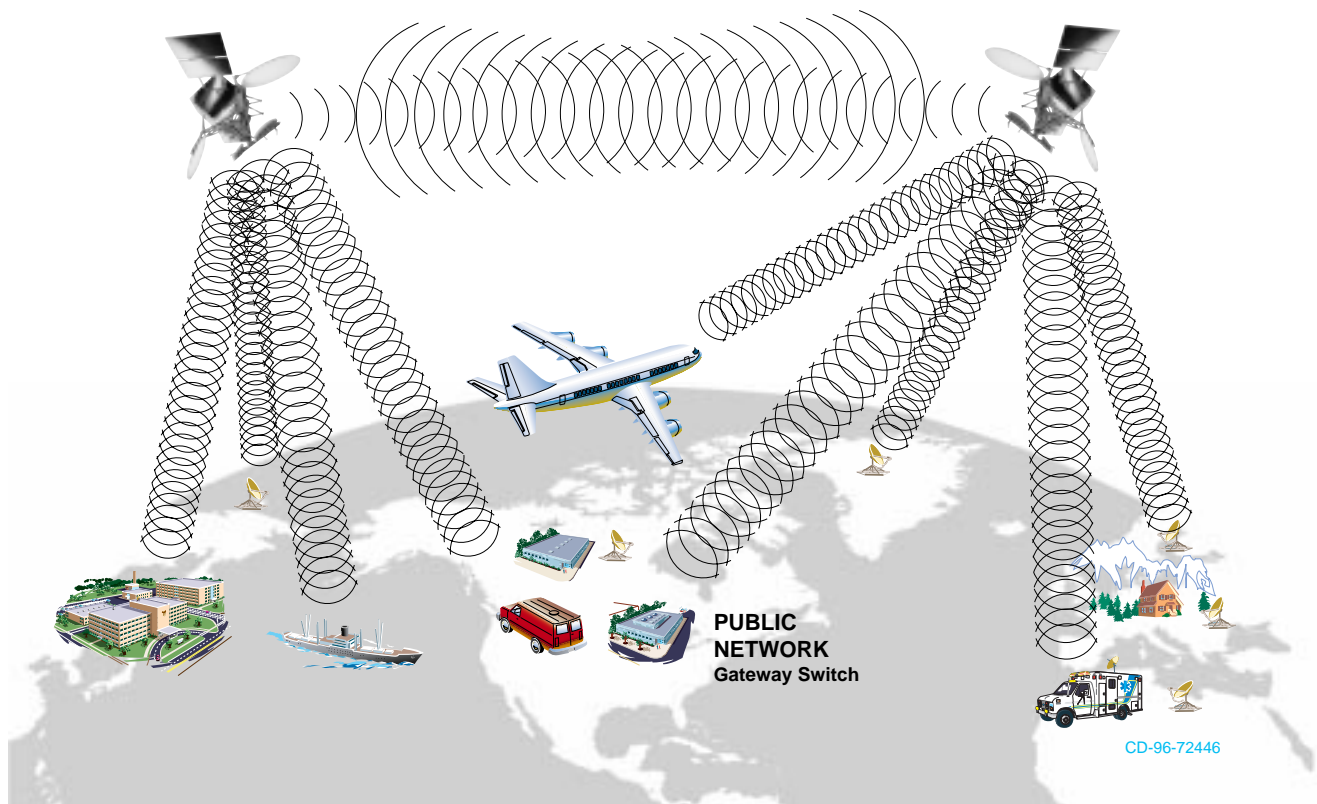
SITF findings were presented to U.S. Vice President Al Gore during the Office of Science and Technology Policy's White House Forum on September 12, 1995, as part of the U.S. Government's efforts to promote the National and Global Information Infrastructure. This meeting was attended by NASA Administrator Daniel Goldin and by senior representatives from the Federal

Communication Commission, the Department of Defense, the Justice Department, and other U.S. agencies, as well as by high-level executives representing the 20 member companies of SITF.

Lewis contacts: Dr. Kul B. Bhasin, (216) 433-3676, and Wayne A. Whyte, Jr., (216) 433-3482
Headquarters program office: OSAT

For more information about Lewis' work with communications satellites, visit our site on the World Wide Web:
<http://sulu.lerc.nasa.gov/>

COMMUNICATIONS SATELLITES IN NATIONAL AND GLOBAL INFORMATION INFRASTRUCTURE



Geostationary, Earth-orbiting satellites (multicast, interactive, delay tolerant, and high rate).

Lewis Helps Examine Feasibility of Fixed Satellite Service and Local Multipoint Distribution Service Sharing the Same Frequency Band

The Federal Communications Commission (FCC) is in the midst of a rule-making procedure that may have a far-reaching effect on the future of Ka-band satellite services. In December 1992, the FCC issued a Notice of Proposed Rule Making that proposed redesignating the 27.5- to 29.5-GHz band (referred to as the 28-GHz band) from fixed, point-to-point services to a new local multipoint distribution service (LMDS).

LMDS is a proposed terrestrial wireless communication service primarily directed at video distribution over small cells. LMDS proponents anticipate that the service would provide cost-effective competition to cable television systems in urban areas.

The 27.5- to 29.5-GHz band also is allocated both domestically and internationally on a primary basis to the Fixed Satellite Service (FSS), and it is currently being used by the NASA Lewis Research Center's Advanced Communications Technology Satellite (ACTS) for uplink transmissions. Seventeen U.S. companies have now filed for commercial satellite communications systems that would utilize the band for uplink and/or feeder link operations.

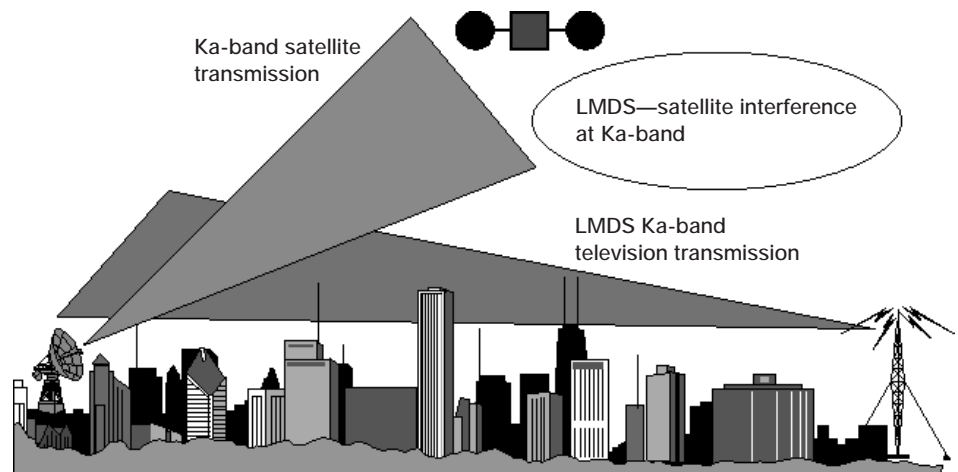
At the time that the FCC released the Notice of Proposed Rule Making on LMDS for comment, the satellite industry was embroiled in the Mobile Satellite Service (MSS) Above 1 GHz Negotiated Rule Making. NASA responded to the Notice of Proposed Rule Making and filed the first discussion regarding the potential for interference between Fixed Satellite Service and LMDS services. (The figure depicts interference paths between these two services.) NASA sensitized the satellite community to the LMDS issues which resulted in further industry opposition to the FCC proposal, citing the inability for future satellite systems to share the 28-GHz band on a cofrequency basis with proposed LMDS systems.

In July 1994, the FCC convened a Negotiated Rule-Making Committee to attempt to resolve the interference issues and

identify rules that would allow frequency cosharing between Fixed Satellite Service and LMDS services. Twenty-five companies and organizations, including NASA, participated in the committee, which represented both satellite and LMDS concerns. Lewis' Space Electronics Division personnel made significant analytical and experimental contributions to the work of the committee.

Despite 60 days of concerted effort by the committee, no sharing solution was found. The primary interference issue centers around the inability to collocate Fixed Satellite Service uplink terminals within reasonable separation distances from LMDS subscriber receivers, and the proposed ubiquitous deployment of Fixed Satellite Service terminals and LMDS receivers within the same service areas.

In an effort to reach a compromise solution that would allow both satellite and LMDS services in the band, the FCC now appears ready to propose segmenting the band. Several segmentation proposals have been filed with the FCC from both satellite and LMDS proponents. These proposals generally satisfy the minimum spectrum requirements of all interests who have filed to date with the FCC for LMDS and satellite systems. The long-term consequences of such a compromise, however, may have a far-reaching and lasting effect on the satellite industry and the future services that it can offer. Limiting the primary spectrum available for satellite services in the 27.5- to 29.5-GHz band will potentially impede the growth of the satellite industry,



Interference scenario between Local Multipoint Distribution Service and Fixed Satellite Service.

reduce competition among satellite providers, and preclude future service opportunities yet to be identified. NASA continues to work with the satellite industry to achieve an outcome that will not hinder the growth potential for Ka-band satellite systems.

For more information about Lewis' work with communications satellites, in general, and ACTS, in particular, visit our sites on the World Wide Web:
<http://sulu.lerc.nasa.gov/>
<http://kronos.lerc.nasa.gov/acts/acts.html>

Lewis contact: Wayne A. Whyte, Jr., (216) 433-3482
Headquarters program offices: OSC and OSAT

Potential Market for Satellite Technology in Meeting Telecommunication Needs of Developing Nations



A recent study examined the potential for satellite technology to meet the telecommunication needs of developing nations. The growth of these nations depends on their attracting and holding the industrial investments of developed nations. This will not be likely with the antiquated telecommunications infrastructure typical of developing nations. On the contrary, it will require an infrastructure that is compatible with international standards. Most of the developing nations perceive this necessity and are pursuing the necessary upgrades. The rate of replacement, types of technology, services affected, and the terrestrial/satellite mix differ by each nation's priorities and gross national product (GNP).

To gain a perspective on the variety of national needs, the NASA Lewis Research Center commissioned Space Systems Loral to perform case studies of Brazil, China, and Mexico. Mexico has made the most progress in terms of percent of population served and the sophistication of services offered. Although China lags behind Mexico in coverage achieved, its recent fiber, cellular, and satellite installations have been impressive, considering the nation has a much larger population and land mass.

In each of these nations, it was found necessary to separate the telecommunications needs of the general population from those of the business community. Because of the expense involved, these nations have concentrated on meeting the needs of the business community first. And this is particularly true of China. In general, the primary telecommunications demand is for conventional telephone service and television. By volume, data services are a smaller niche market,

primarily used by government and business communities. However, this does not mean that the data market is not important. In fact, these governments see data services as playing a critical role in business development. Consequently, the thrust of the telecommunications upgrades tends to favor fiber for urban areas, wireless for outlying areas, and fiber or satellite to connect the two.

China, Brazil, and Mexico are all using satellites to augment their respective telecommunication infrastructures. However, they are not relying solely on satellites to meet their needs. Each of the countries is pursuing both wireless and wired

telecommunications technologies in parallel. For example, China is installing terrestrial fiber networks in urban areas along with wireless cellular systems. In parallel, they are pursuing both a very-small-aperture terminal (VSAT) based backbone data network and a nationwide fiber network interconnection.

Some of the services driving the satellite markets include broadcast television distribution, rural telephone exchange interconnection, private VSAT networks, mobile telephony, and direct-to-home television. For these, terminal equipment must be widely available, inexpensive, and easy to use. Furthermore, for the rural telephone exchange (and perhaps the mobile) application, the overall satellite network must incorporate many of the functions of

the terrestrial telephone system, namely switching, routing, and access control.

Bibliography

Barker, K.; Barnes, C.; and Price, K.M.: Space-Based Communications Infrastructure for Developing Countries. NASA CR-198371, 1995.

For more information about Lewis' work with communications satellites, visit our site on the World Wide Web:

<http://sulu.lerc.nasa.gov/>

Lewis contact: Grady H. Stevens, (216) 433-3463 (E-Mail: gstevens@lerc.nasa.gov)

Headquarters program office: OSAT

Highly Efficient Amplifier for Ka-Band Communications

An amplifier developed under a Small Business Innovation Research (SBIR) contract will have applications for both satellite and terrestrial communications. This power amplifier uses an innovative series bias arrangement of active devices to achieve over 40-percent efficiency at Ka-band frequencies with an output power of 0.66 W. The amplifier is fabricated on a 2.0- by 3.8-mm² chip through the use of Monolithic Microwave Integrated Circuit (MMIC) technology, and it uses state-of-the-art, Pseudomorphic High-Electron-Mobility Transistor (PHEMT) devices.

Although the performance of the MMIC chip depends on these high-performance devices, the real innovations here are a unique series bias scheme, which results in a high-voltage chip supply, and careful design of the on-chip planar output stage combiner. This design concept has ramifications beyond the chip itself because it opens up the possibility of operation directly from a satellite power bus (usually 28 V) without a dc-dc converter. This will dramatically increase the overall system efficiency.

Conventional microwave power amplifier designs utilize many devices all connected in parallel from the bias supply. This results in a low-bias voltage, typically 5 V, and a high-bias current. With this configuration, substantial I^2R losses (current squared times resistance)

may arise in the system bias-distribution network. By placing the devices in a series bias configuration, the total current is reduced, leading to reduced distribution losses. Careful design of the on-chip planar output stage power combiner is also important in minimizing losses. Using these concepts, a two-stage amplifier was designed for operation at 33 GHz and fabricated in a standard MMIC foundry process with 0.20- μm PHEMT devices. Using a 20-V bias supply, the amplifier achieved efficiencies of over 40 percent with an output power of 0.66 W and a 16-dB gain over a 2-GHz bandwidth centered at 33 GHz. With a 28-V bias, a power level of 1.1 W was achieved with a 12-dB gain and a 36-percent efficiency (ref. 1). This represents the best reported combination of power and efficiency at this frequency.

In addition to delivering excellent power and gain, this Ka-band MMIC power amplifier has an efficiency that is 10 percent greater than existing designs. The unique design offers an excellent match for spacecraft applications since the amplifier supply voltage is closely matched to the typical value of spacecraft bus voltage. These amplifiers may be used alone in applications of 1 W or less, or several may be combined or used in an array to produce moderate power, Ka-band transmitters with minimal power combining and less thermal stress owing to the combination of excellent efficiency and power output. The higher voltage operation of this design may also save mass and power because the dc-dc power converter is replaced with a simpler voltage regulator.

Reference

1. Schellenberg, J.M.: A High-Voltage, Ka-Band Power MMIC With 41% Efficiency. Technical Digest 1995. Proceedings of the 17th Annual GaAs IC Symposium, 95CH35851, Oct. 29 - Nov. 1, 1995, pp. 284-287.

To find out more about Lewis' work with communications satellites, visit our site on the World Wide Web:

<http://sulu.lerc.nasa.gov/>

Lewis contact: Dr. Edward J. Haugland, (216) 433-3516

(E-Mail: ejhaugland@lerc.nasa.gov)

Headquarters program office: OSAT

Chemical Vapor-Deposited (CVD) Diamond Films for Electronic Applications

Diamond films have a variety of useful applications as electron emitters in devices such as magnetrons, electron multipliers, displays, and sensors. Secondary electron emission is the effect in which electrons are emitted from the near surface of a material because of energetic incident electrons. The total secondary yield coefficient σ , which is the ratio of the number of secondary electrons to the number of incident electrons, generally ranges from 2 to 4 for most materials used in such applications. It was discovered recently at the NASA Lewis Research Center that chemical vapor-deposited (CVD) diamond films have very high secondary electron yields, particularly when they are coated with thin layers of CsI. For CsI-coated diamond films, the value of σ can exceed 60.

Also, diamond films exhibit field emission at fields that are orders of magnitude lower than for existing state-of-the-art emitters. Present state-of-the-art microfabricated field emitters generally require applied fields above 5×10^7 V/cm. Research on field emission from CVD diamond and high-pressure, high-temperature diamond has shown that field emission can be obtained at fields as low as 2×10^4 V/cm. It has also been shown that thin layers of metals, such as gold, and of alkali halides, such as CsI, can significantly increase field emission and stability. Emitters with nanometer-scale lithography will be able to obtain high-current densities with voltages on the order of only 10 to 15 V.

Bibliography

Mearini, G.T., et al.: Fabrication of an Electron Multiplier Utilizing Diamond Films. *Thin Sol. Fil.*, vol. 253, 1994, pp. 151-156.

Mearini, G.T.; Krainsky, I.L.; and Dayton, J.A., Jr.: Investigation of Diamond Films for Electronic Devices. *Surf. and Interface Anal.*, vol. 21, 1994, pp. 138-143.

Mearini, G.T., et al.: Stable Secondary Electron Emission Observations From Chemical Vapor Deposited Diamond. *Appl. Phys. Lett.*, vol. 65, no. 21, Nov. 1994, pp. 2702-2704.

Mearini, G.T., et al.: Stable Secondary Electron Emission From Chemical Vapor Deposited Diamond Films Coated With Alkali-Halides. *Appl. Phys. Lett.*, vol. 66, no. 2, Jan. 1995, pp. 242-244.

Lamouri, A., et al.: Proc. of the International Vacuum Microelectronic Conference, Portland, OR, 1995.

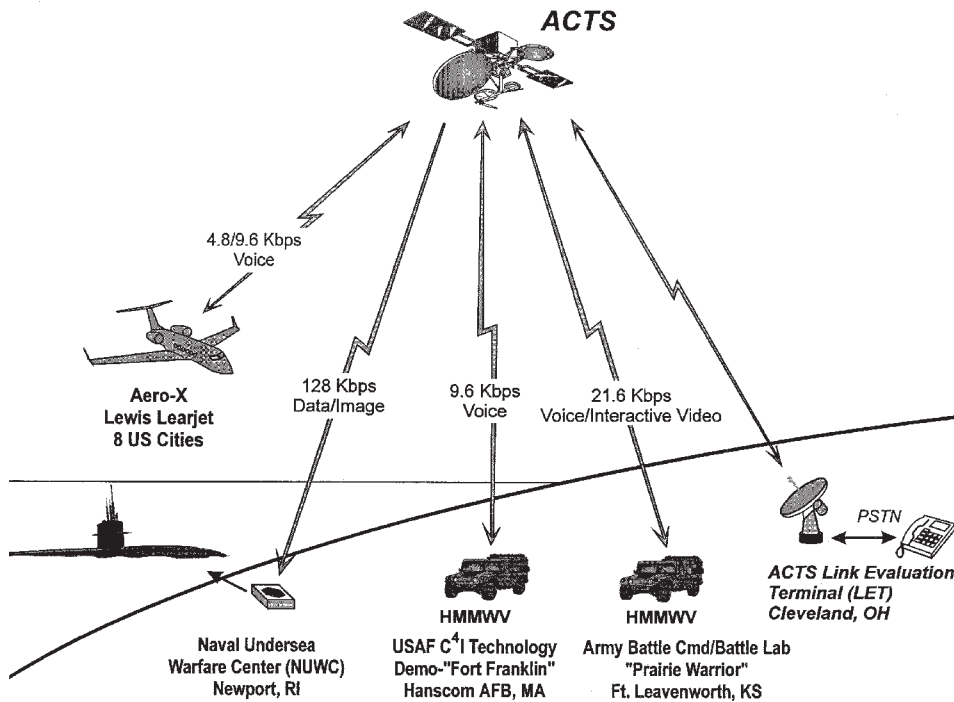
Lewis contact: Dr. Isay L. Krainsky, (216) 433-3509
Headquarters program office: OSAT

Monolithic Microwave Integrated Circuit (MMIC) Phased Array Demonstrated With ACTS

Monolithic Microwave Integrated Circuit (MMIC) arrays developed by the NASA Lewis Research Center and the Air Force Rome Laboratory were demonstrated in aeronautical terminals and in mobile or fixed Earth terminals linked with NASA's Advanced Communications Technology Satellite (ACTS). Four K/Ka-band experimental arrays were demonstrated between May 1994 and May 1995. Each array had GaAs MMIC devices at each radiating element for electronic beam steering and distributed power amplification. The 30-GHz transmit array used in uplinks to ACTS was developed by Lewis and Texas Instruments. The three 20-GHz receive arrays used in downlinks from ACTS were developed in cooperation with the Air Force Rome Laboratory, taking advantage of existing Air Force integrated-circuit, active-phased-array development contracts with the Boeing Company and Lockheed Martin Corporation.

Four demonstrations, each related to an application of high interest to both commercial and Department of Defense organizations, were conducted. The figure shows the location, type of link, and the data rate achieved for each of the applications. In one demonstration—an aeronautical terminal experiment called AERO-X—a duplex voice link between an aeronautical terminal on the Lewis Learjet and ACTS was achieved. Two others demonstrated duplex voice links (and in one case, interactive video links as well) between ACTS and an Army high-mobility, multi-purpose wheeled vehicle (HMMWV, or "humvee"). In the fourth demonstration, the array was on a fixed mount and was electronically steered toward ACTS. Lewis served as project manager for all demonstrations and as overall system integrator. Lewis engineers developed the array system including a controller for open-loop tracking of ACTS during flight and HMMWV motion, as well as a laptop data display and recording system used in all demonstrations. The Jet Propulsion Laboratory supported the AERO-X program, providing elements of the ACTS Mobile Terminal.

The successful performance of experimental, proof-of-concept MMIC K/Ka-band arrays developed with U.S. industry in field demonstrations with ACTS indicates that high-density MMIC integration at 20 and 30 GHz is indeed feasible. The successful development and demonstration of the MMIC array systems was possible only because of significant intergovernmental and Government/industry cooperation and the high level



MMIC phased-array demonstrations with ACTS.

of teamwork within Lewis. The results provide a strong incentive for continuing the focused development of MMIC-array technology for satellite communications applications, with emphasis on packaging and cost issues, and for continuing the planning and conducting of other appropriate demonstrations or experiments of phased-array technology with ACTS.

Given the present pressures on reducing funding for research and development in Government and industry, the extent to which this can be continued in a cooperative manner will determine whether MMIC array technology will make the transition from the proof-of-concept level to the operational system level.

Find out more about ACTS on the World Wide Web:
<http://kronos.lerc.nasa.gov/acts/acts.html>

Lewis contact: Dr. Charles A. Raquet, (216) 433-3471
Headquarters program office: OSAT

B-ISDN Onboard Processing Fast Packet Switch Developed

Future satellite communications applications will require a packet-switched onboard satellite processing system to route packets at very high speeds from uplink beams to different downlink beams. The rapid emergence of point-to-multipoint services, and the important role of satellites in a national and global information infrastructure, makes the multicast function essential to a fast packet switch (FPS). NASA Lewis Research Center's Digital System Technology Branch has been studying possible architectures for high-speed onboard-processing satellite systems. As part of this research, COMSAT Laboratories developed a broadband integrated services digital network (B-ISDN) fast packet switch for Lewis that was delivered on December 1994.

The fast packet switch consists of eight inputs and eight outputs that can receive and transmit data, respectively, at a rate of 155 Mbps. The switch features multiple priorities (three) and multiple-size (three) satellite virtual cells that are similar to ATM cells in length (52 bytes). In addition, the fast packet switch features a congestion-control algorithm that allows users to set

different thresholds for individual destination ports, thus throttling back the traffic from the transmitting port.

To allow for better characterization of the fast packet switch, the Artificial Intelligence Group of Lewis' Digital System Technology Branch developed a user-friendly graphical user interface to the switch. By using the graphical interface, users can efficiently compose commands and generate command script files. Users intuitively select commands from a graphical display by using a mouse. When a command is selected, appropriate parameter options are displayed for further selection. Command instructions and data responses, respectively, are transmitted to and from the fast packet switch via a direct RS-232 serial link. The fast packet switch responses to commands are automatically displayed and can be saved to a file for future reference. In addition, users can build a sequence of commands into a script that can be saved, loaded, edited, and executed at a later time.



Fast packet switch interface.

Errors in command syntax are avoided because only appropriate parameters are offered for the selected command name. Typing errors are avoided because users enter data with the mouse. This intelligent user interface also allows less-experienced users to quickly generate complicated scripts. Users do not have to remember all possible command codes, command options, and corresponding formats. Later, the interface will be integrated with the artificial-intelligence shell Kappa-PC. This shell could help users decide which command or group of commands are needed to perform certain tasks. Also Kappa-PC can help users select appropriate command options.

Find out more about Lewis' work with communications satellites on the World Wide Web:

<http://sulu.lerc.nasa.gov/>

Lewis contacts: Jorge A. Quintana, (216) 433-6519, and Todd Quinn, (216) 977-1103
Headquarters program office: OSAT

Low-Complexity, Digital Encoder/Modulator Developed for High-Data-Rate Satellite B-ISDN Applications

The Space Electronics Division at the NASA Lewis Research Center is developing advanced electronic technologies for the space communications and remote sensing systems of tomorrow. As part of the continuing effort to advance the state-of-the-art in satellite communications and remote sensing systems, Lewis developed a low-cost, modular, programmable, and reconfigurable all-digital encoder-modulator (DEM) for medium- to high-data-rate radiofrequency communication links. The DEM is particularly well suited to high-data-rate downlinks to ground terminals or direct data downlinks from near-Earth science platforms. It can support data rates up to 250 megabits per second (Mbps) and several modulation schemes, including the traditional binary phase-shift keying (BPSK) and quadrature phase-shift keying (QPSK) modes, as well as higher order schemes such as 8 phase-shift keying (8PSK) and 16 quadrature amplitude modulation (16QAM). The DEM architecture also can precompensate for channel disturbances and alleviate amplitude degradations caused by nonlinear transponder characteristics.

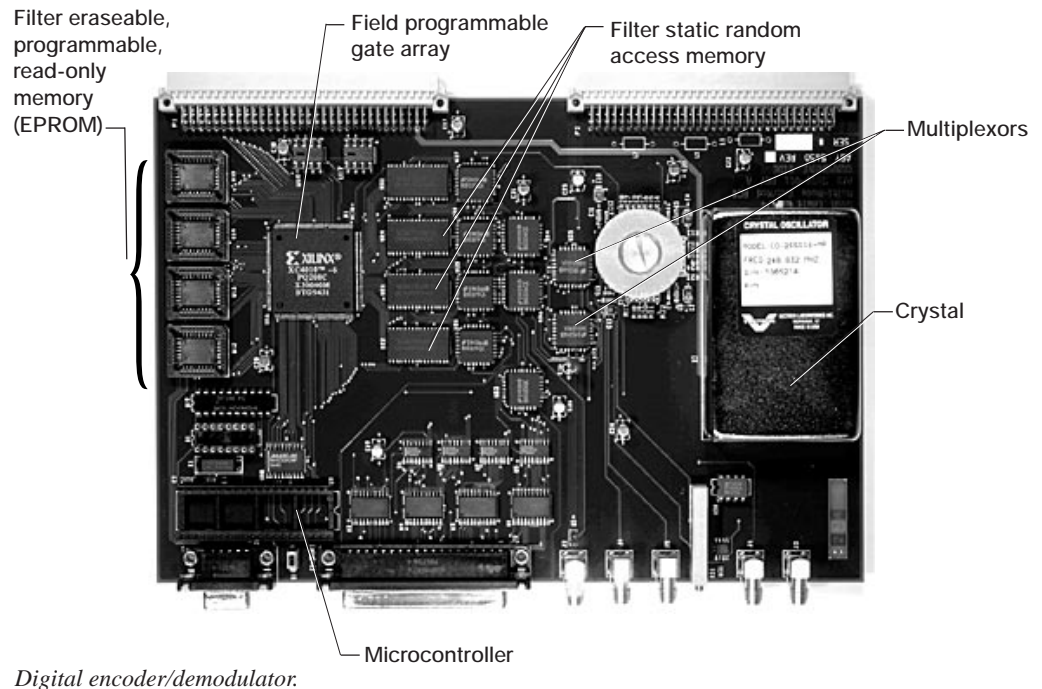
In addition to higher order modulation schemes, a combination of modulation and forward-error correction coding is used to improve the efficiency of conveying information through the power- and bandwidth-limited channels that are characteristic of spaceborne systems. In these systems, onboard power and frequency allocation is at a premium. The DEM's baseline bandwidth efficient modulation technique provides a factor of 2 improvement in bandwidth efficiency over the Consultative Committee for Space Data Systems (CCSDS) standard and nearly 6 orders of magnitude improvement in quality of service. This feature enables bandwidth-efficient, high-data-rate communications without requiring excessively sized, onboard radiofrequency power amplifiers, thus reducing overall spacecraft mass and power.

The modular, programmable, and reconfigurable architecture of the DEM provides a unique level of mission design flexibility, allowing the same package to be used on many kinds of spacecraft with a wide variety of communications needs. Often complex programmable designs become very inefficient in terms of power, size, and mass at other than the highest data rates. The programmable feature allows mission designers to use the same package to provide various levels of communications services depending on the rates required. The unique degree of flexibility afforded by this package will lead to a significant reduction in spacecraft life-cycle costs by reducing nonrecurring development costs for modules that satisfy the needs of only one spacecraft design.

The prototype hardware that is shown in the figure consumes approximately 18 W, is assembled on a 6U by 160-mm VME card, and weighs approximately 40 oz. The use of low-complexity digital signal processing techniques has nearly halved the size and mass of comparable state-of-the-practice designs. Future work will focus on further reducing the size, power, and mass of the unit. An approach under consideration is the design and development of a custom, multichip module to perform the majority of the DEM functions.

Find out more about Lewis' work with communications satellites on the World Wide Web:
<http://sulu.lerc.nasa.gov/>

Lewis contact : Ronald L. Bexten, (216) 433-3535
Headquarters program office: OSAT



Multichannel Error Correction Code Decoder

NASA Lewis Research Center's Digital Systems Technology Branch has an ongoing program in modulation, coding, onboard processing, and switching. Recently, NASA completed a project to incorporate a time-shared decoder into the very-small-aperture terminal (VSAT) onboard-processing mesh architecture. The primary goal was to demonstrate a time-shared decoder for a regenerative satellite that uses asynchronous, frequency-division multiple access (FDMA) uplink channels, thereby identifying hardware and power requirements and fault-tolerant issues that would have to be addressed in a operational system. A secondary goal was to integrate and test, in a system environment, two NASA-sponsored, proof-of-concept hardware deliverables: the Harris Corp. high-speed Bose Chaudhuri-Hocquenghem (BCH) codec and the TRW multichannel demultiplexer/demodulator (MCDD). A beneficial byproduct of this project was the development of flexible, multichannel-uplink signal-generation equipment.

The multichannel ECC decoder (MED) system is a prototype of the uplink portion of a low-rate (64 kbps) FDMA satellite for a mesh VSAT processing satellite. As shown in the schematic, the MED consists of a bit-error-rate test set, uplink signal-generation equipment, the

TRW MCDD (including radiofrequency and link-simulation equipment), and the time-shared decoder. The system can produce four uncoded or coded uplink channels at a channel transmission rate of 64 kbps. The codec uses a BCH block code in block sizes of 224 to 480 bits excluding a 32-bit unique word preamble that identifies the start of a block.

This time-shared decoder has a very good potential for being applied in an onboard-processing circuit-switch environment because individual blocks of data can be processed and routed as soon as a full data block is available. Thus, the amount of storage memory required onboard is reduced. For applications to a packet switch in an asynchronous FDMA environment, the time-shared decoder system would have to be modified to align packets. This procedure would be prohibitively memory intensive and is not recommended.

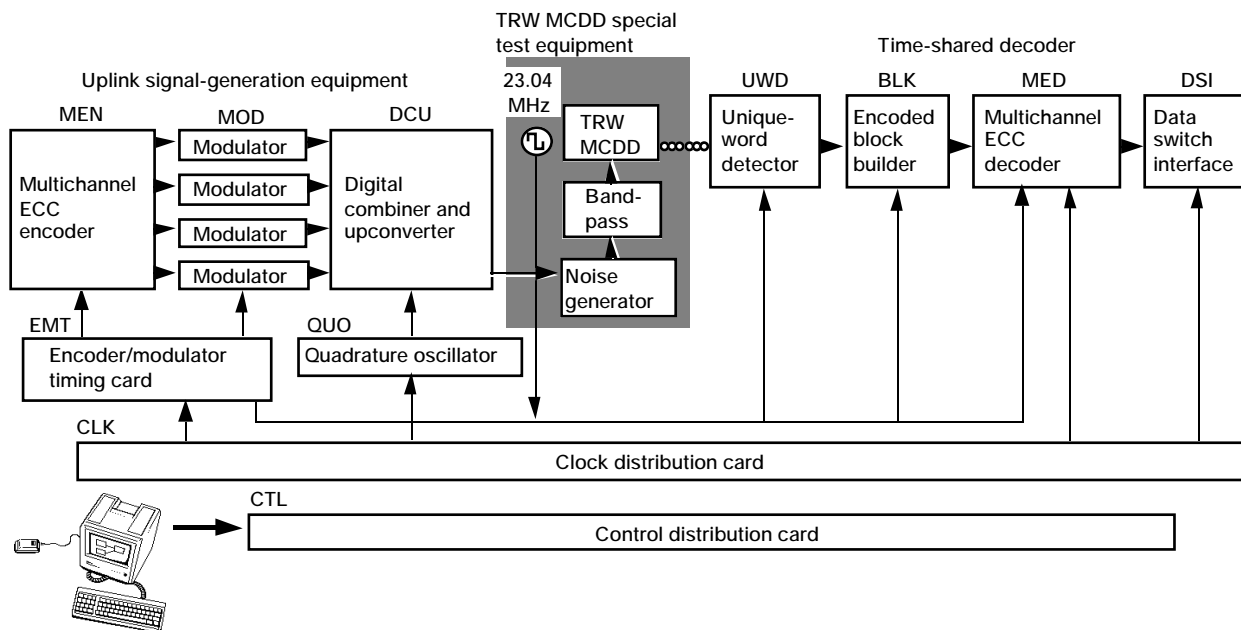
Testing was performed to characterize the information channels through the MCDD at various signal-to-noise levels. In addition, the MCDD's degraded guard channels can be used for transmission with inferior performance. Therefore, the guard channels were also characterized. Some parameters that were investigated include coding block length, data pattern, unique word value, and adjacent-channel interference. A final report of the complete testing and characterization of the system will be available by January 1996.

Bibliography

Wagner, P.K.; and Ivancic, W.D.: Multichannel Error Correction Code Decoder. AIAA Paper 94-1025 (NASA TM-106331), 1994.

Find out more about Lewis' Digital Systems Technology Branch on the World Wide Web:
<http://sulu.lerc.nasa.gov/>

Lewis contacts: Nitin J. Soni, (216) 433-6591, and William D. Ivancic, (216) 433-3494
 Headquarters program office: OSAT



Uplink signal-generation equipment and time-shared decoder. Top: photo. Bottom: schematic.

INTEX Ka-Band Experiment Ground Terminal

The INTEX (interference experiment) Ka-Band Experiment Ground Terminal was developed by NASA Lewis Research Center's Advanced Space Communications Laboratory to enable space communications experiments that use the Advanced Communications Technology Satellite (ACTS). INTEX is used for a wide range of ACTS technology validation and investigation experiments as well as application demonstrations. It also supports experiments for other organizations within and outside of NASA.

The INTEX Ground Terminal includes a 2.4-m parabolic antenna and a 40-W transmitter that can handle data rates from a few kilobits per second up to 300 megabits per second (Mbps) through the ACTS matrix switch mode transponder. The primary experiment data rates and modulations used with the INTEX terminal are T1 (1.544 Mbps) and 48 Mbps using quadrature phase-shift keying (QPSK) modulation and 110 and 220 Mbps using serial minimum-shift-keyed (SMSK) modulation. The SMSK modem is capable of time-division, multiple-access (TDMA) burst transmission at throughput rates of 55, 27.5, and 13.8 Mbps. The INTEX ground terminal also is completely compatible with the ACTS High Burst Rate Link Evaluation Terminal (HBR-LET) terminal, allowing two-terminal duplex link experiments.

Experiments performed so far include: determination of the effects of continuous-wave (CW) interference on a high-data-rate TDMA channel, determination of the two-tone response of the ACTS hardlimiter transponder, determination of the effects of co-channel and adjacent channel interference, performance of multi-signal transmission, characterization of ACTS Ka-band link and transponder performance, evaluation of INTEX and HBR-LET terminal performance, and demonstration of burst high-data-rate transmission between TDMA terminals. Other experiments planned or underway include evaluation of the effects of phase noise on the bit error rate of low- and high-data-rate signals, evaluation of the performance of digital video-compression techniques in the presence of noise and interference, evaluation of the performance of high-ratio image compression applied to medical images, characterization of modulation and coding techniques through the ACTS hardlimiter channel, and demonstration and evaluation of satellite telemammography techniques by transmission to remote medical facilities.

The INTEX terminal can support organizations interested in additional qualified experiments with ACTS for a wide range of investigations and applications demonstrations.

To find out more about ACTS and Lewis' Communications Projects Branch, visit our sites on the World Wide Web:
<http://kronos.lerc.nasa.gov/acts/acts.html>
<http://sulu.lerc.nasa.gov/5660.html>

Lewis contact: Robert J. Kerczewski, (216) 433-3434
Headquarters program office: OSAT

Telemammography Using Satellite Communications

The most effective method for improving survival rates for breast cancer, a leading cause of death among American women, is early detection through mammography. Because of certification requirements and economic reasons, most mammography experts are located in densely populated areas and in large medical facilities. Direct access to such expertise is unavailable for millions of patients in rural, sparsely populated, and economically depressed areas. Telemammography, the electronic transmission of digitized mammograms, can connect these neglected patients with timely, critical medical expertise; however, an adequate terrestrial communications infrastructure does not exist in these areas.

Fortunately, a number of major global satellite networks are being developed for deployment at the end of this decade, bringing a low-cost telecommunications infrastructure connection to virtually any location. NASA Lewis Research Center's Advanced Space Communications Laboratory is now working with leading breast cancer research hospitals, including the Cleveland Clinic and the University of Virginia, to perform the critical research necessary to allow new satellite networks to support telemammography.

The Satellite Telemammography Project recently completed its first live demonstration: several digitized mammography images were transmitted from Lewis to

the ACTS Results Conference via the ACTS satellite T1 VSAT Earth terminals. The Satellite Telemammography Project is working on several critical technology elements required for the future deployment of satellite telemammography systems. One of these elements is the determination of satellite link and image-compression parameters required for telemammography transmission. These parameters are needed to determine the quality of the satellite link needed for transmission and the maximum level of image compression that will maintain diagnostic accuracy. Another element is the need for faster and more efficient image-compression algorithms, which are required to reduce the size of mammography image files from up to 40 megabytes (MB) to 1 MB or less to allow fast transmission over T1 rate links. Also, the process must be integrated with hospital image archiving and communications systems.

Telemammography workstations with high-resolution medical image monitors are configured to allow the study of digitized mammograms and to apply image-

compression algorithms. The Advanced Space Communications Laboratory satellite communications testbed will be used to establish satellite link and image-compression parameters. To provide basic satellite telemammography standards, expert mammographers will participate in studies that fulfill strict medical and statistical requirements. ACTS satellite and ground terminals will be used to test and demonstrate long-distance satellite telemammography between Lewis and digital mammography research hospitals. The Satellite Telemammography Project will provide some of the most important communications technology elements for enabling low-cost satellite telemammography.

For more information about the research of Lewis' Communications Projects Branch, visit our site on the World Wide Web:

<http://sulu.lerc.nasa.gov/5660.html>

**Lewis contact: Robert J. Kerczewski, (216) 433-3434
Headquarters program office: OSAT**

1995 R&T Space Flight Systems

ACTS Project

Compilation and Analysis of 20- and 30-GHz Rain Fade Events at the ACTS NASA Ground Station: Statistics and Model Assessment

Since the beginning of the operational phase of the NASA Research Center's Advanced Communication Technology Satellite (ACTS), signal-fade measurements have been recorded at the NASA Ground Station located in Cleveland, Ohio, with the use of the 20- and 30-GHz beacon signals. Compilations of the daily data have been statistically analyzed on a monthly and yearly basis. Such analyses have yielded relevant parameters as (1) cumulative monthly and yearly probability distributions of signal attenuation by rain, (2) attenuation duration versus attenuation threshold probabilities, and (3) rate-of-fade probabilities. Not only are such data needed for a realistic data base to support the design and performance analysis of future satellite systems, but they are necessary to assess predictions made with the ACTS Rain Attenuation Prediction Model.

Bibliography

Manning, R.M.: Compilation and Analysis of 20- and 30-GHz Rain Fade Events at the ACTS NASA Ground Station: Statistics and Model Assessment. ACTS Results Conference. Cleveland, Ohio. Sept. 11-13, 1995

Find out more about ACTS on the World Wide Web:
<http://kronos.lerc.nasa.gov/acts/acts.html>

Lewis contact: Dr. Robert M. Manning, (216) 433-6750
Headquarters program office: OSAT

Using the ACTS Rain Attenuation Prediction Model to Identify and Specify Communications System Performance Parameters

The Advanced Communication Technology Satellite (ACTS) Rain Attenuation Prediction Model was used in two satellite communication scenarios. In particular, propagation links from ACTS to and from Cleveland, Ohio, and Nashville, Tennessee, were considered. Software for the model, which has existed for 5 years, is known as the NASA Lewis Research Center Satellite Link Attenuation Model program, or LeRC-SLAM, Version 1.1. (This model and its software implementation won the Space Act Award for 1992.) The model is applicable for any location in the continental United States with a spatial resolution of 0.5° in both longitude and latitude. The frequency of operation of the communications link can be within the range inclusive from 1 to 1000 GHz. Other parameters needed to use this software are reviewed in reference 1. The analysis that is given here is for the ACTS communication links mentioned above. In addition to the details given by this version of the LeRC-SLAM software, a new performance parameter, as well as the associated concept of rain fade controller availability ("rain fade" refers to the attenuation of a signal by rain), is used to optimize link performance. It is the purpose of LeRC-SLAM to demonstrate the use of these relevant parameters in the design of such communications links.

Bibliography

Manning, R.M.: Using the ACTS Rain Attenuation Prediction Model to Identify and Specify Communications System Performance Parameters. ACTS Results Conference, Cleveland, Ohio, Sept. 11-13, 1995.

LeRC-SLAM (order number LEW-14979) is available from COSMIC—NASA's Software Technology Transfer Center. Contact COSMIC by phone (706) 542-3265, by fax (706) 542-4807, or on the World Wide Web (<http://www.cosmic.uga.edu/>).

Find out more about ACTS on the World Wide Web:
<http://kronos.lerc.nasa.gov/acts/acts.html>

Lewis contact: Dr. Robert M. Manning (216) 433-6750
Headquarters program office: OSAT

Implications of ACTS Technology on the Requirements of Rain Attenuation Modeling for Communication System Specification and Analysis at the Ka-Band and Beyond

With the advent of the use of the Ka-band for space communications, coupled with the introduction of digital modulation techniques as well as multiple-beam methodology for satellites, the NASA Lewis Research Center has deemed it necessary to reassess the plethora of rain attenuation prediction models in use (computer models that predict the attenuation of signals by rain). The Advanced Communication Technology Satellite (ACTS) project, undertaken by NASA in 1983, offered such challenges to rain attenuation prediction modeling. An examination of the work done in this area shows that, up to 1983, no such single modeling formalism existed that could fulfill the requirements of the ACTS specifications. Not even the work done by the NASA Propagation Experimenters Group had envisioned such requirements, so no dynamic Ka-band data existed from which one could draw conclusions.

In response to this need, Lewis developed the ACTS Rain Attenuation Prediction Model. A detailed discussion of the derivation of the model's basic relations can be found in reference 1. The model as well as its software implementation won the Space Act Award for 1992. In addition to the review of the model, a recommendation is given in reference 2 for a new evaluation of the performance of satellite communication systems, in particular, for those to be operating within the Ka-band and above. These systems will necessarily employ some type of dynamic rain-fade mitigation procedure.

References

1. Manning, R.M.: A Unified Statistical Rain-Attenuation Model for Communication Link Fade Predictions and Optimal Stochastic Fade Control Design Using a Location-Dependent Rain-Statistics Database. *Int. J. Satellite Comm.*, vol. 8, 1990, pp. 11-30.
2. Manning, R.M.: The Implications of ACTS Technology on the Requirements of Rain Attenuation Modeling for Communication System Specification and Analysis at 30/20 GHz and Beyond. ACTS Results Conference, Cleveland, Ohio, Sept. 11-13, 1995.

Find out more about ACTS on the World Wide Web:
<http://kronos.lerc.nasa.gov/acts/acts.html>

Lewis contact: Dr. Robert M. Manning, (216) 433-6750
Headquarters program office: OSAT

ACTS Aeronautical Terminal Experiment (AERO-X)

During the summer of 1994, the performance of an experimental mobile satellite communication system was demonstrated. Using the Advanced Communications Technology Satellite (ACTS) and the ACTS Mobile Terminal (AMT), the system demonstrated an active Monolithic Microwave Integrated Circuit (MMIC) phased-array antenna system. The antenna system was installed onboard one of NASA Lewis Research Center's research aircraft, a Learjet Model 25. It proved the viability of in-flight satellite communications services via small, flush, mountable electronic phased-array antennas. The top left figure illustrates the overall system setup for the ACTS Aeronautical Terminal Experiment (AERO-X). The Link Evaluation Terminal (LET) at Lewis in Cleveland, Ohio, interfaced with fixed-AMT equipment, providing a seamless connection with the Public Service Telephone Network. As the Learjet was flown over several major cities across the U.S., this demonstration system allowed passengers onboard to make telephone calls as if they were using a cellular system. ACTS was operated in its microwave switch matrix mode with a spot beam for the Learjet and another spot beam dedicated to the LET.

ACTS is a proof-of-concept 30/20-GHz satellite launched by the Space Shuttle Discovery (STS-51) in September 1993. It has been operating ever since and continues to validate key technologies such as (1) the satellite multibeam antenna, which produces multiple high-gain spot beams that can be rapidly hopped, scanned, or fixed; (2) the baseband processor, which demodulates, routes individual circuit-switched messages, and remodulates; and (3) the microwave switch matrix, which handles up to 9000-MHz bandwidth signals and provides rapidly reconfigurable connectivity between the spot beams. The bottom figure on the next page shows satellite coverage afforded by the ACTS satellite.

The AMT is a mobile terminal designed to demonstrate the viability of speech (at 2.4, 4.8, and 9.6 kilobits per second (kbps)) and data transmission (at 2.4, 4.8, 9.6, and 64 kbps) in the 30/20-GHz mobile satellite communications environment. The speech codec uses the Government standard LPC-10, the proposed CELP Government standard, and MRELP (Motorola's proprietary algorithm). Its modem implements a simple, but robust, differential phase shift keying (DPSK) scheme with a rate $\frac{1}{2}$ convolutional coding and interleaving.

The MMIC phased-array antenna system (ref. 1) consisted of one transmit array antenna and two receive array antennas. The antennas were mounted inside the Learjet, looking out the standard Plexiglass window. These array antennas incorporated individual GaAs MMIC devices for the individual radiating elements for electronic beam steering and distributed power amplification. An open-loop antenna controller developed by Lewis used information from the global positioning system and aircraft gyroscopes to electronically steer the array beams toward ACTS during flight.

During the demonstration flights, link performance data were recorded with a power meter, a spectrum analyzer, a calibrated 31.8-kHz bandpass filter, and a global positioning system receiver. In the top right figure (which shows the inbound carrier-to-noise ratio), the continuous trace is the measured performance and

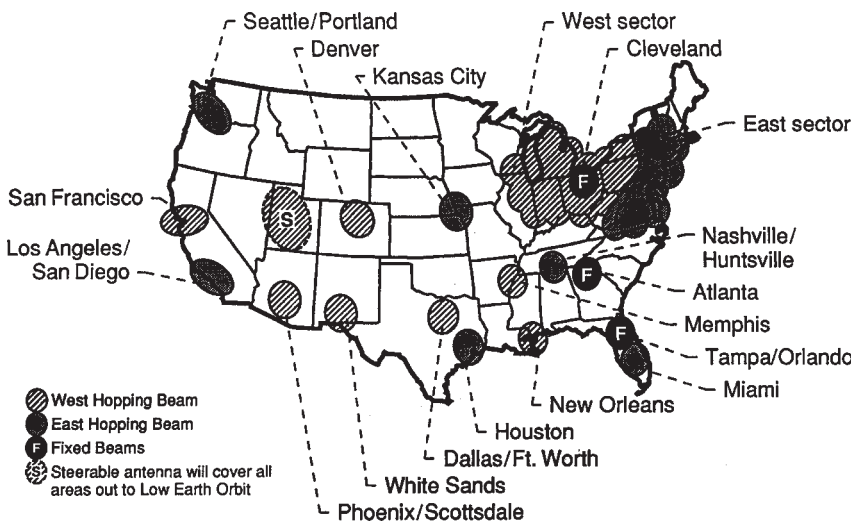
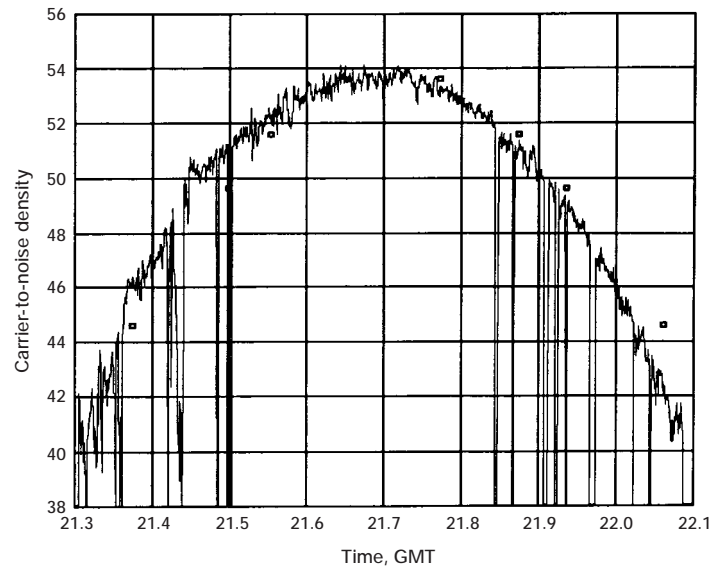
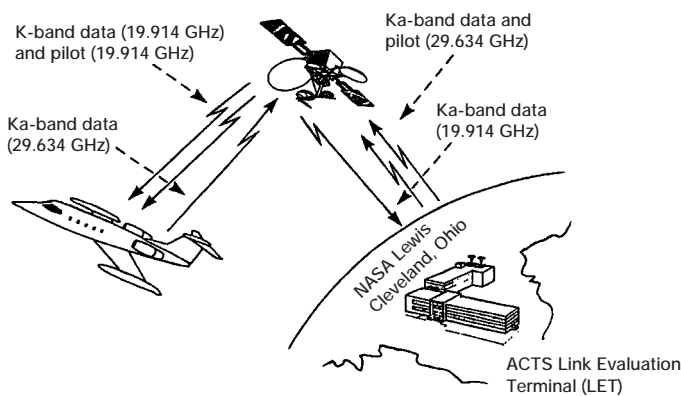
the rectangles represent the predicted performance. The AERO-X program provided an opportunity to showcase many proof-of-concept technologies found in the ACTS satellite, the active phased-array antennas, and the AMT.

Reference

1. Raquet, C., et al.: Ka-Band MMIC Arrays for ACTS Aero Terminal Experiment. Presented at the 43rd Congress of the International Astronautical Federation. Aug. 28 to Sept. 5, 1992.

Find out more about ACTS on the World Wide Web:
<http://kronos.lerc.nasa.gov/acts/acts.html>

Lewis contacts: Sina Javidi, (216) 433-8326, and Richard Reinhart, (216) 433-6588
Headquarters program office: OSAT



Top left: System setup. Top right: Inbound link carrier-to-noise density versus Greenwich Mean Time (GMT). Bottom: ACTS satellite coverage.

Advanced Communication Technology Satellite (ACTS) Multibeam Antenna On-Orbit Performance

Introduction

The NASA Lewis Research Center's Advanced Communication Technology Satellite (ACTS) was launched in September 1993. ACTS introduced several new technologies, including a multibeam antenna (MBA) operating at extremely short wavelengths never before used in communications. This antenna, which has both fixed and rapidly reconfigurable high-energy spot beams (150 miles in diameter), serves users equipped with small antenna terminals.

Extensive structural and thermal analyses have been performed for simulating the ACTS MBA on-orbit performance. The results show that the reflector surfaces (mainly the front subreflector), antenna support assembly, and metallic surfaces on the spacecraft body will be distorted because of the thermal effects of varying solar heating, which degrade the ACTS MBA performance.

Since ACTS was launched, a number of evaluations have been performed to assess MBA performance in the space environment. For example, the on-orbit performance measurements found systematic environmental disturbances to the MBA beam pointing. These disturbances were found to be imposed by the attitude

control system, antenna and spacecraft mechanical alignments, and on-orbit thermal effects. As a result, the MBA may not always exactly cover the intended service area. In addition, the on-orbit measurements showed that antenna pointing accuracy is the performance parameter most sensitive to thermal distortions on the front subreflector surface and antenna support assemblies.

Several compensation approaches were tested and evaluated to restore on-orbit pointing stability. A combination of autotrack (75 percent of the time) and Earth sensor control (25 percent of the time) was found to be the best way to compensate for antenna pointing error during orbit. This approach greatly minimizes the effects of thermal distortions on antenna beam pointing.

Summary of Results

- Analysis and on-orbit measurements of the ACTS MBA performance indicated that thermal distortions are periodic. The table describes the system's effect with and without compensation for ground stations within a single spot beam.

ACTS MULTIBEAM ANTENNA RADIOFREQUENCY POINTING VARIATIONS

| Type | Beam | Magnitude, deg | Axis | Duration | Operational effect |
|-------------------|---------------|------------------------|---------------|----------------|--|
| Rapidly varying | East | Less than 0.1 | Roll | Less than 1 hr | Short-term effect marginal station. Use ESA control during event to minimize effect. |
| Diurnal variation | East and West | .2 | Pitch | 12 hr/event | Significant signal variation can crash stations. Use bias drive to compensate. |
| Quasistatic | East and West | $\pm .04$ $\pm .02$ | Pitch Roll | 14 days | Totally compensated by Autotrack |
| Vibration | Transmit | $\pm .15$ | Pitch | 1 Hz | Generally negligible |

- In future commercial communications satellites that use multibeam reflector systems at the Ka band (or that use gridded reflector structures and materials such as Aztroquartz (GE Astro, East Windsor, New Jersey) at higher frequencies), a sunshade should be employed to avoid large thermal distortions.
- The mechanical oscillations (nonthermal distortions) on the ACTS MBA are very difficult to compensate for. Future communications satellites should consider the mechanical oscillations a driver in their antenna mechanical design.
- The yaw control system can affect the beam pointing drastically, especially for those ground stations located away from either subsatellite longitude or autotrack boresight. Future spacecraft systems should take into account yaw estimation as a primary concern in their design goals.
- The ACTS MBA performance was found to be well within the expected range, and the transmit and receive beam optimization procedures were successfully executed. On-orbit MBA measurements have shown that all design limits have been met and that good pointing performance has been achieved.

Lewis contacts: Dr. Roberto J. Acosta, (216) 433-6640, and David L. Wright, (216) 433-3530
Headquarters program office: OSAT

Space Experiments

Radiative Ignition and the Transition to Flame Spread Investigated in the Japan Microgravity Center's 10-sec Drop Shaft

In space, many things react differently because of the lack of gravity. One area of concern is how fire ignites and reacts in a microgravity environment. Fires in spacecraft pose significant dangers to the crew: toxic products could quickly poison the atmosphere and be difficult to remove, large-scale production of gases at high temperatures could overpressurize the spacecraft, and extinguishing systems might damage the electrical systems. Although momentary ignitions due to electrical short-circuiting or overheating might be an acceptable and recoverable hazard, a transition from an ignition to large-scale fire growth is an unacceptable risk. To stop this transition, the environmental conditions that allow transition must be avoided. These conditions are not yet well known because, on Earth, buoyant flow removes the products of combustion

(carbon dioxide and water vapor) and brings in fresh oxygen for the flame. In the microgravity environment aboard spacecraft, the predominant flows are the very slow air ventilation flows rather than buoyancy.

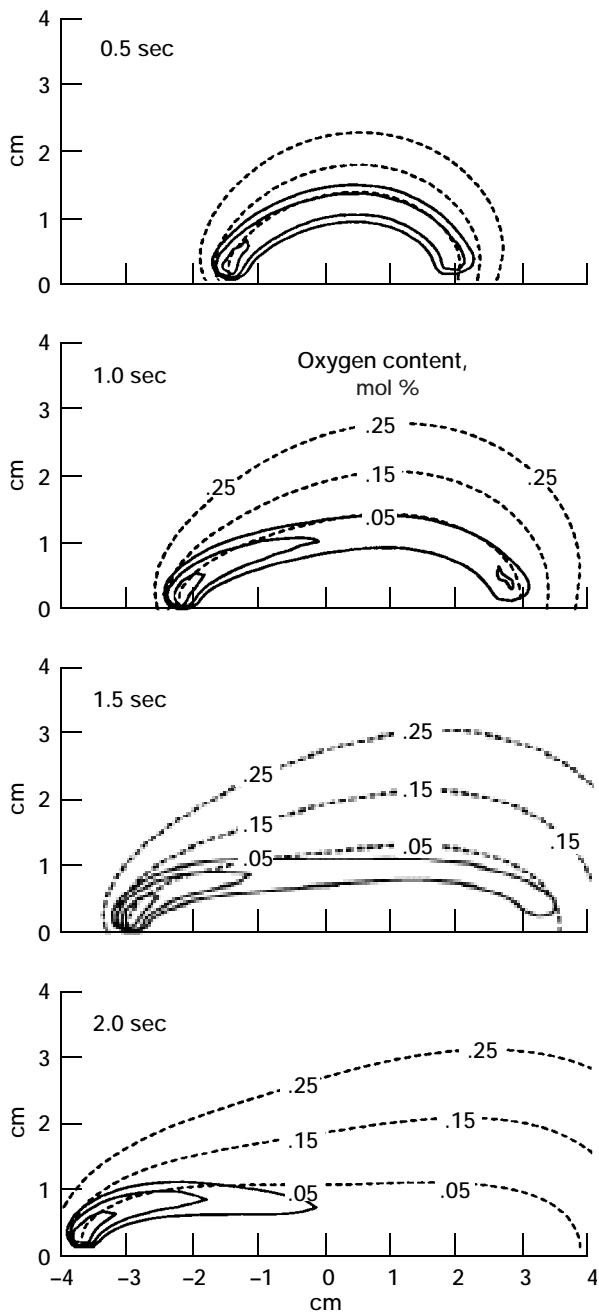
The Radiative Ignition and Transition to Spread Investigation (RITSI) is a shuttle middeck Glovebox combustion experiment developed by the NASA Lewis Research Center, the National Institute for Standards and Technology (NIST), and Aerospace Design and Fabrication (ADF). It is scheduled to fly on the third United States Microgravity Payload (USMP-3) mission in February 1996. The objective of RITSI is to experimentally study radiative ignition and the subsequent transition to flame spread in low gravity in the presence of very low speed air flows in two- and three-dimensional configurations.

Toward this objective, a unique collaboration between NASA, NIST, and the University of Hokkaido was established to conduct 15 science and engineering tests in Japan's 10-sec drop shaft. For these tests, the RITSI engineering hardware was mounted in a sealed chamber with a variable oxygen atmosphere. Ashless filter paper was ignited during each drop by a tungsten-halogen heat lamp focused on a small spot in the center of the paper. The flame spread outward from that point. Data recorded included fan voltage (a measure of air flow), radiant heater voltage (a measure of radiative ignition energy), and surface temperatures (measured by up to three surface thermocouples) during ignition and flame spread. In addition, color video and 35-mm film pictures were taken during the drop.

Data from these tests are still being reduced and analyzed, but some observations can be reported. Radiative ignition in low gravity was successfully achieved for the first time. Preliminary findings indicate that the spread of flames upwind into fresh oxygen was enhanced by the very low speed flows, as was anticipated from model predictions and previous experimental results (refs. 1 and 2). Downwind flame spread was less robust because of the presence of the upwind flame, which vitiates the atmosphere for the downwind flame, in agreement with modeling results, as shown in the figure (ref. 1).

References

1. McGrattan, K.B., et al.: Effects of Ignition and Wind on the Transition to Flame Spread in a Microgravity Environment. Accepted for publication in *Combustion and Flame*, 1996.
2. Olson, S.L.: Mechanisms of Microgravity Flame Spread Over a Thin Solid Fuel: Oxygen and Opposed Flow Effects. *Combust. Sci. Tech.*, vol. 76, 1991, pp. 233-249.



Flame transition to spread after radiative ignition. Gas flow enters from the left. Solid lines are reaction contours, which can be compared to flame shape; and dashed lines are oxygen concentration contours. Note the upstream flame (to the left) is almost immediately more vigorous and that the downstream flame dies away because of the oxygen "shadow" cast by the upstream flame.

Find out more about RITSI and other Lewis microgravity experiments on the World Wide Web:

<http://zeta.lerc.nasa.gov/expr/ritsi.htm>

<http://microgravity.msad.hq.nasa.gov/cScienceProg/subdisc/combust.html>

<http://zeta.lerc.nasa.gov/sedhome.htm>

<http://www.lerc.nasa.gov/WWW/MCFEP/>

Lewis contact: Sandra L. Olson, (216) 433-2859

Headquarters program office: OLMSA (MSAD)

Soot Imaging and Measurement

Soot, sometimes referred to as smoke, is made up primarily of the carbon particles generated by most combustion processes. For example, large quantities of soot can be seen issuing from the exhaust pipes of diesel-powered vehicles. Heated soot also is responsible for the warm orange color of candle flames, though that soot is generally consumed before it can exit the flame. Research has suggested that heavy atmospheric soot concentrations aggravate conditions such as pneumonia and asthma, causing many deaths each year.

To understand the formation and oxidation of soot, NASA Lewis Research Center scientists, together with several university investigators, are investigating the properties of soot generated in reduced gravity, where the absence of buoyancy allows more time for the particles to grow. The increased time allows researchers to better study the life cycle of these particles, with the hope that increased understanding will lead to better control strategies. To quantify the amount of soot present in a flame, Lewis scientists developed a unique imaging technique that provides quantitative and qualitative soot data over a large field of view. There is significant improvement over the single-point methods normally used.

The technique is shown in the sketch, where light from a laser is expanded with a microscope objective,

rendered parallel, and passed through a flame where soot particles reduce the amount of light transmitted to the camera. A filter only allows light at the wavelength of the laser to pass to the camera, preventing any extraneous signals. When images of the laser light with and without the flame are compared, a quantitative map of the soot concentration is produced. In addition to that data, a qualitative image of the soot in the flame is also generated, an example of which is displayed in the photo. This technique has the potential to be adapted to real-time process control in industrial powerplants.

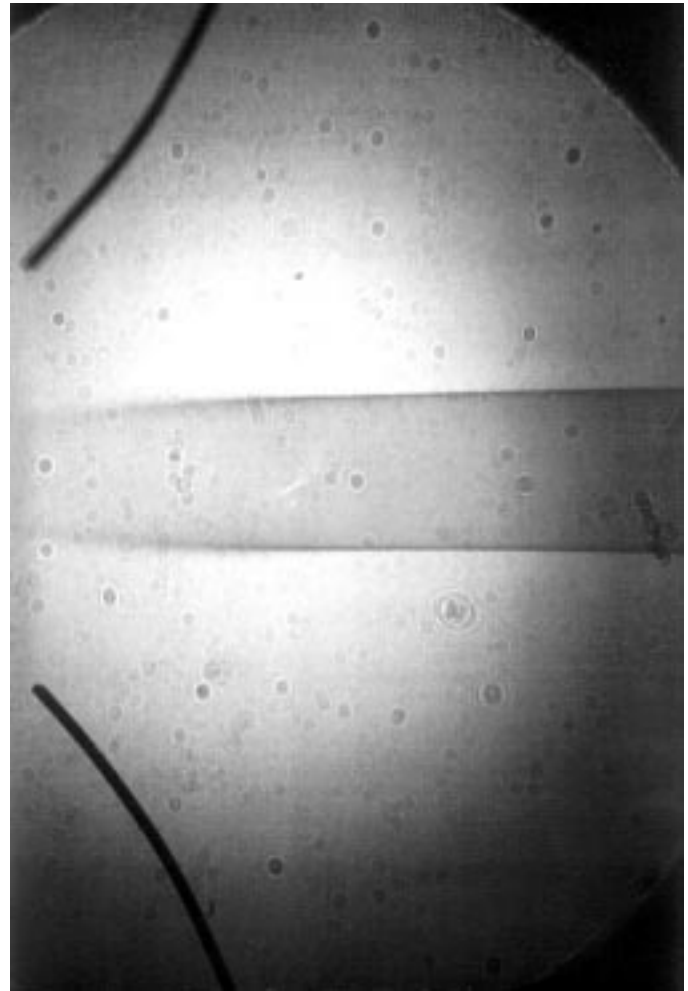
To find out more about Lewis' microgravity experiments, visit our sites on the World Wide Web:

<http://microgravity.msad.hq.nasa.gov/cScienceProg/subdisc/combust.html>

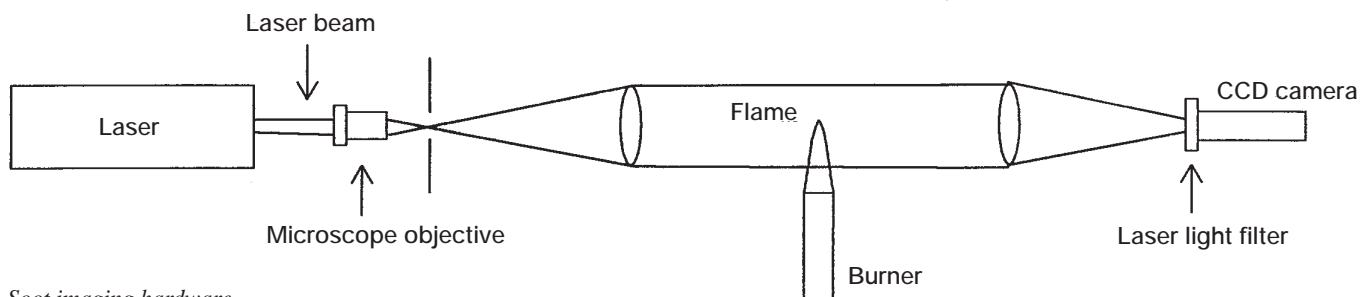
<http://zeta.lerc.nasa.gov/sedhome.htm>

<http://www.lerc.nasa.gov/WWW/MCFEP/>

Lewis contact: Paul S. Greenberg, (216) 433-3621
Headquarters program office: OLMSA (MSAD)



Soot image from a gas-jet diffusion flame.

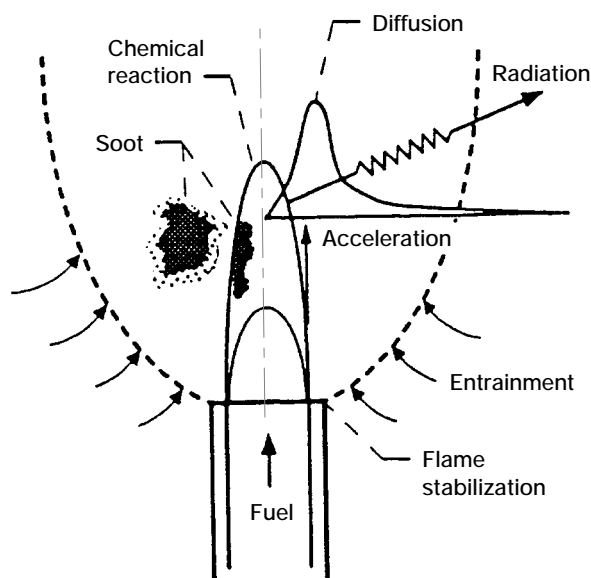


Soot imaging hardware.

Microgravity Turbulent Gas-Jet Diffusion Flames

A gas-jet diffusion flame is similar to the flame on a Bunsen burner, where a gaseous fuel (e.g., propane) flows from a nozzle into an oxygen-containing atmosphere (e.g., air). The difference is that a Bunsen burner allows for (partial) premixing of the fuel and the air, whereas a diffusion flame is not premixed and gets its oxygen (principally) by diffusion from the atmosphere around the flame. Simple gas-jet diffusion flames are often used for combustion studies because they embody the mechanisms operating in accidental fires and in practical combustion systems (see the sketch on the left side of the figure).

However, most practical combustion is turbulent (i.e., with random flow vortices), which enhances the fuel/air mixing. These turbulent flames are not well understood because their random and transient nature complicates analysis. Normal gravity studies of turbulence in gas-jet diffusion flames can be impeded by buoyancy-induced instabilities. These gravity-caused instabilities, which are evident in the flickering of a candle flame in normal gravity, interfere with the study of turbulent gas-jet diffusion flames. By conducting experiments in microgravity, where buoyant instabilities are avoided, we at the NASA Lewis Research Center hope to improve our understanding of turbulent combustion. Ultimately, this could lead to improvements in combustor design, yielding higher efficiency and lower pollutant emissions.

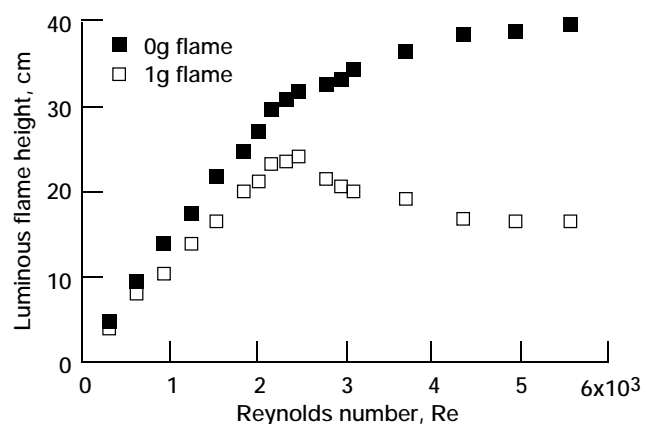


Left: Schematic of the structure of a gas-jet diffusion flame. Right: Measured flame height as a function of injection Reynolds number for propane-air flames in microgravity and normal gravity.

Gas-jet diffusion flames are often researched as model flames, because they embody mechanisms operating in both accidental fires and practical combustion systems (see the first figure). In normal gravity laboratory research, buoyant air flows, which are often negligible in practical situations, dominate the heat and mass transfer processes. Microgravity research studies, however, are not constrained by buoyant air flows, and new, unique information on the behavior of gas-jet diffusion flames has been obtained.

The graph shows the observed flame height as a function of the fuel-injection Reynolds number (which is related to the fuel flow rate for a given injection nozzle size) for flames in both normal gravity and microgravity. Below a Reynolds number of approximately 2000, both flames exhibit laminar characteristics, and the flame height increases with an increase in the Reynolds number. Because of the lack of buoyant convection, which enhances combustion in normal gravity, the microgravity flames are larger.

In the Reynolds number range of 2000 to 3000, the flames undergo a transition process from laminar to turbulent burning. In normal gravity, this process is characterized by a decrease in the flame height and the appearance of instabilities (flame disturbances) that first appear near the flame tip but begin to originate at lower locations with increases in Reynolds number. In



microgravity, the flame height continues to increase, although at a lower rate than in the laminar regime. In contrast to the normal gravity case, flame disturbances in microgravity are first observed near the base of the flame instead of near the tip. Flame instabilities arise primarily at locations of large velocity gradients. In normal gravity, because of buoyant acceleration, velocity gradients are maximum near the flame tip so instabilities are first observed there. In microgravity, velocity gradients are maximum near the base of the flame, and that is where disturbances are first observed.

Beyond a Reynolds number of approximately 3000, turbulent conditions prevail. In normal gravity, in the turbulent regime, the flame height remains constant with the Reynolds number until close to flame blowoff. This feature is explained in terms of a balance between turbulent transport processes and jet momentum. However, in microgravity, the flame height continues to increase with Reynolds number, indicating that jet momentum dominates turbulent transport in this case.

The normal gravity behavior shown in the second figure is similar to that appearing in virtually all combustion science textbooks. It was anticipated that buoyant effects in the turbulent regime would be small and that the behavior of microgravity and normal gravity flames would be identical. This is obviously not the case. We anticipate that microgravity data, which give better insights into the controlling mechanisms for gas-jet diffusion flames, will find its way into textbooks of the future.

Learn more about microgravity on the World Wide Web:

NASA Headquarters:

<http://microgravity.msad.hq.nasa.gov/>

NASA Lewis Research Center:

<http://zeta.lerc.nasa.gov/>

Lewis contact: Dennis P. Stoker, (216) 433-2166

Headquarters program office: OLMSA (MSAD)

Spread Across Liquids: The World's First Microgravity Combustion Experiment on a Sounding Rocket

The Spread Across Liquids (SAL) experiment characterizes how flames spread over liquid pools in a low-gravity environment in comparison to test data at Earth's gravity and with numerical models. The modeling and experimental data provide a more complete understanding of flame spread, an area of textbook interest, and add to our knowledge about on-orbit and Earthbound fire behavior and fire hazards. The experiment was performed on a sounding rocket to obtain the necessary microgravity period. Such crewless sounding rockets provide a comparatively inexpensive means to fly very complex, and potentially hazardous, experiments and perform reflights at a very low additional cost. SAL was the first sounding-rocket-based, microgravity combustion experiment in the world.

It was expected that gravity would affect ignition susceptibility and flame spread through buoyant convection in both the liquid pool and the gas above the pool. Prior to these sounding rocket tests, however, it was not clear whether the fuel would ignite readily and whether a flame would be sustained in microgravity. It also was not clear whether the flame spread rate would be faster or slower than in Earth's gravity.

The SAL experiment flew twice in the past year, and both flights were highly successful, revealing new flame-spread behavior attributable to the absence of gravitational effects and also proving the feasibility in microgravity of several novel, advanced diagnostics and fluid management technologies. The diagnostic instruments, which performed flawlessly, included four flame-imaging cameras, two side-viewing particle image velocimetry (PIV) systems that recorded liquid fuel-flow patterns, an infrared camera that determined the liquid surface temperature field ahead of the flame, and a rainbow schlieren deflectometer that imaged the subsurface-liquid temperature gradients.

In Earth's gravity (1g), flames spread in a regularly pulsating manner. In these microgravity (μ g) tests, however, flames spread very slowly and uniformly across the entire length of the pool (see the graph). Unlike flames in 1g, the microgravity flame was completely blue (soot-free), without any noticeable plume or wavering. (See the comparative photos of a flame in 1g and in microgravity at the bottom of the next page.) The diagnostic instruments showed a large liquid-phase vortical flow extending deep into

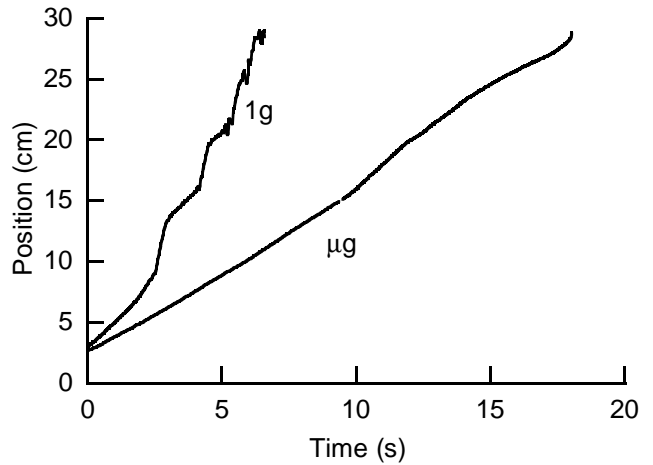
the pool ahead of the flame (see the top photo for the PIV liquid velocity field), very different from the stratified liquid flow that occurs in 1g. These observations showed conclusively that (1) flame spread can persist in microgravity, (2) it is substantially different from that at Earth's gravity, and (3) liquid buoyancy plays a major role in flame spread over flammable liquids. For the past two to three decades prior to these tests, research literature had debated this last point. The acquired data will allow detailed verification of the numerical models in areas such as liquid-phase velocity field (top photo) and temperatures, as well as the flame-spread rate.

The peer-reviewed SAL experiment was conceived and developed by the NASA Lewis Research Center in collaboration with Case Western Reserve University and Aerospace Design & Fabrication (ADF). Experiments are being modeled by the University of California at Irvine.

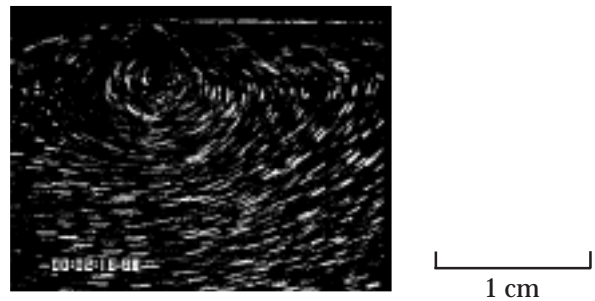
Find out more about SAL and other Lewis microgravity experiments on the World Wide Web:

- <http://zeta.lerc.nasa.gov/expr/sal.htm>
- <http://microgravity.msad.hq.nasa.gov/cScienceProg/subdisc/combust.html>
- <http://zeta.lerc.nasa.gov/sedhome.htm>
- <http://www.lerc.nasa.gov/WWW/MCFEP/>

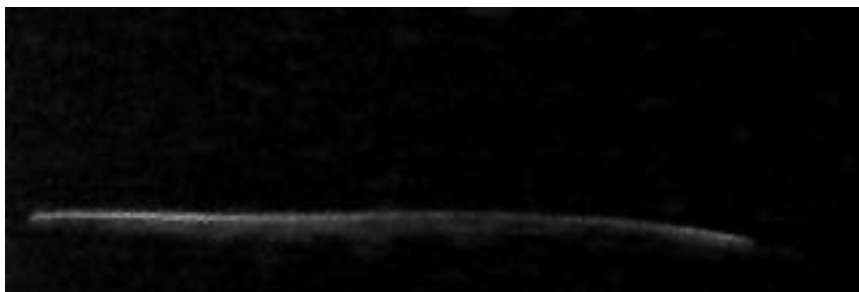
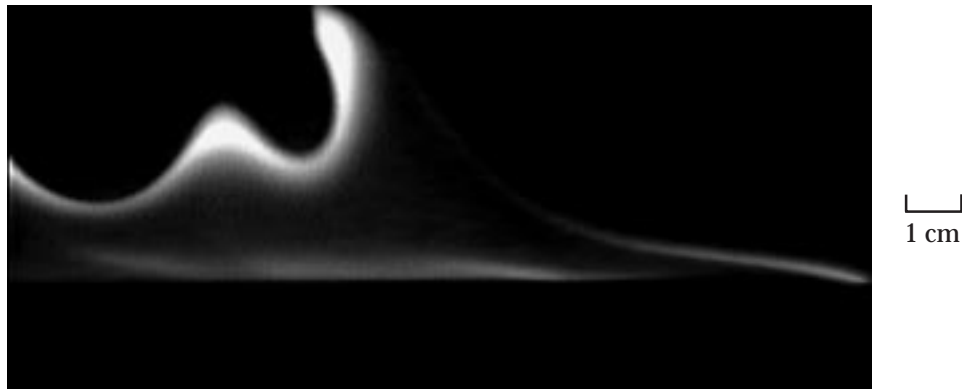
Lewis contact: Dr. Howard D. Ross, (216) 433-2562
Headquarters program office: OLMSA (MSAD)



Flame position versus time for a 2.5-cm-deep butanol pool in an opposed airflow of 30 cm/sec.



Vortical liquid phase velocity field below the flame leading edge.



Top: Flame spread at 1g (normal gravity). Bottom: Flame spread in microgravity.

Two U.S. Experiments to Fly Aboard European Spacelab Facility in 1996

Space provides researchers a way to study the behavior of fluids when the forces of gravity are removed. The studies described here involve international cooperative research projects to study various aspects of fluid behavior in a microgravity environment. These projects utilize the Bubble Droplet Particle Unit (BDPU), which was built by the European Space Agency's (ESA) Technology Center in Noordwijk, The Netherlands. This Spacelab-based multiuser facility flew for the first time in July 1994 on the second International Microgravity Laboratory (IML-2). It is scheduled for reflight on the Life and Microgravity Sciences (LMS) mission in June 1996. This experiment hardware was designed primarily to conduct fluid physics experiments with transparent fluids. LMS will fly both European and U.S. investigations, including experiments defined by Professor R.S. Subramanian of Clarkson University in Potsdam, New York, and Professor S.A. Saville of Princeton University, Princeton, New Jersey.

Professor Subramanian's experiment (a reflight from IML-2), *Thermocapillary Migrations and Interactions of Bubbles and Drops*, will study the bubble's (or droplet's) velocity and shape as it travels (or migrates) through another fluid that has a linear temperature distribution. During the experiment, local temperature gradients around the bubble will impose a surface tension gradient on the bubble interface and produce motion in the interface film. This motion will cause a jetting action that will propel the bubble toward the relatively hotter areas of the surrounding fluid. The LMS experiments will emphasize bubble (and droplet) pair interactions and different fluid combinations to expand the knowledge gained from the IML-2 experiment. The microgravity environment will isolate the thermocapillary phenomena from the normally dominant effects of buoyancy and natural convection on Earth. Results from these types of experiments have applications on Earth in ceramic and glass formation, as well as in metal and alloy solidification. Better understanding of these thermocapillary effects can lead, as well, to superior bubble management techniques for space-based crew life-support systems.

Professor Saville's experiment, *Studies in Electrohydrodynamics*, looks at the stabilizing effects of high-voltage electric fields on liquid columns. Liquid columns of a given length-to-diameter ratio will be established in microgravity and exposed to various electric field strengths. In the absence of an electric field, these columns will deform into increasingly amphoric shapes

and eventually pinch off. The main scientific points of interest to be studied when the electric field is applied will be to determine what minimum electric field strengths are needed to maintain cylindrical columns and what minimum field strengths are required to prevent pinch off. Liquid columns in gas, as well as columns in other immiscible liquids, will be studied.

Long-term microgravity is particularly needed to study liquid columns that are surrounded by a gas. The liquid-in-liquid cases will be compared with similar ground-based experiments. These ground-based tests were done in a simulated low gravity for which the two liquids were density matched. Liquid-gas cases have the advantage of being significantly easier to analyze because of simpler boundary conditions. Applications of improved models and theory from these experiments are expected in processes that involve liquid columns. These processes may, then, be improved through the use of electrohydrodynamics effects. Examples of these processes include fiber spinning, crystal growth, and liquid jets (e.g., for printers).

The Bubble Droplet Particle Unit facility and its various principal-investigator-specific test containers were designed and constructed under the European Space Agency's Technology Center management by various European-based contractors. NASA Lewis Research Center's function is to assist in the design and flight operations of the two U.S. Bubble Droplet Particle Unit experiments.

Find out more about Lewis microgravity experiments on the World Wide Web:

<http://zeta.lerc.nasa.gov/sedhome.htm>
<http://liftoff.msfc.nasa.gov/spacelab/lms>
<http://www.lerc.nasa.gov/WWW/MCFEP/>

Lewis contact: Myron E. Hill, (216) 433-5279
Headquarters program office: OLMSA (MSAD)

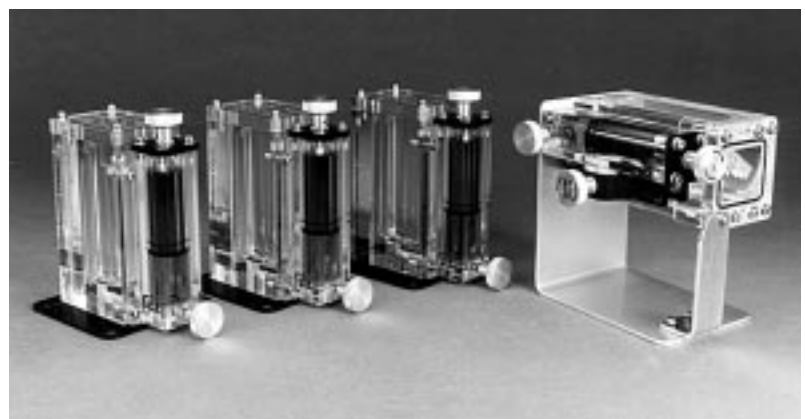
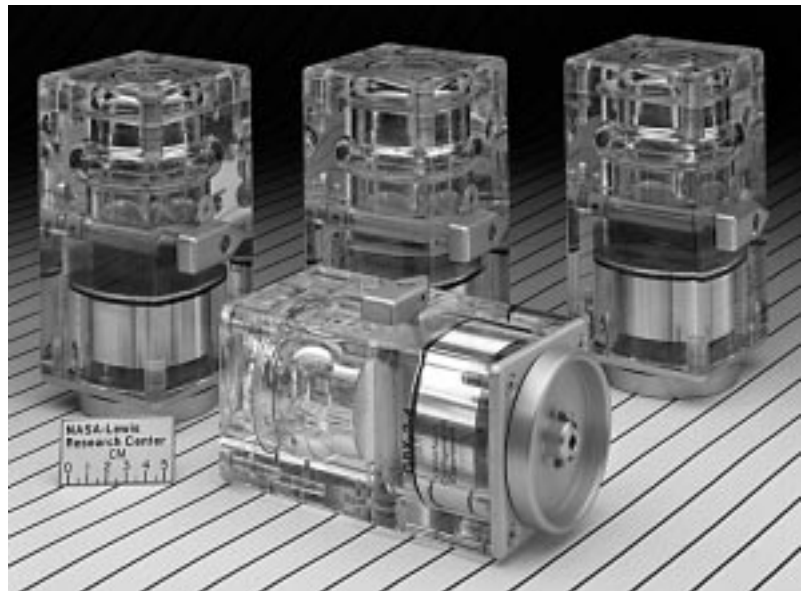
Interface Configuration Experiments (ICE) Explore the Effects of Microgravity on Fluids

The Interface Configuration Experiment (ICE) is actually a series of experiments that explore the striking behavior of liquid-vapor interfaces (i.e., fluid surfaces) in a low-gravity environment under which major shifts in liquid position can arise from small changes in container shape or contact angle. Although these experiments are designed to test current mathematical theory, there are numerous practical applications that could result from these studies. When designing fluid management systems for space-based operations, it is important to be able to predict the locations and configurations that fluids will assume in containers under low-gravity conditions. The increased ability to predict, and hence control, fluid interfaces is vital to systems and/or processes where capillary forces play a significant role both in space and on the Earth. Some of these applications are in general coating processes (paints, pesticides, printing, etc.), fluid transport in porous media (ground water flows, oil recovery, etc.), liquid propellant systems in space (liquid fuel and oxygen), capillary-pumped loops and heat pipes, and space-based life-support systems.

In space, almost every fluid system is affected, if not dominated, by capillarity. Knowledge of the liquid-vapor interface behavior, and in particular the interface shape from which any analysis must begin, is required as a foundation to predict how these fluids will react in microgravity and on Earth. With such knowledge, system designs can be optimized, thereby decreasing costs and complexity, while increasing performance and reliability. ICE has increased, and will continue to increase this knowledge, as it probes the specific peculiarities of current theory upon which our current understanding of these effects is based.

Several versions of ICE were conducted in NASA Lewis Research Center's drop towers and on the space shuttle during the first and second United States Microgravity Laboratory missions (USML-1 and USML-2). Additional tests are planned for the space shuttle and for the Russian Mir space station. These studies will focus on interfacial problems concerning surface existence, uniqueness, configuration, stability, and flow characteristics.

Results to date have clearly demonstrated the need for experimental data regarding the behavior of large-scale capillary surfaces in containers of irregular cross-section. For example, ICE on USML-1 revealed the existence of a globally stable, asymmetric interface configuration in a rotationally symmetric container. For many applications, the possibility of encountering such surfaces must be considered because they may be detrimental to the operation of a system in space. A result from the USML-2 mission revealed that fluid locations after long-duration exposures (days) to low gravity can be significantly different than for short durations (hours). This fact raises concerns both for designers of space systems and for scientists in that true equilibrium for certain capillary surfaces may take days, even weeks, to be achieved.



Top: ICE flight hardware ("exotic" vessels) for USML-1. Bottom: ICE flight cells for USML-2: proboscis (three) and wedge vessels (one).

These experiments were conceived and developed by Paul Concus of Lawrence Berkeley Laboratory and the University of California at Berkeley, Robert Finn of Stanford University, and Mark Weislogel of the NASA Lewis Research Center in Cleveland, Ohio. The hardware was designed and built at Lewis.

To find out more about Lewis' microgravity experiments, visit our sites on the World Wide Web:

<http://microgravity.msad.hq.nasa.gov/cScienceProg/subdisc/fluids.html>

<http://zeta.lerc.nasa.gov/>

Lewis contact: Mark M. Weislogel, (216) 433-2877

Headquarters program office: OLMSA (MSAD)

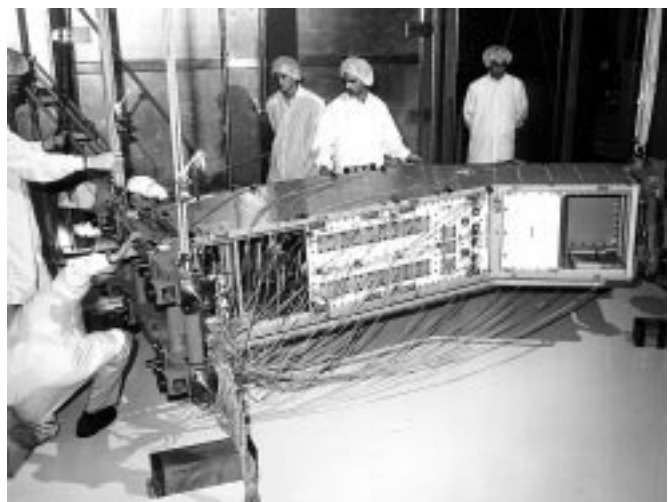
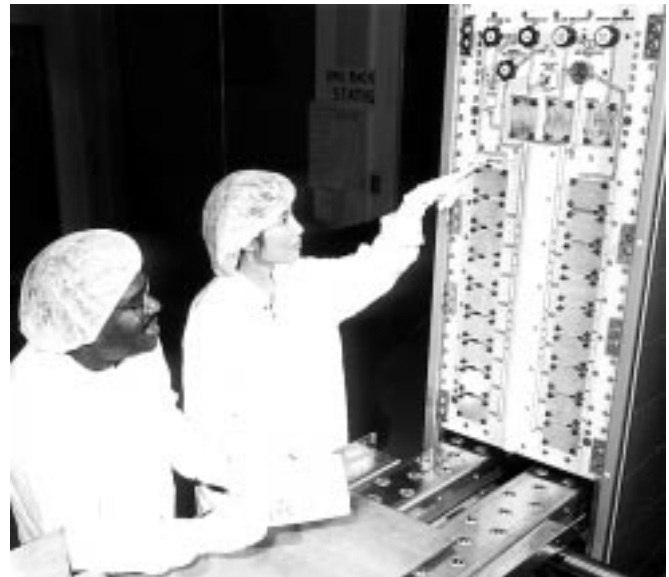
Combustion Module 1: Spacelab Racks Integrated at the Lewis Research Center for the First Time

The Combustion Module-1 (CM-1), NASA's largest (over 1800 lb) and one of the most sophisticated combustion experiments ever to fly on the Spacelab, will be carried on the first Microgravity Science Laboratory (MSL-1) mission aboard the space shuttle flight STS-84 in April 1997. The CM-1 project is a stepping stone to the space station era, because the hardware can support multiple investigators on the same mission and can be integrated at user locations and shipped to the launch site. CM-1 is being developed to accommodate microgravity combustion experiments that are designed to help explain and predict the behavior of combustion processes. Although the two principal investigators for CM-1 are both studying combustion processes, their investigations are quite different. Professor Paul D. Ronney of the University of Southern California will examine the Structures of Flame Balls at Low Lewis Numbers (SOFBALL), in which a variety of fuel-lean gaseous mixtures fill the combustion chamber and are ignited. Professor Gerard M. Faeth of the University of Michigan will investigate Laminar Soot Processes (LSP) by studying the key properties of burning gas jets of fuel, employing different fuels and nozzle sizes.

CM-1's ability to be integrated at user locations is critical in meeting the aggressive schedule for flight on the first Microgravity Science Laboratory. It was necessary to assemble the various hardware packages into the Spacelab racks at the NASA Lewis Research Center in order to fit a shortened development schedule. The normal procedure is to ship the packages

separately to the Kennedy Space Center and integrate the packages into the Spacelab racks there. The complexity of the hardware and the requirement to deliver the hardware nearly 18 months quicker than normal for a project of this size led to the decision for the integration process to take place at Lewis.

Lewis management made other decisions to meet the launch date. One of these decisions was to do the design, development, and fabrication in house and to use the resources available at Lewis and the Greater Cleveland area. To date, nearly 40 fabrication shops across Northeastern Ohio have contributed to making the project a reality. The strategy is working, because the project is still on schedule after 2 years.



Top: Lewis engineers examine Spacelab rack after package installation. Bottom: Personnel from Lewis, Marshall, and Kennedy prepare for modal test of the CM-1 single rack at the NASA Lewis Research Center.

Another factor in keeping the project on schedule has been the teaming relationships that have developed among personnel from several NASA centers: Headquarters, Marshall Space Flight Center, Kennedy Space Center, Johnson Space Center, and Lewis Research Center. Getting a payload of this size and complexity built and delivered has involved many people from many organizations, all playing their parts and keeping the project moving toward its launch date. The CM-1 project has proved that these new ways of doing business are achievable and that the many organizations across NASA are already changing to make them a reality.

To find out more about Lewis' microgravity experiments, visit our sites on the World Wide Web:

<http://microgravity.msad.hq.nasa.gov/cScienceProg/subdisc/combust.html>

<http://zeta.lerc.nasa.gov/sedhome.htm>

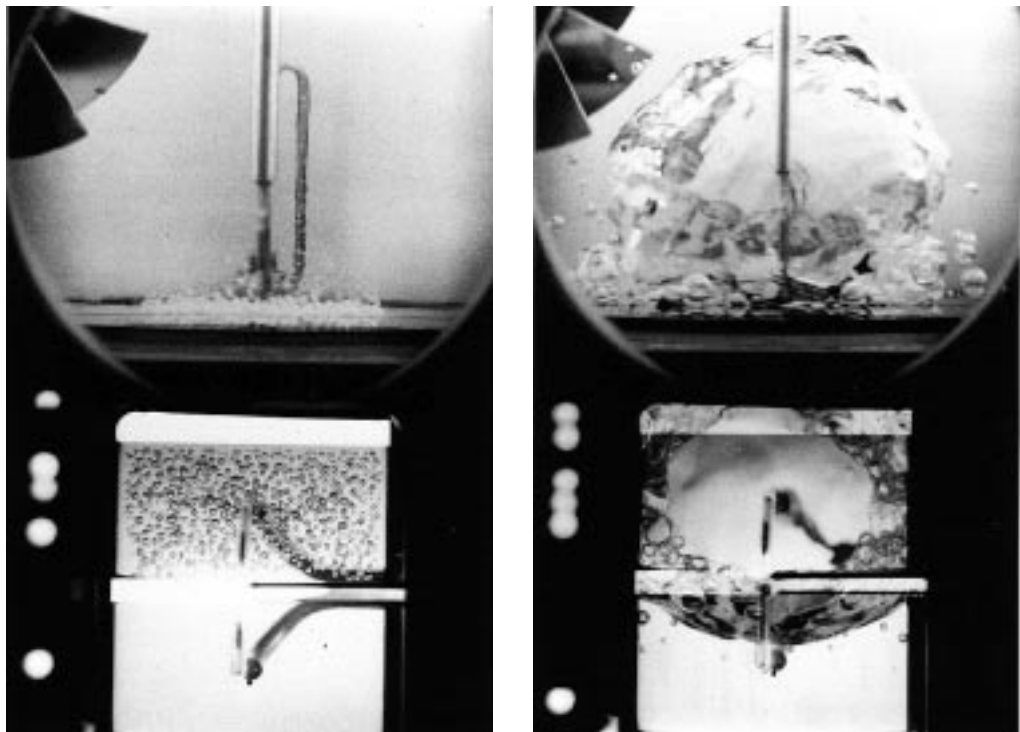
<http://www.lerc.nasa.gov/WWW/MCFEP/>

Lewis contact: Donald F. Martin, (216) 433-8124
Headquarters program office: OLMSA (MSAD)

Pool Boiling Experiment Has Successful Flights

The Pool Boiling Experiment (PBE) is designed to improve understanding of the fundamental mechanisms that constitute nucleate pool boiling. Nucleate pool boiling is a process wherein a stagnant pool of liquid is in contact with a surface that can supply heat to the liquid. If the liquid absorbs enough heat, a vapor bubble can be formed. This process occurs when a pot of water boils. On Earth, gravity tends to remove the vapor bubble from the heating surface because it is dominated by buoyant convection. In the orbiting space shuttle, however, buoyant convection has much less of an effect because the forces of gravity are very small. The Pool Boiling Experiment was initiated to provide insight into this nucleate boiling process, which has many Earthbound applications, such as steam-generation power plants, petroleum, and other chemical plants. Also, by using the test fluid R-113, the Pool Boiling Experiment can provide some basic understanding of the boiling behavior of cryogenic fluids without the large cost of an experiment using an actual cryogen.

The experiment was conceived by Herman Merte of the University of Michigan, was developed by the NASA Lewis Research Center, and is supported by NASA Headquarters' Microgravity Science and Applications



Pool Boiling Experiment.

Division. The pool boiling prototype system, which was initially flown on STS-47 in September 1992, acquired a considerable amount of scientific data. The expected boiling pattern was observed in all high-heat-flux cases, but a different pattern was observed in the low-heat-flux cases. These differences appear to be caused by the rewetting of the heater surface. The film data indicate that the saturated cases experienced a more activated boiling process (more vapor than expected was generated).

Some minor modifications were made in the timing sequences in the test matrix for the next space shuttle flight, STS-57. This was done to increase the probability of observing the initial dynamic vapor bubble growth while the camera was running at the higher speed and to observe the influence of a stirrer on the active boiling process. Observations included the stirrer's effect on the dryout area, the mean heat transfer coefficient, and the nucleate boiling heat transfer coefficient. This latter quantity, which was not originally foreseen as an output from the measurements, resulted from observing the relationships between the mean heater surface temperature and the fractional heater surface dryout area over the long microgravity times available on the shuttle.

Currently, results appear to indicate the potential for quasi-steady nucleate pool boiling in long-term microgravity, with certain combinations of levels of heat flux and bulk liquid subcooling. These were the first experiments of nucleate boiling obtained for long periods of microgravity, and the matrix test conditions were selected in part to cover the reasonably broad range of parameters. Hardware is now being modified for two reflights of this apparatus. Higher subcoolings will be explored in the first flight and lower heat flux values will be studied in the second flight. It is expected that "explosive" bubble growth will occur at low heat flux values.

To find out more about the Pool Boiling Experiment and other Lewis microgravity experiments, visit our sites on the World Wide Web:

<http://zeta.lerc.nasa.gov/expr/pbeinfo.htm>

<http://microgravity.msad.hq.nasa.gov/cScienceProg/subdisc/fluids.html>

<http://zeta.lerc.nasa.gov/>

**Lewis contact: Angel M. Otero, (216) 433-3878
Headquarters program office: OLMSA (MSAD)**

Successful Isothermal Dendritic Growth Experiment (IDGE) Proves Current Theories of Dendritic Solidification are Flawed

The scientific objective of the Isothermal Dendritic Growth Experiment (IDGE) is to test fundamental assumptions about dendritic solidification of molten materials. "Dendrites"—from the ancient Greek word for tree—are tiny branching structures that form inside molten metal alloys when they solidify during manufacturing. The size, shape, and orientation of the dendrites have a major effect on the strength, ductility (ability to be molded or shaped), and usefulness of an alloy. Nearly all of the cast metal alloys used in everyday products (such as automobiles and airplanes) are composed of thousands to millions of tiny dendrites.

Gravity, present on Earth, causes convection currents in molten alloys that disturb dendritic solidification and make its precise study impossible. In space, gravity is negated by the orbiting of the space shuttle. Consequently, IDGE (which was conducted on the space shuttle) gathered the first precise data regarding undisturbed dendritic solidification.

IDGE is a microgravity materials science experiment that uses an apparatus which was designed, built, tested, and operated by people from the NASA Lewis Research Center. This experiment was conceived by the principal investigator, Professor Martin E. Glicksman, from Rensselaer Polytechnic Institute in Troy, New York. The experiment was a team effort of Lewis civil servants, contractors from Aerospace Design & Fabrication Inc. (ADF), and personnel at Rensselaer.

IDGE's first of three planned flights, as part of the United States Microgravity Payload (USMP) series, was highly successful. In fact, by one important measure of the data collected, it was 370-percent successful. This extraordinary success was possible because IDGE is a teleoperable experiment (scientists on the ground can monitor progress and send up commands to alter IDGE programming). During the first flight, dendritic solidification behaved unexpectedly—Experiments could be completed more quickly! Teleoperation, involving some 8000 discrete commands over 9 days, permitted the IDGE team operate the experiment far outside its programmed limits, acquiring much more data than was planned.

IDGE had been planned to produce 20 dendritic growths after supercoolings from 0.1 to 1.0 K. Instead, 58 dendrites were solidified at over 20 different supercoolings, ranging from about 0.05 to 1.93 K. Supercooling is the term used to describe the condition

in which a dendrite solidifies at a temperature below its normal freezing point. The data consisted of over 400 photographs and over 800 television images of dendrites solidifying in space, along with associated supercooling, pressure, and acceleration data. Photographs were possible because the test material was transparent succinonitrile, which mimics the behavior of iron when it solidifies.

Dendrite tip radii, tip solidification speed, and volumetric solidification rates were determined from the space and Earth data. These were compared with predictions made by theorists over the last 50 years—predictions that are currently used for metal production on Earth. The results indicate that the theories, although sound in some respects, are flawed. Corrected theories based on IDGE data should someday improve industrial metal production here on Earth.

IDGE is scheduled to fly aboard the Space Shuttle Columbia, STS-75, for its second flight. The IDGE apparatus was modified to obtain data that will complement the information obtained during the first flight. Until recently, dendrite tips were believed to be parabolas of revolution. Information gathered by the IDGE apparatus proved this assumption to be incorrect. The goal of the second flight of IDGE is to collect data that will definitively determine the three-dimensional shape of the dendrite tip as a function of supercooling.



Members of the Lewis-based IDGE team assemble the flight unit. One of the IDGE 35-mm cameras and the Space Acceleration Measurement System (SAMS) sensor head are visible. IDGE is fully operable by remote control from Earth—this feature contributed to its remarkable success on STS-62.

This will lead to further enhancements of dendritic solidification theories.

To test the universality of advanced solidification theories, a third flight in 1997 will provide solidification data for a different test material. IDGE data will provide a benchmark to test theoretical developments for decades to come.

Find out more about IDGE and other Lewis microgravity experiments on the World Wide Web:

<http://www.rpi.edu/locker/56/000756/index.html>
<http://zeta.lerc.nasa.gov/>

Lewis contact: Diane C. Malarik, (216) 433-3203
Headquarters program office: OLMSA (MSAD)

Microgravity Smoldering Combustion Takes Flight

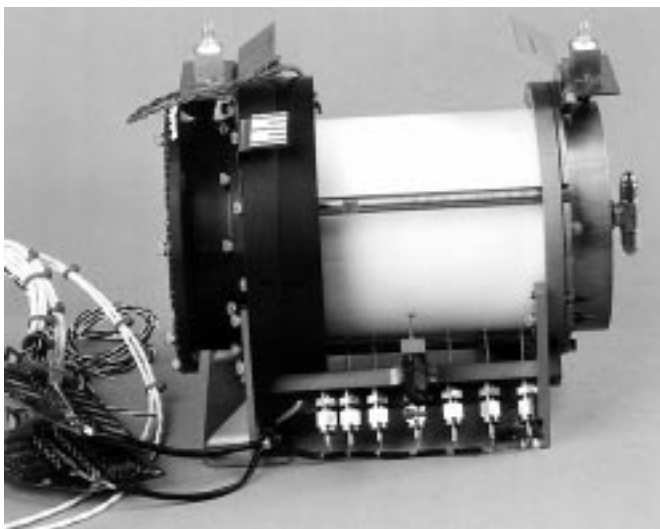
The Microgravity Smoldering Combustion (MSC) experiment lifted off aboard the Space Shuttle Endeavour in September 1995 on the STS-69 mission. This experiment is part of a series of studies focused on the smolder characteristics of porous, combustible materials in a microgravity environment. Smoldering is a nonflaming form of combustion that takes place in the interior of combustible materials. Common examples of smoldering are nonflaming embers, charcoal briquettes, and cigarettes.

The objective of the study is to provide a better understanding of the controlling mechanisms of smoldering, both in microgravity and Earth gravity. As with other forms of combustion, gravity affects the availability of air and the transport of heat, and therefore, the rate of combustion. Results of the microgravity experiments will be compared with identical experiments carried out in Earth's gravity. They also will be used to verify present theories of smoldering combustion and will provide new insights into the process of smoldering combustion, enhancing our fundamental understanding of this frequently encountered combustion process and guiding improvement in fire safety practices.

In the Microgravity Smoldering Combustion experiment during STS-69, two tests were conducted to investigate the spread of smolder along a sample of polyurethane foam (120-mm diameter by 140-mm long) under two experimental conditions: (1) in a still environment of 35 percent oxygen/65 percent nitrogen and (2) in an opposing air flow (1-mm/sec flowing through the foam in the direction opposite to that of the smolder propagation). Each combustion test was conducted in a 20-liter sealed chamber that was instrumented to obtain pressure, temperature, and video data. The flight data have been obtained and are being analyzed by the principal investigator.

Polyurethane foam was selected as the fuel sample because it is representative of materials commonly used on Earth and in space-based facilities. The environmental conditions are part of a matrix of planned experiments in a nonconvective environment with oxygen concentrations higher than in air and in a convective environment with velocities similar to those that can be expected from the ventilating system in space facilities.

The experiment was conceived by Professor A. Carlos Fernandez-Pello at the University of California at Berkeley. The hardware, which was designed and built at the NASA Lewis Research Center by a mixed team of civil servants and contractors from NYMA and Aerospace Design & Fabrication, Inc. (ADF), consists of two sealed aluminum combustion chambers (each one a half cylinder), data acquisition electronics, power distribution electronics, and instrumentation. The hardware is contained in a 5-ft³ Get-Away Special (GAS) canister and flown in the shuttle cargo bay. The



Microgravity Smoldering Combustion fuel sample and test section assembly.

chambers hold the MSC test section (fuel sample) and its temperature and pressure instrumentation. The test section (shown in the figure) consists of a quartz cylinder that contains the polyurethane foam sample and an igniter. This igniter, which is an electrically heated wire sandwiched between two porous ceramic disks, is mounted in contact with the end of the foam sample. An array of 12 thermocouples placed axially and radially along the foam sample provides temperature histories, which are used to determine the rate of smolder propagation and the characteristics of the reaction.

To find out more about the Microgravity Smoldering Combustion experiment and other Lewis Microgravity experiments, visit our sites on the World Wide Web:

<http://zeta.lerc.nasa.gov/expr2/scm.htm>

<http://microgravity.msad.hq.nasa.gov/cScienceProg/subdisc/combust.html>

<http://zeta.lerc.nasa.gov/>

Lewis contact: John M. Koudelka, (216) 433-2852
Headquarters program office: OLMSA (MSAD)

Solid Surface Combustion Experiment Completes a Series of Eight Successful Flights

The Solid Surface Combustion Experiment (SSCE) was the first combustion experiment to fly in the space shuttle and the first such experiment in the NASA spaceflight program since Skylab. SSCE was actually a series of experiments designed to begin to characterize flame spreading over solid fuels in microgravity and the differences of this flame spreading from normal gravity behavior. These experiments should lead to a better understanding of the physical processes involved—increasing our understanding of fire behavior, both in space and on Earth. SSCE results will help researchers evaluate spacecraft fire hazards. These experiments were conceived by the principal investigator, Professor Robert A. Altenkirch, Dean of Engineering at Washington State University.

In the first five flights, the fuel sample—ashless filter paper instrumented with three thermocouples—was mounted in a sealed chamber filled with a 50-percent or 35-percent mixture of oxygen in nitrogen at pressures of 1.0, 1.5, and 2.0 atm. In the next three flights, a polymethyl methacrylate (plexiglass) fuel was instrumented with three thermocouples and tested in a 70-percent or 50-percent mixture of oxygen and nitrogen at pressures

of 1.0 and 2.0 atm. SSCE is a self-contained, battery-operated experiment that can be flown either in the shuttle middeck or in the Spacelab module. Reference 1 provides more information about the hardware configuration.

This past year, the final two of eight flights were completed on STS-64 and STS-63. The NASA Lewis Research Center designed and built the SSCE payload and performed engineering, testing, scientific, and flight operations support. The SSCE project was supported in some way by nearly every major sector of Lewis' organization.

Professor Altenkirch developed a numerical simulation of the flame-spreading process from first principles (of fluid mechanics, heat transfer, and reaction kinetics). The spread rates, flame shape, and thermodynamic data from the SSCE flights are being compared directly with the results of the computational model. Results from the eight flights will be used to formulate an improved solid-phase pyrolysis model. In addition, some results of the flights have been published (ref. 2) and presented at international combustion symposiums. Additional solid fuel combustion experiments are being investigated for future tests with the existing hardware.

References

1. Vento, D.M., et al.: The Solid Surface Combustion Space Shuttle Experiment Hardware Description and Ground-Based Test Results. AIAA Paper 89-0503, 1989.
2. Bhattacharjee, S.; Altenkirch, R.A.; Sacksteder, K.R.: Implications of Spread Rate and Temperature Measurements in Flame Spread Over a Thin Fuel in a Quiescent, Microgravity Space-Based Environment. *Combust. Sci. Tech.*, vol. 91, 1993, pp. 225-242.

To find out more about the Solid Surface Combustion Experiment and other Lewis Microgravity experiments, visit our sites on the World Wide Web:

<http://zeta.lerc.nasa.gov/expr/ssce.htm>

<http://microgravity.msad.hq.nasa.gov/cScienceProg/subdisc/combust.html>

<http://zeta.lerc.nasa.gov/>

**Lewis contact: John M. Koudelka, (216) 433-2852
Headquarters program office: OLMSA (MSAD)**

New Low-Gravity Research Aircraft Takes to the Skies

A new research aircraft began operations at the NASA Lewis Research Center this past year. The aircraft, a McDonnell Douglas Corporation DC-9, began providing researchers funded by NASA Headquarter's Microgravity Science and Applications Division additional opportunities to perform research in a weightless environment, similar to that in orbiting spacecraft.

During a single flight, the aircraft can provide investigators with approximately 40 periods of weightlessness, with each period lasting approximately 22 sec. To provide weightlessness, the pilots fly a special maneuver known as a Keplarian, or parabolic, trajectory. First, the aircraft is put into a shallow dive to increase airspeed. Once at the desired airspeed, the pilots begin to climb, at up to a 60° angle. Once the airspeed drops to the desired level, the pilots "push over," putting the aircraft and its occupants in a free-fall, or weightless, condition. As the aircraft is pushed over, it begins to dive as the weightless condition continues. When the aircraft reaches a 40° downward angle, the pilots return the aircraft to level flight or begin the next parabola, ending the weightless period. During the entry and exit portions of the trajectory, the aircraft and its occupants experience a force of up to twice that of normal Earth gravity (up to 2g).

When Lewis acquired the DC-9, it was configured as a standard passenger aircraft. Lewis and support service contract engineers and technicians spent over a year modifying the aircraft for its new role as an airborne laboratory. All the work was completed at Lewis, with exception of the installation of a cargo door to facilitate the installation and removal of experiments, which was completed under contract. The aircraft is now configured to support up to 8 experiments and 20 experimenters per flight.

Modifications and installations completed at Lewis included a new power system, which was designed and installed to provide the experiments with electrical power. The interior was completely removed, and a new interior was installed to provide a large, unobstructed area for research operation. The cabin interior was then padded to protect the experimenters from being injured while floating about the cabin. The lighting in the cabin was modified to provide adequate light for research while minimizing electrical noise output, which might interfere with experiments. An acceleration measurement and display system was also

installed to help the pilots achieve and maintain a low-gravity environment. Numerous other systems were installed to support research, including an overboard vent, an intercom system, and a video and data recording system.

The DC-9 was completed and began supporting research investigations in combustion, fluid physics, and materials science in mid-May. This aircraft is also used by researchers from other NASA centers, other Government agencies, universities, and international agencies such as the Canadian Space Agency. The DC-9 aircraft will be a valuable research tool for years to come because it provides a low-cost opportunity for researchers to perform basic research and test systems on Earth that are destined for space.

To find out more about Lewis' DC-9, visit Lewis on the World Wide Web:

<http://zeta.lerc.nasa.gov/facility/dc9.htm>

<http://zeta.lerc.nasa.gov/jpw/cover.htm>

Lewis contact: Eric S. Neumann, (216) 433-2608

Headquarters program office: OLMSA (MSAD)



Lewis' DC-9 aircraft beginning a parabolic trajectory.



Research area inside Lewis' DC-9.

Real-Time Data From the Orbital Acceleration Research Experiment (OARE)

The objective of the Orbital Acceleration Research Experiment (OARE) is to measure, with high accuracy, the low-frequency, low-magnitude acceleration levels onboard the space shuttle. The shuttle experiences acceleration from atmospheric drag, gravity gradient forces, shuttle rotations, crew activities, water/waste dumps, and shuttle attitude thrusters. The OARE instrument has successfully flown on five past shuttle missions and is scheduled for five upcoming microgravity science missions. The data collected by OARE will be utilized by microgravity scientists to better predict and analyze the influence and effects of the shuttle's on-orbit microgravity environment on experiments in materials, combustion, and fluids research.

During previous shuttle missions, OARE data were recorded on the space shuttle payload recorder for later transmission to the ground. The second United States Microgravity Laboratory (USML-2), which is scheduled to fly in the fall of 1995, has a requirement for OARE to provide acceleration data to payload scientists in real-time. Payload scientists will use OARE data to verify the predicted microgravity acceleration environment and possibly adjust the orbiter attitude to minimize acceleration disturbances. The OARE instrument has been modified to provide real-time acceleration telemetry data through the shuttle Spacelab High-Rate Multiplexer for transmission to the Payload Operations Control Center at the NASA Marshall Space Flight Center.

OARE acceleration telemetry will be processed and analyzed by members of the Principal Investigator Microgravity Services (PIMS) team from the NASA Lewis Research Center. This team will acquire OARE data at the Payload Operations Control Center, compute sensor bias, perform low-frequency filtering, and display the data with graphics-based workstations. They will also provide expert analysis of the acceleration data provided by OARE.

The OARE and PIMS efforts are part of the Microgravity Measurements and Analysis Project at Lewis. OARE comprises a team of NASA civil servants and contractors from Canopus Systems Incorporated (CSI).

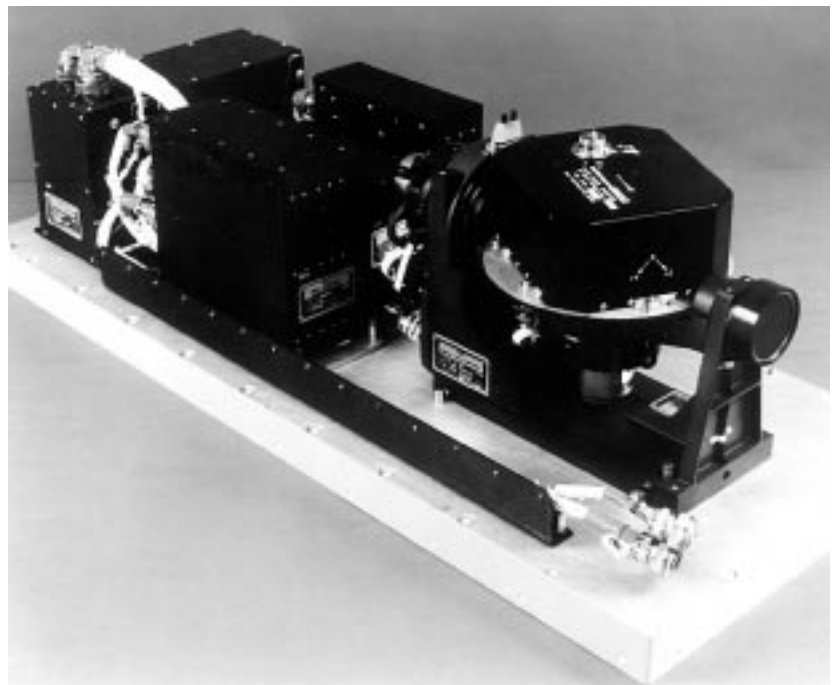
For more information about OARE, PIMS, and Lewis' microgravity experiments, visit our sites on the World Wide Web:

<http://zeta.lerc.nasa.gov/expr/oare.htm>

<http://www.lerc.nasa.gov/WWW/MMAP/PIMS/>

<http://zeta.lerc.nasa.gov/>

**Lewis contact: William O. Wagar, (216) 433-3665
Headquarters program office: OLMSA (MSAD)**



Orbital Acceleration Research Experiment.

Microgravity Environment Measured During Shuttle-Mir Science Program

NASA and the Russian Space Agency are embarking on several cooperative programs in preparation for the international space station program. The Shuttle-Mir Science Program and the NASA-Mir Program are two such programs. These programs will include experiments to help researchers understand the behavior of complex, large structures in space and the effects of microgravity.

One of the first experiments of the Shuttle-Mir Science Program was the Space Acceleration Measurement System (SAMS). The SAMS project at the NASA Lewis Research Center supports microgravity science experiments by measuring microgravity accelerations during on-orbit experiments. The Principal Investigator Microgravity Services (PIMS) project at Lewis supports principal investigators of microgravity experiments as they evaluate the effects of these varying acceleration levels on their experiments.

In August 1994, three U.S. experiments were launched in a Progress vehicle to the Mir station: SAMS, the Tissue Equivalent Proportional Counter, and the Mir Interface to Payload Support. The SAMS experiment was installed in the Kristall module of the Mir complex (see figure), where early U.S. experiments will be operated.

SAMS measures microgravity accelerations during the experiments, characterizing the microgravity environment to which they are exposed. During initial operations, data were collected in seven different time periods to survey the locations of the Protein Crystal Growth Experiment and the Russian Gallar Furnace in the Kristall module. A total of 53 hr and 14 min of microgravity data were collected on two data disks. These were returned to Earth in a Soyuz vehicle in November 1994. Personnel of the Lewis SAMS project quickly processed the data, and the Principal Investigator Microgravity Services project personnel prepared a quick analysis. Results were published in a NASA Technical Memorandum (ref. 1).

The Mir acceleration data were examined by the PIMS team to establish the principal characteristics in the Mir microgravity environment. Having

analyzed similar activity periods on the Mir space station and NASA's space shuttles, we can deduce that the microgravity environment on these vehicles is similar.

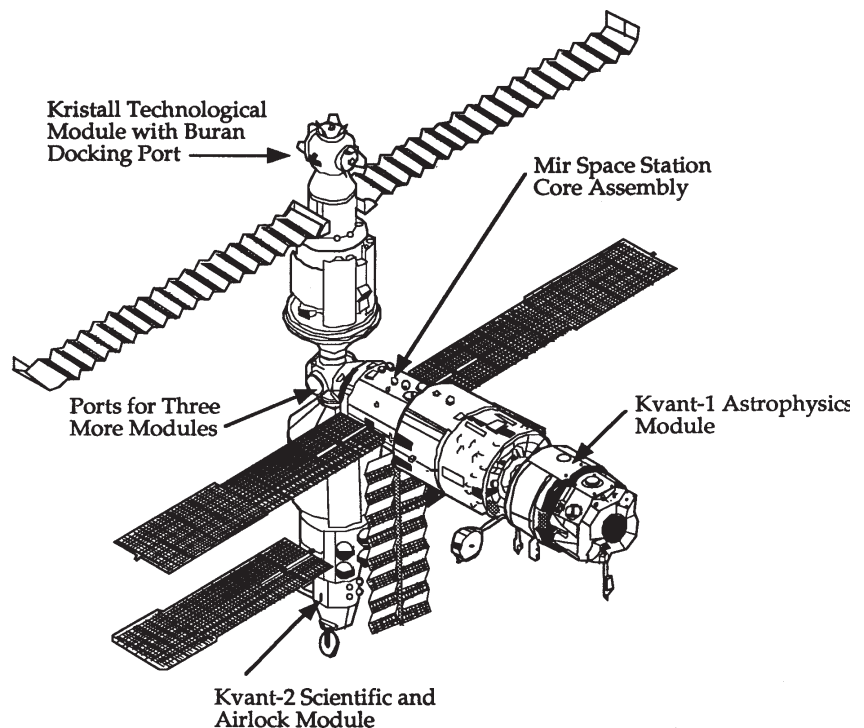
The SAMS Mir data files can be accessed from a file server at Lewis, along with data from other SAMS missions. A request for access instructions may be sent in an electronic mail message to pims@lerc.nasa.gov.

The SAMS unit also will support experiments onboard the Mir space station when more U.S. and Russian experiments are operated in the Priroda module to be installed in 1996. We estimate that an equivalent to 300 days of microgravity data are going to be collected throughout the entire Shuttle-Mir Program and NASA-Mir Program.

Reference

1. DeLombard, R.; and Rogers, M.J.B.: Quick Look Report of Acceleration Measurements on Mir Space Station During Mir-16. NASA TM-106835, 1995.

Lewis contact: Julio C. Acevedo, (216) 433-2471
Headquarters program office: OLMSA (MSAD)



Mir space station.

Advanced Space Analysis

Lewis Mars Pathfinder Microrover Experiments

The NASA Lewis Research Center has a prime role in the Mars Pathfinder mission, the first in the series of Discovery-class missions, sponsored by NASA Headquarter's Office of Space Science. Mars Pathfinder is an engineering proof-of-concept mission intended to demonstrate the successful deployment of scientific instruments, including a small rover, on a planetary body and to gain engineering design information for follow-on systems. The mission is scheduled to be flown in December 1996 and to land on Mars on July 4, 1997.

The Jet Propulsion Laboratory (JPL), which is heading the Pathfinder mission, requested Lewis' aid in developing a means to obtain, using the microrover, information on the abrasiveness and adherence properties of Mars soil and dust. Consequently, Lewis is developing three flight experiments for the Pathfinder Microrover. In addition, Lewis' Plum Brook Station is testing the Pathfinder airbag landing system for JPL.

Lewis' experiments consist of a Wheel Abrasion Experiment (WAE) and two Materials Adherence Experiments (MAE). The Wheel Abrasion Experiment will gain soil abrasion information by observing rover wheel wear. The center section on one of the rover's six wheels will be coated with thin layers of nickel, aluminum, and platinum. Changes in the metal layers' reflectance due to wear will be detected by a photocell. The two adherence experiments consist of (1) a solar cell experiment (MAESC), which compares the power output over time of a rover array cell in a "dirty" configuration (transparent dust cover closed) with the output for a "clean" configuration (dust cover opened briefly to direct illumination), and (2) a quartz crystal monitor experiment (MAEQCM), which measures the mass of dust accumulating with time and correlates this with the power output. This project has been conducted entirely in-house with Lewis and support service contractor personnel.

The development of the experiments was initiated in December 1993, and the flight hardware was delivered to JPL for integration with the microrover in May 1995, where the engineering model checked out successfully with the JPL rover. Integration with the flight unit rover will be concurrent with the rover construction. Principal investigators and engineers from Lewis will continue their involvement through the Pathfinder development and operations phases.



Artist's concept of Mars Pathfinder.

In addition to providing needed information on Mars surface properties, this project will demonstrate Lewis' ability and commitment to NASA's new business philosophies, which are intended to enhance NASA program efficiencies. The project features an in-house, multidirectorate team; low cost; a quick response time; and a cooperative effort with another center (JPL).

Bibliography

Landis, G.A., et al.: Development of a Mars Dust Characterization Instrument. IAF Paper 95-U.4.09, AIAA, 1995.

Jenkins, P.P.; and Landis, G.A.: A Rotating Arm Using Shape-Memory Alloy. 29th Aerospace Mechanisms Symposium. NASA CP-3293, 1995, pp. 167-171.

Siebert, M.W.; and Kolecki, J.C.: Electrostatic Charging of the Pathfinder Rover. AIAA Paper 96-0486, 1996.

Find out more about the Mars Pathfinder on the World Wide Web:

<http://www.lerc.nasa.gov/WWW/OptInstr/mars.html>
http://www.lerc.nasa.gov/WWW/PAO/pressrel/95_26.htm
<http://mpfwww.jpl.nasa.gov>
<http://www.jpl.nasa.gov/mars>

Lewis contact: Steven M. Stevenson, (216) 977-7087
Headquarters program office: OSS

TEMPEST: Twin Electric Magnetospheric Probes Exploring on Spiral Trajectories—A Proposal to the Medium Class Explorer Program

The NASA Lewis Research Center participated as a member of the Twin Electric Magnetospheric Probes Exploring on Spiral Trajectories (TEMPEST) Middle Class Explorer proposal team. This team was composed of Lewis, TRW, the University of California at Los Angeles (UCLA), SwRI, the Aerospace Corporation, the University of Iowa, the University of Maryland, the University of California at Berkeley, the Max Planck Institute, and Rice University. Lewis provided technical information, mission analysis, instrument description and requirements for one scientific experiment, and proposal logistics and publication for the TEMPEST proposal.

The objective of the TEMPEST mission is to understand the nature and causes of magnetic storm conditions in the magnetosphere whether they be manifested classically in the buildup of the ring current, or (as recently discovered) by storms of relativistic electrons that cause the deep dielectric charging responsible for disabling satellites in synchronous orbit, or by the release of energy into the auroral ionosphere and the plasma sheet during substorms.

This mission will be accomplished by two low-mass spacecraft launched by Pegasus rockets into orthogonal 400-km-altitude orbits (high and low inclination) carrying a small complement of instruments to detect, measure, and characterize basic particles and fields. Xenon-ion engines, developed at Lewis and powered by solar arrays, will take these spacecraft on a spiral trajectory from 400 km completely through the magnetosphere to 15 R_E (Earth radii, circular) in 2 years.

One of the science packages is a derivation of Lewis' Solar Array Module Plasma Interaction Experiment (SAMPIE) that was flown on space shuttle flight STS-62. This Spacecraft Interactions Package (SIP) will determine how the spacecraft interacts electrically with its environment. Interactions of interest include spacecraft charging in auroral and geosynchronous plasmas and parasitic current collection from the denser plasmas at low altitude.

The spacecraft xenon ion engines and power-processing units are being developed jointly at Lewis and the Jet Propulsion Laboratory through the NASA Solar Electric Propulsion Technology Assessment Readiness (NSTAR) program. The ion engines' 3300-sec average specific impulse is a key enabler of this mission, allowing a slow spiral through all of the magnetospheric regions of interest. Also key to this mission's success is the capability of the ion engines to throttle over a range of approximately 0.5- to 2.5-kWe input power.

Lewis is providing mission design and analysis for TEMPEST. Lewis' Advanced Space Analysis Office designed and will continue to refine the TEMPEST spacecraft trajectories, including launch window determination, coast phases, inclination changes, and input to the spacecraft guidance, navigation, and control algorithms.



Artist's concept of TEMPEST vehicle.

This mission proposal is being evaluated by NASA Headquarters' Office of Space Science. Should this program be selected, it could be the first application of xenon-ion solar electric propulsion to a NASA space science mission.

Bibliography

Hickman, J.M.; Hillard, G.B.; and Oleson, S.R.: TROPIX: A Solar Electric Propulsion Flight Experiment. NASA TM-106297, 1993.

Hickman, J.M.: Solar Electric Propulsion for Magnetospheric Mapping. AIAA Paper 94-3252, 1994.

Hickman, J.M.; and Hillard, G.B.: A Comprehensive Investigation of Space Environmental Interactions Using Solar Electric Propulsion. AIAA Paper 95-0372, 1995.

Find out more about SAMPIE on the World Wide Web:

<http://zeta.lerc.nasa.gov/expr/sample.htm>

Lewis contact: J. Mark Hickman, (216) 977-7105

Headquarters program office: OSS (SSED and SPD)

1995 R&T Engineering Support

Structural Systems

Improved Acoustic Blanket Developed and Tested

Acoustic blankets are used in the payload fairing of expendable launch vehicles to reduce the fairing's interior acoustics and the subsequent vibration response of the spacecraft. The Cassini spacecraft, to be launched on a Titan IV in October 1997, requires acoustic levels lower than those provided by the standard Titan IV blankets. Therefore, new acoustic blankets were recently developed and tested to reach NASA's goal of reducing the Titan IV acoustic environment to the allowable levels for Cassini.

To accomplish this goal, the Cassini vibroacoustic team—consisting of members from the NASA Lewis Research Center, the Jet Propulsion Laboratory, Lockheed Martin Corporation, and McDonnell Douglas Corporation—developed and coordinated a two-phase test program. In Phase One, 19 different blanket designs were tested in a flat-panel configuration at the Riverbank Acoustical Laboratory in Geneva, Illinois. The parameters evaluated included blanket thickness, blanket batting density, and placement and density of an internal barrier. Each blanket's absorption and transmission loss characteristics were quantified and the two leading designs were selected for the Phase Two test series.

Phase Two consisted of acoustic testing of the two new blanket designs, along with the standard blanket design, in a flightlike, full-scale (60-ft tall) cylindrical payload fairing with a spacecraft simulator. This testing was performed at Lockheed Martin's acoustic chamber in Denver, Colorado. The acoustics and spacecraft vibration measured when the new blankets were used were compared with the acoustics and vibration obtained when the standard Titan IV blankets were used.

Both new blankets designs tested in Phase Two achieved the pretest goal of significantly reducing the fairing's acoustic environment and spacecraft vibration response. The acoustic reduction achieved was 3 to 4 dB (decibels) at the important frequencies. One of the new blanket designs was selected for the Cassini mission. Because of this successful blanket development test program, key and expensive spacecraft components did not have to be redesigned and requalified, and an

estimated \$30 million in cost savings was achieved for the Cassini program.

These blankets can also be used for other Titan IV missions or other launch vehicles. In addition, a wealth of information was obtained about how acoustic blankets work and how these blankets affect the acoustics within a payload fairing.

Bibliography

Hughes, W.O.; and McNelis, A.M.: Cassini/Titan IV Acoustic Blanket Development and Testing. 1996 Proceedings—Institute of Environmental Sciences, 1996.

Find out more about Titan IV and Cassini on the World Wide Web:

<http://sys381.lerc.nasa.gov/analex/titan.htm>
<http://www.jpl.nasa.gov/cassini/>
<http://www.lerc.nasa.gov/WWW/PAO/html/lvpo.htm>

Lewis contacts: William O. Hughes, (216) 433-2597, and Anne M. McNelis, (216) 433-8880
Headquarters program office: OA



Assembly of the payload fairing in the acoustic chamber, with spacecraft simulator and acoustic blankets for Phase Two testing.

MSC/NASTRAN DMAP Alter Used for Closed-Form Static Analysis With Inertia Relief and Displacement-Dependent Loads

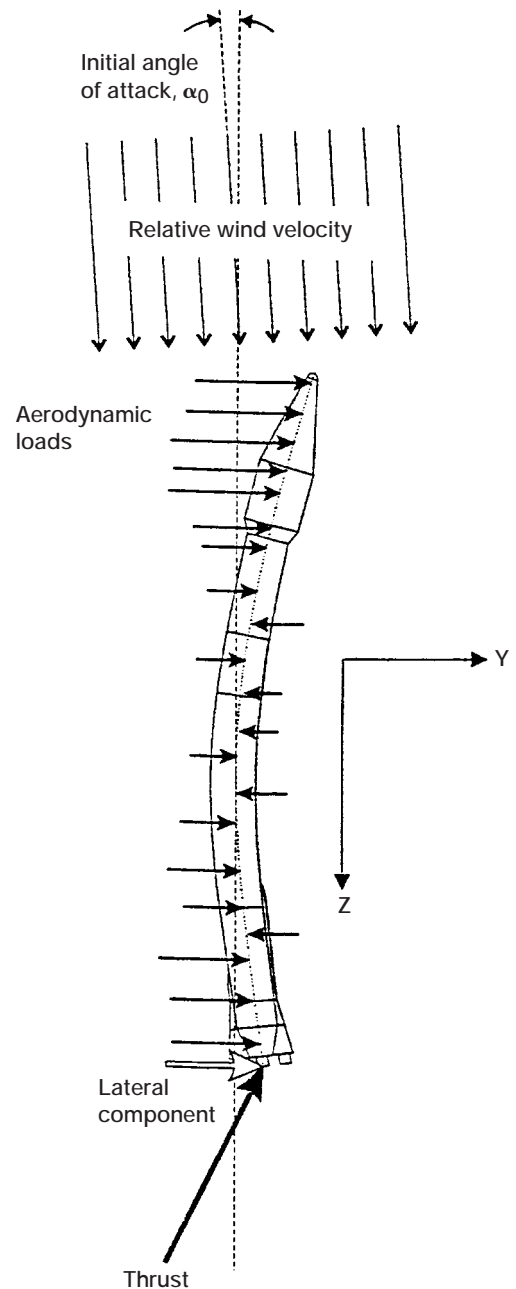
Solving for the displacements of free-free coupled systems acted upon by static loads is a common task in the aerospace industry. Often, these problems are solved by static analysis with inertia relief. This technique allows for a free-free static analysis by balancing the applied loads with the inertia loads generated by the applied loads. For some engineering applications, the displacements of the free-free coupled system induce additional static loads. Hence, the applied loads are equal to the original loads plus the displacement-dependent loads. A launch vehicle being acted upon by an aerodynamic loading can have such applied loads.

The final displacements of such systems are commonly determined with iterative solution techniques. Unfortunately, these techniques can be time consuming and labor intensive. Because the coupled system equations for free-free systems with displacement-dependent loads can be written in closed form, it is advantageous to solve for the displacements in this manner. Implementing closed-form equations in static analysis with inertia relief is analogous to implementing transfer functions in dynamic analysis. An MSC/NASTRAN (MacNeal-Schwendler Corporation/NASA Structural Analysis) DMAP (Direct Matrix Abstraction Program) Alter was used to include displacement-dependent loads in static analysis with inertia relief. It efficiently solved a common aerospace problem that typically has been solved with an iterative technique.

Bibliography

Barnett, A.R.; Widrick, T.W.; and Ludwiczak, D.R.: Closed-Form Static Analysis With Inertia Relief and Displacement-Dependent Loads Using a MSC/NASTRAN DMAP Alter. NASA TM-106836, 1995.

Lewis contacts: Damian R. Ludwiczak, (216) 433-2383; Alan R. Barnett, (216) 977-0168; Timothy W. Widrick, (216) 977-0177; and Kuan Lee, (216) 433-2595
Headquarters program office: OA



Displacement-dependent loads act upon launch vehicles during their ascent to Earth orbit.

Lewis Research Academy

Turbomachinery Flows Modeled

Last year, the average-passage code was released to industry. During the past year, a number of enhancements were made to the code. These enhancements include the modeling of bleed and leakage flows, an improved wall function model for the turbulent shear force, and changes to allow for variable gas properties. In addition, a new coarse grain parallelization execution script allows the code to be executed on clusters made up of workstations, the IBM SP2, and the Cray T3D. Compressors with up to 21 blade rows have been simulated, and the results from these simulations are currently being compared with data.

Lewis contact: Dr. John J. Adamczyk, (216) 433-5829
Headquarters program office: OA

Mixing and Transition Control Studied

Considerable progress in understanding nonlinear phenomena in both unbounded and wall-bounded shear flow transition has been made through the use of a combination of high-Reynolds-number asymptotic and numerical methods. The objective of this continuing work is to fully understand the nonlinear dynamics so that ultimately (1) an effective means of mixing and transition control can be developed and (2) the source terms in the aeroacoustic noise problem can be modeled more accurately.

Two important aspects of the work are that (1) the disturbances evolve from strictly linear instability waves on weakly nonparallel mean flows so that the proper upstream conditions are applied in the nonlinear or wave-interaction streamwise region and (2) the asymptotic formulations lead to parabolic problems so that the question of proper out-flow boundary conditions—still a research issue for direct numerical simulations of convectively unstable shear flows—does not arise. Composite expansion techniques are used to obtain solutions that account for both mean-flow-evolution and nonlinear effects.

A previously derived theory for the amplitude evolution of a two-dimensional instability wave in an

incompressible mixing layer (which is in quantitative agreement with available experimental data for the first nonlinear saturation stage for a plane-jet shear layer, a circular-jet shear layer, and a mixing layer behind a splitter plate) have been extended to include a wave-interaction stage with a three-dimensional subharmonic. The ultimate wave-interaction effects can either give rise to explosive growth or an equilibrium solution, both of which are intimately associated with the nonlinear self-interaction of the three-dimensional component. The extended theory is being evaluated numerically.

In contrast to the mixing-layer situation, earlier comparisons of theoretical predictions based on asymptotic methods and experiments in wall-bounded shear-flow transition have been somewhat lacking in one aspect or another. The current work strongly suggests that the main weakness is the underlying asymptotic representation of the linear “part” of the problem and not the explicit modeling of the nonlinear/wave-interaction effects. Consequently, the long-wave-length/high-Reynolds-number asymptotic limit for the Blasius boundary-layer stability problem was reexamined, and a new dispersion relationship for the instability waves that is uniformly valid for both the upper- and lower-branch regions to the required order of approximation was obtained. A comparison with numerical results, obtained by solving the Orr-Sommerfeld stability problem, shows that the asymptotic formula provides surprisingly good results, even for values of the frequency parameter usually encountered in experimental investigations. This is particularly evident in the dynamically important upper-branch region, where much of the nonlinear interactions in transition experiments are believed to take place. The result is important in that it can be used to greatly improve the accuracy of weakly nonlinear critical-layer-based theories, and a consistent nonlinear theory is currently under evaluation.

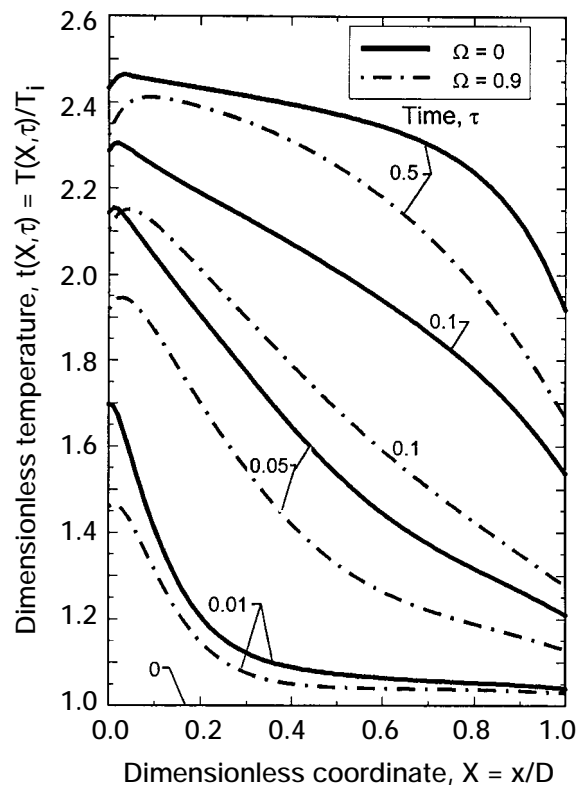
Lewis contact: Dr. Lennart S. Hultgren, (216) 433-6070
Headquarters program office: OA

Transient Analysis Used to Study Thermal Radiation Effects in Single and Composite Semitransparent Layers

To withstand the high temperatures in advanced aircraft engines, some engine parts will need to be made of, or coated with, ceramic materials. However, radiant thermal energy can affect the performance of some ceramics because they are partially transparent in portions of the radiation spectrum. Infrared and visible radiation from hot surroundings, such as in a combustor, will penetrate into the material and heat it internally, similar to penetration and absorption of microwave energy when heating food in a microwave oven. Internal temperatures depend on radiative effects, heat conduction, and heat transfer at the material surfaces. Transient heating behavior is very important because radiant penetration provides more rapid internal heating than conduction alone, and thermal stresses during transients can be more severe than for steady conditions. Because temperatures in an engine are high, emission of radiation from within the hot ceramic material is also very important and must be included.

In a continuing in-house program at the NASA Lewis Research Center, analytical and numerical methods are being developed to apply radiative analysis to predict transient temperature distributions and heat flows in partially transmitting materials. Results have been obtained for a single plane layer, and a transient analysis is being developed for a two-layer composite where each layer has a different refractive index. Because the ceramic refractive indices are larger than one, internal reflections are produced at the surfaces and at the internal interface. As shown in reference 1, reflections tend to distribute energy within a layer, and this affects the transient temperature distributions.

Since the equations to calculate radiative transfer are rather complex integral equations, especially when internal scattering is included, it is important to develop approximate methods that can be conveniently incorporated into computer design programs. One approximate technique that has been shown to be useful and accurate for steady situations is the two-flux method. This method is formulated as simultaneous differential equations that, for transient situations, can be solved along with the transient energy equation in the material. The two-flux equations include scattering without increasing the difficulty in obtaining solutions. In reference 2 the two-flux equations were solved by a shooting method, and transient solutions were obtained for optical thicknesses of a plane layer up to 8. For



Two-flux transient temperatures in a layer, initially at uniform temperature, after exposure to radiative heating on one side and convective cooling on both sides.

optical thicknesses up to 50, a Green's function method was developed (ref. 3). Transient two-flux solutions were compared with exact numerical solutions of the radiative transfer equations from reference 4, and very good agreement was obtained. This method is currently being extended for a two-layer composite.

The figure shows typical solutions obtained by the two-flux method for transient temperature distributions in a plane layer without scattering and with a scattering albedo of 0.9. The plane layer extends from $X = 0$ to 1, and the transient was initiated by suddenly supplying strong radiation to the boundary at $X = 0$, with the layer initially at a uniform temperature. (The layer's refractive index n was 2.) The equations were solved in two spectral regions with optical thicknesses K_D of 1 and 40 at high and low frequencies with approximately equal incident radiation in each frequency range. Energy was removed at both boundaries by convection.

At the beginning of the transient, there was a rapid temperature increase and a large temperature gradient near $X = 0$ because of radiative heating. The temperatures were somewhat reduced when the scattering albedo was increased. Comparisons with results for an opaque layer showed that internal radiation has a large effect.

References

1. Siegel, R.: Refractive Index Effects on Transient Cooling of a Semitransparent Radiating Layer. *J. Thermophys. Heat Transfer*, vol. 9, no. 1, Jan.-Mar. 1995, pp. 55-62.
2. Siegel, R.: Two-Flux Method for Transient Radiative Heat Transfer in a Semitransparent Layer. *Int. J. Heat Mass Transfer*, to be published in 1996.
3. Siegel, R.: Two-Flux and Green's Function Method for Transient Heat Transfer in a Semitransparent Layer. To be published in the Proceedings of the ICHMT International Symposium on Radiative Transfer, Kusadasi, Turkey, August 14-18, 1995.
4. Siegel, R.: Transient Heat Transfer in a Semitransparent Radiating Layer With Boundary Convection and Surface Reflections. *Int. J. Heat Mass Transfer*, vol. 39, no. 1, Jan. 1996, pp. 69-79.

Lewis contact: Dr. Robert Siegel, (216) 433-5831
Headquarters program office: OA

New Theoretical Technique Developed for Predicting the Stability of Alloys

When alloys are being designed for aeronautical and other applications, a substantial experimental effort is necessary to make incremental changes in the desired alloy properties. A scheme to narrow the field to the most promising candidates would substantially reduce the high cost of this experimental screening.

Such a method for determining alloy properties, called the BFS (Bozzolo, Ferrante, and Smith) method, has been developed at the NASA Lewis Research Center. This method was used to calculate the thermal stability and mechanical strength of 200 alloys of Ni_3Al , with Cu and Au impurities forming ternary and quaternary compounds. With recent advances in the method, almost any metallic impurity and crystal structure can be addressed. In addition, thermal effects can be addressed with Monte Carlo techniques. At present, an

experimental program is in progress to verify these results. The method identified a small number of the most promising candidates from the 200 alloys with the largest negative heat of formation and the highest bulk modulus. This calculation required only 5 min of CPU time on a VAX computer.

It is clear that semi-empirical methods have achieved the level of development and reliability to warrant examining this new approach to the problem of alloy design. The present work was meant to demonstrate, perhaps in a rather simple way, this power. This type of application of atomistic simulation methods can narrow the gap and improve the feedback between theoretical predictions and laboratory experimentation.

Bibliography

Bozzolo, G.; and Ferrante, J.: Bulk Properties of Ni_3Al (Gamma Prime) with Cu and Au Additions. To be published in the *Journal of Computer Aided Material Design*, 1995.

Lewis contact: Dr. John Ferrante, (216) 433-6069
Headquarters program office: OA

1995 R&T Technology Transfer

CARES/LIFE Software Commercialization

The NASA Lewis Research Center has entered into a letter agreement with BIOSYM Technologies Inc. (now merged with Molecular Simulations Inc. (MSI)). Under this agreement, NASA will provide a developmental copy of the CARES/LIFE computer program to BIOSYM for evaluation. This computer code predicts the time-dependent reliability of a thermomechanically loaded component. BIOSYM will become familiar with CARES/LIFE, provide results of computations useful in validating the code, evaluate it for potential commercialization, and submit suggestions for improvements or extensions to the code or its documentation.

If BIOSYM/Molecular Simulations reaches a favorable evaluation of CARES/LIFE, NASA will enter into negotiations for a cooperative agreement with BIOSYM/Molecular Simulations to further develop the code—adding features such as a user-friendly interface and other improvements. This agreement would give BIOSYM intellectual property rights in the modified codes, which they could protect and then commercialize. NASA would provide BIOSYM with the NASA-developed source codes and would agree to cooperate with BIOSYM in further developing the code. In return, NASA would receive certain use rights in the modified CARES/LIFE program.

Presently BIOSYM Technologies Inc. has been involved with integration issues concerning its merger with Molecular Simulations Inc., since both companies used to compete in the computational chemistry market, and to some degree, in the materials market. Consequently, evaluation of the CARES/LIFE software is on hold for a month or two while the merger is finalized. Their interest in CARES continues, however, and they expect to get back to the evaluation by early November 1995.

Find out more about Lewis' technology transfer programs and BIOSYM/Molecular Simulations on the World Wide Web:

<http://www.lerc.nasa.gov/WWW/TU/techtran.htm>
<http://www.biosym.com/>

Lewis contacts: James E. Martz, (216) 433-5563 (E-Mail: james.e.martz@lerc.nasa.gov), and Noel N. Nemeth, 433-3215
Headquarters program office: OSAT

Combustion Technology Outreach

Lewis' High Speed Research (HSR) Propulsion Project Office initiated a targeted outreach effort to market combustion-related technologies developed at Lewis for the next generation of supersonic civil transport vehicles. These combustion-related innovations range from emissions measurement and reduction technologies, to diagnostics, spray technologies, NO_x and SO_x reduction of burners, noise reduction, sensors, and fuel-injection technologies. The Ohio Aerospace Institute and the Great Lakes Industrial Technology Center joined forces to assist Lewis' HSR Office in this outreach activity.

From a database of thousands of nonaerospace firms considered likely to be interested in Lewis' combustion and emission-related technologies, the outreach team selected 41 companies to contact. The selected companies represent oil-gas refineries, vehicle/parts suppliers, and manufacturers of residential furnaces, power turbines, nonautomobile engines, and diesel internal combustion engines.

In May 1995, the outreach team held an initial round of telephone interviews with representatives of the 41 firms to determine common areas of interest, grounds for potential collaboration, and preferred methods of interaction. As a result of these interviews, it was determined that the greatest areas of interest involved lowering NO_x and SO_x emissions; developing analysis codes, materials, and instrumentation/diagnostics; and addressing fuel injection, noise reduction, and mixing problems.

The outreach team is now conducting follow-on teleconferences and face-to-face meetings to determine areas of collaboration, assistance, and possible development of consortia.

For more information about Lewis' research and technology transfer programs, visit our sites on the World Wide Web:
<http://www.lerc.nasa.gov/WWW/Infosys/Development/HSR.html>
<http://www.lerc.nasa.gov/WWW/TU/techtran.htm>
<http://www.lerc.nasa.gov>

Lewis contact: Katherine K. Martin, (216) 977-7122
Headquarters program office: OA

Technology Transferred to the Kirby Company

For more than 80 years now, the Kirby Company has been recognized as a leader in the production and development of home-cleaning systems. Today, Kirby's Research and New Product Development Group hopes to evaluate advanced technologies and new concepts that could improve the performance, cost-effectiveness, and quality of its product. Areas of interest include fan and air-flow path improvements for performance; noise reduction; motor and electronic control; light-weight, cost-effective materials; and vibration analysis and control.

Javier Resto and Edward Hronek, of NASA Lewis Research Center's Propulsion Systems Branch, evaluated the structural and vibration characteristics

of the Kirby Model G-4 fan. Modes of vibration and resonance potential were evaluated in the Holography Test Lab at Lewis. As a result of the Lewis tests and rotor structural evaluation, Kirby engineers gained new insights into their existing design, enabling them to develop a more robust fan for use in their vacuum cleaners.

Find out more about Lewis' technology transfer programs on the World Wide Web:

<http://www.lerc.nasa.gov/WWW/TU/techtran.htm>

Lewis contacts: James E. Martz, (216) 433-5563 (E-Mail: james.e.martz@lerc.nasa.gov), and Mark D. Bethea, (216) 433-8161 (E-Mail: msbeth@bomani.lerc.nasa.gov) Headquarters program office: OSAT



A laser beam is used to study the Kirby G-4 fan in the Lewis Holography Test Lab. From left to right are Kirby engineer Dennis Du, consultant Greg Stewart, and Kirby Senior Vice-President of Research and Development John Lackner. Seated is the Chief of Lewis' Propulsion Systems Branch, Edward Hronek.

Flow Visualization Proposed for Vacuum Cleaner Nozzle Designs

In 1995, the NASA Lewis Research Center and the Kirby Company (a major vacuum cleaner company) began negotiations for a Space Act Agreement to conduct research, technology development, and testing involving the flow behavior of airborne particulate flow behavior. Through these research efforts, we hope to identify ways to improve suction, flow rate, and surface agitation characteristics of nozzles used in vacuum cleaner nozzles.

We plan to apply an advanced visualization technology, known as Stereoscopic Imaging Velocimetry (SIV) (ref. 1), to a Kirby G-4 vacuum cleaner. Resultant data will be analyzed with a high-speed digital motion analysis system. We also plan to evaluate alternative vacuum cleaner nozzle designs.

The overall goal of this project is to quantify both velocity fields and particle trajectories throughout the vacuum cleaner nozzle to optimize its "cleanability"—its ability to disturb and remove embedded dirt and other particulates from carpeting or hard surfaces.

Reference

1. Bethea, M.D.: Stereo Imaging Velocimetry. Research & Technology 1995. NASA TM-107111, 1996, pp. 44-45. (World Wide Web URL: <http://www.lerc.nasa.gov/RT1995/5000/5110B.htm>)

Find out more about Lewis' technology transfer programs on the World Wide Web:

<http://www.lerc.nasa.gov/WWW/TU/techtran.htm>

Lewis contacts: James E. Martz, (216) 433-5563 (E-Mail: james.e.martz@lerc.nasa.gov), and Mark D. Bethea, (216) 433-8161 (E-Mail: msbeth@bomani.lerc.nasa.gov)
Headquarters program office: OSAT

CommTech: The Commercial Technology Consultants Program

The Commercial Technology Consultants Program (CommTech), a nationwide Lewis initiative launched in March 1995, provides nonaerospace companies and NASA Lewis Research Center scientists and engineers with a process for forming technical support relationships involving the commercialization of products or processes. The industries targeted in this effort span the environmental, surface transportation (land and sea), and biomedical sectors.

The first CommTech cycle consisted of the following four phases which will extend from fiscal 1995 to fiscal 1997:

- Phase I—Participants Response and Selection
- Phase II—Company Relationship Exploration
- Phase III—Relationship Definition and Agreement
- Phase IV—Agreement Implementation and Execution

In Phase I, 142 company-provided descriptions of long-term product- or process-related technology needs were selected, filtered, compiled, and distributed to 1500 Lewis scientists and engineers. Subsequently, 15 Lewis scientists and engineers applied as individuals and 10 teams applied—bringing the total number of lead and nonlead Lewis scientific and engineering participants to 50. At the end of Phase I, the lead participants selected a total of 73 companies from 21 states for Phase II efforts. Over 80 percent of the selected companies were small- or medium-sized, for-profit businesses.

During Phase II, Lewis' lead participants initiated one-on-one technical-level interactions with the selected companies. A shared budget of \$230,000 was made available to the lead participants to fund limited technology capability demonstrations for selected companies that were unfamiliar with Lewis' capabilities. The companies could then fund further interactions, as desired. As CommTech participants make the transition from Phase II to Phase III, Lewis' lead participants will narrow their focus and each will select one or more companies to support. As of October 1995, 19 lead participants had identified companies interested in further interaction.

A press release about CommTech is available on the World Wide Web:

http://www.lerc.nasa.gov/WWW/PAO/pressrel/95_41.htm

Lewis contact: Gary A.P. Horsham, (216) 433-8316
Headquarters program office: OSAT

NASA Headquarters Program Offices

| | |
|--------------|---|
| OA | Office of Aeronautics |
| | HPCCO High Performance Computing & Communications Office |
| OLMSA | Office of Life & Microgravity Sciences & Applications |
| | MSAD Microgravity Science & Applications Division |
| OSAT | Office of Space Access and Technology |
| | STD Space Transportation Division |
| | SSD Space Systems Division |
| OSC | Office of Space Communications |
| OSMA | Office of Safety and Mission Assurance |
| OSS | Office of Space Science |
| | SSED Solar System Exploration Division |
| | SPD Space Physics Division |

Index of Authors and Contacts

Both authors and contacts are listed in this index. However, only primary contacts are referenced in the actual articles. Articles for these authors and contacts start on the page numbers following the names. When two articles start on the same page, the first article is indicated by the letter "a" after the number and the second article by a "b."

A

Abel, Dr. Phillip B. 51
Abdul-Aziz, Dr. Ali 68
Acevedo, Julio C. 149
Acosta, Dr. Roberto J. 132
Adamczyk, Dr. John J. 155a
Addy, Gene 20
Arnold, Dr. Steven M. 65, 67
Ashpis, Dr. David E. 13

B

Bakhle, Milind A. 75
Banks, Bruce A. 108
Barnett, Alan R. 154
Becks, Edward A. 36
Bethea, Mark D. 44, 159, 160a
Bexten, Ronald L. 124
Bhasin, Dr. Kul B. 117
Bodis, James R. 78a
Bonacuse, Peter J. 69
Bond, Thomas H. 21
Britton, Randall K. 21
Brown, Dr. Gerald V. 76

C

Canacci, Victor A. 22
Castelli, Michael G. 72, 74
Chang, Dr. Clarence T. 15
Chiaramonte, Dr. Fran 142
Chock, Ricaurte 103
Chuang, Dr. Kathy C. 55
Cole, Gary L. 12
Curtis, Henry B. 95

D

DeBonis, James R. 30
De Groh, Kim K. 106, 111
De Groot, Dr. Wilhelmus A. 88
DeLaat, John C. 9
DeLombard, Richard 149

Dever, Joyce A. 107a
DiCarlo, Dr. James A. 50
Dittmar, Dr. James H. 33

E

Ellis, Dr. David L. 47

F

Ferguson, Dr. Dale C. 100, 101, 102
Fernandez-Pello, Prof. A. Carlos 144
Ferrante, Dr. John 157
Forkapa, Mark J. 108
Foss, Dr. Judith K. 16

G

Gaier, Dr. James R. 107b
Garg, Dr. Anita 45
Georgiadis, Nicholas J. 27b
Ghosn, Dr. Louis J. 80
Ginty, Carol A. 43
Gray, Dr. Hugh R. 43
Greenberg, Paul S. 134
Griffin, Dr. Devon W. 134
Guasp, Edwin 96
Gyekenyesi, Dr. John P. 78b

H

Halford, Dr. Gary R. 62, 70
Hamley, John A. 90
Handschuh, Dr. Robert F. 26
Hathaway, Dr. Michael D. 14
Haugland, Dr. Edward J. 121
Hegde, Dr. Uday 136
Heidelberg, Larry J. 34
Heidger, Dr. Susan L. 52
Hendricks, J. Lynne 78a
Herbell, Dr. Thomas P. 48

Hickman, J. Mark 150, 151
Hill, Myron E. 139
Hillard, Dr. Barry 100
Hollansworth, James E. 116
Hopkins, Dale A. 59, 60b
Horsham, Gary A.P. 160b
Hronek, Edward J. 159
Hughes, William O. 153
Hultgren, Dr. Lennart S. 155b
Hung, Dr. Ching-Cheh 109
Hunter, Gary W. 5
Hurwitz, Dr. Frances I. 57

I

Ivancic, William D. 125

J

Jacqmin, Dr. David A. 113
Jacobson, Dr. Nathan S. 58
Jankovsky, Robert S. 87
Janosik, Lesley A. 78b
Javidi, Sina 130b, 132
Jaworske, Dr. Donald A. 110, 111, 112a
Jeracki, Robert J. 33
Johns, Albert L. 27a
Jones, Scott M. 2

K

Kalluri, Dr. Sreeramesh 68, 69, 70
Kascak, Albert F. 76
Kerczewski, Robert J. 127a, 127b
Klem, Mark D. 81
Kolecki, Joseph C. 102
Koudelka, John M. 144, 145
Krainsky, Dr. Isay L. 122a
Krantz, Timothy L. 25

L

Lam, David W. 29
Larkin, Dr. David J. 4
Lawrence, Dr. Charles 40
Lee, Kuan S. 154
Lei, Dr. Jih-Fen 3, 72
Lepicovsky, Dr. Jan 31
Lerch, Bradley A. 61, 62
Lewandowski, Beth 41
Lewicki, Dr. David G. 23, 26

Lopez, Isaac 38
Ludwiczak, Damian R. 154
Lyons, Dr. Valerie J. 19

M

Makel, Darby 5
Malarik, Diane C. 141
Manning, Dr. Robert M. 129a, 129b, 130a
Martin, Donald F. 141
Martin, Katherine K. 78a, 158b
Martz, James E. 158a, 159, 160a
McCartney, Timothy P. 37
McKissock, Barbara I. 94
McNelis, Anne M. 153
Meador, Dr. Mary Ann B. 57
Meador, Dr. Michael A. 55, 56
Merte, Dr. Herman 142
Meyer, Michael L. 83
Miller, Dean R. 20
Miller, Fletcher J. 137
Millis, Marc. G. 92
Mitchell, Kenneth 132
Miyoshi, Dr. Kazuhisa 52
Morales, Dr. Wilfredo 54
Myers, Dr. Roger M. 91

N

Nakamura, Dan 130b
Neiner, George H. 27a
Nemeth, Noel N. 78a, 78b, 158a
Neudeck, Dr. Philip G. 4
Neumann, Eric S. 146
Niedzwiecki, Richard W. 19
Noebe, Ronald D. 61

O

Olson, Sandra L. 133
Oswald, Fred B. 24
Otero, Angel M. 142

P

Palaszewski, Bryan A. 85, 86
Patnaik, Dr. Surya N. 59
Paxson, Daniel E. 8
Pereira, Dr. J. Michael 60a
Piszczor, Michael F. 94, 95
Potapczuk, Dr. Mark G. 22

Powell, J. Anthony 4, 51
Powers, Lynn M. 78b
Prokopius, Paul R. 97

Q

Quinn, Todd 123
Quintana, Jorge A. 123

R

Raj, Dr. Sai V. 45
Rapp, Prof. Robert A. 58
Raquet, Dr. Charles A. 122b, 130b
Reddy, Dr. D.R. 10, 11
Reehorst, Andrew L. 22
Reinhart, Richard 130b
Renz, David D. 98
Ross, Dr. Howard D. 136, 137
Roth, Dr. Don J. 78a
Rutledge, Sharon K. 105

S

Saiyed, Naseem H. 35
Saravanos, Dimitris A. 60b
Schneider, Dr. Steven J. 89
Shaltens, Richard K. 114
Siegel, Dr. Robert 156
Singh, Dr. Mrityunjay 49
Smalley, Robert R. 36, 37
Smith, Timothy D. 87
Soeder, James F. 99
Sohn, Philip Y. 130b
Soni, Nitin J. 125
Sotomayor, Jorge L. 7
Steffen, Christopher J., Jr. 16
Stefko, George L. 75
Steinetz, Dr. Bruce M. 77
Stevens, Grady H. 120
Stevenson, Steven M. 150
Stocker, Dennis P. 136
Strazisar, Dr. Anthony J. 14
Stueber, Thomas J. 112b

T

Taylor, Linda M. 98
Telesman, Jack 80
Thomas, Scott R. 18
Tolbert, Carol M. 113

V

Valco, Dr. Mark J. 17
Vannucci, Raymond D. 56
Veres, Joseph P. 39

W

Wadel, Mary F. 83
Wagar, William O. 148
Wald, Lawrence W. 113
Walker, James F. 84
Warshay, Dr. Marvin 97
Weislogel, Mark M. 140
Welch, Dr. Gerard E. 32
Wernet, Dr. Mark P. 6
Whalen, Mike 78a
Whyte, Wayne A., Jr. 117, 119
Widrick, Timothy W. 154
Wiedenmannott, Barbara E. 1
Wilson, Dr. Jack 32
Wolter, John D. 28
Woo, Dr. Myeung J. 101
Worthern, Dr. Dennis W. 64
Wright, David L. 132

Z

Zaman, Dr. Khairul 16

REPORT DOCUMENTATION PAGEForm Approved
OMB No. 0704-0188

Public reporting burden for this collection of information is estimated to average 1 hour per response, including the time for reviewing instructions, searching existing data sources, gathering and maintaining the data needed, and completing and reviewing the collection of information. Send comments regarding this burden estimate or any other aspect of this collection of information, including suggestions for reducing this burden, to Washington Headquarters Services, Directorate for Information Operations and Reports, 1215 Jefferson Davis Highway, Suite 1204, Arlington, VA 22202-4302, and to the Office of Management and Budget, Paperwork Reduction Project (0704-0188), Washington, DC 20503.

| | | | | |
|---|---|--|---|--|
| 1. AGENCY USE ONLY (Leave blank) | | 2. REPORT DATE March 1996 | 3. REPORT TYPE AND DATES COVERED Technical Memorandum | |
| 4. TITLE AND SUBTITLE Research & Technology 1995 | | | 5. FUNDING NUMBERS None | |
| 6. AUTHOR(S) | | | | |
| 7. PERFORMING ORGANIZATION NAME(S) AND ADDRESS(ES) National Aeronautics and Space Administration Lewis Research Center Cleveland, Ohio 44135-3191 | | | 8. PERFORMING ORGANIZATION REPORT NUMBER E-10017 | |
| 9. SPONSORING/MONITORING AGENCY NAME(S) AND ADDRESS(ES) National Aeronautics and Space Administration Washington, DC 20546-0001 | | | 10. SPONSORING/MONITORING AGENCY REPORT NUMBER NASA TM-107111 | |
| 11. SUPPLEMENTARY NOTES Responsible person, Walter S. Kim, organization code 9400, (216) 433-3742. | | | | |
| 12a. DISTRIBUTION/AVAILABILITY STATEMENT Unclassified - Unlimited Subject Categories 01 and 31 This publication is available from the NASA Center for Aerospace Information, (301) 621-0390. | | | 12b. DISTRIBUTION CODE | |
| 13. ABSTRACT (Maximum 200 words) This report selectively summarizes the NASA Lewis Research Center's research and technology accomplishments for fiscal year 1995. It comprises over 150 short articles submitted by the staff members of the technical directorates. The report is organized into six major sections: aeronautics, aerospace technology, space flight systems, engineering support, Lewis Research Academy, and technology transfer. A table of contents, an author index, and a list of NASA Headquarters program offices have been included to assist the reader in finding articles of special interest. This report is not intended to be a comprehensive summary of all research and technology work done over the past fiscal year. Most of the work is reported in Lewis-published technical reports, journal articles, and presentations prepared by Lewis staff members and contractors (for abstracts of these Lewis-authored reports, visit the Lewis Technical Report Server (LeTRS) on the World Wide Web— http://letrs.lerc.nasa.gov/LeTRS/). In addition, university grants have enabled faculty members and graduate students to engage in sponsored research that is reported at technical meetings or in journal articles. For each article in this report, a Lewis contact person has been identified, and where possible, reference documents are listed so that additional information can be easily obtained. The diversity of topics attests to the breadth of research and technology being pursued and to the skill mix of the staff that makes it possible. For more information about Lewis' research, visit us on the World Wide Web— http://www.lerc.nasa.gov . | | | | |
| 14. SUBJECT TERMS Aeronautics; Aerospace engineering; Space flight; Space power; Materials; Structures; Electronics; Space experiments; Technology transfer | | | 15. NUMBER OF PAGES 178 | |
| | | | 16. PRICE CODE A09 | |
| 17. SECURITY CLASSIFICATION OF REPORT Unclassified | 18. SECURITY CLASSIFICATION OF THIS PAGE Unclassified | 19. SECURITY CLASSIFICATION OF ABSTRACT Unclassified | 20. LIMITATION OF ABSTRACT | |